NEDERL. AKADEMIE VAN WETENSCHAPPEN

PROCEEDINGS

VOLUME XLIV

No. 8

President: J. VAN DER HOEVE
Secretary: M. W. WOERDEMAN

CONTENTS

VENING MEINESZ, F. A.: "Gravity over the continental edges", p. 883.

CLAY, J.: "Cosmic Ray Showers", p. 888.

ITERSON Jr., G. VAN, and A. D. J. MEEUSE: "The shape of cells in homogeneous plant tissues". II. (With one plate), p. 897.

WEITZENBÖCK, R.: "Ueber die Figur dreier Ebenen im R_5", p. 907.

BIEZENO, C. B., and J. J. KOCH: "On the elastic behaviour of the so-called "Bourdon" pressure gauge". II, p. 914.

DEVIVERE, D. VON, and A. DE KLEYN: "A new form of position nystagmus", p. 921.

HEUX, J. W. N. LE: "Recherches sur quelques phénomènes d'interférence des courbes de vibration". (Suite). (Communicated by Prof. P. ZEEMAN). (With one plate), p. 926.

ELTEREN, J. F. VAN: "The orientation of watermolecules round charged particles". (Communicated by Prof. J. D. VAN DER WAALS Jr.), p. 930.

GROOT, J. DE: "Sätze über topologische Erweiterung von Abbildungen". (Communicated by Prof. L. E. J. BROUWER): p. 933.

MONNA, A. F.: "Sur la représentation des fonctions harmoniques". (Communicated by Prof. W. VAN DER WOUDE), p. 939.

WRONA, W.: "Eine Verallgemeinerung des SCHURschen Satzes". (Communicated by Prof. W. VAN DER WOUDE), p. 943.

UVEN, M. J. VAN: "Likelihood as conditioned probability". (Communicated by Prof. H. A. KRAMERS), p. 947.

WOLFF, J.: "Inégalités remplies par les fonctions univalentes". (Communicated by Prof. J. G. VAN DER CORPUT), p. 956.

VEEN, S. C. VAN: "Stark konvergente Entwicklungen für die vollständigen elliptischen Integrale erster und zweiter Art". I. (Communicated by Prof. J. G. VAN DER CORPUT), p. 964.

VEEN, S. C. VAN: "Ueber die Entwicklung der unvollständigen elliptischen Integrale erster und zweiter Art in stark konvergenten Reihen". I. (Communicated by Prof. J. G. VAN DER CORPUT), p. 974

K 244

RUTGERS, J. G.: "Sur des séries et des intégrales définies contenantes les fonctions de BESSEL". V. (Communicated by Prof. J. A. SCHOUTEN), p. 978.

FUNKE, G. L.: "The photoperiodic responses of Anthemis tinctoria in different ranges of wave length". (Communicated by Prof. L. G. M. BAAS BECKING). (With one plate), p. 989.

ROEVER, W. P. DE: "Die permischen Alkaligesteine und die Ophiolithe des timoresischen Faltengebirges". (Communicated by Prof. H. A. BROUWER), p. 993.

BELLEN, R. C. VAN: "Some eocene Foraminifera from the neighbourhood of Ričice near Imotski, E. Dalmatia, Yugoslavia". (Communicated by Prof. L. RUTTEN). (With one plate and one table), p. 996.

KEIJZER, F.: "Eine neue eozäne Foraminiferengattung aus Dalmatien". (Communicated by Prof. L. RUTTEN), p. 1006.

BOL, F. P.: "On the structure of the connective tissue of the anterior lobe of the hypophysis cerebri and the nature of the intraprotoplasmic networks described by Tello in and around the cells of the anterior lobe". (Communicated by Prof. J. BOEKE). (With one plate), p. 1008.

BRUMMELKAMP, R.: "Microgyria and retarded migration". (Communicated by Prof. C. U. ARIËNS KAPPERS). (With one plate), p. 1011.

SEGAAR, J.: "Der Einfluss von Kohlensäure auf die Atmungsbewegungen von Crustaceen". II. (Communicated by Prof. H. J. JORDAN), p. 1017.

ONG SIAN GWAN: "Biophysique. Spectres d'absorption de l'extrait et des protéines du poumon normal et du poumon intoxiqué par le phosgène dans l'ultra-violet". (Troisième mémoire). (Communicated by Prof. W. H. KEESOM), p. 1024.

GERLINGS, P. G.: "Investigations about stimulation and paralysis of the labyrinth by methylamine". (Communicated by Prof. A. DE KLEYN), p. 1031.

BIJTEL, J.: "Some considerations concerning our knowledge of the action of the auditory organ". I. (Communicated by Prof. A. DE KLEYN), p. 1037.

Geophysics. — *Gravity over the continental edges.* By F. A. VENING MEINESZ.

(Communicated at the meeting of September 27, 1941.)

During the gravity expeditions at sea of the Netherlands Geodetic Commission, carried out as it is well-known on board of submarines of the Royal Netherlands Navy, numerous gravity profiles over the edges of the continents have been observed, the stations having been chosen in lines more or less at right angles to the continental slope. At the landside some of the profiles end in a station over the continental shelf, some in a harbour-station occupied during the stay in port of the submarine, and several profiles observed during the expedition of Hr. Ms. K 18 could be continued inland by means of HOLWECK–LEJAY observations during excursions from these ports. In total the writer obtained three profiles at the end of the Channel, one near Lisbon, four at the coast of W. Africa, four at the coast of S. Africa, two at the east-coast of the U.S. near the mouth of the Chesapeake Bay, four at the west-coast of America between Panama and San Francisco of which one is incomplete, six at the east-coast of S. America, two at the west-coast of Australia, one at the south-coast of Ceylon and an incomplete one near Socotra. We shall not mention here the many coastal profiles in the East and West Indies which can not be considered as continental shelf profiles. In this paper the writer wants to discuss the results of the isostatic reduction of these shelf profiles with the new tables for regional and local compensation published this year by the Netherlands Geodetic Commission [1].

The gravity results of these profiles have formerly been isostatically reduced according to three methods, in the first place by means of the HAYFORD–BOWIE tables based on the assumption that the isostatic compensation is evenly distributed between the Earth's surface and a surface at a depth of 113.7 km below it, in the second place by means of the AIRY–HEISKANEN tables for a normal thickness of the crust of 40 km which assume each vertical prism of the crust to float freely on the denser substratum, thus locating the compensation of a density of -0.6 in crustal roots at the lower boundary of the crust, and in the third place by means of provisional tables for regional isostatic reduction which have now been superseded by the more complete new tables. In nearly all the profiles the results of these three reductions have shown an increase of the anomalies of 30—100 mgals when passing from the shelf to deep water. This fairly sudden jump in the anomalies brought about positive anomalies at the ocean-side of most of the profiles, which in many cases continued to exist over great parts of the ocean-crossing. The suddenness of the transition pointed to a cause that can not be deepseated and several suppositions have already been made about it. The new reductions have provided a simple solution. For a better understanding the writer will begin by shortly recalling the principle of these reductions.

They are based on the AIRY supposition of a rigid crust floating on a denser plastic substratum; the densities have been assumed to be 2.67 and 3.27, i.e. the values chosen by HEISKANEN for his tables for local AIRY reduction. Three sets of tables have been computed viz for values of the normal thickness T of the crust of 20 km, 30 km and 40 km. For local reduction we assume that each vertical column of the crust can adjust itself in equilibrium independent of its surroundings, thus bringing about a local isostatic compensation located in roots at the lower boundary of the crust. The new tables for regional isostatic reduction are based on the assumption that each crustal column can not locally adjust itself but that the crust acts as an elastic plate floating on the substratum and that it bends under the load of the topography till equilibrium is readjusted; the

[1] F. A. VENING MEINESZ, Tables for regional and local isostatic reduction (AIRY-system) for gravity values, Waltman, Delft, 1941.

isostatic compensation of an element of the topography is thus also located in a root at the lower boundary of the crust but the root is much broader than the element and it corresponds to the shape of the bending curve. In the practical execution of the tables the compensation has been assumed at the same depth as that of the local reduction but distributed in a horizontal sense round the element according to the shape of the bending curve. This distribution extends as far as the bending goes, i.e. up to a radius R round the element depending on the thickness of the crust and its elastic properties. The tables have been made for values of R of 29.05 km, 58.1 km, 116.2 km, 174.3 km and 232.4 km, and a column has been added for $R = 0$, i.e. for local compensation according to HEISKANEN's assumptions. The tables thus allow the comparizon of local compensation and of five different ranges of regional compensation.

The entire gravity material of the gravity expeditions at sea has been reduced with these new tables. The reductions have been made with all the values for R and for $T = 20$ km and $T = 30$ km. A study of the results for the shelf-profiles shows that the above-mentioned increase of the anomalies over the edge of the shelf disappears for suitable values of R and T. In many profiles this is the case for $T = 30$ km and for $R = 0$ or for small values of R. In many other profiles this occurs for $T = 20$ km or T between 20 and 30 km, in a few also for slightly larger values of T. In cases of profiles leading to oceanic basins where the gravity anomalies are positive the transition becomes gradual. A detailed investigation of all the shelf-profiles will be given in the final report of the gravity expeditions at sea to be published in the next year by the Netherlands Geodetic Commission. The writer may give here two examples in fig. 1 and 2. Fig. 1

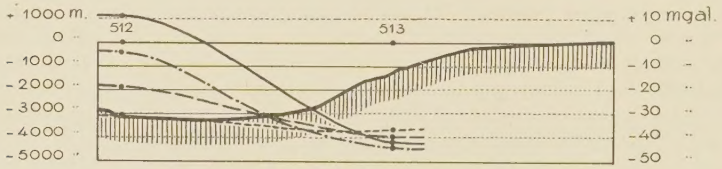

Fig. 1. Shelf-profile SE of Canary Is., horiz. scale 1 : 3000000, vertic. scale 1 : 300000.

is a gravity profile at the west-coast of Africa to the south-east of the Canary-islands and fig. 2 one at the south-coast of Africa south of Humansdorp. In both profiles the

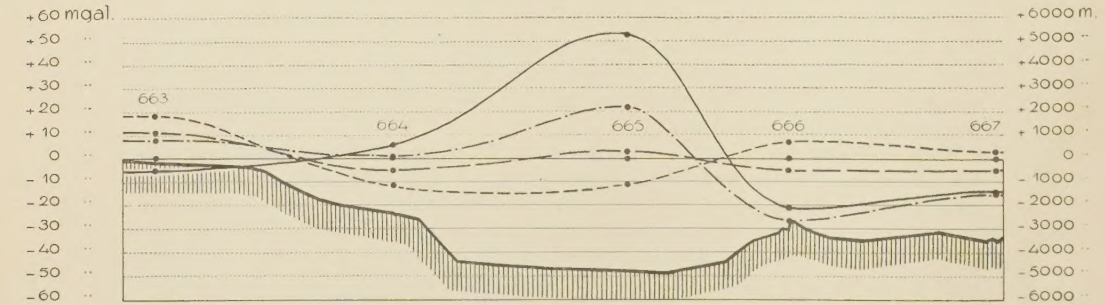

Fig. 2. Shelf-profile S of Humansdorp (S. Africa), horiz. scale 1 : 3000000, vertic. scale 1 : 300000.

dotted line represents the anomalies for $T = 20$ and $R = 0$, the broken line for $T = 30$ km and $R = 0$, the point-dot line for $T = 30$ km and $R = 116.2$ km and the drawn line for $T = 30$ km and $R = 232.4$ km. Fig. 1 shows a case where local compensation for

$T = 20$ km fits best the observed anomalies and fig. 2 one where local compensation combined with a value of T of 30 km meets them best. In the last case the depth-profile is more complicated than for the normal shelf-profile of which fig. 1 is a good example. The drawn curves of both profiles show the sudden increase to positive anomalies at the edge of the shelf in case the gravity results are isostatically reduced for large values of R; the old reductions according to the HAYFORD system, the AIRY–HEISKANEN system with a value of T of 40 km or the old regional system with a large degree of regionality all gave curves similar to these drawn curves.

Several shelf-profiles show more complicated curves than those of the figures given here. Obviously other features are present there besides the main shelf-effect. In most of the cases we can nevertheless determine or at least surmise which reduction best fits the shelf-effect. A method to eliminate more or less the other features without making a detailed study of them is to take the mean of a great number of profiles; the different irregularities of the individual profiles thus merge in the common shelf-effect. For getting a representative figure for this purpose for each profile, we can take the difference of the anomaly of the station at the continental side and of that at the oceanic side of the profile, eventually of mean values of the anomalies of more stations at each of those places. In this way the stations halfway the shelf are left out of account. Taking the mean of the resulting figures for all the 26 available profiles we thus get the following figures for the different sets of anomalies; the mean elevations of the stations at both ends of the profiles are given in the last columns.

Mean shelf difference for all the profiles in mgal.

$R =$	0	29.05 km	58.1 km	116.2 km	174.3 km	232.4 km	Depth shelf	Depth ocean
$T = 30$ km	− 5	− 2	+ 1	+12	+25	+38	230 m	4340 m
$T = 20$ km	−24	−21	−15	+ 1	+16	+33	230 m	4340 m

We see that our conclusion is confirmed [1]; the difference between the shelf and the ocean anomalies disappears for $T = 30$ km and for small regionality of the compensation. This is likewise the case for $T = 20$ km and somewhat larger regionality but even for this small crustal thickness the regionality is less than for many mountain features in the continents and less also than for the oceanic islands of volcanic origin that have been investigated, i.e. the Hawaii archipelago, Madeira [2], St. Vincent (Cape Verde Is.), Fayal, St. Miguel and Bermudas.

We may, therefore, conclude that the crust becomes rather suddenly much thinner at the edge of the continents or, to put it more accurately, those layers of the rigid crust which have less density than the substratum or at least less than the deeper layer. The boundary between these layers does not necessarily coincide with the boundary between rigid and plastic material. Adopting the above-mentioned densities of 2.67 and 3.27 for these layers and 1.027 for sea-water, indicating the sea-depth by d and assuming the shelf to have zero depth, the amount of this decrease of thickness of the upper layer is

$$\left(1 + \frac{2.67 - 1.027}{0.6}\right) d = 3.73\, d.$$

[1] The detailed study of the profiles gives a slightly smaller estimate for the best suited value of T.

[2] VENING MEINESZ, F. A., Gravity over the Hawaiian archipelago and over the Madeira area; conclusions about the Earth's crust, Proc. Ned. Akad. v. Wetensch., Amsterdam, **44**, 1 (1941).

For values of d of 4000—5000 meter this corresponds to 15—19 km. It is difficult to see the cause of this great irregularity in the Earth's crust and in fact this problem is the old problem of the origin of the continents and oceans at the Earth's surface. The above-mentioned results give a slight contribution to the nature of the zone of transition between the continental and oceanic parts of the crust; it tends to the supposition that this transition is rather sudden.

Further light on this problem is shed by the seismic results, which we may shortly recall here. The evidence about crustal structure given by near earthquakes is generally interpreted as pointing to the continental crust consisting of at least two principal layers, an upper layer usually called the granitic layer of about 15 km thickness and a lower layer of about the same thickness generally assumed to be basaltic; on top of the granitic layer we may have a sedimentary layer. In a critical discussion of all the European data JEFFREYS in 1937 [1]) found a thickness of 17 km for the granitic layer and of 9 km for the basaltic or intermediate layer as he calls it. In southern California GUTENBERG [2]) found four crustal layers from top to bottom of 14, 11, 6 and 8 km thickness; in northern California BYERLY and WILSON [3]) obtained three of 13, 12 and 6 km. In both cases the top layer is probably the granitic one. For the oceans no near earthquake data are in general available.

About the thinning of the crustal layers near the shelf as it has been deduced from the gravity results, we may make several suppositions. We can assume all the layers of the crust to become in the same proportion thinner but we can also suppose only the upper one to do so or at least this layer to be the main one responsible for it. The rather sudden character of the change is a slight indication in the latter sense [4]). As the thickness of the upper layer, according to the seismic results, is about the same as the amount of thinning, this supposition would mean that this layer would entirely or nearly disappear at the edge of the shelf. This hypothesis is corroborated by further seismic evidence. In fact most seismologists agree to suppose that the granitic layer is absent in the central Pacific area and that it is thin or also lacking in the deepest parts of the other oceans. This result has been derived from two sources connected with the study of distant earthquakes. In the first place the velocity of the surface waves of short period through the Pacific is considerably larger than through the continents while those of long period show less difference; this effect is given by the Love waves as well as the Rayleigh waves. In the other oceans we find results for the velocities of these waves between those for the Pacific and for the continents. These results point to a surface layer of lower velocity and probably, therefore, of lower density being present in the continents, absent or very thin in the Pacific and thin in the other oceans, or we may assume two layers of the same kind being absent or thin in the Pacific and one of them absent or thin in the other oceans. GUTENBERG favours the hypothesis that the crustal layers of the continents are entirely absent in the central Pacific [5]) while BYERLY [6])

---

[1]) JEFFREYS, H., The structure of the Earth down to the 20° discontinuity. M.N.R.A.S. Geophys. Suppl.; **3**, 401—422 (1936); **4**, 13—39 (1937).

[2]) GUTENBERG, B., Travel-time curves at small distances and wave-velocities in southern California. Gerl. Beitr. Geophysik, **35**, 6—45 (1932).

[3]) BYERLY, P. and WILSON, J. T., The central California earthquakes of May 16, 1933, and June 1, 1934. Seismol. Soc. America, Bull., **25**, 223—246 (1935).

[4]) The seismic results found by EWING at the east-coast of the U.S. and by BULLARD at the end of the Channel seem to point in a contrary direction for these coasts. The writer will come back to these results in the coming detailed report.

[5]) GUTENBERG, B. and RICHTER, C. F., Bearbeitung von Aufzeichnungen einiger Weltbeben, Senckenberg, naturf. Ges. Abh., **40**, 57 (1925).

[6]) BYERLY, P., The dispersion of seismic waves of the Love type and the thickness of the surface layer of the Earth under the Pacific. Gerl. Beitr. Geophysik, **26**, 156—157 (1930).

advocates the alternative explanation of a deeper layer of the continental series to be still present there. The writer is inclined to the latter assumption because otherwise it appears difficult to him to explain the isostatic equilibrium of the Hawaii archipelago and other islands in this ocean. As there is no evidence of any sinking back of these islands we must suppose this equilibrium to be realized and so we need deficiencies of mass lower down for compensating them. For the Hawaiian islands at least we can not easily explain these deficiencies by the blowing out of mass during the volcanic eruptions that gave rise to these islands [1]) because the horizontal spreading out over large areas of these compensating masses as it has been stated by means of the gravity results, could not well be understood in this way. An explanation by regional compensation according to the AIRY system appears to the writer [2]) to be the only acceptable one. But this implies the presence of a crustal layer of smaller density than the plastic substratum and so the writer is inclined to assume at least one such layer to be present in the Pacific area.

Another argument for the absence of the granitic layer in this area is given by GUTENBERG and RICHTER [3]). By studying the amplitudes of the reflected longitudinal waves (*PP*, *PPP*, etc.) they have found that waves of this kind reflected in the central Pacific area and in part of the Arctic basin had smaller amplitudes than those reflected in the continents and in the other oceans and they have ingeniously explained this phenomenon by remarking that the angle of incidence of the wave at the reflecting surface must be larger when no surface layer is present. The writer has not studied this matter but he should wish to venture that the explanation seems to him also to hold true when the number of crustal layers is smaller under the Pacific than elsewhere. As far as the waves having undergone reflections in the other oceans are concerned, it might be possible that they have reflected in parts where remnants of the granitic layer must be admitted or we might suppose, in case we should have to assume no granitic layer at that place, that one layer more than in the Pacific is present there, causing a smaller angle of incidence, although it must be assumed to be larger than in the continents.

Resuming our subject after this short transgression into seismology, it appears to the writer that the most probable explanation of the present seismic and gravimetric data concerning the problem of the presence of oceans and continents at the Earth's surface is to assume the granitic layer only to be present in great thickness in the continents and to end rather suddenly at the edge of the shelf or, if present in some parts of the oceans, to be thin there. The next layer seems to continue under the oceans, perhaps somewhat thinner under the deepest parts of the Atlantic and Indian oceans and certainly thinner under the central part of the Pacific east of the andesite line; it may even be absent in this last area but in this case we must assume a still deeper crustal layer to be present there of a smaller density than the layer below it. The principal part of the gravimetric shelf-profiles as well as of the seismic data could thus be explained.

---

[1]) This explanation was tentatively offered to the writer by Dr. VAN WATERSCHOOT VAN DER GRACHT.

[2]) VENING MEINESZ, F. A., Gravity over the Hawaiian archipelago and over the Madeira area; conclusions about the Earth's crust, Proc. Ned. Akad. v. Wetensch., Amsterdam, **44**, 1 (1941).

[3]) GUTENBERG, B. and RICHTER, C. F., On seismic waves (2nd paper). Gerl. Beitr. Geophysik, **45**, 280—360 (1935).

Physics. — *Cosmic Ray Showers.* By J. CLAY.

(Communicated at the meeting of September 27, 1941.)

Summary.

A summary is given of a number of experiments concerning showers. Especially a comparison is made between the divergence and the penetrating power of showers with small spreading in the first maximum (1,5 cm Pb) and the second maximum (25 cm Pb). The spreading is greater in the second case and the hardness is less. The proportion of the maxima moves between 4 and 3.

Next a distinction is made between the occurring hard showers (of mesons) and shoft showers (electrons) and mixed showers, under thick layers of different matter: air, water, aluminium, iron and lead. The variation with the electron density is determined. The number decreases with increasing atomic number.

The meson showers have greater spreading than the electron showers.

§ 1. When cosmic rays pass through matter bundles of rays (showers) occur, which are formed in consequence of the interaction of the rays and the field of the atomic nuclei. The process of multiplication is such, that in consequence of the reactions the charged corpuscle throws off part of the energy in the form of a photon and this photon loses its energy in forming pairs of electrons, one with a positive, one with a negative charge. Thus arises a multiplication. This process has been treated by many authors, but now BRUINS (1) has succeeded in accounting for it quantitatively. He has been able to describe the process that occurs in the higher layers of the atmosphere and from the phenomena he has estimated the energy distribution of the original spectrum of the incident particles, *which proves to be mostly identical* to the spectrum which has been measured of the mesons in the atmosphere.

§ 2. However in thin layers of matter — where the process was originally found — it is more complicated, because the loss of energy of the particles through ionization is a factor not to be neglected. The theory of it has also been indicated by him in principle but it has not yet been worked out quantitatively.

On measuring *showers* in thin layers of matter there is a difference in relation to the geometrical proportion of the experiment; in the first place how many shower particles are counted and at what distance from the dispersing matter the counters are placed.

In the past year these circumstances have been carefully studied in this laboratory (2). The results have shown in how far the numbers found can be made independent of the geometry of the measuring apparatures.

In thin layers the production is proportional to the square of the atomic number. But the location and the height of the maximum of showers of varying number can only now be tested with the help of the theory of BRUINS.

§ 3. There was however another problem to which we have given our special attention.

When the number of the showers formed under thick layers is examined, it is seen that there must be a second process of a different nature. There is namely a second maximum, indicating that there must be a corresponding multiplication phenomenon, but of particles of more penetrating power. For some time it had been suspected that this must be meson showers. So far, the phenomena found by different investigators, were greatly contradictory (3).

The second maximum, first found by ACKEMAN and HUMMEL (4) under lead, lies at about 16 cm and was also found by us in an earlier investigation under iron at about 26 cm. This was not at all confirmed by some investigators, while under some circumstances others found it, being so evident as to exceed even the first (6).

First of all we determined by three different methods that this maximum and a third maximum certainly exist (7).

Secondly, however, these maxima proved always to be much lower than the first in the proportion of 3 to 4 times. But an even greater difference may be noted. The second maximum, which according to BOTHE and SCHMEISER (6) consists of more penetrating rays, was thought to have less divergence than the showers of soft rays (electrons). In a systematic investigation, carried on for a considerable time, we found the opposite result.

In this investigation we made an arrangement as shown in Figure 1. Four counters of 1 cm diameter are connected parallel, close under a layer of lead A, successively

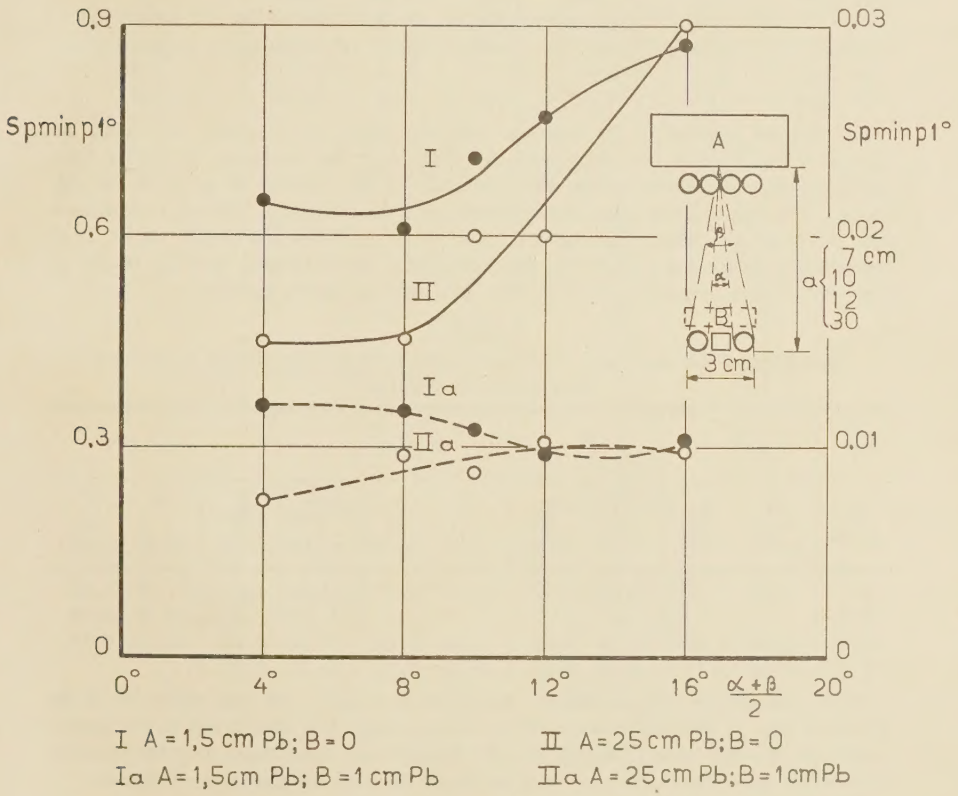

Fig. 1. Showers under 1.5 cm Pb, I and Ia under 25 cm Pb, II and IIa in dependence on their angle of devergence.

1,5 and 25 cm thick. Under it at a distance *a* there are two counters of 1 cm, separated by 1 cm Pb. The distance *a* was varied from 30 to 7,5 cm and thereby the angle of rays from the scattering lead was varied from 2°—6° to 8°—26°. Above the lowest counters layers of lead were placed, varying from 0,5 to 2 cm Pb, in order to measure the absorption of the shower rays. Because the opening becomes larger as the distance is smaller, the numbers were divided by the value of the opening angle and in that way comparable figures were found for different spreading. For 1,5 cm Pb above the counters the figures are given in column 4, the same for a layer of 25 cm Pb in column 7. All observations were continued until at least 150 showers had been observed, so that the uncertainty was no more than 8 %.

TABLE I.

Showers under thin lead, $A_1 = 1.5$ cm Pb and thick lead, $A_2 = 25$ cm Pb at different angles of divergence.

Divergence			$A_1 = 1.5$ cm Pb		$A_2 = 25$ cm Pb		$\frac{S_{A_1}}{S_{A_2}}$
α	β	$\frac{\alpha+\beta}{2}$	S/min	S/min/1°	S/min	S/min/1°	$\frac{\text{max 1.5 cm Pb}}{\text{max 25 cm Pb}}$
2°	6°	4°	0.256	0.065	0.062	0.015	4.1
4°	12°	8°	0.49	0.061	0.12	0.015	4.0
5°	15°	10°	0.72	0.072	0.22	0.020	3.6
6°	18°	12°	0.93	0.077	0.24	0.020	3.9
8°	26°	17°	1.51	0.086	0.54	0.030	3.0

The relative increase of the numbers with the angle of divergence are found in columns 5 and 8. It is seen that under the thick layer the divergence is greater than under the thin one, while further the proportion of the numbers is given in the 8th column. It is seen that this proportion decreases with the divergence. This is in accordance with our experience that the second maximum works out better for greater angles. It is contradictory to the result of BOTHE and SCHMEISER, but in keeping with the results of other investigators, especially TRUMPY (8), and with our results given in § 7.

TABLE II.

Absorption of showers under a thin and under a thick layer of lead at different divergences of the rays.

$\frac{\alpha+\beta}{2}$	4°		8°		10°		12°		17°	
B cm Pb	A 1.5 cm Pb	A 25 cm Pb	A 1.5 cm Pb	A 25 cm Pb	A 1.5 cm Pb	A 25 cm Pb	A 1.5 cm Pb	A 25 cm Pb	A 1.5 cm Pb	A 25 cm Pb
0	1.00	1.00	1.00	1.00	1.00	1.00	1.00	1.00	1.00	1.00
0.5									0.50	0.44
1.0	0.56	0.50	0.58	0.64	0.44	0.45	0.38	0.52	0.35	0.33
2.0	0.24	0.37	0.32	0.29	0.22	0.25	0.22	0.29		

Under a thin layer (1,5 cm Pb) the divergence is therefore less than under 25 cm Pb (Table I, Fig. 1) and the hardness of the showers under the thick layers is not greater than under the thin layer (Table II, Fig. 1). TRUMPY (8) found lately that the hardness is even less under the thick layers and we found the same for a greater divergence.

This is clear from Table II and Fig. 1.

§ 4. In order, however, to distinguish between softer electron showers and hard meson showers, a separate investigation was made, in which four-fold coincidences were measured, but in such a way that the counters were placed two by two above each other, 10 cm, sometimes 15 cm Pb being inserted between them, Fig. 2 a. The experiments were made with four counter boxes of 3 counters, parallel to each other with sensitive area of 840 cm^2.

In this way 3 different cases could be distinguished. If between the two pairs of counters 10 cm Pb (B_1 and B_2) are inserted, it is certain that the two parts necessary for a four-fold coincidence must both have been mesons, for already at 5 cm Pb 10^{11} eVolts is needed, according to HEITLER's theory, and if the energy increases in the same way for the penetration of thicker layers, we arrive at values which do not occur for electrons on the surface of the earth.

TABLE III.

Absorption of soft and of hard shower particles under different kinds of matter in 100 min area 840 cm².

B_1 en B_2	0;0	0;1	0;2	0;3	0;4	0;5	0;10
Open	57	40	40	28	30	28	22
70 cm water	70	51	50	46			30
28 cm aluminium	59	44	39	41			23
33 cm iron	31	24	25	23	19		17.5
15 cm lead	33	25	21				15

By leaving the thickness of lead B_1 10 cm between one pair, and then stating the decrease which arises when the absorption layer between the other counters is varied

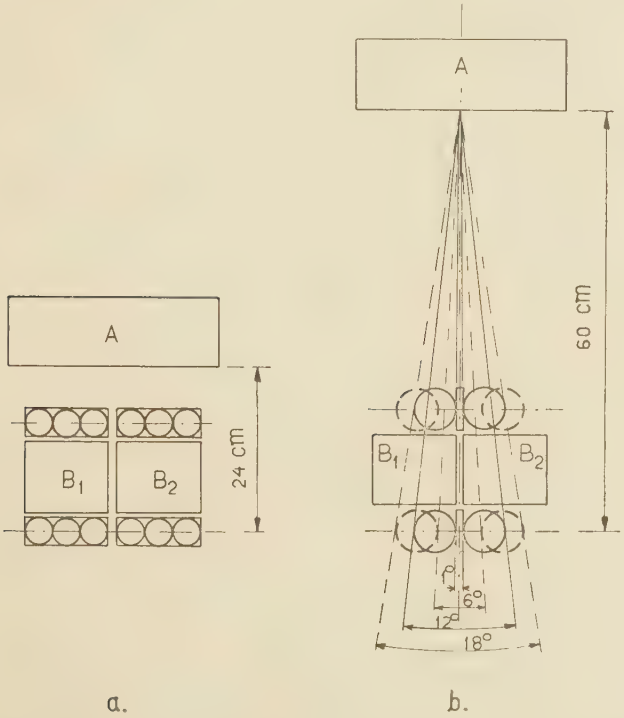

a. b.

Fig. 2. Arrangement of the counters in order to distinguish between electron and meson showers.

a. Four-fold coincidences in 4 boxes each of 3 counters, each of 6 cm diameter and 47 cm long and afterwards 3 counters each 30 cm long and 4 cm diameter.

b. Four-fold coincidences in four counters each 47 cm long and 6 cm diameter in two positions.

from 5 to 15 cm, we finally obtain the absorption of the meson particles in the showers. This is given in Fig. 3 and Table IV. The number is seen to have decreased very little.

When one takes B_1 10 cm Pb, varying B from 0 to 5 cm the absorption is seen to be much greater. The additional showers which are obtained are showers in which one particle must be a meson, but in which the other is most probably an electron. Vide Table V.

TABLE IV.

B_1 and B_2	10; 0	10; 1	10; 2	10; 3	10; 4	10; 5	10; 10	10; 15
Open	22	18	15	13		11	10	7.3
Water	30	24	21			16	12	12.6
Aluminium	27	22	20	20		14	9.1	
Iron	17.5	13	13			10	9	
Lead	15	13				11	8.8	6.4

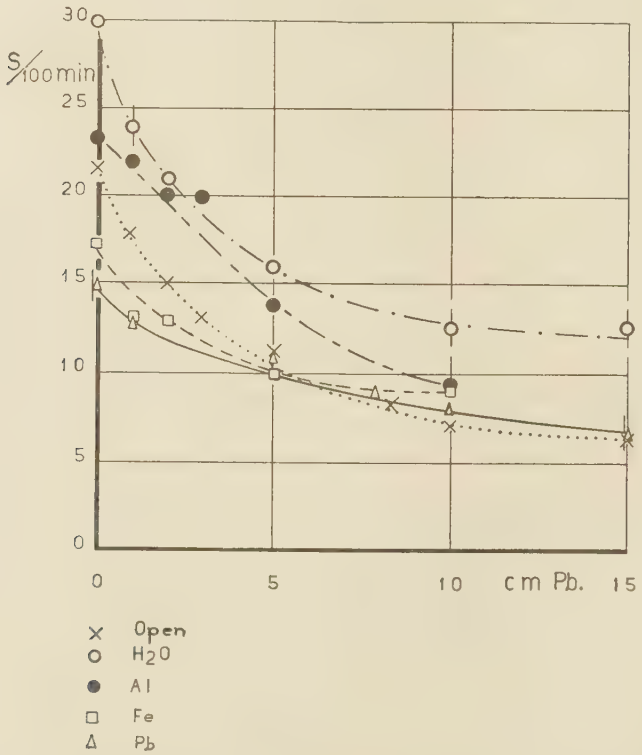

Fig. 3. Decrease of meson showers and mixed showers under air, water, Al, Fe, Pb by absorption in lead from 0—5 and from 5—15 cm. The uncertainty is given for 4 values, but for all the values it is less than 8 %.

TABLE V.

Decrease of soft showers and mixed showers by 1 cm Pb, number in 100 min.

	0; 0—10; 0	0; 1—10; 0	$\frac{0;\,1—10;\,0}{0;\,0—10;\,0}$	0; 10—10; 10	1; 10—10; 10	$\frac{1;\,10—10;\,10}{0;\,10—10;\,10}$
Open	35	18	0.52	12	8	0.67
Water	40	21	0.52	18	12	0.67
Aluminium	36	21	0.58	22	13	0.59
Iron	13.5	6.5	0.48	8.5	4	0.50
Lead	18	10	0.55	6.2	4.2	0.68

These are processes in which the meson throws off an electron from the atomic connection, the processes in which the secondary electron rays are formed. These processes have been observed under thick layers of different material, water, aluminium, iron and lead, in order to attain the condition of saturation (Fig. 4).

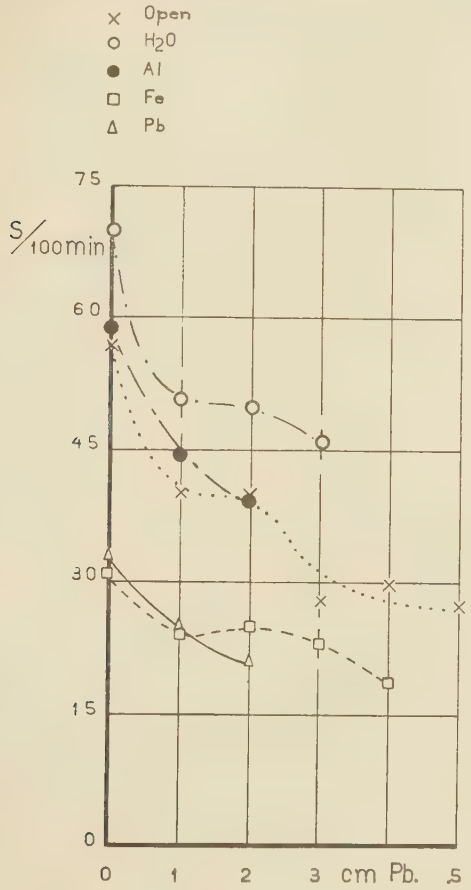

Fig. 4. Decrease of electron showers under thick layers of air, H_2O, Al, Fe and Pb in lead from 0 to 5 cm.

That there are here electrons is apparent from the fact that the decrease by 1 cm Pb (B_2) is of the same value, being only little less than that in soft showers. This is seen from the figures in Table V, where in column 2 the soft showers found are given and in column 3 the cases in which 1 cm Pb is placed in one of the two ways which must be taken by the showers particle; column 4 shows the percentage of the showers left after absorption by 1 cm Pb.

The same is given for the mixed showers in columns 5, 6 and 7. From this it is clear that in this case the remaining particle is not a meson but an electron, although the average energy is a little greater than in the first case.

So in this case we are confronted by à coincidence, in which there is certainly one meson and certainly one electron. A number of such cases is known from WILSON-chamber photographs, namely that an electron rich in energy is produced by a meson (9). When further we deduce the number of coincidences found with $B_1 = 10$ and $B_2 = 0$ from the

number with $B_1 = 0$ and $B_2 = 0$, there is left the number of showers consisting of soft rays i.e. electrons. The decrease of the number in both cases is given in Table V, fig. 4.

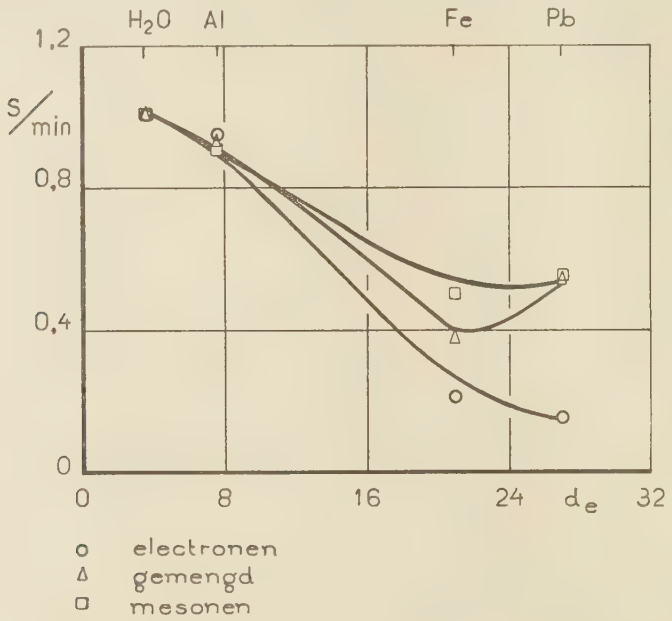

Fig. 5. Decrease of electron showers, mixed showers and meson showers with decrease of the electron density of the material: water, Al, Fe, and Pb.

§ 5. The measurements were all taken under thick layers of different matter. We see that the number of showers under thick layers decreased with the electron density and here we have the same phenomenon as when we measured the number of secondary rays (electrons) with regard to the number of mesons by which they are produced (10). The production is, indeed, proportional to the electron density, but the absorption in the material itself is proportional to the square of the atomic number and consequently, in condition of saturation under thick layers, the number of showers under the material will decrease in proportion to the atomic number.

The number of coincidences found, in which at least one meson and one electron are combined, is less rapid with the electron density of the dispersing material. Here is, however, an irregularity, namely that with lead the number is greater than with iron and this irregularity was tested several times and therefore seems to be real.

TABLE VI.

Number of showers observed under different layers with different absorbing layers, per 100 min, area 360 cm².

	B_1 B_2 0 0	B_1 B_2 0 10	B_1 B_2 5 10	B_1 B_2 10 10
Air	29	16	8.8	4.5
70 cm H_2O	60	22	10	6.9
28 cm Al	56	20	10	6.2
33 cm Fe	17	9	4.9	3.5
15 cm Pb	18	12	6.1	3.8

In order, however, to measure this with certainty a measurement was repeated with another set of four glass counters, this time in quicker succession, the different layers of material being exchanged in order to prevent insufficient constancy of the circumstances during the continued measurements necessary for the absorption. The sensitive area of these counters was 360 cm². It was seen that in the proportion of the hard meson showers the number had decreased approximately in the same proportion as the sensitive area, the proportion for the narrower areas being more favourable for the soft electron showers. This means that in the meson showers there is greater divergence than in the electron showers. This was confirmed in a further investigation, which will be described lower. The figures found are given in Table VI and these values were obtained from a number which was always greater than 150, so that the uncertainty was less than 8 %. The values of table VII were deduced from these data and figures were found for Al, Fe,

TABLE VII.

Number of electron showers (S), combined showers (S & H) and meson showers (H) under different layers of matter of great thickness.

	S		H&S		H		$\frac{S}{H}$	$\frac{H\&S}{P}$
Air	0.13		0.115		0.045		4	2.5
70 cm H_2O	0.38	100	0.15	100	0.069	100	5.5	2.2
28 cm Al	0.36	95	0.138	92	0.062	90	6	2.3
33 cm Fe	0.08	21	0.055	37	0.035	50	2.3	1.6
15 cm Pb	0.06	16	0.082	54	0.038	55	1.6	2.2

and Pb with regard to water. From them is seen the decrease, as the electron density in the material in which they are produced, increases.

§ 6. In figure 6 a separate series of figures is given under iron of varying thickness, in order to state the influence of the thickness of the producing layer of iron. It is seen that the number decreases to a greater extent with the thickness than would agree with the decrease of the entering mesons, except that with the greater thickness there is an irregularity which appears to be greater than only the uncertainty of the observations

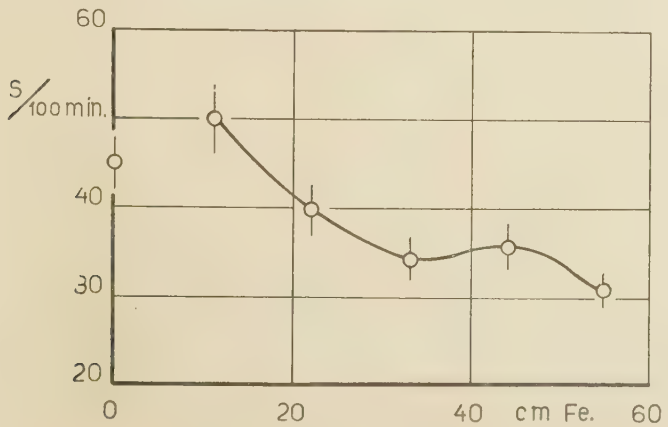

Fig. 6. Meson showers under thick layers of iron.

§ 7. In order to investigate the spreading of the two species of showers an arrangement was made as shown in fig. 2b. We measured under 70 cm of water, the number was determined when the counters were only separated by 1 cm Pb, and secondly when placed at a distance of 6 cm. The results of the two series of measurements for soft and for hard showers given in table VIII clearly show that the divergence of the meson

TABLE VIII.

Comparison of the divergence of electron and meson showers.

	min.	number	S/min.	
Electron showers (no lead between the counters).				
1°—12°	1841	975	0.53	1.00
6°—18°	1362	499	0.37	0.70
For hard showers (10 cm lead between the counters).				
1°—12°	2757	187	0.068	1.00
6°—18°	7593	407	0.055	0.80

showers is greater than of electron showers. This might be expected on the ground of the theory, but after BOTHE and SCHMEISER thought they had found the reverse, WENTZEL (11) investigated what modification must perhaps be made in order to bring the theory in agreement with the phenomena. Therefore it does not seem necessary to insist in this modification.

We will not, as some authors have done, from the decrease of the number of particles with the thickness of the absorbing layer, determine an absorption coefficient with the aid of an exponential absorption formula (12). When one knows the loss of energy of the particles in dependence on the energy, the spectral energy distribution of the entering particles may be deduced from the decrease of the number in layers of increasing thickness (9). This is easy in the case of heavy particles because the loss of energy varies very little with the energy. In the case of known formulas which have been tested in experiment, one should take into consideration the dependence of electrons on energy. For the soft primary rays produced by mesons the distribution is seen not to be exponential, but a proportional to E^{-n}, the value of n but little differing from 1 (10). It will only be possible to make a rough estimate in the case of the small number of shower particles, which can be measured.

In any case, however, it will only be possible to find the decrease of the electrons and the mesons together in thin layers of lead or iron and that of mesons only in thick layers.

REFERENCES.

1. E. M. BRUINS, Physica, **8**, ✳ (1941).
2. J. CLAY and K. H. J. JONKER, Physica, **7**, 94 (1940).
3. Literature showers, R. STEINMAURER, Erg. d. Kosmischen Physik III (1938).
   D. K. FROMAN and J. C. STEARNS, Rev. Mod. Phys., **10**, 138 (1939).
   W. BOTHE, Rev. Mod. Phys., **11**, 303 (1939).
   W. M. NIELSEN and J. E. MORGAN, Rev. Mod. Phys., **11**, 287 (1939).
4. M. ACKEMANN, Z. f. Phys., **32**, 161 (1938).
5. J. CLAY, A. v. GEMERT, J. T. WIERSMA, Physica, **3**, 627 (1936).
6. K. SCHMEISER and W. BOTHE, Ann. d. Phys., **32**, 161 (1938).
7. J. CLAY, A. VENEMA and K. H. J. JONKER, Physica, **7**, 637 (1940).
8. B. TRUMPY, Bergens Museum Årbok (1939).
9. L. LEPRINCE-RINGUET and J. CRUSSARD, J. d. Physique (7), **8**, 207 (1937).
10. J. CLAY, Proc. Ned. Akad. v. Wetensch., Amsterdam, **43**, 1260 (1940).
11. G. WENTZEL, Phys. Rev., **54**, 869 (1938).
12. A. EHMERT, Z. f. Physik, **113**, 234 (1939).

Botany. — *The shape of cells in homogeneous plant tissues.* II. G. VAN ITERSON Jr and A. D. J. MEEUSE.

(Communicated at the meeting of September 27, 1941.)

4. *Suppositions, concerning physical causes of the formation of the cubo-octahedral cellform.*

We have communicated that as early as 1807 MIRBEL suggested that the cells assume their polygonal shape, owing to the fact that originally they are round bodies, flattening each other during their growth.

The idea to connect the form of the cells with the shape which plastic spheres assume, when assemblages of them are compressed through pressure on all sides, or when assemblages of inflatable spherical bodies are freed from their interstices by inflation in an enclosed space, has also been discussed by later investigators.

We shall first discuss the theoretical side of the problem.

When the faces with which the spheres on compression from all sides of the assemblages, or on inflation in an enclosed space, touch and flatten each other, cannot slide over each other, the form of the resulting bodies will be entirely determined by the method of stacking. An assemblage of equal spheres wherein the spheres are placed in the corners of a cubic partitioning of space will produce cubes, and an arrangement according to the closest packing of equal spheres produces rhombic dodecahedrons or extended rhombic dodecahedrons (depending on the position of the spheres in the successive plane layers of the stack) [1]). The way how to pack equal spheres in order to produce on compression orthic tetrakaidecahedrons was calculated for LEWIS by Prof. WILLIAM C. GRAUSTEIN (11); the spheres in the separate plane layers must be placed in squares, but with interstices between the neighouring spheres equal to 0.31 $\times$ the radius, the spheres of a superior layer must rest on four spheres of a lower layer.

Experimentally the proof of the correctness of these considerations cannot easily be furnished. It is difficult to cause uniform pressure on all sides of an assemblage of spheres and it is not easy to find bodies inflating

[1]) As early as 1897 W. BARLOW (A mechanical cause of homogenuity of structure and symmetry geometrically investigated, etc., Scient. Proc. Roy. Dublin Soc. 8, 527—540 (1893—1898)) pointed out the circumstance that an assemblage of equal spheres in closest packing may be constructed in different ways, the centres of the spheres forming point systems with different symmetries. B. G. ESCHER (Over de regulaire en hexagonale dichtste bolstapelingen en de deformatie hunner bollen tot dodecaëders tengevolge van compactie, these Proceedings **43**, 1302—1310 (1940)) lately discussed the bodies which are formed on allsided compression of such arrangements until there is no space left between the spheres. Such bodies are rhombic dodecahedrons and extended rhombic dodecahedrons (for the latter see Fig. 1d in the first part of this communication).

equally in all spatial directions. Some investigators have caused peas to swell in an enclosed space, in imitation of a famous experiment by G. L. L. DE BUFFON (2). One of those who tried this was R. GANE (6) but he was not successful, neither with globes of dough, which he caused to expand by fermentation. F. T. LEWIS (20) informs us that after an experiment with peas, which were made to swell in a brass cylinder, he found an average number of 12.13 faces on 200 peas, and in another experiment with 400 peas the average was 12.14 faces. When he considered that some faces were bounded by intercellular spaces he came to the occurrence of averagely 12 contact faces for one pea with other peas. This result was to be expected if the peas were indeed placed after a closest-packing-arrangement. Yet — for reasons which will be given later — LEWIS calls this experiment "unfortunate".

Some investigators have compressed stacks of equal spheres of plastic material unilaterally. GANE (6) used for this purpose spheres of plasticin, which he rubbed with talc powder and compressed in a cylindrical tumbler, in which he first shook them gently. Here bodies were obtained with lateral faces the number of which varied between 12 and 14. Yet we cannot attach great value to GANE's experiments, seeing that he also compressed equal plastic globes packed as closely as possible in a rectangular space in which experiment he did not get rhombic dodecahedrons, but bodies approaching the orthic tetrakaidecahedron. We have repeatedly made the same experiments and we did get rhombic dodecahedrons or extended rhombic dodecahedrons. On unilateral compressure of equal spheres these bodies naturally did not possess edges of uniform length, but on compression of ellipsoid bodies the resulting bodies had this property. The main fact is that from different stacks of equal spheres bodies with perfectly flat lateral faces and with straight edges are obtained and further it is of importance that on the resulting bodies right and acute angles may be observed and that each body may show more than 3 edges meeting in the same vertex. In the compressed plastic matter these figurations are perfectly stable.

These details exclude the explanation of the tetrakaidecahedral cell form *with curved edges and curved faces* as a result of compressure of originally spherical cells in closest packing and even in a packing after GRAUSTEIN.

A short time ago J. W. MARVIN made some very careful experiments concerning the compression of lead shot in cylinders. A provisional communication (22) appeared in 1937 and this is the treatise which confused LEWIS, making him attribute his own observations of swollen peas to an unfortunate experiment. MARVIN found an average number of lateral faces of 14.17 in shot which had been placed arbitrarily in a cylinder and had been compressed in it in such a way that all intervening space had disappeared, the shot located peripherally in the cylinder being omitted on counting the faces. This figure strikingly approaches the average value which LEWIS found for the number of lateral faces of the cells of elder

pith, and led him to doubt whether shot in the closest packing produces rhombic dodecahedrons on compression.

Since then, in 1939, MARVIN (24) made detailed communications about his experiments. Among others he gives pictures of the result of shot compressed when packed in the closest way, rightly mentioning that in that case rhombic dodecahedrons are obtained. Further he investigated statistically the frequency distribution of the various lateral faces of compressed shot which had been poured into the cylinder without any precautionary measures. There is no doubt that the deviations from the rhombic dodecahedron in the latter case are to be ascribed to the fortuitous arrangement of the shot in this case. It should be borne in mind that even if the bottom layer was placed in such a way that each sphere touched 6 neighbours the arrangement of the shot in the next layers generally would not be the closest possible, as for that purpose the shot of the second layer should fall in *fixed* hollows of the first layer (these hollows are determined as soon as one of the shot of the secund layer has found a place in one of the hollows of the bottom layer). The compressure of spheres in a fortuitous arrangement never can lead to a *homogeneous* assemblage. So in our opinion the agreement of the average number of the lateral faces of compressed shot in these experiments with the average number of the lateral faces of cells in *homogeneous* plant tissues is of no account.

Therefore I shall not discuss the certainly interesting experiments of E. B. MATZKE (25) who compressed mixtures of large and small shot in different proportions until the air in between had disappeared. It will be clear that averagely there were produced more lateral faces on the large shot than on the small.

After what has been said above about the occurrence of tetragonal faces in cells in uniform tissues with sides curved outwards, and about the occurrence of corresponding faces in bodies of membranes of a solution of soap in a homogeneous soap-froth, one might be inclined to consider the shape of the cell as the result of the action of surface tension.

It would be superfluous to recall the fact that there has been a time when surface tension was indeed connected with the position of cell walls with respect to each other. L. ERRERA (4) and afterwards his collaborator E. DE WILDEMAN *compared* the perpendicular position of newly formed cell walls on those present before, and the cell structure of mature tissues with respectively the position of membranes of a soap solution against a moist solid wall and the position of membranes in soap-froth. Meanwhile the conception that in juvenile as well as in mature tissues the surface tension is the *causal force* of the arrangement of the cell walls, has been wrongly ascribed to ERRERA. As a matter of fact the investigator referred the botanist NOLL to an experiment of MACH, when at a congress at Wiesbaden — where ERRERA read a paper on this subject — NOLL remarked that from their origin cell walls should be considered as a solid and not as a liquid matter. From MACH's experiment, which will be discussed

later, it appears that stretched rubber membranes — which are solid — may behave to a certain extent like membranes of a liquid. Yet ERRERA is himself guilty that people had a wrong impression of his conceptions, for in some of his publications he did not avoid the suggestion that the surface tension plays a part at least in determining the position of juvenile cell walls. This can be made clear from the following quotation, which will be of interest in our subsequent considerations. "In mature plant tissues the passive tension of the cell wall through turgor replaces active surface tension. Grouping according to angles of 120° is therefore maintained, or is even reached owing to later shiftings in cases where originally angles of 90° occurred!"

G. BERTHOLD (1) formulated the difference between the arrangement of juvenile cell walls and that of walls in older cell tissues thus that during the development each cell wall tries to become "a plane of *minimal area*" and that in mature tissues the "assemblage of cell walls in its entirety" tries to fulfil the requirements of the principle of the minimal area. For that latter purpose, he thinks, "the cells will later slide over each other and be deformed". BERTHOLD is very certain in his opinion that even the juvenile cell wall should not be considered as a liquid lamella and he tries to account for the perpendicular location of the young wall on the older ones by a tendency to equal division of space of the mother cell over the daughter cells.

It is well-known that in his book mentioned before D'ARCY W. THOMPSON enumerated instances in which the location of the cell walls according to BERTHOLD's principles may be observed. From the recent studies of R. SOUÈGES (30) on the development of vegetable embryos other instances may be taken.

Later investigations about the development of young cell walls and their deformations after the embryonic stages entirely exclude activety of surface tension in the formation of the cubo-octahedral shape. This does not take away from the fact that ERRERA's reference to the experiment of MACH and his observations on the activity of turgor as a deforming action on cell walls have not lost their significance. Therefore I wish to call the attention to that experiment. It was described by MACH (28) at a congress in Prague in 1868. Over the edges of a regular tetrahedron rubber membranes were stretched, after which the space enclosed by those membranes, into which a metal tube entered, was exhausted. The membranes then contracted to the same figure as the membranes of a solution of soap assume when a wire tetrahedron is immersed in a such a solution.

K. GIESENHAGEN (7) enclosed rubber balloons in glass vessels and then exhausted the space round the spheres; the rubber spheres then expended and flattened each other; the partition walls showed positions agreeing with those of cell walls in certain tissues. It was necessary, however, to moisten the balloons with paraffin oil, so that they could slide over each other.

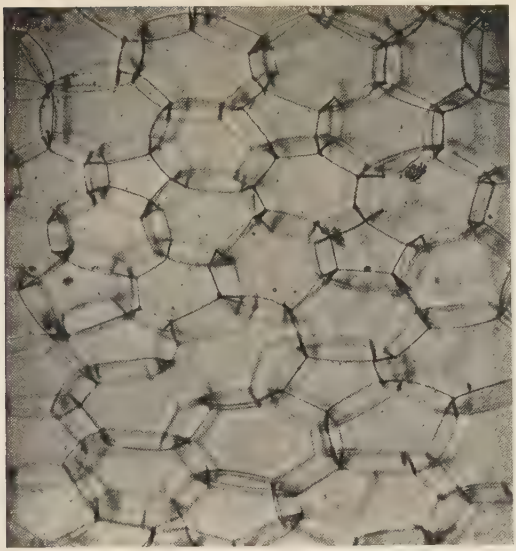

Fig. 1.
Transverse section of the cortical parenchyma of a root tuber of *Asparagus Sprengeri*. Magnif. 50.

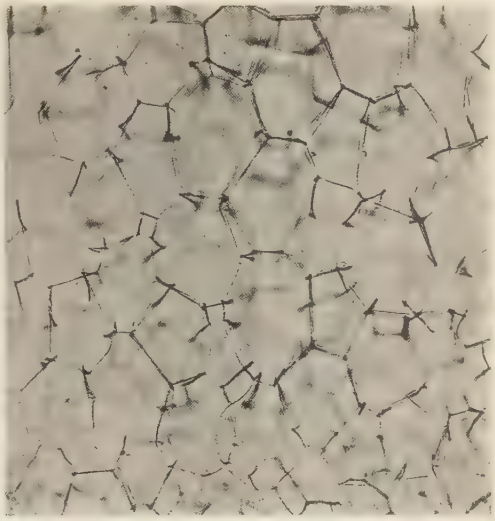

Fig. 2.
Oblique section of the same tissue with many tetragonal faces. Magnif. 50.

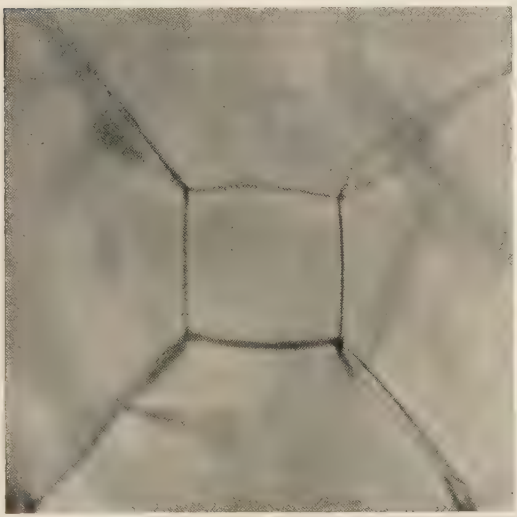

Fig. 3.
A tetragonal face with curved sides and parts of four adjacent hexagonal faces of a cubo-octrahedral cell of the cortical parenchyma of a root tuber of *Asparagus Sprengeri*. Magnif. 200.

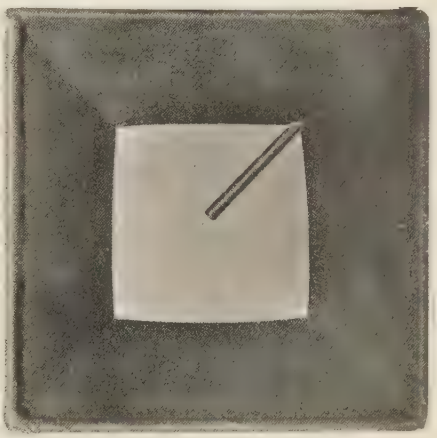

Fig. 4.
The tetragonal plane face with curved sides and the adjacent faces formed in the centre of a rectangular prismatic wire model (the sides of which were 10.2 cm, 8 cm and 10.2 cm). The faces of the model were entirely covered with plane rubber sheet, then it was exhausted by an air pump for which purpose a small tube entered the enclosed room to the centre (this tube is to be seen in the photograph). All the faces in the exhausted model are formed by two membranes. The model was illuminated from the back side, which causes the contrast between the tetragonal face and the other faces.

MACH's experiment may be repeated with other wire figures, for instance with the rectangular prism that Sir WILLIAM THOMSON used to demonstrate the tetragonal plane faces with curved sides of the cubo-octahedron with minimal area (see figure 2 in Part I of this communication); the rubber membranes in the centre of the prism assume a tetragonal shape with curved sides (see fig. 4 on the plate), which entirely corresponds with the shape observed in the experiment of Sir WILLIAM THOMSON with membranes of a solution of soap.

Now it may be assumed with ERRERA that in plant tissues the tension in the cell walls is caused by the turgor pressure of the cells. Further, a hypothetical explanation might be given of what happens in the development of a homogeneous cell tissue with cubo-octahedral cells with curved edges. It may namely be imagined that the cell walls under the influence of their tension take up such a position on growth that in total they assume a minimal area and that if they do not attain that position without changing their mutual arrangement, they will slide over each other in such a way (remember the paraffin oil in GIESENHAGEN's experiments) that they attain that position subsequently.

5. *The significance of the original location and of the growth of the cell walls for the arrangement of the walls of the mature tissues.*

Originally the senior author of this treatise actually thought that the explanation of the occurrence of the "body of Thomson" as the ideal cell form in homogeneous tissues was indeed that juvenile cubic cells, or juvenile cells of a rectangular or a hexagonal prismatic shape, when expending by their growth to maturity, slide over each other, changing their position, until the walls of each cell have obtained the minimal area, possible with the contents of the cells.

Meanwhile it is true that the possibility of the cell walls sliding over each other has often been assumed, but it has also repeatedly been doubted. A dissertation has appeared by A. D. J. MEEUSE (26) in which "the problem of the sliding growth in plant tissues" has once more been thoroughly studied, and from this it can be seen that in plant tissues such growth is out of the question. All the cases in which such growth was assumed may be interpreted differently. The exceptional cases in which cells get into contact with cells with which originally they had no contact must — as is proved by this investigation — be interpreted otherwise than by sliding of a cell wall over other cell walls.

In consequence one may expect the 14 faces of contact of the mature cell with neighbouring cells in homogeneous tissues to be present from the very beginning, that is to say from the moment the cells had been formed through division of other cells. This is actually seen to be the case in the investigation of meristems from which homogeneous plant tissues develop. In those meristems the juvenile cells are hexagonally prismatic, rectangularly prismatic or cubic in shape and in that form they

are already bounded by 14 other cells. The cubo-octahedron develops when 12 out of those 14 faces take up another position when the cells increase in size, namely a position oblique to that of the original one. Two of the faces, those namely which may be considered as upper and lower, or as anterior and posterior faces, only move parallel to themselves. During this development all the edges and eight of the lateral faces of the cell body are curved. The change in the shape of the cells takes place in such a way that the ratio of the contents to the area increases; this may also be formulated by saying that the cell approaches the spherical shape more than would be the case if all the walls had remained plane and the edges straight.

The opposite of the process decribed may be easily pictured, by placing a cubo-octahedron (with straight or with curved edges) of plastic material with a hexagonal face on a horizontal plane, imagining the body stretched vertically in such a way that the six double broken edges connecting the corners of the top and bottom faces of the cubo-octahedron are changed into straight edges, the body thus becoming a hexagonal prism. By horizontal stretching this prism may be changed into a rectangular prism and from that by stretching or compression in two perpendicular directions a cube may be obtained. If the same is imagined to happen to all the cells of a homogeneous tissue of cubo-octahedral cells the walls will not slide over each other; the hexagonal prisms, the rectangular prisms and the cubes that are the result of the deformation will then have 14 contacts with neighbouring prisms or with neighbouring cubes.

On studying juvenile tissues from which homogeneous tissues develop it is seen that they must be counted among the column- or platemeristems in the sense of O. SCHÜEPP (29). As an example we refer to the pictures of longitudinal and transverse sections of the meristem of the pith of *Juncus effusus*, occurring in a publication by R. A. MAAS GEESTERANUS (21), in these Proceedings. Its cells are hexagonal prisms and in the not too juvenile part of the meristem they form vertical columns of cells, owing to the fact that almost exclusively transversely placed partition walls are formed: each cell therefore touches one cell above and one under itself. Besides, these cells have contact sideways with twelve other cells. The same arrangement is found in the columnmeristem from which the cortical parenchyma of the tuber of *Asparagus Sprengeri* develops.

When these cells are inflated by turgor pressure, which will cause tension in the cell walls, then on growth of the cells the result will be the development of "bodies of Thomson", or of bodies which may be derived from them.

It is not necessary to assume that the bounding faces from the very beginning possess surfaces which bear the same ratios to each other as the faces of the "body of Thomson" do. When for instance one of the partitional faces is proportionally too small, there will on inflation be

greater tension in it than in the other faces[1]). As a result the face in question will be more stetched and by growth will more increase its surface than the other faces do. When the inflation is continued long enough, and when the increase of the contents of the cell is equally possible to all sides, the influences discussed here will cause the curving of all the edges and of eight of the faces characteristic of the "body of Thomson", and the ratios of the surfaces of the bounding faces occurring in this body will also be attained.

From what has been said it follows that the shape of the cells in homogeneous cell tissues is determined for the greater part, though not entirely, in the meristem. In order to account for the occurrence of the "body of Thomson", the arrangement of the new cell walls in the meristem has therefore to be considered. I shall restrict myself here to a columnmeristem constructed from hexagonal columns. If the cubo-octahedral cell form is indeed preformed in this meristem, the arrangement of the cell walls in one of the cells forming such a column, and that of some of the walls of adjacent cells, must be approximately as pictured in fig. 5 (in this picture is found a perspective view of the cell and moreover it is folded out in the plane of drawing).

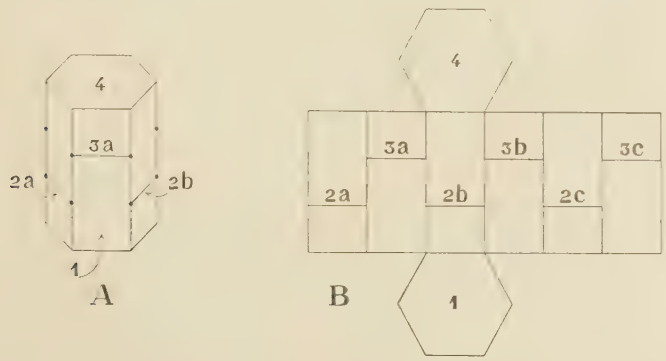

Fig. 5.

A. Hexagonal prismatic meristimatic cell in contact with 14 others. B. The same cell, all faces folded out in the plane of drawing.

The horizontal walls are numbered in the order in which they are supposed to be deposited; the walls 2a, 2b, 2c and 3a, 3b, 3c are horizontal walls of neighbouring cells; the walls indicated by 2a, 2b, 2c are supposed to be formed simultaneously or nearly simultaneously and the same holds good for the walls 3a, 3b, 3c.

If it is assumed that the youngest part of the meristem is found at the top of our picture, it is plausible that the horizontal cell walls have developed in the order indicated by the figures by the side of the walls. In order to explain why the arrangement of the horizontal walls comes about as is shown in our picture, the theory may be brought forward —

[1]) This becomes clear when one imagines a regular, hexagonal network of equally thick and equally tautly stretched rubber threads, and one of the sides of a hexagon shortened.

very plausible in the light of newer investigations — that for the formation of cell walls a certain substance is necessary which is supplied from the older part of the meristem, but which is consumed in the formation of the wall [1]). If at first only wall 1 is imagined to be present and new cell wall forming substance is imagined rising *regularly*, it is more likely that the next cell wall will not be formed within the cell pictured, but in an adjacent cell. If for instance the formation of cell wall 2a follows that of wall 1 it will be most probable, owing to the consumption of the substance in consequence of the formation of the new wall, that other new cell walls are formed in cells not located in the immediate neighbourhood of wall 2a. Thus it may be understood that walls 2b and 2c are formed about simultaneously with wall 2a.

If following the deposition of the walls 2a, 2b and 2c wall-forming substance is imagined to rise with the same regularity, then, owing to the consumption of the substance by the walls which are in course of construction, it will be the turns of walls 3a, 3b and 3c to be formed. It stands to reason that on further supply a new wall in the completely pictured cell, so wall 4, will next be formed.

In a "platemeristem" similar circumstances may account for the preformation of the cubo-octahedral cells, here all-sided supply in the plane of the substance introducing the formation of the cell wall must be assumed. In a "columnmeristem", constructed from columns of cubic cells, we are probably confronted with a case intermediate between a columnmeristem of hexagonal columns and a platemeristem.

Although these considerations are of a purely hypothetical nature, they may serve to make it clear that simple circumstances in the meristems may cause the arrangement of the cell walls according to the scheme discussed.

We will bring forward that these considerations likewise explain the occurrence of cell shapes deviating from the cubo-octahedron, which exceptional shapes occur in great numbers even in highly uniform tissue. Slight disturbances in the supply of the substance, which determines the deposition of the new cell walls, may cause such modifications that they cannot be eliminated by the subsequent regulating activity during the further development of the cell, described in the foregoing pages.

For several of the subjects discussed we finally refer to A. D. J. MEEUSE's dissertation, published lately [2]).

Delft, Laboratory of Technical Botany
of the University College of Technology.

[1]) Naturally nucleus division preceeds the formation of a new wall; properly speaking we should therefore say: the supply of a substance causing nucleus division, but in order to simplify the trend of thought we indicate it as a substance necessary for the formation of a new wall.

[2]) In some respects the considerations exposed here differ from those of MEEUSE; this applies especially to those at the end of this communication. It is to be regretted that MEEUSE has not distinguished between the "body of Thomson" and the "orthic tetrakaidecahedron" (see his dissertation page 61), which makes misunderstandings possible. The above communication may help to remove those.

LITERATURE.

1. BERTHOLD, G., Studien über Protoplasmamechanik, Leipzig 1886, see especially: Kapitel 17 "Theilungsrichtungen und Theilungsfolge, Definitive Ausgestaltung des Zellnetzes".
2. BUFFON, G. L. L. DE, Histoire naturelle, t. **4**, Paris 1753, p. 99—100.
3. DUCHARTRE, P., Elements de botanique, Paris 1867 (see especially page 14, and the heading: "Solide géometrique, formé par chaque cellule").
4. ERRERA, L., a.o. in "Zellenformen und Seifenblasen", Biol. Centralbl. **7**, 728—731 (1888).
5. FEDOROW, E. VON, Theorie der Kristalstructur, Z. Kristall. u. Mineral. **25**, 113—140 (1896).
6. GANE, R., A Method for Demonstrating the Shape of Meristematic Cells in Plants, New Phytologist **29**, 77—99 (1930).
7. GIESENHAGEN, K., Die Richtung der Teilungswand in Pflanzenzellen, Flora **49**, 355—369 (1909).
8. KELVIN, Lord, On Homogeneous Division of Space, Proc. Roy. Soc. London **55**, 1—17 (1894); see also his treatise: "On the molecular factors of a crystal", Robert Boyle Lecture, May 16, 1893, published in "Baltimore Lectures", London 1904, p. 602—621.
9. KIESER, D. G., Ueber die ursprüngliche und eigenthümliche Form der Pflanzenzellen, Verh. der Leop.-Carol. Akad. der Naturforscher **9**, 59—85 (1818). See also by the same author: Mém. sur l'organisation des plantes, Verh. Teyler's Genootschap **18**, Haarlem, 1814.
10. LEWIS, F. T., The typical shape of polyhedral cells in vegetable parenchyma and the restoration of that shape following cell division, Proc. Amer. Acad. Arts and Sc. **58**, 537—552 (1922—1923).
11. ————, A further study of the polyhedral shapes of cells, Proc. Amer. Acad. Arts and Sc. **61**, 1—34 (1925—'26).
12. ————, The effect of cell division on the shape and size of hexagonal cells, Anat. Rec. **33**, 331—335 (1926).
13. ————, The correlation between cell division and the shape and sizes of prismatic cells in the epidermis of Cucumis, Anat. Rec. **38**, 341—376 (1928).
14. ————, The shape of cork cells: a simple demonstration that they are tetrakaidecahedral, Science, New Ser. **68**, 625—626 (1928).
15. ————, A volumetric study of growth and cell division in two types of epithelium, the longitudinally prismatic epidermal cells of Tradescantia and the radially prismatic epidermal cells of Cucumis, Anat. Rec. **47**, 59—99 (1930).
16. ————, A comparison between the mosaic of polygons in a film of artificial emulsion and the pattern of simple epithelium in surface view (Cucumber epidermis and human amnion), Anat. Rec. **50**, 235—265 (1931).
17. ————, The significance of cells as revealed by their polyhedral shapes, with special reference to precartilage, and a surmise concerning nerve cells and neuroglia, Proc. Amer. Acad. Arts and Sc. **68**, 251—285 (1932—'33).
18. ————, Mathematically precise features of epithelial mosaics: observations on the endothelium of capillaries, Anat. Rec. **55**, 323—341 (1933).
19. ————, The Shape of the Tracheids in the Pine, Amer. J. Bot. **22**, 741—762 (1935).
20. ————, The Shape of Compressed Spheres, Science, New Ser. **86**, 609—611 (1937).
21 MAAS GEESTERANUS, R. A., On the development of the stellate form of the pith cells of Juncus species, Proc. Ned. Akad. v. Wetensch., Amsterdam, **44**, 4 and 5 (1941).
22. MARVIN, J. W., Cell Shape Phenomena Interpreted in Terms of Compressed lead Shot. Science, New Ser., **86**, 493—494 (1937).

23. ————, Cell Shape Studies in the Pith of Eupatorium purpureum, Amer. J. Bot., **26**, 487—503 (1939).
24. ————, The Shape of Compressed Lead Shot and its relation to Cell Shapes, Amer. J. Bot., **26**, 280—288 (1939).
25. MATZKE, E. B., An Analysis of the Orthic Tetrakaidecahedron, Bull. Torrey Bot. Club, **54**, 341—348 (1927—'28).
26. MEEUSE, A. D. J., A Study of intercellular relationships among vegetable cells with special reference to cell form and "sliding growth", Dissertation Leyden, Gouda 1941.
27. MIRBEL, C. F. BRISSEAU, Traité d'anatomie et de physiologie végétales, t. **1**, Paris 1802 (see in particular the explanation to the "gravure" added to the work under the heading "Système organique des végétaux", especially what is said under "Du tissue cellulaire").
28 Cited after J. PLATEAU, Statique expérimentale et théorique des liquides soumis aux seules forces moléculaires, Paris 1873, t. **1**, p. 374.
29. SCHÜEPP, O., Meristeme, Bd. **4**, 1. Abt., 2. T1 (Histology) of K. LINSBAUER's "Handbuch der Pflanzenanatomie", Berlin 1926.
30. SOUÈGES, R., Les lois du dévelopment, Exposés d'embryologie et de morphologie végétales **8**, Paris (Hermann et Cie) 1937, in which many works of this author are cited.
31. THOMSON, Sir WILLIAM, On the Division of Space with Minimum Partitional Area, Philos. Mag. 5th Ser., **24**, 503—514 (1887).
32. THOMPSON, D'ARCY WENTWORTH, On Growth and Form, Cambridge 1917.
33. TUTTON, A. E. H., Crystallography and Practical Crystal Measurement, London 1911, p. 536 and following.
34. WILDEMAN, E. DE, Etudes sur l'attache des cloisons cellulaires, Mém. corron. et mém. sav. étr., Acad. roy. Belg., **53**, 1—84 (1894).

Mathematics. — *Ueber die Figur dreier Ebenen im R_5.* Von R. WEITZENBÖCK.

(Communicated at the meeting of September 27, 1941.)

Drei zueinander windschiefe Ebenen des fünfdimensionalen Raumes R_5 bestimmen ein System von ∞^1 solchen Ebenen, die eine dreidimensionale Mannigfaltigkeit dritten Grades M_3^3 erzeugen. Im binären Gebiete dieser ∞^1 erzeugenden Ebenen der M_3^3 stellen die drei gegebenen Ebenen E_1, E_2 und E_3 eine binäre kubische Form dar, deren Kovarianten neue erzeugende Ebenen zugeordnet sind.

Es wird im Folgenden der Zusammenhang letztgenannter Ebenen mit den linearen, zu den drei gegebenen Ebenen gehörigen, kovarianten Ebenenkomplexen des R_5 aufgedeckt. Am Schlusse zeige ich, dass die ∞^1 erzeugenden Ebenen der M_3^3 die Doppelebenen der in der Schaar $\lambda_1 E_1 + \lambda_2 E_2 + \lambda_3 E_3$ enthaltenen Ebenenkomplexe sind.

§ 1.

In den drei paarweise windschiefen Ebenen 1, 2 und 3 mit den Gleichungen

$$E_1 = (a^3 \pi^3) = (1^3 \pi^3) = 0 \ , \ E_2 = (\alpha^3 \pi^3) = (2^3 \pi^3) = 0 \ , \ E_3 = (p^3 \pi^3) = (3^3 \pi^3) = 0$$

seien A_1, A_2, A_3, B_1, B_2, B_3 und C_1, C_2, C_3 je drei Punkte. Davon wählen wir A_1, A_2, A_3 willkürlich. Wir verbinden A_i mit der dritten Ebene 3; der Verbindungs-R_3 schneidet die zweite Ebene in B_i. Die Gerade $A_i B_i$ trifft dann die dritte Ebene in C_i. Diese Konstruktion ergibt

$$B_i = 2\,(2^2 A_i 3^3). \quad . \quad . \quad . \quad . \quad . \quad . \quad . \quad . \quad (1)$$

und

$$C_i = B_i - \tfrac{1}{3} A_{23} A_i, \quad . \quad . \quad . \quad . \quad . \quad . \quad . \quad . \quad (2)$$

wobei A_{23} die Invariante

$$(2^3 3^3) = (a^3 \alpha^3) = 36 \sum a_{123}\, \alpha_{456}$$

bedeutet. Wir setzen

$$(A_1 A_2 A_3)_{ijk} = a_{ijk} = 1_{ijk} = \tfrac{1}{6} (1^3)_{ijk} \ ; \ E_1 = 6\,(A_1 A_2 A_3 \pi^3) \quad . \quad (3)$$

Nach (1) haben wir, wenn 2_1 und 2_2 mit 2 äquivalent sind:

$$(B_1 B_2 B_3 \pi^3) = (22_1\, 2_2 \pi^3)\,(2^2 A_1 3^3)\,(2_1^2 A_2 3_1^3)\,(2_2^2 A_3 3_2^3) \, . \quad . \quad . \quad (4)$$

und dies lässt sich umformen auf

$$(B_1 B_2 B_3 \pi^3) = -\tfrac{1}{2\,7} \cdot \tfrac{1}{6} \cdot A_{23}^2 A_{31}\,(2^3 \pi^3) = -\tfrac{1}{2\,7} \cdot \tfrac{1}{6} \cdot A_{23}^2 A_{31} \cdot E_2 \, . \quad (5)$$

Setzt man analog zu (1)

$$A_i^* = 1\,(1^2 B_i 3^3) \quad . \quad . \quad . \quad . \quad . \quad . \quad . \quad . \quad . \quad (6)$$

und hierin B_i von (1) ein, so ergibt sich

$$A_i^* = 1\,(1^2 23^3)\,(2^2 A_i 3^3),$$

oder, nach Umformung der rechten Seite:

$$A_i^* = -\tfrac{1}{9} A_{23} A_{31} \cdot A_i. \quad . \quad . \quad . \quad . \quad . \quad . \quad . \quad . \quad (7)$$

§ 2.

Wir nehmen jetzt auf den drei Geraden $A_i B_i$ je einen Punkt $A_i + \mu_i B_i$ an; ihre Verbindungsebene hat die Gleichung

$$(A_1 + \mu_1 B_1, A_2 + \mu_2 B_2, A_3 + \mu_3 B_3 \pi^3) = 0. \quad . \quad . \quad . \quad . \quad (8)$$

Sie ist dann und nur dann erzeugende Ebene der durch die drei Ebenen bestimmten $M_3{}^3$, wenn sie von allen Treffgeraden dieser drei Ebenen geschnitten wird. Diese ∞^2 Treffgeraden sind durch AB gegeben mit

$$A = \lambda_1 A_1 + \lambda_2 A_2 + \lambda_3 A_3 \ , \ B = \lambda_1 B_1 + \lambda_2 B_2 + \lambda_3 B_3.$$

AB trifft die Ebene (8) wenn die Determinante

$$\left.\begin{matrix} (A_1 + \mu_1 B_1 \, , A_2 + \mu_2 B_2 \, , A_3 + \mu_3 B_3 \, , \\ \lambda_1 A_1 + \lambda_2 A_2 + \lambda_3 A_3 \, , \lambda_1 B_1 + \lambda_2 B_2 + \lambda_3 B_3, X) \end{matrix}\right\} . \quad . \quad (9)$$

für jedes X und jedes λ_i verschwindet.

Wertet man (9) aus und setzt die Koeffizienten von $\lambda_i \lambda_k$ gleich Null, so ergeben sich die Gleichungen

$$\left.\begin{matrix} (\mu_3 - \mu_2) \, . \, [(A_1 \, A_2 \, A_3 \, B_2 \, B_3 \, X) + \mu_1 \, (B_1 \, B_2 \, B_3 \, A_2 \, A_3 \, X)] \equiv 0 \\ (\mu_1 - \mu_3) \, . \, [(A_1 \, A_2 \, A_3 \, B_3 \, B_1 \, X) + \mu_2 \, (B_1 \, B_2 \, B_3 \, A_3 \, A_1 \, X)] \equiv 0 \\ (\mu_2 - \mu_1) \, . \, [(A_1 \, A_2 \, A_3 \, B_1 \, B_2 \, X) + \mu_3 \, (B_1 \, B_2 \, B_3 \, A_1 \, A_2 \, X)] \equiv 0 \end{matrix}\right\} . \quad (10)$$

Dies muss identisch in allen X gelten. Wegen $(A_1 \, A_2 \, A_3 \, B_1 \, B_2 \, B_3) \neq 0$ sind die sechs Räume $(A_1 \, A_2 \, A_3 \, B_2 \, B_3 \, X) = 0$ u.s.f. von (10) linear-unabhängig und es folgt

$$\mu_1 = \mu_2 = \mu_3 = \mu,$$

d.h. aus (8) wird

$$(A_1 + \mu \, B_1 \, , A_2 + \mu \, B_2 \, , A_3 + \mu \, B_3 \, \pi^3) = 0,$$

oder, entwickelt:

$$\left.\begin{matrix} (A_1 \, A_2 \, A_3 \, \pi^3) + \mu . \, [(A_2 \, A_3 \, B_1 \, \pi^3) + (A_3 \, A_1 \, B_2 \, \pi^3) + (A_1 \, A_2 \, B_3 \, \pi^3)] + \\ + \mu^2 . \, [(A_1 \, B_2 \, B_3 \pi^3) + (A_2 B_3 B_1 \pi^3) + (A_3 B_1 B_2 \pi^3)] + \mu^3 \, . \, (B_1 \, B_2 \, B_3 \pi^3) = 0. \end{matrix}\right\} \quad (11)$$

Hier wird der erste Term nach (3)

$$(A_1 \, A_2 \, A_3 \, \pi^3) = \tfrac{1}{6} \, (1^3 \, \pi^3) = \tfrac{1}{6} \, E_1.$$

Beim Koeffizienten von μ in (11) ersetzen wir B_i durch die Ausdrücke (1) und formen

$$(A_2 \, A_3 \, 2 \, \pi^3) \ (2^2 \, A_1 \, 3^3) \quad . \quad . \quad . \quad . \quad . \quad . \quad . \quad (12)$$

um, indem wir A_1 in den ersten Klammerfaktor bringen. Hierdurch wird dieser Koeffizient zu

$$(A_1 \, A_2 \, A_3 \, \pi^3) \ (2^3 \, 3^3) - 3 \, (A_1 \, A_2 \, A_3 \, 2 \, \pi^2) \ (2^2 \, \pi \, 3^3) =$$
$$= \tfrac{1}{6} \, (1^3 \, \pi^3) \, . \, A_{23} - \tfrac{1}{2} \, . \, (1^3 \, \pi^2 \, 2) \ (2^2 \, \pi \, 3^3) = \tfrac{1}{6} \, A_{23} \, E_1 - \tfrac{1}{2} \, J_{1\pi 23} = - \tfrac{1}{2} \, J_{\pi 123};$$

denn es ist [1])

$$J_{1\pi 23} = J_{\pi 123} + \tfrac{1}{3} \, A_{1\pi} \, A_{23}.$$

Beim Koeffizienten von μ^2 in (11) ersetzen wir zuerst A_i durch A_i^*: nach (7) wird dann

$$(A_1 \, B_2 \, B_3 \, \pi^3) = - \frac{9}{A_{23} \, A_{31}} \, (A_1^* \, B_2 \, B_3 \, \pi^3),$$

---

[1]) Vgl. diese Proceedings **35** (1932), p. 1029, Formel (12).

also nach (6)

$$= -\frac{9}{A_{23}\,A_{31}}\,(B_2\,B_3\,1\,\pi^3)\,(1^2\,B_1\,3^3)$$

und hier kann man dieselbe Umformung wie bei (12) ausführen und die drei B_i im ersten Klammerfaktor vereinigen. Man erhält

$$-\frac{9}{A_{23}\,A_{31}}\,\{A_{13}\,(B_1\,B_2\,B_3\,\pi^3) - 3\,(B_1\,B_2\,B_3\,1\,\pi^2)\,(1^2\,\pi\,3^3)\},$$

also nach (5):

$$\tfrac{1}{18}\,A_{23}\,\{A_{13}\,E_2 - 3J_{2\pi 13}\} = -\tfrac{1}{6}\,A_{23}\,J_{\pi 213}.$$

Somit kommt statt (11), wenn wir den Faktor $\frac{1}{6}$ weglassen:

$$E_1 - 3\mu\,J_{\pi 123} - \mu^2\,A_{23}\,J_{\pi 213} - \tfrac{1}{27}\,\mu^3\,A_{23}^2\,A_{31}\,E_2 = 0. \quad . \quad . \quad (13)$$

Nun ist

$$J_{\pi 213} = J_{\pi 123} + \tfrac{1}{9}\,(A_{13}\,A_{\pi 2} + A_{32}\,A_{\pi 1} + A_{21}\,A_{\pi 3})$$

$$J_{\pi 213} = J_{\pi 123} + \tfrac{1}{9}\,(A_{23}\,E_1 + A_{31}\,E_2 + A_{12}\,E_3) \quad . \quad . \quad . \quad . \quad (14)$$

und wenn wir die in allen vier Indizes symmetrische Komitante

$$S = S_{123\pi} = \tfrac{1}{24}\,\Sigma J_{123\pi}$$

$$= J_{\pi 123} - \tfrac{1}{6}\,A_{\pi 1}\,A_{23} + \tfrac{1}{18}\,A_{\pi 2}\,A_{31} - \tfrac{1}{18}\,A_{\pi 3}\,A_{12}$$

$$S = S_{123\pi} = J_{\pi 123} + \tfrac{1}{6}\,A_{23}\,E_1 - \tfrac{1}{18}\,A_{31}\,E_2 + \tfrac{1}{18}\,A_{12}\,E_3$$

einführen, so wird

$$J_{\pi 123} = S - \tfrac{1}{6}\,A_{23}\,E_1 + \tfrac{1}{18}\,A_{31}\,E_2 - \tfrac{1}{18}\,A_{12}\,E_3 \quad . \quad . \quad . \quad (15)$$

$$J_{\pi 213} = S - \tfrac{1}{18}\,A_{23}\,E_1 + \tfrac{1}{6}\,A_{31}\,E_2 + \tfrac{1}{18}\,A_{12}\,E_3. \quad . \quad . \quad . \quad (16)$$

Damit erhält (13) die Gestalt:

$$\left.\begin{aligned} E_1\,.\,(1 + \tfrac{1}{2}\,\mu\,A_{23} + \tfrac{1}{18}\,\mu^2\,A_{23}^2) - E_2\,.\,\tfrac{1}{6}\,\mu\,A_{31}\,(1 + \mu\,A_{23} + \tfrac{2}{9}\,\mu^2\,A_{23}^2) + \\ + E_3\,.\,\tfrac{1}{6}\,\mu\,A_{12}\,(1 - \tfrac{1}{3}\,\mu\,A_{23}) - \mu\,.\,S\,(3 + \mu\,A_{23}) = 0. \end{aligned}\right\} \quad . \quad (17)$$

§ 3.

Bezeichnen wir den Schnittpunkt der Geraden $A_i\,B_i$ mit dieser Ebene (17) durch D_i, setzen also nach (8)

$$D_i = A_i + \mu\,B_i, \quad . \quad . \quad . \quad . \quad . \quad . \quad . \quad . \quad . \quad (18)$$

so folgt nach (?), dass bei

$$\mu\,A_{23} = -3\,\delta. \quad . \quad . \quad . \quad . \quad . \quad . \quad . \quad . \quad . \quad (19)$$

die Grösse δ gleich dem Doppelverhältnis $(A_i B_i D_i C_i)$ wird. Aus (17) folgt dann, wenn die Ebene (17) E_δ genannt wird:

$$\left.\begin{aligned} E_\delta = E_1\,.\,A_{23}\,\tfrac{1}{2}\,(\delta - 1)\,(\delta - 2) + E_2\,.\,A_{31}\,\delta\,(\delta - 1)\,(\delta - \tfrac{1}{2}) - \\ - E_3\,.\,A_{12}\,\tfrac{1}{2}\,\delta\,(1 + \delta) + S\,.\,9\,\delta\,(1 - \delta). \end{aligned}\right\} \quad . \quad (20)$$

Hierdurch werden die erzeugenden Ebenen der M_3^3 durch den Parameter δ dargestellt. Den Werten $\delta = 0,\ \infty,\ 1$ entsprechen die Ebenen E_1, E_2 und E_3.

Führt man nach (19) das Doppelverhältnis δ statt der Grösse μ in die Gleichung (13) ein, so ergibt sich

$$E_\delta = E_1 \,.\, A_{23} + 9\,\delta \,.\, J_{\pi 123} - 9\,\delta^2 \,.\, J_{\pi 213} + \delta^3 \,.\, E_2 \,.\, A_{31} = 0 \quad . \quad (21)$$

in Uebereinstimmung mit einer früher abgeleiteten Gleichung [2]). Setzt man nämlich in (21) $\pi_{ijk} = s_{ijk}$ als gegeben voraus, so stellt (21) eine Gleichung dritten Grades für δ dar. Ihren drei Wurzeln entsprechen die drei Transversalebenen der $M_3{}^3$, die dem linearen Komplexe s_{ijk} angehören. Ist s_{ijk} speziell, so bedeutet dies, dass diese drei Transversalebenen die Ebene s_{ijk} schneiden. Die zugehörigen Punkte D_i sind demnach die Schnittpunkte der Ebene s_{ijk} mit der $M_3{}^3$.

§ 4.

Die ∞^1 erzeugenden Ebenen E_δ werden nach (20) durch ein Polynom dritten Grades in δ gegeben, also, wenn man durch $\delta = \frac{\delta_1}{\delta_2}$ zu homogenen Parametern übergeht, durch eine kubische Binärform $f(\delta_1, \delta_2)$ dargestellt. Die drei Basisebenen E_1, E_2 und E_3 sind dann durch die Form

$$f_0 = \delta_1\,\delta_2\,(\delta_1 - \delta_2)$$

dargestellt. Deren kubische Kovariante Q_0 wird

$$Q_0 = 2\,\delta_1^3 - 3\,\delta_1^2\,\delta_2 - 3\,\delta_1\,\delta_2^2 + 2\,\delta_2^3;$$

ihre Nullpunkte sind also durch die Gleichung

$$2\,\delta^3 - 3\,\delta^2 - 3\delta + 2 = 0$$

gegeben, was die Parameterwerte

$$\delta_1 = 2,\ \delta_2 = \tfrac{1}{2},\ \delta_3 = -1$$

ergibt. Die hierzu gehörigen Ebenen werden dann nach (20):

$$\left.\begin{aligned} F_1 &= \quad A_{31}\,E_2 - A_{12}\,E_3 - 6\,S = 0 \\ F_2 &= -A_{23}\,E_1 \quad + A_{12}\,E_3 - 6\,S = 0 \\ F_3 &= \ A_{23}\,E_1 - A_{31}\,E_2 \quad - 6\,S = 0 \end{aligned}\right\} \quad . \ . \ . \quad (22)$$

Hieraus folgt

$$F_1 + F_2 + F_3 = 18\,S; \quad . \ . \ . \ . \ . \ . \ . \quad (23)$$

hierdurch ist der lineare Ebenenkomplex $S = 0$ als Linearkombination dreier Ebenen dargestellt. Es ist aber S auch durch zwei erzeugende Ebenen der $M_3{}^3$ darstellbar. Die HESSE'sche Kovariante der Grundform $f_0 = \delta_1\,\delta_2\,(\delta_1 - \delta_2)$ ist bis auf einen Zahlenfaktor durch

$$\delta_1^2 - \delta_1\,\delta_2 + \delta_2^2$$

gegeben, was auf die Nullpunkte

$$\delta = \tfrac{1}{2}\,(1 \pm \sqrt{-3})$$

führt. Setzt man dies in (20) ein und setzt

$$T = A_{23}\,E_1 + A_{31}\,E_2 + A_{12}\,E_3, \quad . \ . \ . \ . \ . \quad (24)$$

---

[2]) Diese Proceedings **35** (1932), p. 1125, Formel (12). Bei dieser muss im dritten Term J_{4213} statt J_{1342} stehen.

so erhält man die beiden erzeugenden Ebenen

$$\left.\begin{aligned} H_1 &= S + \tfrac{1}{18}\sqrt{-3}\,T \\ H_2 &= S - \tfrac{1}{18}\sqrt{-3}\,T \end{aligned}\right\} \quad \ldots\ldots\ldots \quad (25)$$

wonach also

$$S = \tfrac{1}{2}(H_1 + H_2)\ ,\ T = \frac{9}{\sqrt{-3}}(H_1 - H_2). \quad \ldots\ldots \quad (26)$$

Die geometrische Bedeutung der linearen Ebenenkomplexe $T = 0$ und $S = 0$ ist leicht anzugeben. Wenn die durch (21) gegebene kubische Binärform mit der Grundform

$$f_0 = \delta_1\,\delta_2\,(\delta_1 - \delta_2)$$

konjugiert (apolar) sein soll, so folgt $T = 0$; ist aber (21) zur Kovariante

$$Q_0 = 2\,\delta_1^3 - 3\,\delta_1^2\,\delta_2 - 3\,\delta_1\,\delta_2^2 + 2\,\delta_2^3$$

konjugiert, so folgt $S = 0$, wie schon E. A. WEISS bewiesen hat [3]).

§ 5.

Für die beiden Ebenen H von (25), die im binären Gebiete der erzeugenden Ebenen der $M_3{}^3$ den Nullpunkten der HESSE'schen Kovariante von f_0 entsprechen, lässt sich leicht eine geometrische Deutung in Bezug auf die Komplexe T und S geben.

Zunächst eine Vorbemerkung. Ein linearer Ebenenkomplex K im R_5

$$K = A_{K\pi} = (a^3\,\pi^3) = 0 \quad \ldots\ldots\ldots \quad (27)$$

hat eine Komitante

$$R_K = (a^3\,b^2\,c)\ (b\,c^2\,\pi^3) = J_{KKK\pi} = A_{R_K\pi}, \quad \ldots\ldots \quad (28)$$

die, gleich Null gesetzt, wieder einen linearen Ebenenkomplex darstellt. Die bilineare Invariante

$$J_K = A_{R_K K} = (a^3\,b^2\,c)\,(bc^2\,d^3) = J_{KKKK} \quad \ldots\ldots \quad (29)$$

der beiden Komplexe R_K und K ist die einzige Invariante des Komplexes K.

Die beiden Komplexe

$$H_K = R_K \pm \sqrt{-\tfrac{1}{6}}\,J_K\,.\,K = 0 \quad \ldots\ldots\ldots \quad (30)$$

sind dann speziell und geben die sogen. „Doppelebenen" des Komplexes K. Bei $J_K \neq 0$ ist die Beziehung zwischen K und R_K gegenseitig, d.h. R_{R_K} führt auf K zurück. Man hat nämlich

$$R_{R_K} = -\tfrac{1}{36}\,J_K^2\,.\,K\,. \quad \ldots\ldots\ldots \quad (31)$$

$$J_{R_K} = A_{R_{R_K} R_K} = -\tfrac{1}{36}\,J_K^2\,.\,A_{KR_K} = \tfrac{1}{36}\,J_K^3 \quad \ldots\ldots \quad (32)$$

Wir setzen nun $K = T$ (Gleichung (24)). Dann folgen

$$A_{T1} = 0\ ,\ A_{T2} = 0\ ,\ A_{T3} = 0\,. \quad \ldots\ldots\ldots \quad (33)$$

und nach leichter Rechnung

$$R_T = 6\,A_{23}\,A_{31}\,A_{12}\,.\,S \quad \ldots\ldots\ldots \quad (34)$$

Es ist also S der zum Komplexe T kovariante Ebenenkomplex und umgekehrt.

---

[3]) Diese Proceedings **36** (1933), p. 74—75.

Weiter folgt für die Invariante von T:

$$J_T = 2\,(A_{23}\,A_{31}\,A_{12})^2. \quad . \quad . \quad . \quad . \quad . \quad . \quad . \quad . \quad (35)$$

Aus (31) und (34) ergeben sich

$$R_s = -\frac{4}{6^5}\,A_{23}\,A_{31}\,A_{12}\,.\,T, \qquad J_s = \frac{4}{3.6^5}(A_{23}\,A_{31}\,A_{12})^2 \quad . \quad (36)$$

und nach (30)

$$H_T = 6\,A_{23}\,A_{31}\,A_{12}\,(S \pm \tfrac{1}{18}\sqrt{-3}\,T) \quad . \quad . \quad . \quad . \quad (37)$$

in Uebereinstimmung mit (25).

§ 6.

Zu den erzeugenden Ebenen der $M_3{}^3$ gelangt man noch auf einem anderen Wege. Die drei Ebenen E_i bestimmen eine lineare Schaar von ∞^2 linearen Ebenenkomplexen, die wir in der Gestalt

$$\Sigma = \sigma_1\,A_{23}\,E_1 + \sigma_2\,A_{31}\,E_2 + \sigma_3\,A_{12}\,E_3 = A_{\sigma\pi} = (\sigma^3\,\pi^3) \quad . \quad . \quad (38)$$

schreiben. Für den zu Σ kovarianten Komplex R_Σ (Gleichung (28)) erhält man:

$$\left.\begin{aligned} R_\Sigma = J_{\sigma\sigma\sigma\pi} = 2\,\sigma_1\,\sigma_2\,\sigma_3\,A_{23}\,A_{31}\,A_{12}\,.\sum_c J_{123\pi} + \\ + \tfrac{1}{3}\,A_{23}\,A_{31}\,A_{12}\,.\sum_c \sigma_1\,A_{23}\,(\sigma_3\,\sigma_1 - \sigma_1\,\sigma_2 - \sigma_2\,\sigma_3)\,E_1, \end{aligned}\right\} \quad . \quad (39)$$

wobei $\sum_c$ zyklische Summierung andeutet.

Da nun nach (15) und (24)

$$\sum_c J_{123\pi} = J_{123\pi} + J_{231\pi} + J_{312\pi} = 3\,S + \tfrac{1}{6}\,T = 3\,S + \tfrac{1}{6}\sum_c A_{23}\,E_1 \quad (40)$$

wird, ergibt sich

$$R_\Sigma = J_{\sigma\sigma\sigma\pi} = 6\,\sigma_1\,\sigma_2\,\sigma_3\,A_{23}\,A_{31}\,A_{12}\,.\,S + \tfrac{1}{3}\,A_{23}\,A_{31}\,A_{12}\sum_c \sigma_1^2(\sigma_3 - \sigma_2)\,A_{23}\,E_1 \quad (41)$$

Wegen

$$A_{S1} = \tfrac{1}{9}\,A_{31}\,A_{12}, \quad A_{S2} = \tfrac{1}{9}\,A_{12}\,A_{23}, \quad A_{S3} = \tfrac{1}{9}\,A_{23}\,A_{31} \quad . \quad . \quad (42)$$

$$A_{1\Sigma} = A_{31}\,A_{12}(\sigma_2 - \sigma_3), \quad A_{2\Sigma} = A_{12}\,A_{23}(\sigma_3 - \sigma_1), \quad A_{3\Sigma} = A_{23}\,A_{31}(\sigma_1 - \sigma_2) \quad (43)$$

folgen

$$A_{S\Sigma} = \tfrac{1}{9}\,A_{23}\,A_{31}\,A_{12}\,(\sigma_1 + \sigma_2 + \sigma_3) \quad . \quad . \quad . \quad . \quad . \quad (44)$$

$$\left.\begin{aligned} J_\Sigma = A_{R_\Sigma\Sigma} = \tfrac{1}{3}\,(A_{23}\,A_{31}\,A_{12})^2\,[2\,\sigma_1\,\sigma_2\,\sigma_3\,(\sigma_1 + \sigma_2 + \sigma_3) - \sum_c \sigma_1^2\,(\sigma_2 - \sigma_3)^2] = \\ = -\tfrac{2}{3}\,(A_{23}\,A_{31}\,A_{12})^2\,[(\sum_c \sigma_2\,\sigma_3)^2 - 4\,\sigma_1\,\sigma_2\,\sigma_3\,(\sum_c \sigma_1)]. \end{aligned}\right\} \quad (45)$$

Für

$$(\sigma_2\,\sigma_3 + \sigma_3\,\sigma_1 + \sigma_1\,\sigma_2)^2 = 4\,\sigma_1\,\sigma_2\,\sigma_3\,(\sigma_1 + \sigma_2 + \sigma_3) \quad . \quad . \quad . \quad (46)$$

ist also Σ halb-speziell und R_Σ wird speziell und hat wegen $A_{ik} \neq 0$ nach (41) die Gleichung:

$$S = \tfrac{1}{18}\sum_c \frac{\sigma_1^2\,(\sigma_2 - \sigma_3)}{\sigma_1\,\sigma_2\,\sigma_3}\,A_{23}\,E_1 = 0. \quad . \quad . \quad . \quad . \quad . \quad (47)$$

Gehen wir hier zu inhomogenen Parametern

$$\sigma = \frac{\sigma_1}{\sigma_3},\ \tau = \frac{\sigma_2}{\sigma_3}$$

über und setzen

$$\tau = (1-\delta)^2,$$

so ergibt sich aus (46)

$$\sigma = \frac{(\delta-1)^2}{\delta^2}$$

und aus (47) wird

$$S - \tfrac{1}{18}\frac{\delta-2}{\delta} A_{23} E_1 - \tfrac{1}{18}(2\delta-1) A_{31} E_2 - \tfrac{1}{18}\frac{1+\delta}{1-\delta} A_{12} E_3 = 0$$

in voller Uebereinstimmung mit (20).

Die erzeugenden Ebenen der M_3^3 sind also die Doppelebenen der in der Schaar enthaltenen halbspeziellen Ebenenkomplexe.

Die Doppelebenen H_Σ von Σ haben nach (30), (41) und (45) die Gleichung

$$S - \tfrac{1}{18}\sum_c \left(\frac{\sigma_1(\sigma_2-\sigma_3)}{\sigma_2\sigma_3} \pm \frac{1}{\sigma_2\sigma_3}\sqrt{(\sum_c \sigma_2\sigma_3)^2 - 4\sigma_1\sigma_2\sigma_3(\sum_c \sigma_1)} \right) A_{23} E_1 = 0. \quad (48)$$

Setzt man hier

$$\delta = \frac{1}{2\sigma_2\sigma_3}\left(\sigma_2\sigma_3 + \sigma_1\sigma_2 - \sigma_1\sigma_3 \pm \sqrt{(\sum_c \sigma_2\sigma_3)^2 - 4\sigma_1\sigma_2\sigma_3(\sum_c \sigma_1)}\right) \quad (49)$$

so ergibt sich wiederum (20). *Die Doppelebenen aller Komplexe Σ sind also erzeugende Ebenen der M_3^3.* Im Besonderen ist E_δ von (20) Doppelebene aller Σ mit

$$\sigma_2\sigma_3 \,.\, \delta(\delta-1) + \sigma_3\sigma_1 \,.\, \delta + \sigma_1\sigma_2(1-\delta) = 0. \quad . \quad . \quad . \quad (50)$$

Mechanics. — *On the elastic behaviour of the so-called "Bourdon" pressure gauge.* II. By C. B. BIEZENO and J. J. KOCH.

(Communicated at the meeting of September 27, 1941.)

4. *The iterative method.* Provisionally we introduce in the endplanes V_1 and V_2 a system of tangential stresses σ_1, such that:

1°. each plane is loaded by an equilibrium system,

2°. the material points of V_1 and V_2 remove to planes V_1' and V_2', the relative position of which is defined by the specific quantities ε_1 and ω_1, (differing from the definitive values ε_0 and ω_0 mentioned in § 3).

3°. for the points of any cross-section the displacements in the direction y are given by v_1.

These stresses can easily be found by considering a fibre intersecting the meridional plane of symmetry of the ring in the point (x, y). The original length of this fibre is $(r + y)d\psi$ whereas its new length is given by:

$$(r + y + v_1)\, d\psi + \varepsilon_1\, r\, d\psi + (y + v_1)\, \omega_1\, d\psi.$$

The specific elongation ε therefore is:

$$\varepsilon = \frac{v_1\, d\psi + \varepsilon_1\, r\, d\psi + (y + v_1)\, \omega_1\, d\psi}{(r + y)\, d\psi}.$$

In the numerator we neglect the product $v_1\omega_1$ against terms of the first degree in v_1, ε_1 and ω_1; in the denominator y in all actual cases is negligible with respect to r. Hence:

$$\varepsilon = \frac{v_1}{r} + \varepsilon_1 + \frac{y}{r}\, \omega_1$$

and consequently

$$\sigma_1 = E\varepsilon = E\left[\frac{v_1}{r} + \varepsilon_1 + \frac{y}{r}\, \omega_1\right].$$

The equilibrium of the force-system produced by the stresses σ_1 requires — if dF denotes the surface element on which σ_1 acts —

$$\int_F E\left[\frac{v_1}{r} + \varepsilon_1 + \frac{y}{r}\, \omega_1\right] dF = 0$$

$$\int_F E\left[\frac{v_1}{r} + \varepsilon_1 + \frac{y}{r}\, \omega_1\right] y\, dF = 0.$$

On account of symmetry $\int_F y\,dF$ as well as $\int_F v_1\,dF$ is zero, so that the equations pass into:

$$E\,\varepsilon_1\,F=0$$

$$\frac{E}{r}\int_F [v_1+\omega_1\,y]\,y\,dF=0$$

from which we derive:

$$\varepsilon_1=0 \qquad \omega_1=-\frac{\int_F v_1\,y\,dF}{\int_F y^2\,dF}.$$

With these values σ_1 becomes

$$\sigma_1=\frac{E}{r}\left[v_1-\frac{\int_F v_1\,y\,dF}{\int_F y^2\,dF}\,y\right].$$

As a matter of course we replace the integrals $\int_F v_1\,y\,dF$ and $\int_F y^2\,dF$ by the sums $\Sigma\,v_1\,y\,\triangle F$ and $\Sigma\,y^2\,\triangle F$, where $\triangle F$ stands for the meridional surface of a segment of the length s.

The product $v_1\,y$, the sums $\frac{1}{4}\Sigma\,v_1\,y\,\triangle F$ and $\frac{1}{4}\Sigma\,y^2\,\triangle F$ and the expression

$$v_1^*=v_1-\frac{\Sigma\,v_1\,y\,\triangle F}{\Sigma\,y^2\,\triangle F}\,y$$

can be read from the columns 20—23 of table I.

The introduction of the stress systems

$$\sigma_1=\frac{E}{r}\,v_1^*$$

in the endplanes V_1 and V_2 unfortunately does not bring our problem to an end. For the forces $\sigma_1\,\triangle F$ in two corresponding elements of the planes V_1 and V_2 include an angle $d\psi$, and therefore produce a resultant force

$$\sigma_1\,\triangle F\,.\,d\psi$$

in the direction of the negative y-axis.

Consequently the ring is submitted to a new flexure due to forces P_{2y}

TABLE II. 2nd iteration.

1	2	3	4	5	6	7	8	9	10	11	12	13	14	15	16	17	18
joint	x	y	Δx	Δy	$P_{2y} = -\frac{E}{r^2}\Delta F\, v_1^*$	K_{2y}	$K_{2y}\Delta x$	M_2^*	M_2^{**}	M_2	$\Delta\varphi_2$	φ_2	$\Delta v_2 = -\varphi_2\Delta x$	v_2	$v_2 y \Delta F$	$\frac{\Sigma v_2 y \Delta F}{\Sigma y^2 \Delta F} y$	$v_2^* = v_2 - \frac{\Sigma v_2 y \Delta F}{\Sigma y^2 \Delta F} y$
0	0	262			−1703			0	−1972	−1972	− 986			−2331	−305	−1490	−841
			75	− 1		1703	128					− 986	74				
1	75	261			−3164			128	−1973	−1845	−1845			−2257	−589	−1485	−772
			75	− 3		4867	365					−2831	212				
2	150	258			−2457			493	−1973	−1480	−1480			−2045	−528	−1468	−577
			75	− 6		7324	549					−4311	323				
3	225	252			−1364			1042	−1973	− 931	− 931			−1722	−434	−1433	−289
			75	− 9		8688	652					−5242	393				
4	300	243			− 94			1694	−1973	− 279	− 279			−1329	−323	−1382	53
			74	−11		8782	650					−5521	409				
5	374	232			1434			2344	−1972	372	372			− 920	−213	−1320	400
			74	−17		7348	544					−5149	381				
6	448	215			2858			2888	−1973	915	915			− 539	−116	−1223	684
			70	−28		4490	314					−4234	296				
7	518	187			3741			3202	−1973	1229	1229			− 243	− 45	−1064	821
			58	−49		749	43					−3005	174				
8	576	138			3467			3245	−1973	1272	1272			− 69	− 10	− 785	716
			36	−65		−2718	−98					−1733	62				
9	612	73			2055			3147	−1973	1174	1174			− 7	− 1	− 415	408
			12	−73		−4773	−57					− 559	7				
10	624	0			0			3090	−1972	1118	559			0	0	0	0
								$\Sigma = 19728$							$\Sigma = -2564$		
	$10^{-3}\alpha$	$10^{-3}\alpha$	$10^{-3}\alpha$	$10^{-3}\alpha$	$10^{-5}\frac{E}{E^*}\frac{s^2h}{I r^2}\frac{\alpha^5}{\beta^2\gamma^2}p$	$10^{-5}\frac{E}{E^*}\frac{s^2h}{I r^2}\frac{\alpha^5}{\beta^2\gamma^2}p$	$10^{-5}\frac{E}{E^*}\frac{s^2h}{I r^2}\frac{\alpha^6}{\beta^2\gamma^2}p$	$10^{-5}\frac{E}{E^*}\frac{s^2h}{I r^2}\frac{\alpha^6}{\beta^2\gamma^2}p$	$10^{-5}\frac{E}{E^*}\frac{s^2h}{I r^2}\frac{\alpha^6}{\beta^2\gamma^2}p$	$10^{-5}\frac{E}{E^*}\frac{s^3h}{I r^2}\frac{\alpha^7}{\beta^5\gamma^2}p$	$10^{-5}\frac{E}{E^*}\frac{s^3h}{I r^2}\frac{\alpha^7}{\beta^5\gamma^2}p$	$10^{-5}\frac{E}{E^*}\frac{s^3h}{I r^2}\frac{\alpha^8}{\beta^5\gamma^2}p$	$10^{-5}\frac{E}{E^*}\frac{s^3h}{I r^2}\frac{\alpha^8}{\beta^5\gamma^2}p$	$10^{-5}\frac{E}{E^*}\frac{s^4h^2}{I r^2}\frac{\alpha^{10}}{\beta^4\gamma^2}p$	$10^{-5}\frac{E}{E^*}\frac{s^3h}{I r^2}\frac{\alpha^8}{\beta^5\gamma^2}p$	$10^{-5}\frac{E}{E^*}\frac{s^3h}{I r^2}\frac{\alpha^8}{\beta^5\gamma^2}p$

TABLE III. 3nd iteration.

1	2	3	4	5	6	7	8	9	10	11	12	13	14	15	16	17	18
joint	x	y	Δx	Δy	$P_{3y} = -\frac{E}{\tau^2}\Delta F v_2^*$	K_{3y}	$K_{3y}\Delta x$	M_3^*	M_3^{**}	M_3	$\Delta\varphi_3$	φ_3	$\Delta v_3 = -\varphi_2\Delta x$	v_3	$v_3 y\Delta F$	$\frac{\Sigma v_3 y\Delta F}{\Sigma y^2\Delta F} y$	$v_3^* = v_3 - \frac{\Sigma v_3 y\Delta F}{\Sigma y^2\Delta F} y$
0	0	262			420			0	4610	4610	2305			5329	698	3388	1941
			75	— 1		— 420	— 315					2305	—173				
1	75	261			772			— 315	4610	4295	4295			5156	1346	3375	1781
			75	— 3		—1192	— 894					6600	—495				
2	150	258			577			—1209	4609	3400	3400			4661	1203	3336	1325
			75	— 6		—1769	—1327					10000	—750				
3	225	252			289			—2536	4610	2074	2074			3911	986	3258	653
			75	— 9		—2058	—1544					12074	—906				
4	300	243			— 53			—4080	4610	530	540			3005	730	3142	— 137
			74	—11		—2005	—1484					12604	—933				
5	374	232			—400			—5564	4610	— 954	— 954			2072	481	3000	— 928
			74	—17		—1605	—1188					11650	—862				
6	448	215			—684			—6752	4609	—2143	—2143			1210	260	2780	—1570
			70	—28		— 921	— 645					9507	—665				
7	518	187			—821			—7397	4610	—2787	—2787			545	102	2418	—1873
			58	—40		— 100	— 58					6720	—390				
8	576	138			—716			—7455	4610	—2845	—2845			155	21	1784	—1629
			36	—65		616	221					3875	—140				
9	612	73			—408			—7234	4610	—2624	—2624			15	1	944	— 929
			12	—73		1024	123					1251	— 15				
10	624	0			0			—7111	4609	—2502	—1251			0	0	0	0
								$\Sigma = -45097.5$							$\Sigma = 5828$		
		$10^{-3}\alpha$	$10^{3}\alpha$	$10^{-3}\alpha$	$10^{-5}\frac{E^2}{E^{*2}}\frac{s^4h^2}{\bar{I}^2 r^4}\overline{\beta^4}_{,\gamma^4} P^{\alpha^9}$	$10^{5}\frac{E^2}{E^{*2}}\frac{s^4h^2}{\bar{I}^2 r^4}\overline{\beta^4}_{,\gamma^4} P^{\alpha^9}$	$10^{-6}\frac{E^2}{E^{*2}}\frac{s^4h^2}{\bar{I}^2 r^4}\overline{\beta^4}_{,\gamma^4} P^{\alpha^{10}}$	$10^{-6}\frac{E^2}{E^{*2}}\frac{s^4h^2}{\bar{I}^2 r^4}\overline{\beta^4}_{,\gamma^4} P^{\alpha^{10}}$	$10^{6}\frac{E^2}{E^{*2}}\frac{s^4h^2}{\bar{I}^2 r^4}\overline{\beta^4}_{,\gamma^4} P^{\alpha^{10}}$	$10^{-6}\frac{E^2}{E^{*3}}\frac{s^5h^2}{\bar{I}^3 r^4}\overline{\beta^4}_{,\gamma^4} P^{\alpha^{10}}$	$10^{-6}\frac{E^2}{E^{*3}}\frac{s^5h^2}{\bar{I}^3 r^4}\overline{\beta^4}_{,\gamma^4} P^{\alpha^{11}}$	$10^{-6}\frac{E^2}{E^{*3}}\frac{s^5h^2}{\bar{I}^3 r^4}\overline{\beta^7}_{,\gamma^4} P^{\alpha^{11}}$	$10^{-6}\frac{E^2}{E^{*3}}\frac{s^5h^2}{\bar{I}^3 r^4}\overline{\beta^7}_{,\gamma^4} P^{\alpha^{12}}$	$10^{-6}\frac{E^2}{E^{*3}}\frac{s^5h^2}{\bar{I}^3 r^4}\overline{\beta^7}_{,\gamma^4} P^{\alpha^{12}}$	$10^{-6}\frac{E^2}{E^{*3}}\frac{s^6h^3}{\bar{I}^3 r^4}\overline{\beta^6}_{,\gamma^4} P^{\alpha^{10}}$	$10^{-6}\frac{E^2}{E^{*3}}\frac{s^5h^2}{\bar{I}^3 r^4}\overline{\beta^7}_{,\gamma^4} P^{\alpha^{12}}$	$10^{-6}\frac{E^2}{E^{*3}}\frac{s^5h^2}{\bar{I}^3 r^4}\overline{\beta^7}_{,\gamma^4} P^{\alpha^{12}}$

parallel to the y-axis of the magnitude (pro unit of surface):

$$P_{2y} = -\frac{\sigma_1 \triangle F\, d\psi}{r\, d\psi} = -\frac{E \triangle F}{r^2} v_1^* .$$

The displacements v_2 caused by this load can be calculated after the scheme of table I (see table II, column 1—15). They renew the problem in as far as they are responsible for a new distortion of the endplanes V_1 and V_2. Therefore a new set of normal stresses has to be introduced in these planes, which on their part give rise to other displacements v_3 a.s.o.

If the process of iteration herewith described, converges, we get three series of quantities M_i, ω_i, σ_i, which summed up, give rise to the ultimate bending moment M, the ultimate ω_0, and the ultimate tangential stress σ.

As will be seen from the two tables II, III, the set of values M_3 is nearly proportional to the set of values M_2.

Therefore the iteration needs not to be continued any longer; for if we put $M_3 : M_2 = \lambda$, obviously $M_4 : M_3$ will be λ too, a.s.o. so that

$$M = M_1 + M_2 + M_3 + \ldots = M_1 + M_2 + \frac{M_3}{1-\lambda}.$$

Analogous remarks hold for ω and σ.

5. *Numerical results.* It follows from table I, II and III that

$$\omega_1 = -\frac{\Sigma v_1 y \triangle F}{\Sigma y^2 \triangle F} = -\frac{13014}{4508} \cdot \frac{10^{-1} \cdot s\alpha^3}{E^* I \beta^3} p = -0{,}2887 \frac{s\alpha^3}{E^* I \beta^3} p$$

$$\omega_2 = -\frac{\Sigma v_2 y \triangle F}{\Sigma y^2 \triangle F} = +\frac{2564}{4508} \cdot \frac{10^{-1} E s^3 h \alpha^7}{E^* I^2 r^2 \beta^5 \gamma^2} p = 0{,}05688 \frac{s\alpha^3}{E^* I \beta^3} \cdot \frac{E s^2 h \alpha^4}{E^* I r^2 \beta^2 \gamma^2} p$$

$$\omega_3 = -\frac{\Sigma v_3 y \triangle F}{\Sigma y^2 \triangle F} = -\frac{5828}{4508} \cdot \frac{10^{-2} E^2 s^5 h^2 \alpha^{11}}{E^{*2} I^3 r^4 \beta^7 \gamma^4} p = -0{,}01293 \frac{s\alpha^3}{E^* I \beta^3} \cdot \left[\frac{E s^2 h \alpha^4}{E I r^2 \beta^2 \gamma^2}\right]^2 p$$

$$\lambda = \frac{\omega_3}{\omega_2} = -\frac{0{,}01293}{0{,}05688} \cdot \frac{E s^2 h \alpha^4}{E^* I r^2 \beta^2 \gamma^2} .$$

With $r = 3{,}15$ cm, $h = 0{,}06$ cm, $s = 0{,}075$ cm, $E = 10^6$ kg/cm² (the data of the pressure gauge under consideration), we find:

$$\omega = \omega_1 + \omega_2 + \frac{\omega_3}{1-\lambda} = \left[-1{,}127 + 0{,}3933 \frac{\alpha^4}{\beta^2 \gamma^2} - \frac{0{,}1584 \left(\frac{\alpha^4}{\beta^2 \gamma^2}\right)^2}{1 + 0{,}403 \frac{\alpha^4}{\beta^2 \gamma^2}}\right] \cdot 10^{-3} \frac{\alpha^3}{\beta^3} p.$$

For the standard pressure gauge itself, we get — putting $\alpha = \beta = \gamma = 1$ —

$$\omega = 0{,}8465 \cdot 10^{-3} p.$$

Experiments made on this gauge gave

$$\omega = 0{,}7260 \,.\, 10^{-3}\, p.$$

The agreement of both results is quite satisfactory, and probably would have still been better if we had used the real modulus of elasticity instead of the standard value 10^6 kg/cm^2.

For the moment M we get in a similar manner:

$$M = \left[M_1 + 0{,}1772 \frac{\alpha^4}{\beta^2 \gamma^2} M_2 + \frac{0{,}0314 \left(\frac{\alpha^4}{\beta^2 \gamma^2} \right)^2}{1 + 0{,}403 \frac{\alpha^4}{\beta^2 \gamma^2}} M_3 \right] 10^{-4} \alpha^2 p.$$

In this formula the values of M_1, M_2, M_3, following from table I, II, III, for the point (i) have to be substituted if the total bending moment at this point (i) is required. The greatest bending stress σ_b is given by

$$\sigma_b = \frac{M}{\frac{1}{6} h^2 \beta^2} = \frac{10^4 M}{6 \beta^2}.$$

Finally the total tangential normal stress is given by

$$\sigma_t = \frac{E}{\gamma r} \left[v_1^* + 1{,}772 \frac{\alpha^4}{\beta^2 \gamma^2} v_2^* + \frac{0{,}314 \left(\frac{\alpha^4}{\beta^2 \gamma^2} \right)^2}{1 + 0{,}403 \frac{\alpha^4}{\beta^2 \gamma^2}} v_3^* \right] \frac{10^{-5}\, s \alpha^4}{E^* I \beta^3} p.$$

Again the values v_1^*, v_2^*, v_3^* following from table I, II, III for the point (i) have to be substituted in this formula if the total tangential stress at this point (i) is required.

To conclude we reproduce in table IV the stress distribution of the standard gauge, characterized by the parameters $\alpha = \beta = \gamma = 1$.

The columns 1, 2, 3 contain the values M_1, M_2 and M_3: $(1 - \lambda)$; the value of λ used in the third column agrees with the value of λ, used with the quantity ω $\left(\lambda = -\frac{0{,}01293}{0{,}05688} = -0{,}403\right)$. The total moment M is inserted in column 5. The common multiplying factor of all columns 2—5 is 10^{-4} p. The quantities occurring in the following columns are expressed in kg/cm^2, and relate to the pressure $p = 60$ kg/cm^2, for which the gauge was said to be designed. Column 6 gives the greatest bending stress, column 10 the total tangential stress as a sum of the stresses σ_1, σ_2 and σ_3 : $(1 - \lambda) = \sigma_3 : 1{,}403$, and column 11 the so-called "ideal" stress, which is equal to the absolute value of the difference of the extreme principal stresses. In calculating this stress, it must be observed, that σ_b (column 6) bas been calculated for the outer surface of the gauge, and that an equal bending stress, but of opposite sign, occurs at the inner surface. From two

corresponding points of the outer and inner surface, *that* point is to be considered as the most dangerous one, for which the difference of the two

TABLE IV.

1	2	3	4	5	6	7	8	9	10	11
	M_1	M_2	$\frac{M_3}{1{,}403}$	M	σ_b	σ_1	σ_2	$\frac{\sigma_3}{1{,}403}$	σ_t	$\sigma_{id.}$
0	722	—349	103	476	4760	2534	—1109	323	1748	6508
1	697	—327	96	466	4660	2354	—1018	286	1622	6282
2	621	—262	76	435	4350	1828	— 761	221	1288	5638
3	494	—165	46	375	3750	1015	— 381	109	743	4493
4	319	— 49	12	282	2820	70	70	— 23	117	2937
5	97	66	—21	142	1420	—1067	527	—154	— 694	2114
6	—170	162	—48	— 56	— 560	—2126	902	—261	—1485	2045
7	—452	218	—62	—296	—2960	—2783	1082	—312	—2013	4973
8	—689	225	—64	—528	—5280	—2580	944	—271	—1907	7187
9	—836	208	—59	—687	—6870	—1529	538	—155	—1146	8016
10	—884	198	—56	—742	—7420	0	0	0	0	7420
	$10^{-4}p$	$10^{-4}p$	$10^{-4}p$	$10^{-4}p$						

extreme principal stresses is the greater; and it is seen at once that this is the point for which σ_b and σ_t have opposite signs. With this remark in mind the absolute value of σ_{id} is obtained by adding the corresponding *absolute* values of σ_b and σ_t.

A glance at column 11 learns that very high stresses indeed occur, and that the manifold ruptures of pressure-gauges which are registered in practice, are in full accordance with what has to be expected. It is worth while to state, that the greatest ideal stress occurs in the neighbourhood of point 10, and not in the point 10 itself, which is in full agreement with the experiment.

Finally it must be remarked that our calculations only hold for gauges, the cross section of which is similar to that of our standard gauge. To get reliable results for other cross sections, the calculations given here are to be repeated.

Medicine. — *A new form of position nystagmus.* By D. VON DEVIVERE and A. DE KLEYN.

(Communicated at the meeting of September 27, 1941.)

Position nystagmus is a nystagmus, developing when a certain position of the head exists; this can be a position of the head in space or a position of the head with relation to the trunk [1]). In such cases the stimulations caused by that special position are nearly always sufficient to elicit a nystagmus.

Only a few cases exist where the nystagmus also develops when a certain position of the head is present but where this position must be accompanied by another stimulation.

In 1936 this phenomenon was observed for the first time in a patient of 38 years of age. Therefore the medical history of this patient will be recorded somewhat more extensively. Owing to some circumstances the examination was not complete, however.

Mrs. B. consulted the clinic on October 26th 1936. She stated the following previous history:

Since August 1936 she suffered from dizziness as soon as she lay down. *It appeared that these attacks only developed when the patient turned to her left side after having lain on the right side for some time.* No dizziness developed when the patient, in dorsal position, turned immediately to the left lateral position, or, when in sitting position, turned the head to the right.

She had always been in good health and the previous medical history showed no abnormalities except the fact that about a year ago the patient had suddenly become dizzy on a station, which she did not remember, however.

The above-mentioned attacks of dizziness being of short duration, were not accompanied by nausea.

Present history: Internal examination: no abnormalities except a congenital vitium cordis. Both the WASSERMANN reaction and the reaction of SACHS GEORGI were negative. The blood-pressure was low (105/70); the blood-picture and sedimentation rate were normal. The basal metabolism was –18 %.

Neurological examination: The fundi showed no abnormalities. Sometimes the abdominal reflexes were absent, on other occasions these could be elicited. The BABINSKI reflex was present on the right, though not constantly. No further abnormalities, the lumbar fluid was completely normal.

Acoustic examination: The whispering voice was heard bilaterally at a normal distance.

Vestibular examination: No spontaneous nystagmus in different directions (patient in dorsal or sitting position); no spontaneous past-pointing, no abnormalities when walking with closed eyes, during test of ROMBERG, etc.

Post-rotation nystagmus: horizontal nystagmus:
10 × to the right, 28 movements in 20″
10 × to the left, 34 movements in 23″.

Stimulation of the right labyrinth, either with cold or warm water gave normal results; a typical past-pointing was present.

Contrarily to this stimulation of the left labyrinth, both with cold and warm water, gave no reaction; reactive past-pointing was also absent.

Moreover the following disturbances were found:

On the first examination, a nystagmus with its quick component upward (↑), developed immediately after turning the head backward and then to the left lateral position. As is known this movement causes a disturbance of the circulation in the right arteria verte-

---

[1]) DE KLEYN, A., Proc. Ned. Akad. v. Wetensch., Amsterdam, **44**, 153 (1941).

bralis [2]). The above-mentioned fact could be noticed once again; as for the rest every nystagmus was absent on turning the head backward and then to the right or left lateral position. Yet, under other circumstances, it was quite possible to elicit a nystagmus. Later examination on several days, gave always the following results:

I. No nystagmus developed if the patient (in sitting or dorsal position) turned the head backward and then to the right or left lateral position.

II. When the head of the patient, who was lying on a stretcher for 5 minutes, — either in the right lateral position (the head symmetrically in relation to the trunk) or in dorsal position with the head in the right lateral position — was turned backward and then to the left lateral position, a strong vertical nystagmus upward developed immediately, lasting for 14". Sometimes this nystagmus was combined with a rotatory nystagmus.

III. No nystagmus developed if the head was kept in the right lateral position for 5 minutes and after this turned backward and to the right lateral position.

IV. If the patient was completely or only with the head in the left lateral position, no nystagmus developed. The same thing took place if the patient was in the dorsal position for 5 minutes after which the head was turned backward and to the left lateral position.

That the vertical nystagmus was for the first time observed when the head was turned backward and to the left lateral position accounted for the fact that in further examinations we always brought the head into that position. As mentioned above, a disturbance in the circulation of the arteria vertebralis is then caused. An examination made to see if the nystagmus also developed when the head of the patient or the patient herself was brought into the left lateral position without turning the head backward, thus not causing the disturbances of the circulation in the arteria vertebralis, was omitted, but this development is most probable as, according to the previous history, the attacks of vertigo also developed when the patient lay in bed for some time in the right lateral position and after this turned to the left lateral position.

The complaints gradually diminished in the next half year and then they disappeared completely.

Summary: This patient always showed a vertical nystagmus with its quick component upward, provided she kept her head for some time in the right lateral position after which it was turned backward and to the left lateral position.

It was hardly ever possible to elicit such a nystagmus if the head was immediately turned backward and to the left lateral position, without being kept previously in the right lateral position.

Patient II.

This patient has already been described by one of us [3]). She suffered from a spondylitis tuberculosa. A rotatory horizontal nystagmus to the left developed with the patient in the left lateral position, provided this position was preceded by a right lateral position of the head; the same nystagmus, turned to the right, was seen after a preceding left lateral position of the head with the patient in the right lateral position.

When the head was kept in the dorsal position for some minutes and then turned to the right or left lateral position, no nystagmus developed (for further details see the article in the Conf. Neurol.). Owing to the general condition of the patient an extensive examination could not be performed.

Patient III.

This female achondroplastic patient, 36 years of age, showed, in 1938 symptoms analogous with those of patient I. Her previous history was also typical. *She stated*

---

[2]) DE KLEYN, A. and NIEUWENHUYSE, Acta Oto-Laryng., **11**, 155 (1927).

[3]) DE KLEYN, A., Confinia Neurologia, **2**, 257 (1940).

spontaneously that *the attacks of dizziness only developed if she had been lying in the right lateral position and after this turned to the left lateral position.* The patient also suffered from a bilateral otitis media. Extensive examination proved that a gross long-lasting horizontal nystagmus to the left only developed when the patient (either in symmetric or in non-symmetric position with relation to the trunk) kept her head in the right lateral position for some time (2 minutes or more) and then turned it to the left lateral position. It made no difference if the patient turned completely to the left lateral position or when the trunk remained in the dorsal position and the head was turned to the left lateral position. Such a nystagmus was not seen if the head was first kept in the dorsal position; neither was it seen when the head was kept for some time in the left lateral position and then turned to the right lateral position.

Except a slight horizontal nystagmus to the left in all directions and positions, no other vestibular disturbances were found: the separate forms of post-rotation nystagmus (horizontal, vertical and rotatory) on turning to the right and to the left were symmetric and of equal duration. The tilting reactions of RADEMAKER–GARCIN showed no disturbances.

From the extensive examination we mention the following facts:

Internal examination: no disturbances except a typical achondroplasia.

Extensive neurological examination (Department of Professor BROUWER) gave the following diagnosis: achondroplasia + brachialgia [4]).

Since January 1941 the patient had been admitted again to the neurological Department with a left-sided hemiparesis, probably due to a thrombosis cerebri (arteriosclerosis).

Roentgenological examination: On neither side pneumatisation of the ossa petrosa. Examination of the extremities revealed typical achondroplastic symptoms.

Rhinological examination: no abnormalities.

Acoustic examination: On the right the whispering voice was heard at about 6 metres; there was a small perforation without secretion. On the left the whispering voice was heard ad concham; also on this side a small perforation without secretion was found. The tuning-fork tests were typical for a middle ear affection.

Summary: This patient only developed a definite slow horizontal nystagmus to the left when, after having been in the right lateral position, she turned her head to the left lateral position.

Patient IV.

This patient, 46 years of age, suffered from a middle ear deafness due to a prior otitis media. She now had heavy attacks of turning dizziness with vomiting. Extensive internal, neurological, ophthalmological and roentgenological examination revealed no disturbances except some symptoms of a vasomotoric affection. Vestibular examination proved that the right labyrinth could be more easily stimulated than the left one. Spontaneous nystagmus was absent. A rotatory nystagmus to the left developed if the head, after having been for some minutes in the right lateral position, was brought from this position into the left lateral position; a rotatory nystagmus to the right if the head took the right lateral position after having been in the left lateral position.

Summary: A woman, suffering from attacks of dizziness, developed a rotatory nystagmus in both lateral positions, provided the head had been kept for some time in the opposite direction.

Patient V.

Previous history: 4 weeks before examination, after an influenza the patient developed attacks of turning-dizziness with vomiting. The surroundings seemed to turn in the opposite way of the direction of the hands of the clock. Her gait had become unsteady. Except some childhood diseases she had never had any serious affection until she was

---

[4]) BIEMOND, A., Proc. Kon. Ned. Akad. v. Wetensch., Amsterdam, **42**, 370 (1939) (Patient 2).

21 years of age: she then developed pneumonia with pleuritis; when she was 27 years of age she had typhoid. Information from the "Valeriuskliniek" revealed that in 1934 the patient had a neuritis of the right plexus brachialis which complaints persisted in later years. Family history: no abnormalities.

Internal examination: no disturbances. Reactions of WASSERMANN, SACHS GEORGI and KAHN were negative.

Ophthalmologic examination: no abnormalities.

Neurological examination (Department of Professor Dr. BROUWER): revealed that no distinct symptoms of the right plexus brachialis were present; the following facts, however, were now noted: tongue protruded to the right; hypaesthesia of the right auricle and on the right cheek (which could not be circumscribed).

The lumbar fluid was normal.

The most probable diagnosis was a right-sided neuritis of the plexus brachialis (marked in 1934, scarcely present in 1938) and a neuritis of the cerebral nerves (right vestibularis, right trigeminus, right hypoglossus).

Rhinological examination: no abnormalities.

Acoustic examination: the whispering voice was heard bilaterally at a normal distance. Tuning-fork tests: no abnormalities.

Vestibular examination: neither a spontaneous nor a simple position nystagmus was found. Horizontal post-rotation nystagmus:

10 × to the right, frequent after-nystagmus during 30 minutes, to the left.
10 × to the left: less frequent after-nystagmus during 15 minutes to the right.

Caloric examination of both labyrinths with cold and warm water gave normal reactions and revealed that a distinct "Nystagmusbereitschaft" was present for a nystagmus with its quick component to the left, e.g.:

5 cc. 36° C. right ear: nystagmus to the left.
5 cc. 36° C. left ear: no nystagmus.
5 cc. 39° C. right ear: no nystagmus.
5 cc. 39° C. left ear: nystagmus to the left.

On examination of the singular form of position nystagmus which is the subject of this paper, the following appeared:

I. Patient in dorsal position, head in left lateral position during two minutes: no nystagmus.

II. After this the head was brought into the right lateral position: horizontal-rotatory nystagmus to the left (⇉) preceded by some movements downward (↓).

III. Patient completely in left lateral position during 2 minutes: no nystagmus.

IV. After this patient was brought into the right lateral position: horizontal nystagmus to the left (→), preceded by some movements downward (↓).

V. Patient in right lateral position during two minutes: no nystagmus.

VI. Patient turned in left lateral position: no nystagmus.

VII. Patient in dorsal position during 2 minutes: no nystagmus.

VIII. Head brought into right or left lateral position: no nystagmus.

Summary: In this case the nystagmus could only be elicited when the head was brought into the right lateral position after having been kept for some minutes in the left lateral position.

Summarizing it appears that the common symptom shown by the 5 patients described above, is a position nystagmus developing when the head was brought into a certain lateral position after it had been in the opposite lateral position for some minutes.

This position nystagmus showed different forms: once a horizontal, once a rotatory, once a vertical and once a rotatory-horizontal nystagmus developed while in the last case some vertical movements were followed by some horizontal ones. Of the horizontal and rotatory nystagmus the quick component was in 3 cases directed to the left with

patient in left lateral position, and to the right with patient in right lateral position. In one case (patient V) the nystagmus had its quick component horizontally to the left with the patient in right lateral position. In one case an unaldulterated vertical nystagmus upward was found.

It is very probable that inductive symptoms of SHERRINGTON play an important part in this form of position nystagmus.

To comprehend this symptom the patients must be supposed to have a "Bereitschaft" for a position nystagmus when being in a certain lateral position, e.g. in the left one; however, this mere lateral position offers no sufficient stimulation to elicit the nystagmus. If, however, the opposite (right) lateral position by which the irritability of the antagonistic centra is enlarged (induction of SHERRINGTON) is taken first, the changing to the left lateral position accounts sufficiently for the eliciting of a position nystagmus.

All patients showing the above-mentioned form of position nystagmus were females. However, the number (5) was too small to draw conclusions.

In literature we found only one case [5]) which more or less belonged to this category. In 1916 at the Otological Society of Vienna, VIKTOR URBANTSCHITSCH demonstrated a patient suffering from a chronic purulent discharge of the ear and formation of cholesteatoma together with a fistula symptom which when operated upon proved to be due to a fistula in the horizontal semi-circular canal. Some days after operation patient stated that he became dizzy and nauseated when lying on the right side. Extensive examination by URBANTSCHITSCH revealed the following facts:

Lying in dorsal or left lateral position caused no dizziness. When patient was lying in right lateral position he became dizzy, at the same time a marked rotatory nystagmus could be seen, provided pressure was brought to bear on a small spot at the back of the head near the posterior edge of the processus mastoideus. This nystagmus lasted only 5 seconds, a repeated attempt to elicit this nystagmus was only successful after ¼—½ hour. Simple pressure (Patient in dorsal or sitting position) was not sufficient to cause a nystagmus.

If patient in sitting position strongly inclined the head to the right side, in this way bringing the head into the right lateral position after which pressure was brought to bear on the above-mentioned spot, a nystagmus developed immediately. This was not the case if the pressure was exerted with the head inclined backward or to the left.

This nystagmus cannot be explained merely as a fistula symptom: chloraethyl-anaesthetization of the above-mentioned spot prevented the development of the nystagmus, whereas, as soon as the anaesthetization had ended, the nystagmus could be elicited.

Another entirely analogous case was also recorded by URBANTSCHITSCH. A woman with completely healthy ears (with the head in right lateral position) after pressure on the same above-mentioned place, also developed a rotatory nystagmus [6]); this however, made the sickness so bad, that the patient had to change her position immediately.

URBANTSCHITSCH identifies these cases with those with a reflectory nystagmus, without complaining further why this nystagmus only developed in the right lateral position. His cases in so far agree with the above-mentioned cases that these patients also had a "Nystagmusbereitschaft" with the head in right lateral position, though there exists one difference: in the cases of URBANTSCHITSCH a sensible stimulation was sufficient to cause the nystagmus, whereas in our case this had to be preceded by the opposite lateral position and the accompanying inductive symptoms. The reason why in the cases of URBANTSCHITSCH pressure on a certain spot of the skull was necessary to elicit the nystagmus, has not yet been explained.

---

[5]) URBANTSCHITSCH, V., Monatschr. f. Ohrenheilk., **50**, 199 (1916).

[6]) The direction was not mentioned.

Physics. — *Recherches sur quelques phénomènes d'interférence des courbes de vibration.* (Suite.) Par J. W. N. LE HEUX. (Communicated by Prof. P. ZEEMAN.)

(Communicated at the meeting of September 27, 1941.)

1. Dans l'étude suivante, je me propose de donner une explication de la naissance des franges noires, dites isogyres principales, que l'on observe dans une lame cristalline biaxale, coupée perpendiculairement au 1er diamètre, en lumière convergente et homogène.

Cette explication résulte de l'étude de la courbe générale

$$x = a \cos \alpha \cos \varphi \ , \ y = a \cos (\alpha + \theta) \cos (\varphi + \triangle),$$

déjà publiée dans mes recherches antérieures et ainsi elle diffère de la méthode usuelle, qui s'occupe de la discussion de la formule

$$I = a^2 \sin^2 2 \varphi \sin^2 \frac{\pi d}{\lambda} (n_2 — n_1)$$

exprimant l'intensité de la lumière.

2. Proposition: Apparemment, l'image d'interférence des cristaux biaxials ne montre qu'*un* système de lemniscates.

En réalité, il y a deux systèmes. Chaque exemplaire d'un système coïncide en partie avec deux exemplaires consécutifs de l'autre système. Les parties non-coïncidentes des deux systèmes forment les isogyres principales.

Dans la position normale, les grands axes des lemniscates sont croisés, dans la position diagonale, ils coïncident.

3. Dans un travail antérieur [1]), j'ai fait les deux observations suivantes:

a. L'image des lemniscates se produit par la superposition de deux spirales elliptiques S_1 et S_3 qui satisfont à de certaines conditions.

b. Chacune de ces deux spirales n'est que la moitié d'une courbe de vibration C. Ainsi, la courbe C_1 est composée d'une spirale verticale S_1 et d'une spirale horizontale S_2 et la courbe C_2 est composée de S_3 et S_4. Comme les spirales S_1 et S_2 (et de même S_3 et S_4) sont symétriques par rapport à la bisectrice de l'angle droit des coördonnées et que cette bisectrice est aussi axe de symétrie pour l'image des lemniscates, il s'ensuit que les spirales S_2 et S_4 donneront une image d'interférence, qui coïncide avec l'image des spirales S_1 et S_3.

4. Les images d'interférence furent tracées à l'aide d'un appareil à quatre pendules. Cet appareil permet de dessiner par approximation un système de six ou huit lemniscates, chaque fois que les conditions trouvées sont remplies, mais il ne permet pas (à cause de l'épaisseur des traits d'encre) de dessiner une superposition de deux systèmes de lemniscates, c'est à dire de quatre spirales superposées. Donc, il faut conclure par raisonnement à l'énoncé ci-dessus, concernant la coïncidence des deux systèmes de lemniscates. Cependant, une observation plus exacte révèle deux points de vue nouveaux, savoir:

a. Dans un système de lemniscates, obtenu par la superposition de deux spirales elliptiques, les courbes suivent le mouvement de l'ellipse intérieure à l'ellipse extérieure, c'est à dire, elles semblent tourner d'un angle de 45°.

b. Les spirales S_1 et S_2 peuvent être symétriques par rapport à la bisectrice, mais en général, elles ne le sont pas.

---

[1]) Proc. Kon. Ned. Akad. v. Wetensch., Amsterdam, **43**, N° 1 (1940).

5. Quant à 4a, ce phénomène se présente le mieux, quand l'image d'interférence est composée d'anneaux elliptiques. (Voir Table X, fig. 1.) On voit que le grand axe de l'anneau intérieur est à peu près vertical, tandis que le grand axe de l'anneau extérieur fait un angle de 45° avec le vertical.

Appelons les spirales composantes et verticales S_1 et S_3. Comme nous l'avons dit (3), ces spirales sont les moitiés de deux courbes de vibration C_1 et C_2. Les autres moitiés sont les spirales horizontales S_2 et S_4, qui donneront un système d'anneaux elliptiques, dont l'anneau intérieur est presque horizontal, tandis que l'anneau extérieur coïncide avec celui de C_1 (Table X, fig. 2).

Donc: la superposition de C_1 et C_2 donne deux systèmes d'anneaux croisés, ou, en général, deux systèmes de lemniscates croisées.

6. Quant à 4b, il faut répéter la construction d'une spirale elliptique qui, du reste, confirme le changement de direction des ellipses.

La formule $x = a \cos \alpha \cos \varphi$, $y = a \cos (\alpha + \theta) \cos (\varphi + \triangle)$, qui sert de base à toutes nos recherches, comprend l'ensemble des ellipses $x = \cos \varphi$, $y = \cos (\varphi + \triangle)$

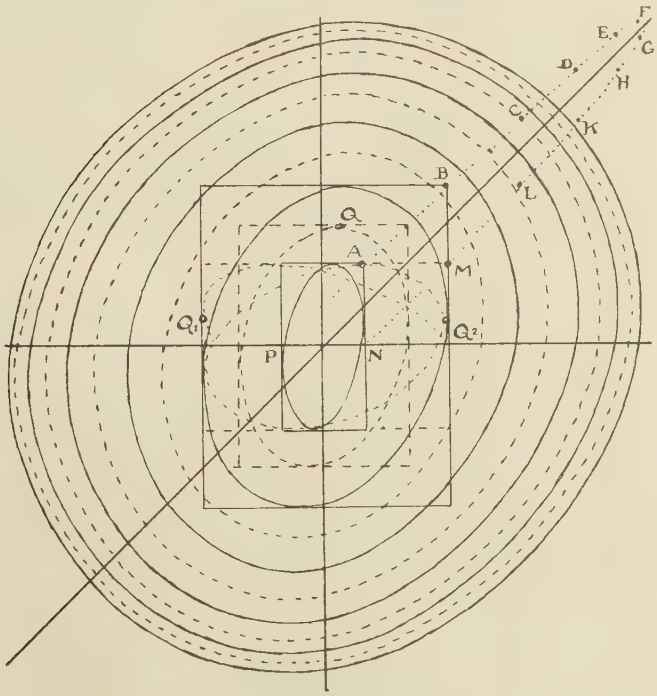

Fig. 17.

($\triangle$ constant) inscrites dans les rectangles sur les doubles coördonnées des points de l'ellipse $x = a \cos \alpha$, $y = a \cos (\alpha + \theta)$ (θ constant) et unies par une courbe continue C_1 ou C_2).

Cette courbe est composée de deux spirales S_1 et S_2.

Les ellipses qui fournissent la spirale S_1 (voir fig. 17) sont inscrites dans les rectangles *A, B, C, D, E* et *F* — les ellipses de la spirale S_2 sont inscrites dans les rectangles *G, H, K, L, M* et *N*.

Les ellipses, symétriques aux dernières par rapport à la bisectrice sont pointillées et l'on voit, qu'elles ne peuvent pas coïncider avec les ellipses tracées.

Il s'ensuit que les deux spirales S_1 et S_2 sont différentes: une est, par manière de dire, la „négative" de l'autre.

Dans le seul cas, où les points de la partie supérieure de l'ellipse $x = a \cos \alpha$, $y = a \cos (\alpha + \theta)$ et les points de la partie inférieure sont choisis de façon à être symétriques par rapport à la bisectrice, on trouvera deux spirales égales S_1 et S_2.

Pour se faire une idée nette d'une courbe C, on peut procéder de la façon suivante. Dessiner toutes les ellipses de la figure 17, copier les ellipses tracées et dessiner la spirale S_1, qui les réunit. De même, sur une autre feuille de papier transparent, copier les ellipses pointillées et dessiner la spirale S_2. Faire incliner cette spirale d'un angle de 90°, puis tourner le papier et faire coïncider les axes. Les deux spirales formeront ainsi une courbe continue.

Pour les spirales S_3 et S_4 (courbe C_2) on peut dire la même chose: en général, ces spirales ne sont pas égales. Surtout, quand elles sont composées d'un très grand nombre d'ellipses, il est permis de dire que la spirale S_4 est la „négative" de la spirale S_3.

Cela posé, nous concluons que l'image d'interférence des spirales S_2 et S_4 sera la „négative" de l'image des spirales S_1 et S_3, c'est à dire: après la petite rotation, déjà mentionnée (5), les anneaux clairs d'une figure coïncideront avec les anneaux obscurs de l'autre (voir Table X, fig. 1 et 2).

7. En combinant ces deux nouvelles observations, celle du changement de direction des exemplaires d'un système et celle de la différence des deux spirales d'une même courbe de vibration, nous trouvons:

l'Image des lemniscates, résultant de la superposition de deux vibrations elliptiques complètes, est composée de deux systèmes de courbes. Chaque exemplaire d'un système est situé entre deux exemplaires consécutifs de l'autre, mais un peu croisé, ce qui admet la possibilité de quatre parties communes. Pour illustrer cet énoncé, les anneaux d'interférence des figures 1 et 2 de la table X sont réunis dans la fig. 3. Les lignes „en zig-zag" des parties non-coïncidentes forment les isogyres principales dans le cas de la position normale.

8. Etudions maintenant l'effet d'une petite rotation de la courbe C_2.

Comme la courbe C_1 est composée des deux spirales S_1 et S_2 et la courbe C_2 des deux spirales S_3 et S_4, nous avons effectué cette rotation par celles des spirales S_3 et S_4, toutes les deux dans le même sens et d'un angle égal (Table X, fig. 4 et 5).

l'Image d'interférence des spirales S_1 et S_3 change un peu et devient une figure, qui est symétrique par rapport à la deuxième bisectrice. l'Image des spirales S_2 et S_4 se comporte de la même manière. Maintenant, les grands axes des anneaux ou des lemniscates coïncident avec la bisectrice. Après avoir réuni les anneaux d'interférence des fig. 4 et 5 dans la fig. 6, on voit qu'après la rotation, les parties coïncidentes sont situées sur les extrémités des deux axes des anneaux. Entre ces parties, on voit de nouveau quatre lignes „en zig-zag", qui forment les isogyres principales dans la position diagonale.

9. Avec la théorie précédente, il devient possible de deviner les parties des courbes, cachées derrière les franges noires dans les photos usuels des phénomènes d'interférence.

Les figures 7, 8, 9 et 10 de la Table X en donnent quelques exemples, empruntés à l'ouvrage de HAUSWALDT [1]).

Fig. 7 et 8, qui sont les plus simples, montrent (en gris) l'image de Sanidine, à droite dans la position diagonale, à gauche dans la position normale. Dans ce dernier cas, il est également possible que la deuxième courbe intérieure est composée de deux ovales.

Dans les fig. 9 et 10 on voit un cas plus compliqué (ammonium — magnésium — phosphate), qui explique la naissance des petits traits, qui traversent les ovales les plus petits dans l'image totale. Un tel ovale, avec son diamètre apparent, consiste donc en réalité en deux ovales, dont un est la moitié de l'autre et qui se touchent à l'intérieur.

---

[1]) Interferenz-Erscheinungen an doppeltbrechenden Krystallplatten im konvergenten polarisirten Licht. Photografisch aufgenommen von HANS HAUSWALDT in Magdeburg. Mit einem Vorwort von TH. LIEBISCH in Göttingen. Magdeburg 1902.

TABLE X

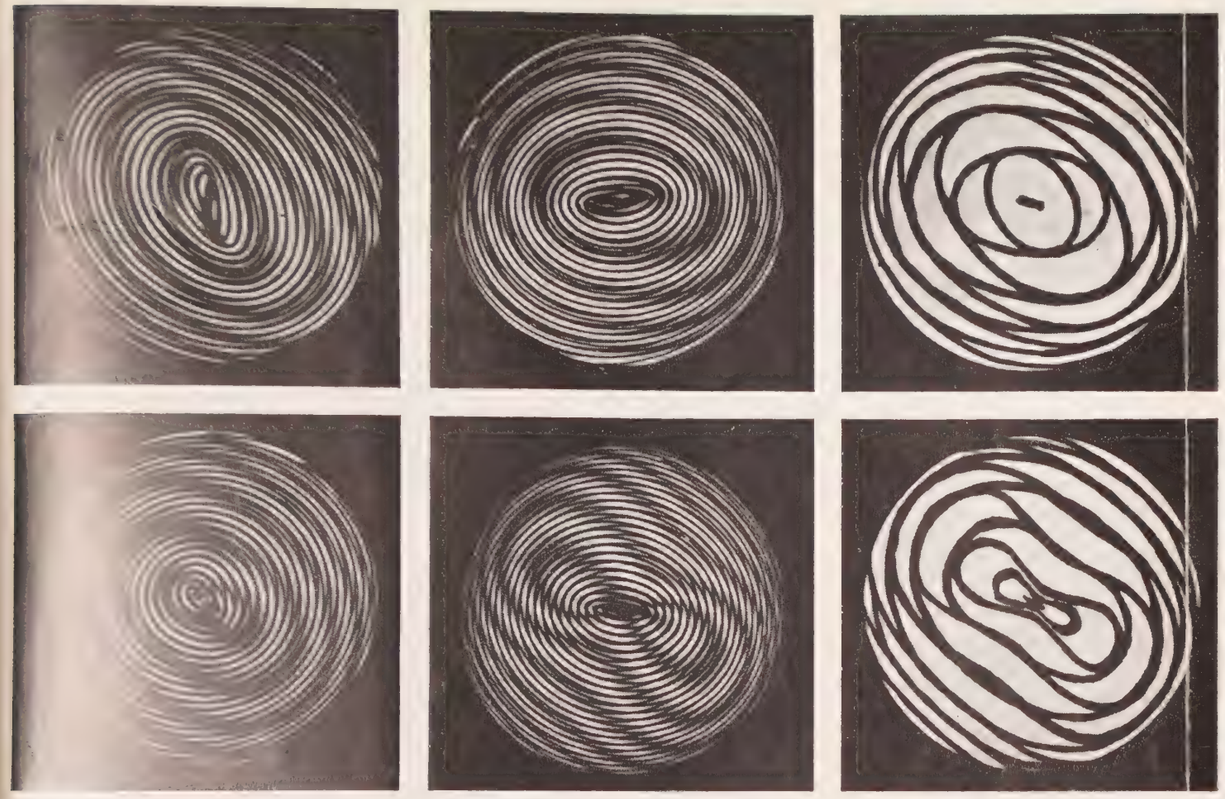

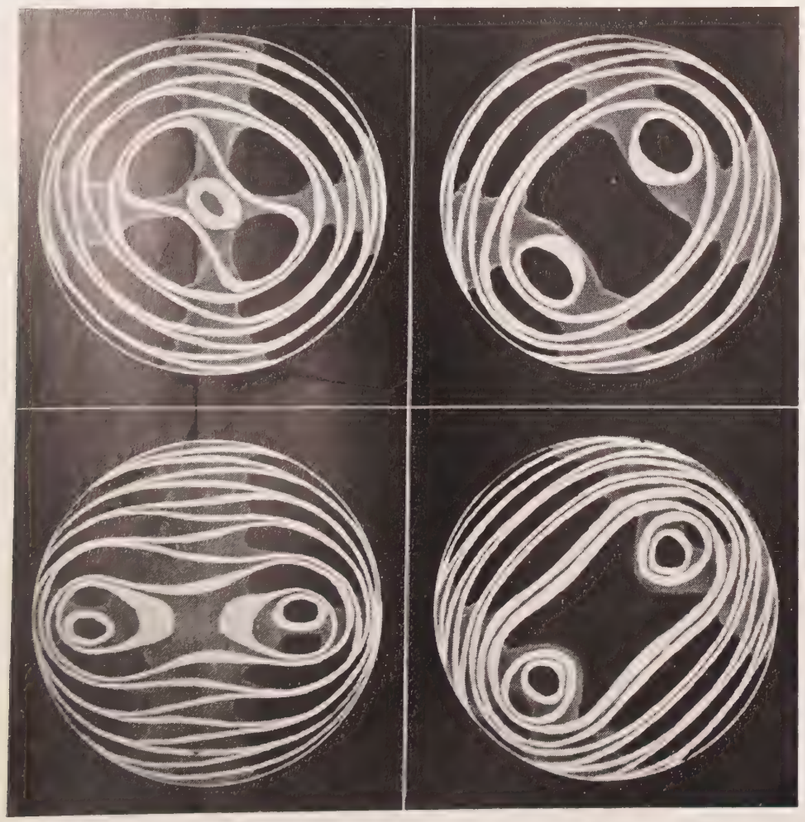

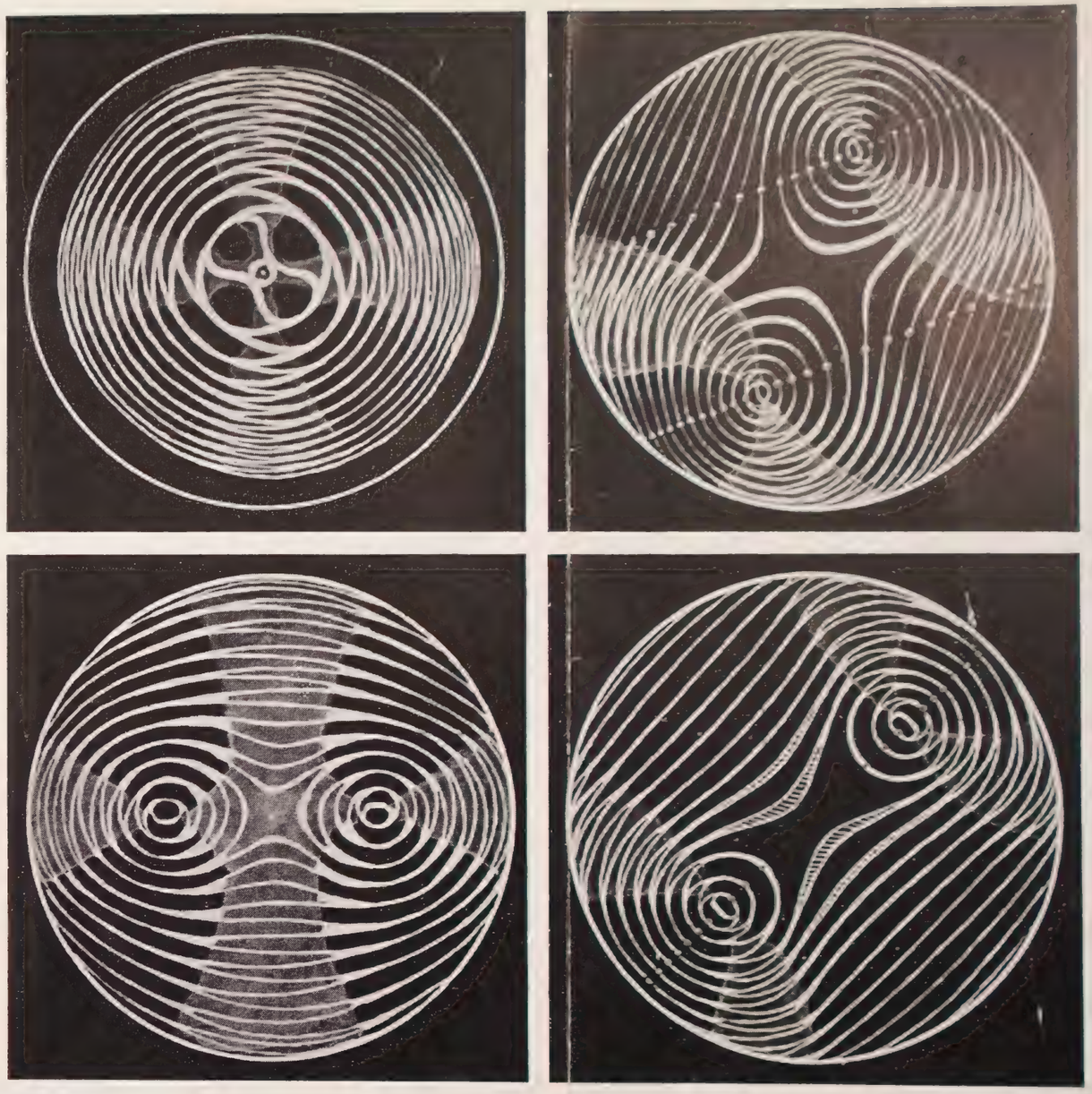

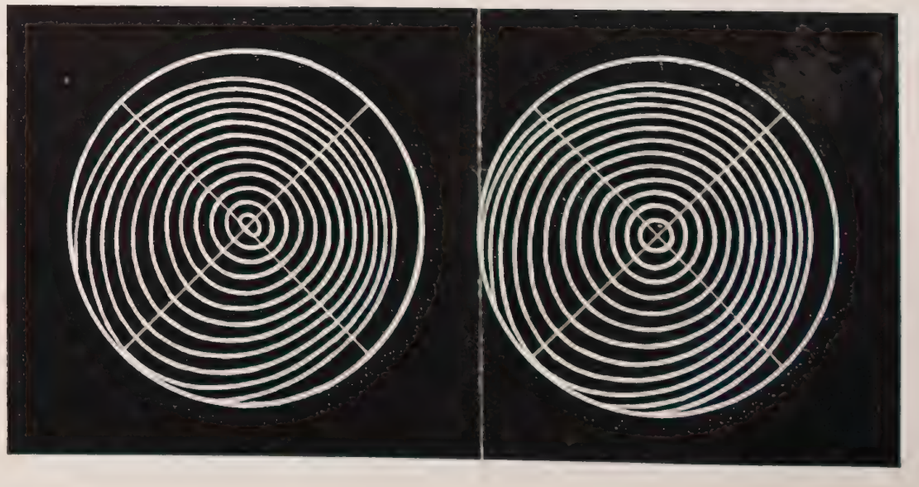

Dans la position normale les traits ne peuvent pas être en ligne droite à cause de la rotation.

Dans les photos, on constatera qu'un est situé plus bas que le prolongé de l'autre.

Les taches blanches font voir que les courbes d'interférence ont une certaine „épaisseur variable", qui dépend de l'angle, sous lequel les spires des spirales se coupent et qui contribue au contour et à l'aire des isogyres.

Fig. 11 de la table XI, zirkonium, est un exemple d'un cristal unaxial, qui ne semble pas se distinguer de la fig. 7.

10. Maintenant, il est possible de dessiner des projets d'un grand nombre d'images d'interférence.

En augmentant le nombre des ovales autour d'un pôle, le dessin ressemble à la construction d'une famille de cercles, dont chaque exemplaire est tangent au précédent et au suivant dans les extrémités d'un diamètre. Pour beaucoup d'ovales, les parties non-coïncidentes formeront les deux franges noires de l'image d'interférence d'un cristal biaxial, coupé sous un angle droit avec une binormale en lumière convergente. J'ai discuté une telle construction dans une étude antérieure [1]) et pour des cercles de rayon $r = a \cos n\,\alpha$ (α très petit). Ici on peut remarquer, qu'en dessinant ces cercles pour les valeurs paires de n et puis séparément pour les valeurs impaires de n, la première figure est „la négative" de l'autre. Par une petite rotation (ou, ce qui revient au même, une petite translation) on voit paraître les lignes „en zig-zag", qui forment les isogyres. En répétant ce dessin pour un deuxième pôle et après avoir dessiné p.e. six ovales, il faut envelopper les deux systèmes de lemniscates. A ce moment, les isogyres, limitées jusqu'ici par des lignes droites, font une courbure et les contours de ces taches noires ressemblent quelque peu à des hyperboles.

Les dessins (fig. 12, 13 et 14) donnent en outre une explication de la variation en épaisseur des courbes que l'on voit en observant les photos des images d'interférence.

Les figures 15 et 16 montrent les deux systèmes d'ovales, qui, par superposition, donnent les deux isogyres de l'image d'une lame de topaze, coupée perpendiculairement à une binormale (position diagonale) [2]).

LITTERATURE.

Pour le problème fondamental:

D. J. KORTEWEG, Verslag Kon. Akad. v. Wet. Amsterdam, Afd. Natuurk. Vol. **5**, No. 8 (1897); Arch. Néerl., Vol. I, série 2, pp. 229—260.

Pour la théorie des courbes-enveloppes:

H. J. E. BETH, Verslag Kon. Akad. v. Wet. Amsterdam, Afd. Natuurk., Vol. **27** et **28** (1919/20); Phil. Mag. Aug. 1913.

Pour les images d'interférence obtenues à l'aide d'un appareil à quatre pendules, les communications suivantes de ma main:

J. W. N. LE HEUX, Verslag Kon. Akad. v. Wet. Amsterdam, Afd. Natuurk., Vol. **23**, No. 8; Vol. **24**, No. 4 et 5; Vol. **25**, No. 3 et 4; Vol. **32**, No. 10 (1929); Vol. **41**, No. 4 (1938); Vol. **43**, No. 1 (1940). Avec la littérature qui s'y rapporte.

---

[1]) Proc. Kon. Ned. Akad. v. Wetensch., Amsterdam, **41**, N°. 4 (1938).

[2]) POCKELS, Kristalloptik, Tafel V, Fig. 1.

Physics. — *The orientation of watermolecules round charged particles.* By J. F. VAN ELTEREN. (Communicated by Prof. J. D. VAN DER WAALS Jr.)

(Communicated at the meeting of September 27, 1941.)

The question is, how watermolecules are arranged round colloidal particles or, generally speaking, round charged particles. We must distinguish between positively and negatively charged particles. No question can arise about the orientation of the watermolecules round the positive particles, for the place of the points of charge in a watermolecule is known [1]). (Fig. 1.) With a positively charged particle the negative pole of the watermolecule will

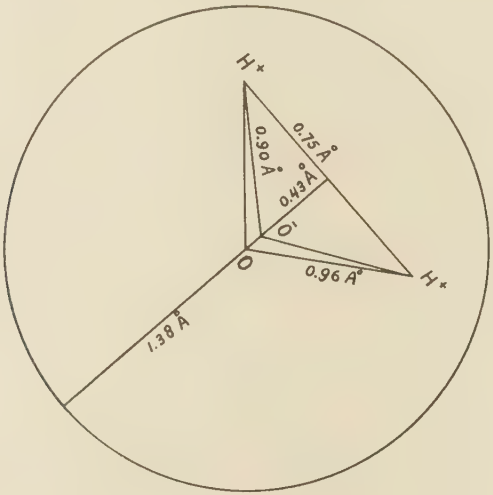

Fig. 1.

be directed to that particle; but both the positive charges are turned away. With negative particles the matter becomes more complicated. It is impossible to say at first sight, what the direction of the watermolecule will be. Two positions are possible, one symmetrical, the other non-symmetrical. In the non-symmetrical position one of the positive charges approaches as near as possible to the charged particle. We can, however, state at once, that in the non-symmetrical position the potential energy will decrease more quickly in proportion to the distance of the centre of the charged particle than in the symmetrical position. For, generally speaking, the potential energy of a dipole in its relation to a charged particle is inversely proportional to the square of the distance, whereas for a quadrupole it is inversely proportional to the cube of the distance. The forces operating between a dipole and a charged particle will cause a symmetrical orientation, but a non-symmetrical orientation in the case of a quadrupole. To show the working of this process, small rounds of blottingpaper, dipped in paraffin, on which little magnets had been placed, were brought on a surface of water. One of the poles of a magnet represented an ion,

[1]) FOWLER–BERNAL, Trans. Far. Soc., **29**, 1049 (1933).

the diameter of which was represented by test-tubes of various sizes. It appeared, (Fig. 2, 3, 4) that with a small ionic radius the non-symmetrical position was stable, and with a greater ionic radius the symmetrical position. Hence it was clear, that between water and single-charged ions both positions were possible.

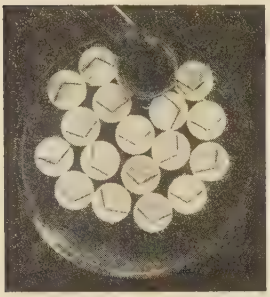

Fig. 2.
negative ion
small ionic radius

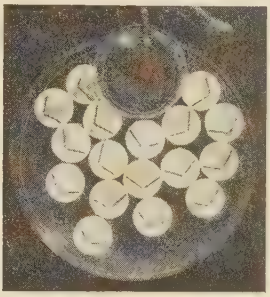

Fig. 3.
negative ion
great ionic radius

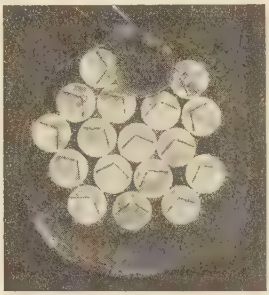

Fig. 4.
positive ion

The potential energy of the watermolecule in relation to a charged particle was computed in dependence on the radius of the charged particle. The result of this computation is shown in the graph. (Fig. 5.) The ionic radii of F, Cl, Br and J, and of K, Na, Rb, Cs are shown on the absciss. From this graph some conclusions may be drawn.

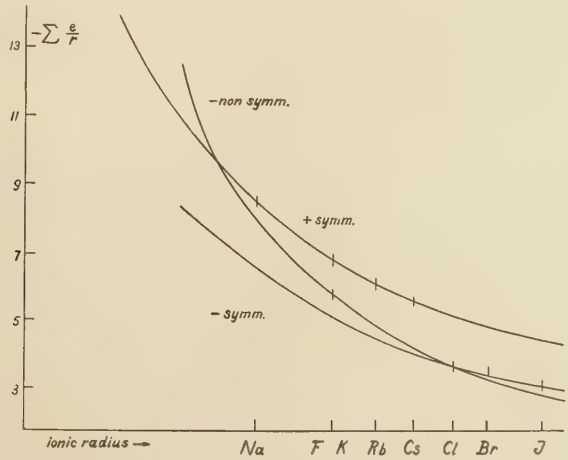

Fig. 5.

The F-ion takes up a peculiar place. In the first layer round the F-ion the watermolecule will take up a non-symmetrical position. In former computations of the hydration-energy this had never been taken into account. The lyotropic numbers are connected with this hydration-energy according to: $I/H = aL + b$. Here H and L are respectively the hydration-energy and the lyotropic number; a and b are constants. It often appears, that the F-ion does not correspond to the linear relation between this lyotropic number and the

effect obtained [2]). The deviations can be explained by the particular position of the watermolecules.

We cannot conclude from this, how their position will be round colloïdal particles. We shall have to give an answer to the question, whether the charge of these colloidal particles must be considered as points of charge which are found on the surface and each of which binds the watermolecules, or whether we are allowed to consider the charge as concentrated in the centre of the colloidal particle.

From the graph it is clear, that in the case of positive particles $-\Sigma e/r$ is greater than in the case of negative ones. In the literature on this subject it is assumed, that with an equal ionic radius negative ions will have a greater hydration-energy than positive ones; for the positive pole of a water dipole is situated nearer to the periphery than the negative one [3]). Exactly the opposite, however, appears from our own computations, as the computed numbers are a measure of this hydration-energy; which is evident from the table. Here the relations to the hydration-energy are shown. Indications of this may also be found in the literature of the colloid-chemistry. E.g. SPEELMAN [4]) states, that in

	$-\Sigma e/r$	H	$-\Sigma e/r/H$
F	5.8	123	0.047
Cl	3.65	84	0.044
Br	3.4	73	0.047
J	3.0	64	0.047

flocculation-experiments with serumalbumen the alcohol number appears as non-symmetrical on both sides of the iso-electric point. With a low p_H, therefore with positively charged particles, the alcohol number is greater than with a high p_H. Which points to a stronger binding of the watermantle to positive particles.

Measurements of viscosity and other properties render a similar result.

SUMMARY.

1. F appears to deviate from Cl, Br and J. Experiments have borne this out.
2. In case of an equal ionic radius positive ions seem to bind the watermolecules more strongly than negative ones.
3. A possibility of computing hydration-energies is offered, in which, of course, the various correcting factors must be taken into account.

In a following article we hope to speak on this subject more at large. My thanks are due to Dr. E. H. BÜCHNER, who suggested the idea on which these considerations are based.

---

[2]) BÜCHNER, Recueil, **59**, 703 (1940).
SARLUY, Thesis, Amsterdam (1940).
[3]) VAN ARKEL en DE BOER, Chemische Binding (1930).
[4]) SPEELMAN, Thesis, Amsterdam (1937).

Chemical Laboratory of the University,
Colloid Chemistry Dept., Amsterdam.

Mathematics. — *„Sätze über topologische Erweiterung von Abbildungen".* By J. DE GROOT. (Communicated by Prof. L. E. J. BROUWER.)

(Communicated at the meeting of September 27, 1941.)

1. *Fragestellung.* Unter einer Erweiterung topologischer Abbildungen versteht man folgendes: man betrachtet eine Punktmenge A eines Raumes und in demselben oder in einem anderen Raume eine mit A homöomorphe Punktmenge A'. Bisweilen ist es jetzt möglich zwei (zu A und A' fremde) Punktmengen B und B' zu finden von der Art, dasz $A+B$ topologisch abzubilden ist auf $A'+B'$, während die durch diese Abbildung induzierte Abbildung von A auf A' mit einer vorgegebenen topologischen Abbildung übereinstimmt. Die Abbildung von A auf A' ist also erweitert zu einer topologischen Abbildung von $A+B$ auf $A'+B'$.

Dieses Problem ist unter verschiedenen Voraussetzungen der Mengen A, B, A' und B' schon wiederholt bearbeitet worden. Ich nenne z.B. die Namen: L. ANTOINE (J. Math. Pures Appl. (8) **4** (1921), S. 221), H. M. GEHMANN (Trans. Am. Math. Soc. **28** (1926), S. 252; **31** (1929), S. 241. Am. J. of Math. **51** (1929), S. 385. Bull. Am. Math. Soc. **42** (1936), S. 79), M. LAVRENTIEFF (Compt. Rend. **178** (1924), S. 187. Fund. Math. **6** (1924), S. 149), S. STOÏLOW (Rev. Math. Union Inter-Balkan **1** (1936), S. 97), H. WOLKENSTÖRFER (Dissertation, München 1929). Man sehe auch die Fusznote auf Seite 3.

1.1. Wir werden im allgemeinen die Terminologie von P. ALEXANDROFF und H. HOPF verwenden [1]).

Unseren Betrachtungen legen wir einen normalen Raum R mit abzählbarer Basis (bisweilen auch den n-dimensionalen Zahlenraum R_n) zugrunde und beschränken das Problem in folgender Weise:

1^0 B ist eine Teilmenge der abgeschlossenen Hülle $\overline{A}$ der Menge A, also $B \subset \overline{A}$. Ebenfalls gilt $B' \subset \overline{A}'$.

2^0 Es soll *jede* topologische Abbildung von A auf A' erweiterungsfähig sein.

2. Der denkbar einfachste Fall ist wohl der, dasz B (bzw. B') nur einen Punkt P (bezw. P') enthält. Es gilt folgender einfacher Satz:

Satz I. *In R sind gegeben zwei (in sich) kompakte Mengen $A+P$ und $A'+P'$; sind A und A' homöomorph, so kann man jede topologische Abbildung van A auf A' erweitern zu einer Abbildung von $A+P$ auf $A'+P'$.*

Beweis. Ist P ein isolierter Punkt der Menge $A+P$, so ist P notwendig isolierter Punkt von $A'+P'$. Sonst würde A kompakt und A' nicht-kompakt sein in widerspruch zur Homöomorphie. Somit liegen beide Punkte isoliert und es ist nichts zu beweisen.

Wir nehmen also an $P \subset \overline{A}$ und $P' \subset \overline{A}'$. Denken wir uns jetzt eine beliebige, aber im Folgenden festgehaltene topologische Abbildung T von A auf A'. Eine gegen P konvergente, zu A gehörige Punktfolge a_i wird abgebildet auf eine Folge $a_i' \subset A'$, welche wenigstens einen Häufungspunkt $Q' \subset A'+P'$ besitzt. Es ist aber $Q' \subset A'$, denn sonst würde es eine gegen Q ($Q \subset A$) konvergente Teilfolge von a_i geben, weil T^{-1} topologisch ist. Es musz also $Q'=P'$ sein.

Das Bild jeder gegen P konvergenten und zu A gehörigen Folge ist somit eine gegen

---

[1]) P. ALEXANDROFF, H. HOPF, Topologie I, Berlin, Springer, 1935.

P' konvergente und zu A' gehörige Folge, und umgekehrt. M. a. W.: das Bild jeder Umgebung von P in der Menge $A+P$ (abgekürzt: $U(P|A+P)$) ist eine $U(P'|A'+P')$, und umgekehrt, wenn die Punkte P und P' einander zugeordnet werden.

2. 1. Fordert man in Satz I statt Kompaktheit zum Beispiel totale Beschränktheit [1]) oder Abgeschlossenheit, so verliert er seine Geltung. Man nehme etwa für $A+P$ den zweidimensionalen Zahlenraum R_2, und setze $A'=A$, $P'=P$, $\varphi'=\varphi$, $r'=\frac{1}{r}$ $(P=0{,}0)$ gibt eine topologische Abbildung von A auf A', welche nicht erweiterbar ist. Ebenso leicht konstruiert man Abbildungen von total-beschränkten, aber nicht abgeschlossenen Mengen aufeinander, welche nicht erweiterungsfähig sind.

2. 2. Betrachten wir jetzt den Fall, dasz die Mengen B und B', jede für sich, endlich viel Punkte enthalten. Das Analogon des Satzes I ist schon unrichtig. Dieser Tatbestand erhellt folgendermaszen: man verbiege ein Dreieck ABC in der Weise, dasz die Punkte B und C zusammenfallen; ein mit ABC kongruentes Dreieck $A'B'C'$ verbiege man in der Weise, dasz A' und B' zusammenfallen. Aus der ersten verbogenen Figur entferne man die Punkte A und B $(=C)$, aus der zweiten C und A $(=B)$. Eine kongruente Abbildung von ABC (ohne Eckpunkte) auf $A'B'C'$ (ohne Eckpunkte) induziert eine topologische Abbildung der beiden soeben konstruierten Figuren. Es leuchtet unmittelbar ein, dasz diese Abbildung sich nicht erweitern läszt zu einer Abbildung der beiden verbogenen Figuren.

Sind aber im n-dimensionalen Zahlenraum R_n die Punkte von B (bzw. B') innere Punkte der Menge $A+B$ (bzw. $A'+B'$) in bezug auf R_n, so gilt

Satz II. *In R_n $(n\geq 2)$ sind gegeben zwei beschränkte abgeschlossene Mengen $A+B$ und $A'+B'$; A und A' sind homöomorph, während B (bzw. B') eine (endliche oder unendliche) isolierte Punktmenge ist, deren Punkte innere Punkte der Menge $A+B$ (bzw. $A'+B'$) in bezug auf R_n sind. Jede topologische Abbildung von A auf A' ist jetzt erweiterbar zu einer Abbildung von $A+B$ auf $A'+B'$.*

Der Beweis folgt nachher.

Dieser Satz gilt nicht für $n=1$, da A und A' in diesem Falle nicht zusammenhängend sind. Man nehme zum Beispiel in R_1 nacheinander die Punkte A, P_1, P_2, B und B', Q_1, Q_2, A'. Das lineare Bild von AP_1 (ohne P_1) sei $A'Q_2$ (ohne Q_2), von P_1P_2 Q_1Q_2, und von P_2B (ohne P_2) Q_1B' (ohne Q_1). Entfernt man aus den Strecken AB und $B'A'$ die Punkte P_1, P_2, Q_1 und Q_2, so hat man durch diese Abbildungen zusammen eine topologische Abbildung der Restmengen aufeinander. Man kann aber nicht die Punkte P und Q einander zuordnen in der Art, dasz die genannte Abbildung erweiterbar ist.

2. 3. Es erhebt sich jetzt die Frage nach Aussagen für den Fall, dasz B und B' allgemeinere Punktmengen sind. In 3 werden wir diese Frage beantworten. B und B' werden dabei nulldimensionale [2]) Punktmengen sein. Für n-dimensionale $(n>0)$ Punktmengen B und B' wird es aber schwer, wenn nicht unmöglich sein, etwas Allgemeines und Positives auszusagen. Wir erläutern diesen Tatbestand an folgendem einfachem Beispiel, wobei B und B' zwei eindimensionale Simplices sind, welche sogar ganz im Inneren der Mengen A und A' liegen. In der gezeichneten Figur sind die beiden von den Rechtecken berandeten Flächenstücke die Mengen $A+B$ und $A'+B'$; B und B' sind die Strecken XY und $X'Y'$. Man konstruiert leicht eine topologische Abbildung von A auf A', bei der das Dreieck SPA (ohne A) übergeführt wird in das Rechteck $S'P'Q'R'$ (ohne $R'Q'$). Diese Abbildung ist aber nicht erweiterbar, denn sie kann nicht einmal eineindeutig sein.

[1]) Eine Menge heiszt total beschränkt, wenn sie sich für jedes $\delta>0$ als Summe endlich vieler Mengen von Durchmessern $\leq\delta$ darstellen läszt.

[2]) Im BROUWER–URYSOHNschen Sinne.

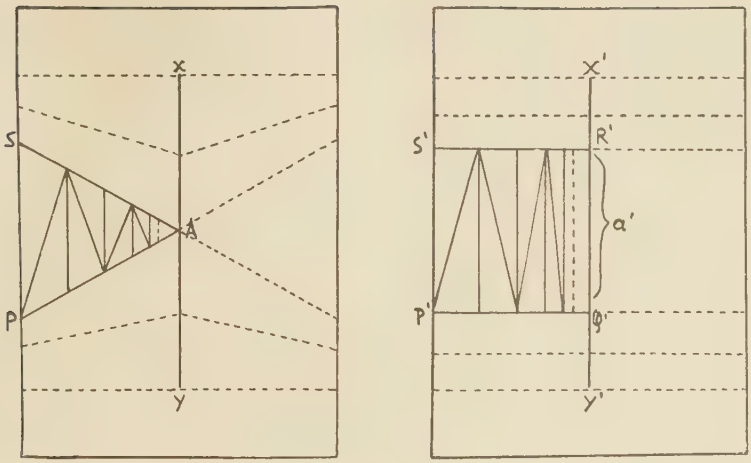

Fig. 1.

3. Wir brauchen folgendes Lemma.

Lemma. In R ist gegeben eine Menge $A+B$; es gilt $B \subset \overline{A}$.

Wenn eine eindeutige Abbildung f von $A+B$ auf eine Menge $A'+B'$ in jedem Punkte von $A+B$ stetig in bezug auf A ist, so ist f eine stetige Abbildung von $A+B$ auf $A'+B'$.

Beweis. f ist eine stetige Abbildung von $A+B$ auf $A'+B'$, wenn es zu jeder Umgebung $U(P'|A'+B')$ eines Punktes $P' \subset A'+B'$ eine Umgebung $U(P|A+B)$ gibt, deren Bild zu der $U(P'|A'+B')$ gehört. Wir dürfen annehmen, dasz die Umgebung $U(P'|A'+B')$ eine abgeschlossene Menge ist. Der Durchschnitt von $U(P'|A'+B')$ und $A'+P'$ ist eine Umgebung $U(P'|A'+P')$. Da f in P stetig in bezug auf A ist, gibt es eine Umgebung $U(P|A+P)$, deren Bild in der $U(P'|A'+P')$ enthalten ist.

Die Menge $U(P|A+P)$ und die Menge der zu $A+B$ gehörigen Häufungspunkte von $U(P|A+P)$ geben zusammen — wie man leicht einsieht — eine Umgebung $U(P|A+B)$. Jede gegen den Punkt $Q \subset A+B$ konvergierende Punktfolge $a_i \subset A$ wird aber abgebildet auf eine gegen Q' konvergierende Folge a'_i. Aus dem Obigen geht also jetzt hervor, dasz das Bild der konstruierten $U(P|A+B)$ zu der $U(P'|A'+B')$ gehört, was zu beweisen war.

Bemerkung. Wenn auszerdem $A+B$ (in sich) kompakt und f eineindeutig ist, so leitet man — mit Hilfe eines bekannten Satzes — sofort ab, dasz f topologisch ist.

3.1. Mit Hilfe dieses Lemma beweisen wir folgenden Satz.

Satz III. *In R sind gegeben zwei kompakte Mengen $A+B$ und $A'+B'$; A und A' sind homöomorph, und es gilt $B \subset \overline{A}$, $B' \subset \overline{A'}$.*

Wenn die Mengen $A+B$ und $A'+B'$ die Eigenschaften 1 und 2 besitzen, so ist jede topologische Abbildung von A auf A' erweiterbar zu einer Abbildung von $A+B$ auf $A'+B'$.

Die Eigenschaften [1]), ausgesprochen für die Mengen A und B, sind:

---

[1]) H. FREUDENTHAL — dem ich an dieser Stelle herzlichst danke für seinen wertvollen Rat — war so freundlich, meine Aufmerksamkeit zu lenken auf seine Dissertation „Ueber die Enden topologischer Räume und Gruppen" (Math. Z.schr. **33** (1931)), insbesondere Satz 7, und auf einen Aufsatz von L. ZIPPIN „On semicompact spaces" (Am. J. of Math.

1. *die Menge A ist zusammenhängend im kleinen in der Nähe der Menge B. Das heiszt: für jeden Punkt $P \subset B$ gibt es beliebig kleine Umgebungen $U(P|A)$, welche zusammenhängend sind* [1]).
2. *B ist eine nulldimensionale Punktmenge (zum Beispiel: B ist eine diskontinuierliche F_σ-Menge* [2])).

Beweis. Wenn B nulldimensional ist, so gibt es offenbar zu jedem Punkt $P \subset B$ beliebig kleine (offene) Umgebungen $U(P|R)$, deren Begrenzungen keine Punkte von B enthalten.

Unser Ziel ist jetzt zu beweisen, dasz eine beliebige Umgebung $U(P|A+P)$ eines Punktes $P \subset B$ übergeführt wird in eine $U(P'|A'+P')$, wenn wir eine gewisse topologische Abbildung von A auf A' betrachten, und die Punkte $P \subset B$ und $P' \subset B'$ einander in geeigneter Weise zuordnen. Wir brauchen dazu folgenden bekannten Satz: Wenn eine zusammenhängende Menge S sowohl mit der offenen Menge U wie auch mit der Menge $R-U$ wenigstens einen Punkt gemein hat, so hat S wenigstens einen Punkt mit der Begrenzung von U gemeinsam.

Eine beliebige $U'(P|A+P)$ ist Durchschnitt von $A+P$ und einer $U'(P|R)$. Wir nehmen eine (offene) $U(P|R)$ mit $U(P|R) \subset U'(P|R)$, deren Begrenzung G zu B fremd ist. Der Durchschnitt von $U(P|R)$ und $U'(P|A+P)$ ist wieder eine $U(P|A+P)$.

G und $A+B$ sind abgeschlossene Mengen; die Menge $N=(A+B)\cdot G$ ist also ebenfalls eine (vielleicht leere) abgeschlossene Menge. Das Bild $N' \subset A'$ ist wieder abgeschlossen.

Betrachten wir eine zu $U(P|A+P)$ gehörige und gegen P konvergente Punktfolge a_i. Die Bildfolge a_i' hat wenigstens einen Häufungspunkt P' mit $P' \subset B'$. Wir ordnen P' dem Punkte P zu (später wird hervorgehen, dasz P diesen Punkt P' eindeutig bestimmt). Angenommen, das Bild von $U(P|A+P)$ sei keine Umgebung $U(P'|A'+P')$; dann gibt es in jeder Nähe von P' einen Punkt $Q' \subset A'$, der nicht zum Bilde von $U(P|A+P)$ gehört. Der Originalpunkt Q von Q' gehört also nicht zu $U(P|A+P)$ und auch nicht zu $U(P|R)$, weil Q zu A gehört. Wegen Eigenschaft 1 gibt es beliebig kleine zusammenhängende Umgebungen $U(P'|A')$. Wir wählen diese $U'(P'|A')$ in der Weise, dasz der Durchschnitt von $U(P'|A')$ und N' leer ist (die Menge N' ist abgeschlossen!).

In $U(P'|A')$ liegt ein Punkt Q' der oben erwähnten Art und ein Punkt a_k'; diese beiden Punkte sind also verbunden durch die Menge $U(P'|A')$. Die inverse topologische Abbildung bildet $U(P'|A')$ ab auf eine zusammenhängende Menge $M \subset A$, welche Q und a_k enthält. Es gilt offenbar $Q \subset R-U(P|R)$, $a_k \subset U(P|R)$; M hat also wenigstens einen Punkt mit N gemeinsam in Widerspruch zu der Tatsache, dasz das Bild $U(P'|A')$ von M keinen

---

57 (1935)), welcher Erweiterungen von FREUDENTHALs Arbeit enthält. Durch ZIPPIN wird u.a. ein Satz abgeleitet, welcher, an Stelle der Bedingungen 1 und 2, die folgenden Bedingungen fordert: *a.* A ist zusammenhängend; *b.* A ist im kleinen zusammenhängend; *c.* B ist eine diskontinuierliche F_σ-Menge; *d.* B ist „totally avoidable", d.h. in jeder zusammenhängenden, in $A+B$ offenen Menge D mit $D \subset A+B$ ist $D\cdot A$ zusammenhängend. Aus diesen vier Bedingungen sind sofort die Bedingungen 1 und 2 abzuleiten; das Umgekehrte ist aber nicht der Fall. Tatsächlich ist es möglich, Beispiele ausfindig zu machen, welche den Anforderungen 1 und 2, aber nicht *a* und (oder) *b* entsprechen. Unser Satz III sagt also wesentlich Neues aus.

Von diesem Berührungspunkt abgesehen kann man ZIPPINs und unsere Resultate nicht miteinander vergleichen, da wir verschiedene Ausgangspunkte und Ziele haben.

[1]) Man bemerke, dasz $U(P|A)$ den Punkt P nicht enthält.

[2]) $F_\sigma = \sum_n F_n$, jedes F_i abgeschlossen. Eine abzählbare Menge ist z.B. ein F_σ.

Ein diskontinuierliches F_σ ist eine nulldimensionale Menge, denn jede Menge F_i ist eine abgeschlossene und diskontinuierliche, also eine nulldimensionale Menge (sehe z.B.: K. MENGER, Dimensionstheorie, S. 213). Aus dem „Summensatz" der Dimensionstheorie geht jetzt die Behauptung hervor.

Punkt von N' enthält. Das Bild jeder $U(P|A+P)$ ist also eine $U(P'|A'+P')$. Es geht jetzt auch unmittelbar hervor, dasz P' der einzige Häufungspunkt der Folge a_i' ist. Gäbe es nämlich zwei Häufungspunkte P' und P'', so könnte man die inverse topologische Abbildung von A' auf A betrachten, und genau wie oben nachweisen, dasz jede $U(P''|A'+P'')$ und jede $U(P'|A'+P')$ übergeführt wird in Umgebungen $U(P|A+P)$. Wählt man die Umgebungen von P' und P'' fremd zueinander, so erhält man leicht einen Widerspruch. Die Beziehung zwischen den Punkten $P \subset B$ und $P' \subset B'$ ist also eineindeutig.

Mit Hilfe des Lemmas schlieszen wir jetzt sofort auf die Erweiterungsfähigkeit der Abbildung.

4. Als erste Anwendung des soeben bewiesenen Satzes nennen wir Satz II. Es ist einleuchtend, dasz die Daten den Anforderungen entsprechen. Uebrigens kann man Satz II auch direkt — ohne Hilfe des Lemmas — beweisen; dazu braucht man nur eine Vereinfachung der im Satze III angewendeten Beweisführung.

4. 1. Um zu einer zweiten Anwendung zu gelangen, teilen wir die Punkte des Zahlenraumes R_n in zwei Klassen ein: in die erste Klasse die Punkte mit ausschlieszlich rationalen Koordinaten, das sind die „rationalen" Punkte; in die zweite Klasse die übrigen, das sind die „irrationalen" Punkte.

Satz IV. *Jede topologische Abbildung der irrationalen Punkte zweier n-dimensionaler Elemente in R_n $(n > 1)$ aufeinander ist erweiterbar zu einer Abbildung der beiden n-dimensionalen Elemente.*

Beweis. Die rationalen Punkte bilden eine abzählbare, also gewsiz eine nulldimensionale Punktmenge. Wir haben also nur mehr Eigenschaft 1 nachzuprüfen. Diese Eigenschaft ist aber unmittelbar klar für die inneren Punkte eines n-dimensionalen Elementes E.

Zum Nachweis für die (rationalen) Randpunkte bilden wir E topologisch ab auf eine n-dimensionalen Vollkugel E'. Das Bild $U(P'|E')$ einer Umgebung $U(P|E)$ eines rationalen Randpunktes $P \subset E$ enthält eine $U_\varepsilon(P'|E')$. Je zwei zu dieser Umgebung gehörigen Punkte kann man verbinden durch eine in der Umgebung liegende Strecke. Die Originalmenge $U'(P|E)$ von $U_\varepsilon(P'|E')$ ist also ebenfalls stetig zusammenhängend. Wir haben jedoch nachzuweisen, dasz jede zwei zu $U'(P|E)$ gehörigen *irrationalen* Punkte zu verbinden sind durch einen nur *irrationalen* Punkte enthaltenden einfachen Jordanbogen. Wir erreichen jetzt unser Ziel durch eine Approximation.

Angenommen die zwei irrationalen Punkte, welche wir verbinden wollen, gehören nicht zum Rande S von E. Ein die zwei Punkte verbindender zu $U'(P|E)$ gehöriger Jordanbogen hat eine positive Entfernung δ von der Menge $S+G$ (G bedeutet die Begrenzung der offene Menge $U'(P|E)$). Wir konstruieren jetzt eine Einteilung des R_n in n-dimensionale Würfel, deren Randpunkte alle irrational sind. Die Kantenlänge jedes Würfels wählen wir $< \frac{\delta}{n}$. Betrachten wir die Menge der Würfel, welche wenigstens einen Punkt mit dem Jordanbogen gemeinsam haben. Man ist nun sofort im Stande einen zur Menge der Würfel und deshalb zu $U'(P|E)$ angehörigen Weg von irrationalen Punkten zu bestimmen, welcher die zwei irrationalen Punkte verbindet.

Wenn einer der beiden irrationalen Endpunkte K des Jordanbogens b zum Rande S von E gehört, so bestimmen wir eine Einteilung von b in eine Folge von einfachen Jordanbogen b_i

$$b = b_1 + b_2 + \ldots\ldots$$

derart, dasz b_k und b_{k+1} genau einen Punkt gemeinsam haben und die Folge der Bogen b_i gegen K konvergiert. Jetzt approximieren wir jeden Bogen b_i durch einen Weg w_i in der oben angegebenen Weise. Setzen wir

$$w = w_1 + w_2 + \ldots\ldots$$

so konvergieren die w_i gegen den Punkt K. Die Menge $w + K$ ist also ein Jordanbogen, der den Anforderungen entspricht.

Gehören die beiden irrationalen Endpunkte des Jordanbogens b zum Rande S, so führt natürlich eine analoge Betrachtung zum Ziel.

4. 2. Bekannt ist folgender Satz: jede abzählbare überall dichte Menge A im R_n ist der Menge A' der rationalen Punkte des R_n homöomorph. Man kann sogar eine topologische Abbildung von A auf A' bestimmen, welche sich erweitern läszt zu einer Selbstabbildung des ganzen Raumes R_n. Diese Behauptung gilt aber nicht für *jede* topologische Abbildung von A auf A' [1]). Ebensowenig gilt Satz IV, wenn wir das Wort irrational durch das Wort rational ersetzen. Erläutern wir diesen Tatbestand durch folgendes Beispiel [2]):

Ein Quadrat mit irrationalen Seiten teile man durch eine irrationale Strecke in zwei irrationale Rechtecke *ABCD* und *CDEF*. Wir dürfen annehmen, dasz bei der kongruenten Abbildung von *ABCD* auf *DCBA* die rationalen Punkte in rationale Punkte übergeführt werden. Diese Abbildung gibt zusammen mit der identischen Abbildung des Rechteckes *CDEF* eine topologische Abbildung der rationalen Punkte des Quadrates, welche offenbar nicht erweiterungsfähig ist.

Jetzt bringen wir noch eine einfache Anwendung des Satzes IV.

Korollar. Jede topologische Abbildung der irrationalen Punkte zweier n-dimensionalen Elemente in R_n $(n > 1)$ aufeinander ist eine gleichmäszig stetige Abbildung.

Die Abbildung ist nämlich erweiterbar zu einer Abbildung von zwei beschränkten abgeschlossenen Mengen. Diese letzte Abbildung, und also auch die erste, ist gleichmäszig stetig.

4. 3. Erwähnen wir noch eine letzte Anwendung des Satzes III.

Satz V. *In der Ebene R_2 sind gegeben zwei beschränkte abgeschlossene Mengen $A + B$ und $A' + B'$; A und A' sind homöomorph, B (bzw. B') ist eine (beschränkte) abgeschlossene diskontinuierliche Punktmenge, während die Punkte von B (bzw. B') innere Punkte der Menge $A + B$ (bzw. $A' + B'$) in bezug auf R_2 sind.*

Es ist jetzt jede topologische Abbildung von A auf A' erweiterbar zu einer topologischen Abbildung von $A + B$ auf $A' + B'$.

Beweis. Ein bekannter Satz besagt, dasz man durch B (bzw. B') eine Jordankurve J legen kann. Zu jedem Punkte $P \subset B$ gibt es auf beiden Seiten von P auf J eine nach P konvergente und zu A gehörige Punktfolge, da B eine diskontinuierliche Menge ist. Auszerdem ist eine Jordankurve in jedem ihrer Punkte glatt und erreichbar, sowohl für das Innere wie auch für das Aeuszere der Kurve [3]); mit Hilfe dieser Eigenschaften leuchtet sofort ein, dasz die Eigenschaft 1 vorhanden ist.

[1]) Für den Beweis dieser und analoger Sätze sehe man L. E. J. BROUWER, *Some remarks on the coherence type η.* Proc. Kon. Akad. v. Wetensch., Amsterdam, **15**, S. 1256—1263 (1913), **16**, S. 336 (1913).

[2]) Andere Beispiele gibt L. E. J. BROUWER, l.c., S. 1262.

[3]) Siehe: A. SCHOENFLIES, Math. Ann. **62** (1906), S. 296 oder B. v. KERÉKJÁRTÓ, Vorlesungen über Topologie, S. 65.

Mathematics. — *Sur la représentation des fonctions harmoniques.* Par A. F. MONNA. (Communicated by Prof. W. VAN DER WOUDE).

(Communicated at the meeting of September 27, 1941.)

1. Dans le numéro précédent de ce journal j'ai fait quelques remarques concernant la possibilité de la représentation des fonctions harmoniques dans un domaine par une intégrale de STIELTJES—RADON. Aucune condition ne fut imposée au domaine Ω et les fonctions harmoniques ne furent supposées que d'être bornées supérieurement. Cependant une étude de plus près m'a fait voir qu'il est difficile à rendre la démonstration exacte sans quelques conditions, qui sont données dans ce qui suit.

On remarque d'abord que les fonctions d'ensemble μ_n^P, $\theta_n^{P_0}$, etc, peuvent être considérées comme définies sur tous les ensembles de l'espace trois-dimensionnel (pour autant qu'ils sont mesurables relativement à μ_n^P, etc.), en les posant zéro hors Σ.

2. Dans la démonstration est utilisée que les intégrales

$$\int_e \gamma^P(Q)\, d\theta^{P_0}(Q), \quad \int_{e_n} \gamma_n^P(Q)\, d\theta_n^{P_0}(Q). \quad . \quad . \quad . \quad . \quad (1)$$

où e et e_n désignent respectivement des sous-ensembles de Σ et de Σ_n, tendent vers zéro avec la mesure harmonique de e et de e_n [1]). Puisque γ^P et γ_n^P sont bornés et positifs, il faut et il suffit pour cela que θ^{P_0} et $\theta_n^{P_0}$ s'annulent sur les ensembles de mesure harmonique nulle. Posons alors $u(P) = -v(P)$. On a alors

$$\theta_n^{P_0}(e) = \int_{e_n} v(Q)\, d\mu_n^{P_0}(Q). \quad . \quad . \quad . \quad . \quad . \quad . \quad . \quad (2)$$

$v(Q)$ est continu sur Σ_n fermé, et donc borné; $v \leqq M_n$. Donc

$$0 \leqq \theta_n^{P_0}(e_n) \leqq M_n\, \mu_n^{P_0}(e_n).$$

Par conséquent $\theta_n^{P_0}(e_n) \to 0$ si $\mu_n^{P_0}(e_n) \to 0$. Si v est borné dans Ω (donc si u est non seulement borné supérieurement, mais aussi borné inférieurement), $M_n \leqq M$, un passage à la limite montre que le même est vrai pour θ^{P_0}. Cependant, pour conclure que $\theta^{P_0}(e) \to 0$ si $\mu^{P_0}(e) \to 0$, il n'est pas nécessaire que v est borné.

Il faut et il suffit que les intégrales (2) *sont uniformement et absolument continues par rapport à la mesure harmonique sur le* Σ_n *correspondant,* c. a. d. s'il existe pour tout $\varepsilon > 0$ donné un nombre $\delta(\varepsilon) > 0$ tel que

$$\theta_n^{P_0}(e) = \int_e v(Q)\, d\mu_n^{P_0}(Q) < \varepsilon$$

pour $n > N(\varepsilon)$ dès que $\mu_n^{P_0}(e) < \delta(\varepsilon)$.

[1]) On ne l'a utilisé que pour les ensembles $e = \Sigma - \Sigma''$ et $e_n = \Sigma_n - \Sigma_n''$.

Ceci résulte immédiatement de ce qu'on a $\lim_{n\to\infty} \mu_n^{P_0}(e) = \mu^P(e)$ et $\lim_{n\to\infty} \theta_n^{P_0}(e) = \theta^{P_0}(e)$ pour tout e ainsi dit „régulier".

Remarquons que toute intégrale (2) est absolument continue sur le Σ_n correspondant (u étant supposé seulement borné supérieurement), de sorte que seulement l'uniformité de cette continuité désigne une restriction.

La condition imposée à $u(P)$ est superflue si la dérivée de $\mu^P(e)$ par rapport à $\mu^{P_0}(e)$ existe en chaque point Q de Σ.

3. Pour pouvoir conclure à la convergence de $\gamma_n^P(Q_n)$ vers $\gamma^P(Q)$ sur les Σ_n' il faut imposer une condition à Ω. A savoir, il n'est pas certain sans plus qu'il existe un ensemble e de mesure harmonique positive, tel qu'on a

$$\left| \frac{\mu^P(e)}{\mu^{P_0}(e)} - \gamma^P(Q) \right| < \tfrac{1}{3}\varepsilon; \quad \left| \frac{\mu_n^P(e)}{\mu_n^{P_0}(e)} - \gamma_n^P(Q_n) \right| < \tfrac{1}{3}\varepsilon \quad . \quad . \quad . \quad (3)$$

et la possibilité de ceci est essentielle dans la démonstration.

On peut arriver à une condition suffisante comme il suit.

A. Supposons que la frontière Σ de Ω est telle que la portion de Σ contenue dans une sphère de rayon ϱ et centrée dans un point Q quelconque de Σ, a une mesure harmonique positive.

Soit alors $\{Q_n\}$ une suite de points de $\{\Sigma_n\}$ tendant vers Q. Désignons par e_n l'intérieure de la sphère de rayon ϱ et de centre Q_n; de même par e l'intérieur de la sphère de rayon ϱ et de centre Q. Pour $\varepsilon > 0$ donné arbitrairement il existe un nombre $\varrho_n(\varepsilon) > 0$ tel que pour $\varrho \leqq \varrho_n$

$$\left| \frac{\mu_n^P(e_n)}{\mu_n^{P_0}(e_n)} - \gamma_n^P(Q_n) \right| < \tfrac{1}{3}\varepsilon. \quad . \quad . \quad . \quad . \quad . \quad . \quad . \quad . \quad (4)$$

De même il existe un nombre $\varrho^*(\varepsilon) > 0$ tel que pour $\varrho \leqq \varrho^*$

$$\left| \frac{\mu^P(e)}{\mu^{P_0}(e)} - \gamma^P(Q) \right| < \tfrac{1}{3}\varepsilon. \quad . \quad . \quad . \quad . \quad . \quad . \quad . \quad . \quad (5)$$

On a supposé ici que les dérivés de μ^P et μ_n^P existent en Q et Q_n (en vertu de no. 1 les autres points n'ont pas d'importance). Remarquons que ceci est, comme conséquence de la condition A, compatible avec la supposition que $Q_n \to Q$. Supposons maintenant que

B. Pour $n > N(\varepsilon)$ on a $\varrho_n > \eta > 0$.

Alors, à partir d'un certain nombre n, les sphères de rayon ϱ_n contiennent tous Q. En prenant les ϱ_n suffisamment petits, on peut arranger que toutes ces sphères sont contenues dans la sphère de rayon ϱ^* et de centre Q. Alors évidemment l'intérieur e_0 de la sphère de rayon $\eta > 0$ et de centre Q satisfait aux inégalités (3); en vertu de A cet ensemble a une mesure harmonique positive.

La condition B doit être vérifié dans tous les points de Σ', c.a.d. partout sur Σ sauf aux points d'un ensemble de mesure harmonique nulle. Alors $\gamma^P(Q)$ est presque partout continu sur Σ, donc sauf aux points d'un ensemble de mesure harmonique nulle.

La condition B, de même que A, signifie une restriction pour Ω et non pour la fonction harmonique considérée.

4. La condition A est certainement vérifiée en tout point de Σ si Ω n'a qu'une frontière extérieure. Pour montrer cela, soit S_ϱ la partie (fermée) de la surface de la sphère de rayon ϱ, située dans $\Omega + \Sigma$ et soit Σ_ϱ la partie de Σ située dans cette sphère. Σ_ϱ et S_ϱ constituent la frontière d'un domaine Ω_ϱ. La mesure harmonique de Σ_ϱ relativement à

Ω vaut au moins la mesure harmonique de Σ_ϱ relativement à Ω_ϱ (principe de CARLEMAN de l'extension du domaine). Il suffit donc de montrer que cette dernière mesure est positive. Or, on a, en désignant la mesure par rapport à Ω_ϱ par μ,

$$\mu(\Sigma_\varrho + S_\varrho) = 1,$$

$$\mu(\Sigma_\varrho) + \mu(S_\varrho) = 1.$$

Il faut donc montrer que $\mu(S_\varrho) < 1$. Désignons par $\mu^*(S_\varrho)$ la mesure harmonique de S_ϱ relativement à l'intérieur de la sphère. Par le même principe on a $\mu^*(S_\varrho) \geqq \mu(S_\varrho)$. Maintenant $\mu^*(S_\varrho)$ est < 1, puisque le complément de S_ϱ par rapport à la surface de la sphère a des points intérieurs (la frontière est extérieure) et a donc une mesure harmonique positive (la somme des mesures des deux parties de la surface vaut 1).

Il est aisé de généraliser ce résultat pour des cas particuliers de domaines ayant une frontière intérieure.

La condition B n'a qu'un rapport très indirecte aux propriétés de Σ. Le problème se pose donc de chercher des conditions d'un caractère plus géométrique. Des conditions nécessaires et suffisantes (s'il faut poser des conditions) ne sont pas connues. Il semble cependant que la condition B, qui doit être vérifiée presque partout, ne signifie pas une restriction grave pour Ω. L'exemple facile suivant montre p. ex. que la régularité de Ω, c.a.d. la possibilité de la résolution du problème de DIRICHLET, pour des valeurs-frontière continues quelconques, n'est pas nécessaire pour la représentation intégrale. Il suffit de prendre, si $E \subset \Sigma$,

$$\mu^P(E) = \int_\Sigma \gamma^P(Q)\, d\bar{\mu}^{P^0}(e_Q)$$

si

$$\bar{\mu}^{P_0}(e) = \begin{cases} \mu^{P_0}(e) & \text{pour } e \subset E \\ 0 & \text{pour } e \subset \Sigma - E \end{cases}$$

et de remarquer que $\mu^P(E)$ est une fonction harmonique de P.

On peut voir comme il suit que la condition B est compatible avec l'irrégularité de Ω. Montrons cela d'abord pour la condition plus restrictive.

B'. *Pour* $n > N(\varepsilon)$ *on a* $\varrho_n > \eta > 0$ *quelque soit la suite croissante* $\{\Omega_n\}$ *tendant vers* Ω.

Supposons donc que B' est vérifié dans le point Q_0. Soit alors B_ϱ la sphère fermée de rayon ϱ arbitrairement petit et de centre Q. Soit $\{\Omega_n\}$ une suite quelconque de domaines croissants, tendant vers Ω, et telle que $\Omega_n + \Sigma_n \subset \Omega + \Sigma$; supposons de plus que Ω_n et Ω, donc aussi Σ_n et Σ, coïncident dans B_ϱ. Pour Ω_n les fonctions $\mu_n^{P_0}(e)$ et $\gamma_n^P(Q)$ sont bien définies. Par un raissonnement comme dans l'article précédent on voit alors que $\gamma_n^P(Q_0)$ tend vers $\gamma^P(Q_0)$ si $n \to \infty$; la restriction dans B' „quelque soit la suite croissante $\{\Omega_n\}$ tendant vers Ω" est ici essentielle. $\gamma^P(Q)$ est donc une fonctionnelle continue du domaine dans le sens mentionné.

Le même est vrai pour le quotient $\dfrac{\mu_n^P(e)}{\mu_n^{P_0}(e)}$ (si la mesure harmonique est positive). On en tire que la condition B', vérifié dans Q_0, a un caractère local, c.a.d. reste vérifié si le domaine hors B_ϱ diminue tandis que ϱ est arbitrairement petit. En effet. Soit $\bar{\Omega}$ le domaine varié et $d \neq 0$ la plus grande distance de sa frontière Σ à Σ. On peut choisir $\bar{\Omega}$, en prenant d assez petit, tel que pour $n > N(\lambda)$ les quotients

$$\frac{\bar{\mu}_n^P(e_0)}{\mu_n^{P_0}(e_0)} \quad \text{et} \quad \frac{\mu_n^P(e_0)}{\mu_n^{P_0}(e_0)}$$

différent moins que le nombre $\lambda > 0$, donné arbitrairement; remarquons seulement qu'on peut arranger que les suites croissantes de domaines tendant vers $\overline{\Omega}$ et Ω coïncident dans B_ϱ. Pour n suffisamment grand, $n > N(\alpha)$, et d suffisamment petit la quantité

$$\left| \frac{\mu_n^P(e_n)}{\mu_n^{P_0}(e_n)} - \gamma_n^P(Q_n) \right|$$

varie donc moindre qu'un nombre $\alpha > 0$, donné arbitrairement. Remarquons alors qu'on peut choisir dès le début les rayons $\varrho(\varepsilon)$ tels qu'on a, pour tous les n suffisamment grand,[1])

$$\tfrac{1}{3}\varepsilon - \left| \frac{\mu_n^P(e_n)}{\mu_n^{P_0}(e_n)} - \gamma_n^P(Q_n) \right| > \alpha.$$

Alors les inégalités (4) subsistent pour le domaine varié Ω.

En partant de $\overline{\Omega}$ on peut répéter le procédé.

Il suit de ce qui précède que, serait-il donc impossible que B' soit vérifié dans un point irrégulier, il est cependant possible que Ω a des points irréguliers: par une diminution convenable de Ω hors B_ϱ on peut arranger que le domaine a un point irrégulier hors B_ϱ et la condition B', si vérifiée dans Q_0, reste alors vérifiée.

A fortiori, la condition B, qui est moins restrictive, est donc compatible avec l'irrégularité de Ω.

La possibilité de la représentation intégrale fut démontrée en admettant que B est vérifié presque partout (μ) sur Σ. Cela signifie cependant par une restriction quant à la possibilité de points irréguliers sur Σ, puisque les points irréguliers constituent un ensemble de capacité nulle, donc de mesure harmonique nulle. Il est donc probable que la représentation intégrale des fonctions harmoniques qui vérifient la condition donnée ci-dessus de continuité uniforme est possible pour des domaines très généraux.

Pour des domaines à frontière suffisamment régulière (p. ex. l'intérieure ou l'extérieure d'une sphère) la condition B est satisfaite en tout point[2]). Ceci résulte de ce qu'on a alors

$$\mu^P(e) = \frac{1}{4\pi} \int_e \frac{\partial G}{\partial n}\, d\sigma$$

G étant la fonction de GREEN de Ω avec pôle P; n la normale intérieure. Il s'en suit que la représentation intégrale est possible pour tout domaine dont la frontière, entièrement extérieure, consiste en un nombre fini ou une infinité dénombrable de parties de telles surfaces, puisque les points où B n'est peut être pas vérifié constituent alors au plus un ensemble dénombrable d'ensembles de mesure harmonique nulle, qui a donc lui même une mesure nulle.

Dordrecht, août 1941.

---

[1]) En effet, si cette inégalité n'est pas vérifiée, on change la correspondance de ϱ_n et ε en faisant correspondre les ensembles de rayon ϱ_n au nombre $\varepsilon + 3\alpha$ et donc les ensembles de rayon ϱ_n $(\varepsilon - 3\alpha)$ à ε (prendre α tel que $\varepsilon - 3\alpha > 0$).

[2]) Dans le cas deux dimensionnel p. ex. la condition B est satisfaite si Σ est une courbe analytique sans points singuliers.

Mathematics. — *Eine Verallgemeinerung des* SCHURschen *Satzes.* Von W. WRONA.
(Communicated by Prof. W. VAN DER WOUDE.)

(Communicated at the meeting of September 27, 1941.)

In einer früheren Arbeit [1]) haben wir den Begriff der skalaren Krümmung einer m-Richtung in einer RIEMANNschen Mannigfaltigkeit V_n eingeführt. Unter die skalare Krümmung einer m-Richtung verstehen wir nämlich die erzwungene skalare Krümmung einer in V_n eingebetteten V_m, die diese m-Richtung enthält. Für $m = 2$ fällt dieser Begriff mit dem des RIEMANNschen Krümmungsmasses [2]) zusammen.

Eine wichtige Eigenschaft des RIEMANNschen Krümmungsmasses drückt der bekannte Satz von F. SCHUR aus. Dieser Satz lautet: *Ist das* RIEMANN*sche Krümmungsmass einer V_n örtlich konstant (d.h. unabhängig von der gegebenen 2-Richtung), so ist es auch unabhängig vom Ort* [3]).

Im Folgenden werden wir mit Hilfe des Begriffes der skalaren Krümmung eine Verallgemeinerung des SCHURschen Satzes beweisen.

Hauptsatz. I. *Ist in einer V_n für ein bestimmtes m, wobei $1 < m < n$ ist, die skalare Krümmung einer m-Richtung örtlich konstant, so ist sie auch unabhängig vom Ort.*

II. *Darüber hinaus folgt unter derselben Voraussetzung, dass*

1) *für $m < n-1$ die V_n eine S_n (eine Mannigfaltigkeit konstanter Krümmung) ist,*

2) *für $m = n-1$ die V_n eine* EINSTEIN*sche Mannigfaltigkeit ist.*

Beweis. Den Fall $n = 3$ brauchen wir nicht zu betrachten, weil in diesem Falle unser Satz mit dem SCHURschen zusammenfällt.

Für $n > 3$ müssen wir zwei Möglichkeiten unterscheiden und zwar: 1) $m < n-1$ und 2) $m = n-1$.

1) $m < n-1$. Betrachten wir in einem Punkte der V_n zwei m-Richtungen, welche eine gemeinsame $(m-1)$-Richtung besitzen. Die diesen zwei m-Richtungen entsprechenden Fundamentaltensoren bezeichnen wir mit $b^{\mu\lambda}$ und $\bar{b}^{\mu\lambda}$. Man kann sie in folgender Form ausdrücken:

$$\left.\begin{aligned} b^{\mu\lambda} &= c^{\mu\lambda} + \underset{p}{\varepsilon}\, p^\mu p^\lambda \qquad \underset{p}{\varepsilon} = p^\varkappa p_\varkappa \\ \bar{b}^{\mu\lambda} &= c^{\mu\lambda} + \underset{q}{\varepsilon}\, q^\mu q^\lambda \qquad \underset{q}{\varepsilon} = q^\varkappa q_\varkappa \end{aligned}\right\}, \quad \ldots\ldots \quad (1)$$

wo $p^\varkappa$ und $q^\varkappa$ zur $(m-1)$-Richtung senkrechte Einheitsvektoren sind und der Fundamentaltensor der $(m-1)$-Richtung mit $c^{\varkappa\lambda}$ bezeichnet ist. Die skalaren Krümmungen dieser zwei m-Richtungen sind entsprechend gleich:

$$k_m = \frac{1}{m(m-1)} K_{\nu\mu\lambda\varkappa}\, b^{\mu\lambda} b^{\nu\varkappa}, \quad \bar{k}_m = \frac{1}{m(m-1)} K_{\nu\mu\lambda\varkappa}\, \bar{b}^{\mu\lambda} \bar{b}^{\nu\varkappa} \quad [4]). \qquad (2)$$

---

[1]) J. HAANTJES und W. WRONA, Ueber konformeuklidische und EINSTEINsche Räume gerader Dimension. Proc. Ned. Akad. v. Wetensch., **42**, 7, 626—636 (1939).

[2]) J. A. SCHOUTEN und D. J. STRUIK, Einführung in die neueren Methoden der Differentialgeometrie I, Noordhoff Groningen, S. 117 und II, S. 134. Weiter zitiert als Einführung. L. P. EISENHART, RIEMANNian Geometry. S. 79—81.

[3]) T. LEVI-CIVITA, Der absolute Differentialkalkül. Springer Berlin, S. 136. L. P. EISENHART, l.c. S. 82.

[4]) J. HAANTJES und W. WRONA, l.c. S. 626.

Nach Voraussetzung bekommen wir aus (1) und (2):

$$K_{\nu\mu\lambda\varkappa}(c^{\mu\lambda}\,c^{\nu\varkappa} + 2\underset{p}{\varepsilon}\,c^{\mu\lambda}\,p^{\nu}\,p^{\varkappa} + p^{\mu}\,p^{\lambda}\,p^{\nu}\,p^{\varkappa}) =$$
$$= K_{\tau\mu\lambda\varkappa}(c^{\mu\lambda}\,c^{\tau\varkappa} + 2\underset{q}{\varepsilon}\,c^{\mu\lambda}\,q^{\tau}\,q^{\varkappa} + q^{\mu}\,q^{\lambda}\,q^{\tau}\,q^{\varkappa})$$

und daraus

$$\underset{p}{\varepsilon}\,K_{\tau\mu\lambda\varkappa}\,c^{\mu\lambda}\,p^{\tau}\,p^{\varkappa} = \underset{q}{\varepsilon}\,K_{\tau\mu\lambda\varkappa}\,c^{\mu\lambda}\,q^{\tau}\,q^{\varkappa}\,. \quad . \quad . \quad . \quad . \quad . \quad . \quad (3)$$

Die letzte Gleichung gilt für alle zu der $(m-1)$-Richtung senkrechte Einheitsvektoren p^{λ} und q^{λ}. Daraus geht hervor [5]), dass

$$K_{\tau\mu\lambda\varkappa}\,c^{\mu\lambda}\,r^{\tau}\,s^{\varkappa} = 0 \quad . \quad . \quad . \quad . \quad . \quad . \quad . \quad . \quad (4)$$

ist, wo r^{ν} und s^{ν} zwei beliebige, gegenseitig und zu der betrachteten $(m-1)$-Richtung senkrechte Vektoren sind. Diese Gleichung kann man nun wieder für $m-1 \geqq 2$ für verschiedene $\overline{c}^{\lambda\varkappa}$ und $\overline{\overline{c}}^{\lambda\varkappa}$, die zwei $(m-1)$-Richtungen mit gemeinsamer $(m-2)$-Richtung entsprechen, anschreiben:

$$K_{\nu\mu\lambda\varkappa}\,\overline{c}^{\mu\lambda}\,r^{\nu}\,s^{\varkappa} = 0\,, \quad K_{\nu\mu\lambda\varkappa}\,\overline{\overline{c}}^{\mu\lambda}\,r^{\nu}\,s^{\varkappa} = 0\,.$$

Wenn wir die letzten zwei Gleichungen voneinander subtrahieren, ergibt sich in ähnlicher Weise wie oben

$$K_{\nu(\mu\lambda)\varkappa}\,u^{\nu}\,v^{\varkappa}\,r^{\mu}\,s^{\lambda} = 0 \quad . \quad . \quad . \quad . \quad . \quad . \quad . \quad . \quad (5)$$

für jedes System von vier gegenseitig senkrechten Vektoren $u^{\varkappa}$, $v^{\varkappa}$, $r^{\varkappa}$, $s^{\varkappa}$. Im Falle $m = 2$ ist die Beziehung (5) eine unmittelbare Folge der Gleichung (4); dieser Fall wurde aber schon von SCHUR erledigt.

Aus (5) geht durch Verwechslung von $v^{\varkappa}$ und $s^{\varkappa}$

$$K_{\nu(\mu\varkappa)\lambda}\,u^{\nu}\,v^{\varkappa}\,r^{\mu}\,s^{\lambda} = 0 \quad . \quad . \quad . \quad . \quad . \quad . \quad . \quad . \quad (6)$$

hervor. Subtraktion der letzten zwei Gleichungen ergibt wegen $K_{[\nu\mu\lambda]\varkappa} = 0$

$$3\,K_{\nu\mu\lambda\varkappa}\,u^{\nu}\,v^{\varkappa}\,r^{\mu}\,s^{\lambda} = 0\,, \quad . \quad . \quad . \quad . \quad . \quad . \quad . \quad . \quad (7)$$

Für jedes orthogonale Bezugssystem verschwinden also alle Bestimmungszahlen des Krümmungsaffinors mit vier ungleichen Indizes. Die V_n ist demzufolge konformeuklidisch [6]) und der Krümmungsaffinor nimmt folgende Gestalt an [7])

$$K_{\nu\mu\lambda\varkappa} = \frac{4}{n-2}\,a_{[\nu\,[\lambda}\,L_{\mu]\,\varkappa]}\,, \quad \left(L_{\mu\varkappa} = -\,K_{\mu\varkappa} + \frac{1}{2\,(n-1)}\,K\,a_{\mu\varkappa}\right). \quad (8)$$

Für die skalare Krümmung k_m einer m-Richtung bekommen wir jetzt folgenden Ausdruck

$$k_m = \frac{4}{(n-2)\,(m-1)\,m}\,a_{[\nu\,[\lambda}\,L_{\mu]\,\varkappa]}\,b^{\nu\varkappa}\,b^{\mu\lambda} = \frac{-2}{m\,(n-2)}\,L_{\mu\varkappa}\,b^{\mu\varkappa}\,, \quad . \quad (9)$$

wo $b^{\mu\varkappa}$ der Fundamentaltensor der betrachteten m-Richtung darstellt.

Um jetzt zu schliessen, dass unsere V_n eine S_n ist, würde es nach dem bekannten Resultat von SCHOUTEN und STRUIK [8]) genügen noch nachzuweisen, dass unsere V_n EINSTEINsch ist. Wir kommen aber schneller zum Ziel indem wir direkt zeigen werden, dass $L_{\mu\varkappa}$ proportional zu $a_{\mu\varkappa}$ ist. Zu diesem Zweck schreiben wir nun den Ausdruck (9)

---

[5]) J. HAANTJES, Eine Charakterisierung der konformeuklidischen Räume. Proc. Ned. Akad. v. Wetensch., Amsterdam, **43**, 1, 91—94 (1940).

[6]) Einführung II, S. 204.

[7]) Einführung II, S. 202.

[8]) L. P. EISENHART, l.c., S. 93.

für beide in (1) angegebenen Fundamentaltensoren $b^{\mu\varkappa}$ und $\bar{b}^{\mu\varkappa}$ an. Nach der Voraussetzung ($k_m = \bar{k}_m$) erhalten wir

$$\underset{p}{\varepsilon}\, L_{\mu\nu}\, p^{\mu}\, p^{\nu} = \underset{q}{\varepsilon}\, L_{\mu\nu}\, q^{\mu}\, q^{\nu} \quad . \quad . \quad . \quad . \quad . \quad . \quad . \quad (10)$$

für jede zwei Einheitsvektoren $p^{\varkappa}$ und $q^{\varkappa}$. Aus (10) folgt, dass die mit $L_{\mu\varkappa}$ gemessene Länge der Vektoren proportional zu der mit $a_{\mu\varkappa}$ gemessenen Länge ist. Es ist also

$$L_{\mu\varkappa} = \sigma\, a_{\mu\varkappa} . \quad . \quad . \quad . \quad . \quad . \quad . \quad . \quad . \quad . \quad (11)$$

Der Krümmungsaffinor nimmt also folgende Gestalt an:

$$K_{\nu\mu\lambda\varkappa} = \frac{4}{n-2}\, \sigma\, a_{[\nu\,[\lambda}\, a_{\mu]\,\varkappa]} . \quad . \quad . \quad . \quad . \quad . \quad . \quad . \quad (12)$$

Setzen wir nun in (12)

$$\sigma = -\frac{n-2}{2}\, \varkappa , \quad . \quad . \quad . \quad . \quad . \quad . \quad . \quad . \quad . \quad (13)$$

so erhalten wir

$$K_{\nu\mu\lambda\varkappa} = -2\,\varkappa\, a_{[\nu\,[\lambda}\, a_{\mu]\,\varkappa]} . \quad . \quad . \quad . \quad . \quad . \quad . \quad . \quad (14)$$

Die V_n ist daher eine Mannigfaltigkeit konstanter Krümmung [9]) und folglich ist $\varkappa$ eine Konstante. Aus (9), (11) und (13) finden wir

$$k_m = \varkappa . \quad . \quad . \quad . \quad . \quad . \quad . \quad . \quad . \quad . \quad . \quad (15)$$

Die skalare Krümmung einer m-Richtung ist daher eine Konstante, die auch von m unabhängig und gleich der skalaren Krümmung der V_n ist. Damit haben wir den ersten Teil des Satzes bewiesen.

2) $m = n-1$. In diesem Falle können wir die Fundamentaltensoren $d^{\mu\varkappa}$ und $\bar{d}^{\mu\varkappa}$ zweier beliebigen $(n-1)$-Richtungen in folgender Form ausdrücken

$$\left.\begin{aligned} d^{\mu\varkappa} &= a^{\mu\varkappa} - \underset{p}{\varepsilon}\, p^{\mu}\, p^{\varkappa} \qquad \underset{p}{\varepsilon} = p^{\mu}\, p_{\mu} = \pm 1 \\ \bar{d}^{\mu\varkappa} &= a^{\mu\varkappa} - \underset{q}{\varepsilon}\, q^{\mu}\, q^{\varkappa} \qquad \underset{q}{\varepsilon} = q^{\mu}\, q_{\mu} = \pm 1 \end{aligned}\right\} . \quad . \quad . \quad . \quad (16)$$

Nach Voraussetzung bekommen wir

$$K_{\nu\mu\lambda\varkappa}\, d^{\nu\varkappa}\, d^{\mu\lambda} = K_{\nu\mu\lambda\varkappa}\, \bar{d}^{\nu\varkappa}\, \bar{d}^{\mu\lambda} , \quad . \quad . \quad . \quad . \quad . \quad (17)$$

woraus nach (16)

$$K - 2\,\underset{p}{\varepsilon}\, K_{\mu\lambda}\, p^{\mu}\, p^{\lambda} = K - 2\,\underset{q}{\varepsilon}\, K_{\mu\lambda}\, q^{\mu}\, q^{\lambda} , \quad . \quad . \quad . \quad . \quad (18)$$

also

$$\underset{p}{\varepsilon}\, K_{\mu\lambda}\, p^{\mu}\, p^{\lambda} = \underset{q}{\varepsilon}\, K_{\mu\lambda}\, q^{\mu}\, q^{\lambda} \quad . \quad . \quad . \quad . \quad . \quad . \quad . \quad (19)$$

hervorgeht. Aus (19) folgt (vgl. (10))

$$K_{\mu\lambda} = \lambda\, a_{\mu\lambda} . \quad . \quad . \quad . \quad . \quad . \quad . \quad . \quad . \quad . \quad (20)$$

Die V_n ist daher eine EINSTEINsche und λ ist bekanntlich eine Konstante. Rechnen wir

---

[9]) Einführung I, S. 126.

jetzt die skalare Krümmung k_{n-1} einer $(n-1)$-Richtung aus. Nach (18) erhalten wir

$$k_{n-1} = \frac{1}{(n-1)(n-2)} [K - 2 \underset{p}{\varepsilon} \lambda a_{\mu\lambda} p^{\mu} p^{\lambda}] = \frac{1}{(n-1)(n-2)} (K - 2\lambda). \quad (21)$$

Aus (20) folgt aber, dass

$$\lambda = \frac{K}{n} \quad . \quad . \quad . \quad . \quad . \quad . \quad . \quad . \quad . \quad . \quad . \quad (22)$$

ist, daher

$$k_{n-1} = \frac{K}{n(n-1)} = \varkappa$$

ist, wo $\varkappa$ die skalare Krümmung der V_n bezeichnet. Daraus sehen wir, dass die skalare Krümmung der $(n-1)$-Richtung konstant ist. Damit haben wir auch den Fall $m = n-1$ erledigt.

Bemerkung 1. Den Fall $n = 3$ haben wir vom vornherein ausgeschlossen, da er durch den SCHURschen Satz erledigt ist. Das obige Verfahren gilt aber auch für $n = 3$ und zwar deswegen, da eine EINSTEINsche V_3 immer konformeuklidisch, also auch von konstanter Krümmung ist.

Bemerkung 2. Aus obigem Beweise kann man sofort folgende zwei Sätze schliessen.

I. *Ist in jedem Punkte einer V_n für ein bestimmtes m $(1 < m < n)$ die skalare Krümmung einer m-Richtung von der besonderen Wahl dieser m-Richtung unabhängig, so ist die V_n* EINSTEINsch.

II. *Die notwendige und hinreichende Bedingung dafür, dass eine V_n $(n \geqq 3)$* EINSTEINsch *sei, besteht darin, dass in jedem Punkte die skalaren Krümmungen aller $(n-1)$-Richtungen einander gleich seien.*

Mathematics. — *Likelihood as conditioned probability.* By Prof. M. J. VAN UVEN. (Communicated by Prof. H. A. KRAMERS.)

(Communicated at the meeting of September 27, 1941.)

In his paper "On the Mathematical Foundations of Theoretical Statistics" [1]) Prof. R. A. FISHER has recommended the "Method of maximum Likelihood" for determining the likeliest values of the *a-priori* probabilities ruling a given frequency distribution, c.q. of the variables on which these probabilities depend. Here Prof. FISHER emphasizes the distinction between the concept of probability and the concept of "likelihood", which, according to him, only formally agrees with inverse frequency distribution. However, likelihood may be considered as (the density of) conditioned probability, and the efficacy of the method of maximum likelihood is due, as it appears to us, to the circumstance, that this conditioned probability is independent of the choice of the variables on which the *a-priori* probabilities are considered to depend, and that the formulae for the most probable values and their accuracy are proof against transition from one set of variables to another.

An experiment may have n different events $E_h\,(h = 1, \ldots, n)$ mutually excluding each other and having the *a-priori* probabilities

$$p_h\,(h = 1, \ldots, n, \sum_{h=1}^{n} p_h = 1).$$

Then the probability that out of N experiments F_h have the event E_h, is

$$w_F^{(p)} = \mathfrak{w}\,(F_1, \ldots, F_n; p_1, \ldots, p_n) = \frac{N!}{\Pi F_h!}\,\Pi p_h^{F_h}. \quad . \quad . \quad . \quad (1)$$

Hence $\mathfrak{w}\,(F_1, \ldots, F_n; p_1, \ldots, p_n)$, or, abbreviated, $\mathfrak{w}\,(F; p)$, is the probability of the frequency set $[F_h]$ $(\sum_{h=1}^{n} F_h = N)$.

$\mathfrak{w}\,(F; p)$ satisfies

$$\sum_{F_1=0}^{N} \sum_{F_2=0}^{N-F_1} \cdots \sum_{F_{n-1}=0}^{N-F_1-\ldots-F_{n-2}} \mathfrak{w}\,(F_1, \ldots, F_n; p_1, \ldots, p_n) = 1. \quad . \quad . \quad (2)$$

The *a-priori* probabilities p_h may be connected, besides by $\Sigma\, p_h = 1$, by some other relations; then they may be (univalent) functions of a set of s indepedent continuous variables $\zeta_k\,(k = 1, \ldots, s; s \leqq n - 1)$; these functions $p_h\,(\zeta_1, \ldots, \zeta_s)$, or, shorter, $p_h\,(\zeta)$, must satisfy the identity

$$\sum_{h=1}^{n} p_h\,(\zeta) \equiv 1. \quad . \quad . \quad . \quad . \quad . \quad . \quad . \quad . \quad . \quad . \quad (3)$$

[1]) Phil. Trans. Ser. A, Vol. 222 (1922), pp. 309—368.

The ζ_k, being continuous, have infinitesimal probabilities. We suppose that the set $[\zeta]$ has the *a-priori* probability (irrespective of F_h):

$$dw_\zeta = \chi(\zeta_1, \ldots, \zeta_s)\, d\zeta_1 \ldots d\zeta_s,$$

or, briefly,

$$dw_\zeta = \chi(\zeta)\, d\zeta_1 \ldots d\zeta_s. \quad . \quad . \quad . \quad . \quad . \quad . \quad . \quad . \quad (4)$$

If ζ_k ranges from α_k unto β_k, we have

$$\int_{\zeta_1=\alpha_1}^{\beta_1} \ldots \int_{\zeta_s=\alpha_s}^{\beta_s} \chi(\zeta)\, d\zeta_1 \ldots d\zeta_s = 1. \quad . \quad . \quad . \quad . \quad . \quad . \quad . \quad (5)$$

The probability differential (4) is also the probability of the set $p_h(\zeta)$, as $p_h(\zeta)$ is wholly determined by $\zeta_1, \ldots, \zeta_s$. It is the *a-priori* probability of the set $[\zeta]$ (or of the set $[p_h(\zeta)]$) without any supposition concerning the (empirical) frequencies F_h.

The compound probability 1^0 that the variables ζ_k assume given values (with ranges $d\zeta_k$), 2^0 that, with these values of ζ_k, the frequencies F_h occur, amounts to

$$dw_{F;\zeta} = dw_\zeta \,.\, w_F^{(\zeta)} = \mathfrak{w}(F; p(\zeta)) \,.\, \chi(\zeta)\; d\zeta_1 \ldots d\zeta_s. \quad . \quad . \quad . \quad (6)$$

Denoting the probability w_F of the frequency set $[F_h]$, occurring with any set $[\zeta]$, by $g(F_1, \ldots, F_n)$, or, shorter, by $g(F)$, we obtain this *a-priori* probability of the set $[F_h]$ by integrating (6) over $\zeta_1, \ldots, \zeta_s$; hence

$$w_F = g(F) = \int_{\zeta_1=\alpha_1}^{\beta_1} \ldots \int_{\zeta_s=\alpha_s}^{\beta_s} \mathfrak{w}(F; p(\zeta)) \,.\, \chi(\zeta)\, d\zeta_1 \ldots d\zeta_s \quad . \quad . \quad . \quad (7)$$

Of course $g(F)$ satisfies

$$\sum_{F_1=0}^{N} \sum_{F_2=0}^{N-F_1} \ldots \sum_{F_{n-1}=0}^{N-F_1-\ldots-F_{n-2}} g(F) = 1. \quad . \quad . \quad . \quad . \quad . \quad (8)$$

Now we consider the (infinitesimal) probability $dw_\zeta^{(F)}$ of the set $[\zeta]$ with given frequencies F_h, hence the conditioned probability of the set $[\zeta]$. Its density being $\omega(\zeta_1, \ldots, \zeta_s; F_1, \ldots, F_n)$, or, abbreviated, $\omega(\zeta; F)$, we have

$$dw_\zeta^{(F)} = \omega(\zeta; F)\, d\zeta_1 \ldots d\zeta_s. \quad . \quad . \quad . \quad . \quad . \quad . \quad . \quad (9)$$

So we find for the compound probability: 1^0 that the frequencies F_h assume a given set of values, 2^0 that these frequencies are accompanied by the values ζ_k, the expression:

$$dw_{\zeta;F} = w_F \,.\, dw_\zeta^{(F)} = g(F) \,.\, \omega(\zeta; F)\, d\zeta_1 \ldots d\zeta_s. \quad . \quad . \quad (6\ bis)$$

Now this compound probability equals the compound probability (6).

For the probability dw_{ζ} of the set $[\zeta]$, irrespective of the frequency set $[F_h]$, we have

$$dw_{\zeta} = \sum_{F_1=0}^{N} \sum_{F_2=0}^{N-F_1} \cdots \sum_{F_{n-1}=0}^{N-F_1-\ldots-F_{n-2}} dw_{\zeta;F},$$

or, by (4) and (6 bis),

$$\chi(\zeta) = \sum_{F_1=0}^{N} \sum_{F_2=0}^{N-F_1} \cdots \sum_{F_{n-1}=0}^{N-F_1-\cdots-F_{n-2}} g(F) \cdot \omega(\zeta; F). \quad . \quad . \quad . \quad (10)$$

As $\mathfrak{w}(F; p(\zeta))$ has a well-defined shape, the equation (7) determines $g(F)$ when $\chi(\zeta)$ is known, whereas $\chi(\zeta)$, $g(F)$ being given, can be computed by solving (7) as integral equation.

The conditioned probability of the set $[\zeta]$, with given frequencies F_h, follows by equating (6) and (6 *bis*). Its density is

$$\omega(\zeta; F) = \frac{\mathfrak{w}(F; p(\zeta))}{g(F)} \cdot \chi(\zeta). \quad . \quad . \quad . \quad . \quad . \quad . \quad . \quad (11)$$

As a rule the function $\chi(\zeta)$, hence also the function $g(F)$, is unknown. So the density $\omega(\zeta; F)$ of the conditioned probability, depending, by (11), on the *a-priori* probability distribution $\chi(\zeta)$ of the set $[\zeta]$, also contains an element of uncertainty.

The problem: to find the most probable values ζ_k^* of ζ_k, when the frequencies F_h are given, might be solved by postulating that the most probable set $[\zeta]$ makes the (conditioned) probability density $\omega(\zeta; F)$ a maximum. But then the transition from one set of variables $[\zeta]$ into another set $\tau_i = \theta_i(\zeta_1, \ldots, \zeta_s)$ $(i = 1, \ldots, s)$ would alter the probability density, and so also its maximum, and the most probable values τ_i^* of τ_i would not correspond to the most probable values ζ_k^* in virtue of the relations $\tau_i = \theta_i(\zeta_1, \ldots, \zeta_s)$.

We may avoid this drawback by passing from the general variables ζ_k to particular, so-called "canonical" variables $z_1, \ldots, z_s$, which range from 0 to 1 with constant probability density, so that the probability that z_i lies within the interval dz_i precisely equals dz_i:

$$dw_{z_i} = dz_i. \quad . \quad . \quad . \quad . \quad . \quad . \quad . \quad . \quad . \quad . \quad (12)$$

So the probability of the set $[z]$ is

$$dw_z = dz_1 \ldots dz_s.$$

From $dw_{\zeta} \rightleftarrows dw_z$ follows, that the canonical variables are such functions $z_i(\zeta_1, \ldots, \zeta_s)$ of $\zeta_1, \ldots, \zeta_s$, that

$$dz_1 \ldots dz_s \rightleftarrows \chi(\zeta)\, d\zeta_1 \ldots d\zeta_s,$$

or

$$\frac{\partial(z_1, \ldots, z_s)}{\partial(\zeta_1, \ldots, \zeta_s)} = \chi(\zeta). \quad . \quad . \quad . \quad . \quad . \quad . \quad . \quad . \quad (13)$$

In order to provide an example of canonical variables, we suppose, that the variables ζ_k are the probabilities $p_1, \ldots, p_{n-1}$ themselves, and

that p_h runs trough the interval $1-p_1 \ldots -p_{h-1}$ with constant probability density. Then we put

$$p_1 = z_1,\ p_2 = (1-p_1)\, z_2,\ p_3 = (1-p_1-p_2)\, z_3, \ldots,\ p_{n-1} = (1-p_1-\ldots-p_{n-2})\, z_{n-1},$$

whence

$$p_1 = z_1,\ p_2 = (1-z_1)\, z_2,\ p_3 = (1-z_1)\,(1-z_2)\, z_3, \ldots,$$
$$p_{n-1} = (1-z_1)\,(1-z_2) \ldots (1-z_{n-2})\, z_{n-1},$$

The equation (11) must now be replaced by

$$u(z; F) = \frac{\mathfrak{w}(F; p(z))}{g(F)} \quad \ldots\ldots\ldots \quad (14)$$

Reintroducing the former (general) variables ζ_k, the function $u(z; F)$ is transformed into the function

$$\varphi(\zeta; F) = \frac{\mathfrak{w}(F; p(\zeta))}{g(F)} \quad \ldots\ldots\ldots \quad (14')$$

Before we attack the main problem: to obtain the most probable values of ζ_k, and, moreover, to compute their accuracy (represented by the asymptotically averaged error-squares (variances) and error-products), we will derive a preparatory theorem.

We consider a function $y = \psi(\zeta)$ of the s quantities ζ_k. This function may, by the substitution $\zeta_k \rightarrow z_i(\zeta_1, \ldots, \zeta_s)$, be transformed into the function $y = v(z_1, \ldots, z_s)$, or, briefly, $y = v(z)$. Hence

$$y = \psi(\zeta) = v(z). \quad \ldots\ldots\ldots \quad (15)$$

In the following we make use of the notation with lower and upper indices, applied in Tensor Analysis, and drop the summation sign Σ over corresponding upper and lower indices (contraction). The covariant forms are denoted with upper indices, the contravariant forms with lower indices.

So we put [1])

$$\left.\begin{aligned}
&\psi^k \equiv \frac{\partial \psi}{\partial \zeta_k},\ \psi^{kl} \equiv \frac{\partial^2 \psi}{\partial \zeta_k\, \partial \zeta_l},\ \Psi \ldots \psi^{kl} \ldots,\ \Psi_{kl} \ldots \frac{\partial \Psi}{\partial \psi^{kl}} \\
&\qquad\qquad\qquad\qquad \text{(complementary minor of } \psi^{kl}\text{)} \\
&v^i \equiv \frac{\partial v}{\partial z_i},\ v^{ij} \equiv \frac{\partial^2 v}{\partial z_i\, \partial z_j},\ V \equiv |v^{ij}|,\ V_{ij} \equiv \frac{\partial V}{\partial v^{ij}} \\
&\qquad\qquad\qquad\qquad \text{(complementary minor of } v^{ij}\text{)} \\
&z_i^k \equiv \frac{\partial z_i}{\partial \zeta_k},\ z_i^{kl} \equiv \frac{\partial^2 z_i}{\partial \zeta_k\, \partial \zeta_l},\ Z \equiv |z_i^k|,
\end{aligned}\right\} \quad (16)$$

[1]) The determinants Ψ and V are written without indices, though they are not invariant; but there is no danger of misunderstanding, as we are mainly concerned with the quotients $\psi_{kl} = \frac{\Psi_{kl}}{\Psi}$ and $v_{ij} = \frac{V_{ij}}{V}$, which are really contravariant with respect to $\zeta_k, \zeta_l; z_i, z_j$.

whence

$$Z = \frac{\partial (z_1, \ldots, z_s)}{\partial (\zeta_1, \ldots, \zeta_s)} . \quad . \quad . \quad . \quad . \quad . \quad . \quad . \quad . \quad (17)$$

Moreover

$$\psi^k = v^i z_i^k \ , \ \psi^{kl} = v^i z_i^{kl} + v^{ij} z_i^k z_j^l .$$

At the extremum of $y = \psi(\zeta) = v(z)$ we have

$$\psi^k = 0 \ (k = 1, \ldots, s) \quad \text{and} \quad v^i = 0 \ (i = 1, \ldots, s).$$

Therefore

$$\text{At } y \text{ extr.} \qquad \psi^{kl} = v^{ij} z_i^k z_j^l , \quad . \quad . \quad . \quad . \quad . \quad . \quad . \quad . \quad (18)$$

whence

$$\text{At } y \text{ extr.} \qquad \Psi = VZZ. \quad . \quad . \quad . \quad . \quad . \quad . \quad . \quad . \quad (19)$$

Let ζ_k^*, resp. z_i^*, be the values of ζ_k, resp. z_i, for which y has its extremum, and $\triangle \zeta_k = \zeta_k - \zeta_k^*$, $\triangle z_i = z_i - z_i^*$ the deviations (errors) in the neighbourhood of the centre ζ_k^* (z_i^*). Then, for small deviations, we have approximately

$$\triangle z_i = z_i^k \triangle \zeta_k ;$$

here z_i^k represents the value of $\frac{\partial z_i}{\partial \zeta_k}$ at the centre.

The asymptotic error-products are respectively

$$\mu_{kl} \equiv \langle \triangle \zeta_k \, . \, \triangle \zeta_l \rangle \quad , \quad m_{ij} \equiv \langle \triangle z_i \, . \, \triangle z_j \rangle ;$$

they are connected by the relation $\langle \triangle z_i \, . \, \triangle z_j \rangle = z_i^k z_j^l \langle \triangle \zeta_k \, . \, \triangle \zeta_l \rangle$, or

$$m_{ij} = \mu_{kl} z_i^k z_j^l . \quad . \quad . \quad . \quad . \quad . \quad . \quad . \quad . \quad (20)$$

Putting

$$M = |m_{ij}| \quad , \quad \mathrm{M} = |\mu_{kl}| ,$$

we derive from (20)

$$M = \mathrm{M} ZZ, \quad . \quad . \quad . \quad . \quad . \quad . \quad . \quad . \quad . \quad (21)$$

whence, by (19),

$$VM = \Psi \mathrm{M} \ ^1). \quad . \quad . \quad . \quad . \quad . \quad . \quad . \quad . \quad (22)$$

By differentiating Ψ with respect to v^{ij} we find on the one hand, by (19),

$$\frac{\partial \Psi}{\partial v^{ij}} = ZZ \frac{\partial V}{\partial v^{ij}} = ZZ V_{ij},$$

on the other hand, by (18),

$$\frac{\partial \Psi}{\partial v^{ij}} = \frac{\partial \Psi}{\partial \psi^{kl}} \cdot \frac{\partial \psi^{kl}}{\partial v^{ij}} = \Psi_{kl} \, . \, z_i^k z_j^l .$$

---

1) Another simple relation follows from (18) and (20):

$$m_{ij} v^{ij} = \mu_{kl} v^{ij} z_i^k z_j^l = \mu_{kl} \psi^{kl}.$$

Hence

$$\text{At } y \text{ extr.} \qquad V_{ij} = \frac{1}{ZZ} \Psi_{kl} z_i^k z_j^l, \quad \ldots \ldots \ldots \quad (23)$$

or

$$\frac{V_{ij}}{V} = \frac{1}{VZZ} \cdot \Psi_{kl} z_i^k z_j^l,$$

so, by (19),

$$\text{At } y \text{ extr.} \qquad \frac{V_{ij}}{V} = \frac{\Psi_{kl}}{\Psi} z_i^k z_j^l. \quad \ldots \ldots \ldots \quad (23\,bis)$$

Let ϱ be an invariant function, c.q. a constant. Them from (20) and (23 *bis*) follows

$$\text{At } y \text{ extr.} \qquad m_{ij} - \varrho \frac{V_{ij}}{V} = \left(\mu_{kl} - \varrho \frac{\Psi_{kl}}{\Psi} \right) z_i^k z_j^l. \quad \ldots \ldots \quad (24)$$

Therefore, if for one set $[\zeta]$

$$\text{At } y \text{ extr.} \qquad \mu_{kl} - \varrho \frac{\Psi_{kl}}{\Psi} = 0 \quad \left(\begin{matrix} k \\ l \end{matrix} \right\} = 1, \ldots, s \Big),$$

then also for any other set $[z]$

$$\text{At } y \text{ extr.} \qquad m_{ij} - \varrho \frac{V_{ij}}{V} = 0 \quad \left(\begin{matrix} i \\ j \end{matrix} \right\} = 1, \ldots, s \Big)$$

holds. Hence

At $y = \psi(\zeta) = v(z)$ extr.:

$$\left.\begin{aligned} &\text{From } \mu_{kl} - \varrho \frac{\Psi_{kl}}{\Psi} = 0 \left(\begin{matrix} k \\ l \end{matrix} \right\} = 1, \ldots, s \Big) \text{ follows} \\ &\qquad\qquad m_{ij} - \varrho \frac{V_{ij}}{V} = 0 \left(\begin{matrix} i \\ j \end{matrix} \right\} = 1, \ldots, s \Big), \\ &\text{where} \\ &\mu_{kl} \equiv \langle \triangle \zeta_k \,.\, \triangle \zeta_l \rangle \,;\; \psi^{kl} \equiv \frac{\partial^2 \psi}{\partial \zeta_k \, \partial \zeta_l}, \; \Psi \equiv |\psi^{kl}|, \; \Psi_{kl} \equiv \frac{\partial \Psi}{\partial \psi^{kl}}, \\ &m_{ij} \equiv \langle \triangle z_i \,.\, \triangle z_j \rangle \,;\; v^{ij} \equiv \frac{\partial^2 v}{\partial z_i \, \partial z_j}, \; V \equiv |v^{ij}|, \; V_{ij} \equiv \frac{\partial V}{\partial v^{ij}}. \end{aligned}\right\} \quad (25)$$

This is the preparatory theorem alluded to above.

We now return to the (conditioned) probability density $\varphi(\zeta; F)$, and we suppose, that, at its maximum, it has approximately the character of normal correlation. This supposition is, as a rule, the more justified the larger the total sum N of the frequencies is.

Introducing the true errors $\tau_k = \zeta_k - \zeta_k^*$, we may represent $\varphi(\zeta; F)$, at its maximum, by

$$\varphi(\zeta; F) \simeq \sqrt{\frac{A}{(2\pi)^s}} \cdot e^{-\frac{1}{2} a^{\varkappa\lambda} \tau_\varkappa \tau_\lambda} \text{ with } A = |a^{\varkappa\lambda}|. \quad \ldots \quad (26)$$

In order to derive our conclusions more easily, we shall sometimes distinguish formally a^{kl} from a^{lk} (resp. $a^{\varkappa\lambda}$ from $a^{\lambda\varkappa}$).

Putting $\psi(\zeta) = -\log \varphi(\zeta)$, we have

$$\psi(\zeta) = \frac{s}{2}\log(2\pi) - \tfrac{1}{2}\log A + \tfrac{1}{2}\, a^{\varkappa\lambda}\,\tau_\varkappa\,\tau_\lambda =$$

$$= \frac{s}{2}\log(2\pi) - \tfrac{1}{2}\log A + \tfrac{1}{2}\{a^{11}\,\tau_1\,\tau_1 + (a^{12}+a^{21})\,\tau_1\,\tau_2 + \ldots + a^{ss}\,\tau_s\,\tau_s\};$$

hence

$$\psi^k \equiv \frac{\partial\psi}{\partial\zeta_k} = \frac{\partial\psi}{\partial\tau_k} = \tfrac{1}{2}\{2\,a^{kk}\,\tau_k + \sum_{\lambda\neq k}(a^{k\lambda}+a^{\lambda k})\,\tau_\lambda\} = \sum_{\lambda=1}^{s} a^{k\lambda}\,\tau_\lambda = a^{k\lambda}\,\tau_\lambda$$

and

$$\psi^{kl} \equiv \frac{\partial^2\psi}{\partial\zeta_k\,\partial\zeta_l} = \frac{\partial^2\psi}{\partial\tau_k\,\partial\tau_l} = a^{kl},$$

whence

$$\Psi = A, \Psi_{kl} \equiv \frac{\partial\Psi}{\partial\psi^{kl}} = \frac{\partial A}{\partial a^{kl}} \equiv A_{kl}.$$

Here we have

$$\mu_{kl} \equiv \langle \triangle\zeta_k \,.\, \triangle\zeta_l\rangle = \langle \tau_k\,\tau_l\rangle = \int_{\tau_1=-\infty}^{+\infty}\!\!\cdots\int_{\tau_s=-\infty}^{+\infty} \tau_k\,\tau_l\,\varphi(\zeta;F)\,d\tau_1\ldots d\tau_s =$$

$$= \sqrt{\frac{A}{(2\pi)^s}}\cdot\int_{\tau_1=-\infty}^{+\infty}\!\!\cdots\int_{\tau_s=-\infty}^{+\infty} \tau_k\,\tau_l\,e^{-\frac{1}{2}a^{\varkappa\lambda}\tau_\varkappa\tau_\lambda}\,d\tau_1\ldots d\tau_s.$$

As

$$\frac{\partial\,(e^{-\frac{1}{2}a^{\varkappa\lambda}\tau_\varkappa\tau_\lambda})}{\partial a^{kl}} = -\tfrac{1}{2}\,\tau_k\,\tau_l\,e^{-\frac{1}{2}a^{\varkappa\lambda}\tau_\varkappa\tau_\lambda},$$

we may write

$$\mu_{kl} = \sqrt{\frac{A}{(2\pi)^s}}\cdot -2\,\frac{\partial}{\partial a^{kl}}\int_{\tau_1=-\infty}^{+\infty}\!\!\cdots\int_{\tau_s=-\infty}^{+\infty} e^{-\frac{1}{2}a^{\varkappa\lambda}\tau_\varkappa\tau_\lambda}\,d\tau_1\ldots d\tau_s. \quad . \quad (27)$$

Now

$$\int_{\tau_1=-\infty}^{+\infty}\!\!\cdots\int_{\tau_s=-\infty}^{+\infty} \varphi(\zeta;F)\,d\tau_1\ldots d\tau_s = 1,$$

or, by (26),

$$\int_{\tau_1=-\infty}^{+\infty}\!\!\cdots\int_{\tau_s=-\infty}^{+\infty} e^{-\frac{1}{2}a^{\varkappa\lambda}\tau_\varkappa\tau_\lambda}\,d\tau_1\ldots d\tau_s = (2\pi)^{\frac{s}{2}}\,A^{-\frac{1}{2}};$$

hence

$$\frac{\partial}{\partial a^{kl}}\int_{\tau_1=-\infty}^{+\infty}\cdots\int_{\tau_s=-\infty}^{+\infty} e^{-\frac{1}{2}a^{\varkappa\lambda}\tau_\varkappa\tau_\lambda}d\tau_1\ldots d\tau_s=(2\pi)^{\frac{s}{2}}\cdot -\tfrac{1}{2}A^{-\frac{3}{2}}\frac{\partial A}{\partial a^{kl}}=-\tfrac{1}{2}(2\pi)^{\frac{s}{2}}\cdot\frac{A_{kl}}{A^{\frac{3}{2}}};$$

so equation (27) furnishes the well-known result

$$\mu_{kl}=\frac{A_{kl}}{A},$$

or, in the ψ-notation

$$\mu_{kl}=\frac{\Psi_{kl}}{\Psi}.$$

Since $\varphi(\zeta;F)$ maximum corresponds with $\psi(\zeta)$ minimum, we may apply (25), and so obtain, with $\varrho=1$,

$$m_{ij}-\frac{V_{ij}}{V}=0\quad\left(\begin{matrix}i\\j\end{matrix}=1,\ldots,s\right),$$

where

$$m_{ij}=\langle\triangle z_i\,.\,\triangle z_j\rangle;\quad v(z)=-\log u(z;F),$$

$$v^{ij}=\frac{\partial^2 v}{\partial z_i\,\partial z_j},\quad V=|v^{ij}|,\quad V_{ij}=\frac{\partial V}{\partial v^{ij}},$$

$u(z;F)$ being the function into which $\varphi(\zeta;F)$ passes by changing the variables ζ_k into the variables z_i.

Therefore:

If $\varphi(\zeta;F)$ at its maximum behaves as the probability density of normal correlation, we have for any other system of variables, c.q. $[z]$:

$$\left.\begin{aligned}&\text{At } u \text{ max.}\quad m_{ij}=\frac{V_{ij}}{V}\quad\left(\begin{matrix}i\\j\end{matrix}=1,\ldots,s\right),\\ &\text{where}\\ &m_{ij}=\langle\triangle z_i\,.\,\triangle z_j\rangle;\quad v(z)=-\log u(z;F),\\ &\qquad\qquad v^{ij}=\frac{\partial^2 v}{\partial z_i\,\partial z_j},\quad V=|v^{ij}|,\ V_{ij}=\frac{\partial V}{\partial v^{ij}}.\end{aligned}\right\}\tag{28}$$

Now for canonical variables the density of conditioned probability coincides with the density of unconditioned probability ($dw_z=dz_1\ldots dz_s$).

Hence, using canonical variables z_i, we may safely consider that set $[z]$ as the most probable one, which maximizes the probability density $u(z;F)$, and thus minimizes the function $v(z)=-\log u(z;F)$.

So the most probable values z_i^* derive from

$$v^i=\frac{\partial v}{\partial z_i}=\frac{\partial(-\log u(z;F))}{\partial z_i}=0\quad(i=1,\ldots,s),\ldots\tag{29}$$

and their error-products from

$$m_{ij} \equiv \langle \triangle z_i \,.\, \triangle z_j \rangle = \left(\frac{V_{ij}}{V} \right)_{v \text{ min.}} \qquad \left(\begin{matrix} i \\ j \end{matrix} \right) = 1, \ldots, s \Big). \quad . \quad (30)$$

The formulae (29) and (30) have been deduced for the canonical variables.

But the theorem (25) enables us to apply the formulae (29) and (30) also to any set $[\zeta]$ of (independent) variables ζ_k. Hence:

The most probable values ζ_k^* of ζ_k are those for which

$$\eta'_k \equiv \frac{\partial \eta'}{\partial \zeta_k} \equiv \frac{\partial \left(\log q \, (\zeta ; F) \right)}{\partial \zeta_k} \equiv 0 \qquad (k = 1, \ldots, s),$$

where

$$\varphi \, (\zeta ; F) \equiv \frac{\mathfrak{w} \, (F ; p \, (\zeta))}{g \, (F)} \,.\, ^{1}) \quad . \quad . \quad . \quad . \quad . \quad . \quad . \quad (31)$$

Here the solution-values ζ_k^* and z_l^* are really connected by the general substition-formulae $z_l (\zeta_1, \ldots, \zeta_s)$: $z_l^* = z_l (\zeta_1^*, \ldots, \zeta_s^*)$.

The error-products (c.q. variances) are furnished by

$$\mu_{kl} \equiv \langle \triangle \zeta_k \,.\, \triangle \zeta_l \rangle = \left(\frac{\Psi_{kl}}{\Psi} \right)_{\psi \text{ min.}} \qquad \left(\begin{matrix} k \\ l \end{matrix} \right) = 1, \ldots, s \Big). \quad . \quad (32)$$

The equations (31) and (32) are the well-known formulae of Prof. R. A. FISHER's method of maximum likelihood.

It is particularly the property (25) at the extremum of a function $\eta = \psi \, (\zeta) = v \, (z)$, which releases us from distinguishing between the concept "likelihood" and the concept "conditioned probability (density)", in such cases where the frequency distribution $[F_h]$ is given, and where we are concerned with the most probable values of the variables ζ_k, on which the *a-priori* probabilities p_h depend, and with their error-products, c.q. variances.

[1]) The particular from (14') of $q \, (\zeta ; F)$ is irrelevant.

Mathematics. — *Inégalités remplies par les fonctions univalentes.* Par Prof. J. WOLFF. (Communicated by Prof. J. G. VAN DER CORPUT.)

(Communicated at the meeting of September 27, 1941.)

Dans la présente communication on suppose que $f(z) = f(x + iy)$ soit holomorphe, bornée et univalente dans le demi-plan $D(x > 0)$, d'où

$$\iint_D f'^{\,2}\, dx\, dy < \infty \quad . \quad . \quad . \quad . \quad . \quad . \quad . \quad . \quad . \quad (1)$$

THÉORÈME I. **$x f'(z)$ tend vers zéro quand x tend vers zéro, c'est à dire: toute suite z_n dans D, sur laquelle $x_n \to 0$, satisfait à $x_n f'(z_n) \to 0$.**

Démonstration. Dans le cas contraire il existerait un nombre $\varepsilon > 0$ et une suite z_n dans D satisfaisant à $x_n \to 0$ et $x_n |f'(z_n)| > \varepsilon$, $n = 1, 2, \ldots$. Dans le cercle de centre z_n et de rayon x_n $f(z)$ est holomorphe et univalente. Le théorème de KOEBE permet de conclure que dans le cercle γ_n de centre z_n et de rayon $x_n/2$

$$|f'(z_n)| > \frac{k\varepsilon}{x_n}, \quad k = \text{constante positive.}$$

Donc

$$\iint_{\gamma_n} |f'^{\,2}\, dx\, dy > \pi \cdot \frac{x_n^2}{4} \cdot \frac{k^2 \varepsilon^2}{x_n^2} = \frac{k^2 \pi \varepsilon^2}{4} \cdot \quad . \quad . \quad . \quad . \quad . \quad (2)$$

Parce que $x_n \to 0$, (2) est valable pour une infinité de cercles γ_n extérieurs l'un à l'autre, en contradiction avec (1).

Il est clair que dans l'énoncé on peut remplacer $x_n \to 0$ par $z_n \to \infty$.

Pour les fonctions $\phi(z)$ holomorphes, bornées et univalentes dans le cercle-unité $|z| < 1$ le théorème équivaut au

THÉORÈME IA. **$(1 - |z|)\ \phi'(z) \to 0$ quand $|z| \to 1$.**

On le voit au moyen d'une homographie. Ce dernier théorème entraîne une propriété de la longueur $L(\varrho)$ de l'image du cercle $|z| = \varrho$, $0 < \varrho < 1$ réalisée par la représentation conforme $w = \phi(z)$. En effet

$$(1-\varrho)\, L(\varrho) = (1-\varrho) \int_0^{2\pi} |\Phi'(\varrho e^{i\varphi})|\, \varrho\, d\varphi,$$

donc, parce que $(1-\varrho)\phi'(\varrho e^{i\varphi}) \to 0$ uniformément $(0 \leqq \varphi \leqq 2\pi)$ pour $\varrho \to 1$, il vient

$$(1-\varrho)\, L(\varrho) \to 0 \text{ pour } p \to 1.$$

Cependent, tout en restant dans le même ordre d'ideés nous allons améliorer ce résultat en montrant le

THÉORÈME II. **$(1-\varrho)^{\frac{1}{2}}\, L(\varrho) \to 0$ pour $\varrho \to 1$** [1].

---

[1]) M. A. DENJOY (Comptes Rendus de l'Ac. des Sc., Paris, 23 Juin 1941, p. 1072) a montré que $(1-\varrho)^{\frac{1}{2}}\, L(\varrho) \to 0$ *approximativement*. La même page contient le théorème I A.

Démonstration. Remarquons d'abord que

$$\int_0^1 \int_0^{2\pi} |\Phi'|^2 \varrho \, d\varrho \, d\varphi < \infty . \quad . \quad . \quad . \quad . \quad . \quad . \quad . \quad . \quad (3)$$

D'autre part, en vertu de l'inégalité de SCHWARZ:

$$\{L(\varrho)\}^2 = \left\{ \int_0^{2\pi} |\Phi'(\varrho e^{i\varphi})| \, \varrho \, d\varphi \right\}^2 \leqq 2\pi \int_0^{2\pi} |\Phi'|^2 \varrho^2 \, d\varphi . \quad . \quad (4)$$

D'après (3) et (4):

$$\int_0^1 \{L(\varrho)\}^2 \, d\varrho < \infty \quad . \quad . \quad . \quad . \quad . \quad . \quad . \quad . \quad . \quad (5)$$

Soit $\varepsilon > 0$. Admettons pour un instant qu'il existe une suite $\varrho_n \to 1$ telle que

$$(1-\varrho_n)^{\frac{1}{2}} L(\varrho_n) > \varepsilon, \qquad n = 1, 2, \ldots \quad . \quad . \quad . \quad . \quad . \quad . \quad (6)$$

Soit $\alpha = \varrho_n e^{i\varphi}$ un point arbitraire du cercle $|z| = \varrho_n$. Dans le cercle de centre α et de rayon $1 - \varrho_n$ la fonction $\phi(z)$ est holomorphe et univalente, donc dans le cercle de centre α et de rayon $(1-\varrho_n)/2$ on a en vertu du théorème de KOEBE

$$|\Phi'(z)| > k \, |\Phi'(\alpha)| . \quad . \quad . \quad . \quad . \quad . \quad . \quad . \quad . \quad . \quad (7)$$

En vertu de (6) et (7), pour $\varrho_n \leqq \varrho \leqq (1+\varrho_n)/2$:

$$L(\varrho) > k \, L(\varrho_n) > k\varepsilon \, (1-\varrho_n)^{-\frac{1}{2}}$$

$$\int_{\varrho_n}^{\frac{1+\varrho_n}{2}} \{L(\varrho)\}^2 \, d\varrho > \frac{k^2 \varepsilon^2}{1-\varrho_n} \cdot \frac{1-\varrho_n}{2} = \frac{k^2 \varepsilon^2}{2} . \quad . \quad . \quad . \quad . \quad (8)$$

Cela étant pour une infinité de nombres $0 < \varrho_n \to 1$ nous aboutissons à une contradiction avec (5), ce qui démontre le théorème II.

Revenons au demi-plan D. Considérons une droite verticale $x = c > 0$. Admettons pour un instant que sur $x = c$:

$$\int_{-\infty}^{\infty} |f'|^2 \, dy = \infty . \quad . \quad . \quad . \quad . \quad . \quad . \quad . \quad . \quad . \quad (9)$$

Le théorème de KOEBE montre immédiatement que

$$\int_{-\infty}^{\infty} |f'|^2 \, dy = \infty \text{ sur } x = c', \; \tfrac{1}{2} c \leqq c' \leqq \tfrac{3}{2} c. \quad . \quad . \quad . \quad (10)$$

Or (1) contredit (10). Par conséquent

$$\int_{-\infty}^{\infty} |f'(c+iy)|^2 \, dy < \infty, \, c > 0, . \quad . \quad . \quad . \quad . \quad . \quad (11)$$

Indiquons par $L(n)$ la longueur de l'image du segment rectiligne $x = c, \; 0 \leqq y \leqq n$.

Alors d'après l'intégalité SCHWARZ, N étant un nombre positif fixe,

$$L(n) = \int_0^n f' \, dy = L(N) + \int_N^n f' \, dy \leqq L(N) + (n-N)^{\frac{1}{2}} \left\{ \int_N^n f'^{\,2} \, dy \right\}^{\frac{1}{2}}, \quad n > N.$$

$\varepsilon > 0$ étant donné, fixons N tel que

$$\int_N^\infty f'^{\,2} \, dy < \varepsilon^2$$

Alors

$$L(n) \leqq L(N) + \varepsilon (n-N)^{\frac{1}{2}}, \; n > N, \text{ d'où}$$

$$n^{-\frac{1}{2}} L(n) < 2\varepsilon \text{ pour } n \text{ suffisamment grand.}$$

Nous avons démontré le

THÉORÈME III. Sur toute droite $x = c > 0$ la longueur $L(y)$ de l'image du segment $[c, c + y i]$ satisfait à

$$L(y) = o(|y|^{\frac{1}{2}}) \text{ pour } |y| \to \infty.$$

Pour les fonctions $\phi(z)$ holomorphes, bornées et univalentes dans le cercle-unité $|z| < 1$ nous avons donc le

THÉORÈME IIIA. Sur toute circonférence tangente intérieurement à la circonférence $|z| = 1$ la longueur $L(z)$ de l'image de l'arc entre un point initial z_0 et un point z tendant vers le point de contact α satisfait à

$$L(z) = o(|z-\alpha|^{-\frac{1}{2}})$$

Considérons dans D une demi-droite $d(y = mx)$, $-\infty < m < \infty$. Indiquons par $L(z)$ la longueur de l'image d'un segment $z_0 z$ de d. Du théorème I résulte immédiatement le

THÉORÈME IV. z_0 étant fixe et z tendant vers zéro on a

$$L(z) = o\,|\log|z||.$$

Même majoration pour $z \to \infty$.

Pour $\phi(z)$ holomorphe, bornée et univalente dans le cercle-unité $|z| < 1$ il vient

THÉORÈME IVA. Sur toute corde $\alpha\beta$ du cercle-unité la longueur $L(z)$ de l'image du segment $z_0 z$, z_0 étant fixe et z tendant vers α, satisfait à

$$L(z) = o(|\log|z-\alpha||).$$

Soit $p > 0$, $a > 0$ et considérons dans D les courbes Γ_t d'équations

$$y = ax^{-p} + t, \qquad -\infty < t < \infty \; . \; . \; . \; . \; . \; . \quad (12)$$

L'inégalité (1) exige que

$$\int_\alpha^\infty dt \int_{\Gamma_t} |f'|^2 \, dx < \infty. \; . \; . \; . \; . \; . \; . \; . \quad (13)$$

Montrons que

$$\int_{\Gamma_t} |f'|^2 \, dx < \infty, \qquad -\infty < t < \infty. \; . \; . \; . \; . \quad (14)$$

En admettant que pour une certaine valeur de t

$$\int_{\Gamma_t} |f'|^2\,dx = \infty, \quad \ldots\ldots\ldots \quad (15)$$

soit $z = x + iy$ un point de Γ_t et $z_1 = x_1 + iy$ un point de Γ_{t_1}, $t_1 \neq t$, ayant même ordonnée y que z. Alors le rapport $x_1/x = (y - t/y - t_1)^p$ tend vers l'unité quand $y \to +\infty$, c'est à dire quand $x \to 0$. Le théorème de KOEBE assure l'existence d'une constante positive K telle que $|f'(z_1)| > K|f'(z)|$ pour les valeurs suffisamment petites de x. D'autre part considérons sur Γ_{t_1} un point $z' = x + iy'$ ayant même abscisse x que z. Pour x suffisamment grand le disque circulaire de centre z et de rayon $x/2$ contient z'; le théorème de KOEBE assure l'existence d'une autre constante positive $\bar{K}$ telle que $|f'(z')| > \bar{K}|f'(z)|$ pour les valeurs suffisamment grandes de x. Donc (15) entraîne la divergence de cette intégrale pour toutes les valeurs de t, en contradiction avec (13); par suite (14) est démontré.

Soit $L(n)$ la longueur de l'image de l'arc $[y - t = a\,x^{-p},\ t + 1 \leqq y \leqq n]$ de Γ_t, réalisée par la représentation conforme $w = f(z)$. Etant fixé un nombre $\varepsilon > 0$, fixons un nombre $N > t$ tel que sur Γ_t

$$\int_{y=N}^{\infty} |f'|^2\,dx < \varepsilon^2.$$

Alors sur Γ_t pour $n \to \infty$ il vient en vertu de l'inégalité de SCHWARZ

$$L(n) = L_N + O\left\{\int_N^n |f'|\,dy\right\} = L_N + O\left\{\int_{y=N}^n |f'|\,x^{-p}\,.\,dx\right\} =$$

$$= L_N + O\left\{\int_{y=N}^{\infty} |f'|^2\,.\,|dx|\,.\int_{y=N}^n x^{-2p-2}\,.\,|dx|\right\}^{\frac{1}{2}} =$$

$$= L_N + \varepsilon\, O\left\{\int_N^n y^{1+\frac{1}{p}}\,dy\right\}^{\frac{1}{2}} = \varepsilon\, O\left(n^{1+\frac{1}{2p}}\right).$$

ε étant arbitraire nous concluons que $L(n) = o\left(n^{1+\frac{1}{2p}}\right)$.

Nous avons démontré le

THÉORÈME V. La longueur L(z) de l'image de l'arc de Γ_t entre un point initial z_0 et un point z, dont l'abscisse x tend vers zéro, satisfait à

$$L(z) = o\left(z^{1+\frac{1}{2p}}\right).$$

Une homographie conduit au théorème correspondant pour les fonctions holomorphes, bornées et univalentes dans le cercle-unité $|z| < 1$:

THÉORÈME VA. Sur toute courbe dans $|z| < 1$ tangente au cercle $|z| = 1$ et dont l'équation au voisinage du point de contact α est

$$|z - \alpha| = b\,(1 - |z|)^q\ ,\ 0 < q < \tfrac{1}{2}\ ,\ b > 0,$$

la longueur $L(z)$ de l'image de l'arc entre un point initial z_0, et un point z tendant vers α, satisfait à

$$L(z) = o\left(|z - \alpha|^{-\frac{1}{2q}}\right).$$

Dans ce qui précède les majorations sont valables au voisinage de chaque point de la frontière $x = 0$ ou $|z| = 1$. Nous allons montrer que la frontière contient toujours un ensemble considérable de points, aux voisinages desquels les majorations peuvent être améliorées et où en outre $f(z)$, $\phi(z)$ respectivement, montre une conduite assez régulière.

Appelons avec M. DENJOY „plénitude" d'un ensemble E tout sous-ensemble e de E tel que $E - e$ est de mesure nulle.

Considérons dans D les courbes Γ_t convexes vers la gauche d'équations

$$y = \psi(x) + t,\ \psi(x) > 0 \text{ pour } x > 0,\ \psi(0) = 0,\ -\infty < t < \infty.$$

L'inégalité (1) exige que l'axe imaginaire contienne une plénitude de points it tels que

$$\int_{\Gamma_t} |f'|^2 dx < \infty \quad . \quad . \quad . \quad . \quad . \quad . \quad . \quad . \quad . \quad (16)$$

D'autre part l'axe imaginaire contient, en vertu d'un théorème de FATOU, une plénitude de points it tels que la limite

$$\lim_{x \to 0} f(x + it) = l(t) \text{ existe} \quad . \quad . \quad . \quad . \quad . \quad . \quad . \quad (17)$$

Sur la plénitude e commune aux deux plénitudes $> <$ (16) et (17) sont vrais. Sans perte de généralité supposons que l'origine $O(z = 0)$ appartienne à e.

Admettons pour un instant que Γ_0 contienne une suite $z_n \to 0$ telle que

$$|f'(z_n)| \geqq \frac{\varepsilon \sqrt{y_n}}{x_n},\ n = 1, 2, \ldots \quad . \quad . \quad . \quad . \quad . \quad . \quad (18)$$

Soit Q_n le carré $[|x - x_n| \leqq x_n/2, |y - y_n| \leqq x_n/2]$. Le segment de droite $O z_n$ coupe la droite $y = y_n - x_n/2$ au point d'abscisse $x = (x_n^2/2y_n)$. Or de la convexité de Γ_0 il suit que sur l'arc γ_n de Γ_0, qui traverse Q_n, la variation de x surpasse la quantité $x_n^2/2y_n$. Il existe par conséquent en vertu du théorème de KOEBE une constante positive k indépendente de n, telle que sur γ_n: $|f'| > k\,|f'(z_n)|$, donc d'après (18)

$$\int_{\gamma_n} |f'|^2 dx \geqq k^2 \varepsilon^2 \frac{x_n^2}{2 y_n} \cdot \frac{y_n}{x_n^2} = \frac{k^2 \varepsilon^2}{2},\ n = 1, 2 \ldots \quad . \quad . \quad . \quad (19)$$

Cela étant sur une infinité d'arcs γ_n extérieurs l'un à l'autre, nous rencontrons une contradiction avec (16). Nous avons donc démontré le

THÉORÈME VI. L'axe imaginaire contient une plénitude e de points it tels que, z tendant vers it sur une courbe convexe vers la gauche,

$$f'(z) = o\left(\frac{\sqrt{|y - t|}}{x}\right).$$

Pour les fonctions $\phi(z)$ holomorphes, bornées et univalentes dans le cercle-unité nous avons donc le théorème

THÉORÈME VIA. La circonférence $C(|z| = 1)$ contient une plénitude de points α tels que, z tendant vers α sur un arc de courbe qui est convexe dans la direction $O\alpha$

$$\phi'(z) = o\left(\frac{\sqrt{|z - \alpha|}}{1 - |z|}\right).$$ [1]

[1]) M. DENJOY a acquis ce résultat pour les courbes satisfaisant à

$$\limsup_{z \to \alpha} \frac{\log(1 - |z|)}{\log|z - \alpha|} \leqq 2.$$

(Comptes rendus de l'Ac. des Sc., Paris, 21 Juillet 1941, p. 117).

Prenons, comme exemple, pour cette courbe convexe un arc de cercle tangent à C en un point α de la plénitude. Nous trouvons

$$\Phi'(z) = o(|z-\alpha|^{-\frac{3}{2}}),$$

donc, en utilisant la notation du théorème IIIA,

$$L(z) = o(|z-\alpha|^{-\frac{1}{2}}).$$

Nous ne trouvons rien de nouveau, car le théorème IIIA est beaucoup plus général. Mais prenons une corde $\alpha\beta$, α étant sur la plénitude. Nous trouvons

$$\Phi'(z) = o(|z-\alpha|^{-\frac{1}{2}}),$$

donc, en utilisant la notation du théorème IVA,

$$L(z) \text{ est finie, } ^{2})$$

résultat dépassant largement celui énoncé par le théorème IVA pour *toutes les cordes* du cercle.

Prenons les courbes du théorème VA; α étant sur la plénitude, nous trouvons pour $z \to \alpha$

$$\Phi'(z) = o\left(|z-\alpha|^{\frac{1}{2}-\frac{1}{q}}\right),$$

donc

$$L(z) = o\left(|z-\alpha|^{\frac{3}{2}-\frac{1}{q}}\right).$$

Or, si $q > \frac{1}{3}$, $\frac{3}{2} - \frac{1}{q} > -\frac{1}{2q}$, donc la majoration dépasse alors celle du théorème VA.

Enfin considérons dans D les courbes Γ_t d'équations

$$y = a x^q + t \ , \ a > 0, \ 1 \geqq q \geqq \tfrac{1}{2} \ , \ -\infty < t < \infty .$$

Sur une plénitude e de points it de l'axe imaginaire (16) et (17) sont vrais. Supposons que l'origine appartienne à e. Ecrivons l'inégalité (1) en coordonnées polaires:

$$\iint_D |f'|^2 \varrho \, d\varrho \, d\varphi < \infty \quad . \quad . \quad . \quad . \quad . \quad . \quad . \quad (20)$$

Soit $\varepsilon > 0$. Montrons que, pour ϱ suffisamment petit, le segment d'extrémités $\varrho/2$ et ϱ contient au moins **un** point ϱ' tel que la longueur $L(\varrho')$ de l'image du demi-cercle $|z| = \varrho', -\frac{\pi}{2} < \varphi < \frac{\pi}{2}$ soit $< \varepsilon$, donc que

$$L(\varrho') = \int_{-\frac{\pi}{2}}^{\frac{\pi}{2}} |f'(\varrho' e^{i\varphi})| \, \varrho' \, d\varphi < \varepsilon. \quad . \quad . \quad . \quad . \quad . \quad (21)$$

En effet, dans le cas contraire il existerait une suite $\varrho_n \to 0$ telle que

$$\int_{\frac{\varrho_n}{2}}^{\varrho_n} \{L(\varrho)\}^2 \, d\varrho \geqq \frac{\varepsilon^2 \varrho_n}{2}, \quad n = 1, 2, \ldots \quad . \quad . \quad . \quad . \quad (22)$$

---

2) Voir les notes de DENJOY et de WOLFF, Comptes rendus de l'Ac. des Sc., 23 Juin 1941.

Donc, en vertu de l'inégalité de SCHWARZ, C_n étant la couronne $\frac{\varrho_n}{2} \leqq \varrho \leqq \varrho_n$,

$$\frac{\varepsilon^2 \varrho_n}{2} \leqq \int_{\frac{\varrho_n}{2}}^{\varrho_n} |L(\varrho)|^2 \, d\varrho = \int_{\frac{\varrho_n}{2}}^{\varrho_n} \left| \int_{-\frac{\pi}{2}}^{\frac{\pi}{2}} |f'| \, \varrho \, d\varphi \right|^2 d\varrho \leqq \pi \varrho_n \iint_{C_n} |f'|^2 \varrho \, d\varrho \, d\varphi. \quad (23)$$

De (23) on conclut que les aires des images des couronnes C_n, $n = 1, 2, \ldots$, surpassent $\varepsilon^2/2\pi$ ce qui contredit (20). Par suite l'énoncé est vrai.

Cela posé, soient z_1 et z_2 deux points sur Γ_0. Posons $|z_1| = \varrho_1$, $|z_2| = \varrho_2$. Aux valeurs suffisamment petites de ϱ_1 et ϱ_2 correspondent des nombres ϱ_1' et ϱ_2' satisfaisant à

$$\frac{\varrho_1}{2} \leqq \varrho_1' \leqq \varrho_1, \; \frac{\varrho_2}{2} \leqq \varrho_2' \leqq \varrho_2, \; L(\varrho_1') < \varepsilon, \; L(\varrho_2') < \varepsilon. \quad . \quad . \quad (24)$$

Les demi-cercles dans D de rayons ϱ_1' et ϱ_2' coupent Γ_0 en deux points z_1' et z_2'. Il vient

$$f(z_2) - f(z_1) = \int_{z_1}^{z_2} f' \, dz = \left(\int_{\varrho_1'}^{\varrho_2'} + \int_{z_1'}^{\varrho_1'} + \int_{\varrho_2'}^{z_1'} + \int_{z_1}^{z_2'} - \int_{z_1'}^{z_2} \right) f' \, dz. \quad (25)$$

Supposons dorénavant ϱ_1 et ϱ_2 suffisamment petits. Alors d'après (17)

$$\left| \int_{\varrho_1'}^{\varrho_2'} f' \, dz \right| = |f(\varrho_2') - f(\varrho_1')| < \varepsilon. \quad . \quad . \quad . \quad . \quad . \quad (26)$$

D'après (21) et (24):

$$\left(\int_{z_1'}^{\varrho_1'} + \int_{\varrho_2'}^{z_2'} \right) f' \, dz < L(\varrho_1') + L(\varrho_2') < 2\varepsilon. \quad . \quad . \quad . \quad (27)$$

Enfin calculons les deux dernières intégrales dans (25) sur Γ_0, en utilisant l'inégalité de SCHWARZ et l'hypothèse $1 \geqq q \geqq \frac{1}{2}$. Il vient

$$\int_{z_1}^{z_1'} f' \, dz \leqq 2 \int_{z_1}^{z_1'} f' \, dy = 2 \int_{z_1'}^{z_1} y^{\frac{1}{2}} |f'| \cdot \frac{dy}{y^{\frac{1}{2}}} \leqq 2 \left(\int_{z_1'}^{z_1} |f'|^2 y \, dy \right)^{\frac{1}{2}} \cdot \left(\int_{z_1'}^{z_1} \frac{dy}{y} \right)^{\frac{1}{2}} =$$

$$= 2a q^{\frac{1}{2}} \cdot \left(\log \frac{y_1}{y_1} \right)^{\frac{1}{2}} \cdot \left(\int_{z_1'}^{z_1} |f'|^2 \, dx \right)^{\frac{1}{2}}.$$

D'après (16) et (24) il vient donc

$$\left| \int_{z}^{z_1'} f' \, dz \right| < \varepsilon \text{ et de la même manière } \left| \int_{z'}^{z_1} f' \, dz \right| < \varepsilon. \quad . \quad (28)$$

De (25), (26), (27) et (28) résulte que, pour ϱ_1 et ϱ_2 assez petits,

$$|f(z_2) - f(z_1)| < \varepsilon.$$

Nous avons donc démontré que, z tendant vers O sur Γ_0, $f(z)$ tend vers une limite. De même sur la courbe Γ_0 d'équation $y = -a x^q$. Par suite, z tendant vers O, en restant

dans le domaine $y^2 < a^2 x^{2q}$, $f(z)$ tend vers une limite unique $l(0)$. Nous avons démontré le

THÉORÈME VII. L'axe imaginaire contient une plénitude de points it tels que, z tendant vers it dans le domaine $|y-t| < a x^q$, $q \geqq \frac{1}{2}$. $f(z)$ tend vers une limite unique $I(t)$ [1]).

Traduisons ce théorème en un théorème sur les fonctions holomorphes, bornées et univalentes dans le cercle-unité, en nous bornant au cas $q = \frac{1}{2}$. Faisons d'abord une remarque: q étant fixé, la plénitude figurant dans le théorème VII dépend de a. Mais soit a_n une suite de nombres positis tendant vers l'infini. Les plénitudes correspondantes e_n ont en commun une plénitude e, et sur e l'énoncé VII est vrai, quelque soit $a > 0$. Il est clair que dans la traduction les nouvelles courbes peuvent être remplacées par des cercles tangent au cercle-unité.

Nous avons donc le

THÉORÈME VIIA. Etant donnée une fonction $\varphi(z)$ holomorphe, bornée et univalente dans le cercle-unité, la frontière $C(|z| = 1)$ contient une plénitude de points α tels que, z tendant vers α dans un cercle quelconque tangent à C en α, $\varphi(z)$ tend vers une limite unique $I(\alpha)$.

---

[1]) M. DENJOY a obtenu ce résultat pour les courbes satisfaisant à

$$\limsup_{z \to it} \frac{\log x}{\log |y-t|} < 2.$$

(Comptes rendus de l'Ac. des Sc. Paris, 7 Juillet 1941, p. 15). Cet ensemble de courbes ne contient pas les courbes du théorème VII correspondant à $q = 2$.
Les théorèmes VI et VII se trouvent dans deux notes de J. WOLFF, à paraître aux Comptes rendus.

Mathematics. — *Stark konvergente Entwicklungen für die vollständigen elliptischen Integrale erster und zweiter Art.* I. Von S. C. VAN VEEN. (Communicated by Prof. J. G. VAN DER CORPUT).

(Communicated at the meeting of September 27, 1941.)

Einleitung.

Seit den bahnbrechenden Arbeiten von JACOBI nnd WEIERSTRASS in Bezug auf die Theorie der Theta-Funktionen ist es üblich geworden, speziell bei numerischen Rechnungen, die älteren hypergeometrischen Reihenentwicklungen für die vollständigen elliptischen Integrale erster und zweiter Art, nämlich

$$K(k) = \int_0^{\frac{\pi}{2}} \frac{d\varphi}{\sqrt{1-k^2 \sin^2 \varphi}} = \frac{\pi}{2} F(\tfrac{1}{2}, \tfrac{1}{2}; 1; k^2)$$

und

$$E(k) = \int_0^{\frac{\pi}{2}} \sqrt{1-k^2 \sin^2 \varphi}\, d\varphi = \frac{\pi}{2} F(-\tfrac{1}{2}, \tfrac{1}{2}; 1; k^2),$$

wegen ihrer oft ungenügend starken Konvergenz, durch ein unvergleichlich stärkeres konvergentes Rechnungsverfahren mittels der Theta-Reihen zu ersetzen.

In der vorliegenden Arbeit wird gezeigt, dass die obengenannten hypergeometrischen Reihen in prinzipiell einfacher Weise in andere, ebenfalls hypergeometrische Reihen, deren Konvergenzstärke der der Theta-Reihen nicht nur gleichkommt, sondern beliebig weit übersteigen kann, transformiert werden können. Dazu kommt, dass in formeller Hinsicht diese Entwicklungen, als hypergeometrische Reihen, einfacher und regelmässiger als die notwendigen Umkehrungen der Theta-Reihen gebildet sind.

Diese Konvergenz ist dermassen stark, dass schon das sehr einfach gebildete Hauptglied *in allen vorkommenden Fällen* für reelles k eine *zehnstellige*, ja sogar oft eine *neunzehnstellige* Genauigkeit verbürgt.

Im § 1 betrachten wir den Fall, dass k nicht in der Nähe von 1 liegt. Vorläufig wird k reell vorausgesetzt, mit $0 \leqq k < 1$. Unter wiederholter Anwendung der LANDENschen Transformation wird die hypergeometrische Reihe $F(\frac{1}{2}, \frac{1}{2}; 1; k^2)$ in $F(\frac{1}{2}, \frac{1}{2}; 1; k_n^2)$ transformiert, wo k_n nach einigen Transformationen sehr klein ist, selbst wenn die Differenz zwischen 1 und k ziemlich klein ist. Das Bildungsverfahren der Grössen k_n wird dabei wesentlich auf das klassische Verfahren des arithmetisch-geometrischen Mittels von GAUSS zurückgeführt. (Satz I).

Als Beispiel dieser Entwicklungen nennen wir

$$K(k) = \frac{2\pi}{(1+\sqrt[4]{1-k^2})^2} F\left(\tfrac{1}{2}, \tfrac{1}{2}; 1; \left(\frac{1-\sqrt[4]{1-k^2}}{1+\sqrt[4]{1-k^2}}\right)^4\right). \qquad (K\,III)$$

Noch viel stärker konvergiert die Reihe

$$K(k) = \frac{2\pi}{\left(\cos\frac{\alpha}{2} + \sqrt[4]{\cos\alpha}\right)^2} F\left(\tfrac{1}{2}, \tfrac{1}{2}; 1; \left(\frac{\cos\frac{\alpha}{2} - \sqrt[4]{\cos\alpha}}{\cos\frac{\alpha}{2} + \sqrt[4]{\cos\alpha}}\right)^4\right),$$

$$\text{mit } \sin\alpha = k. \qquad (K\,IV)$$

deren Hauptglied

$$K(k) \approx \frac{2\pi}{\left(\cos\frac{\alpha}{2} + \sqrt[4]{\cos\alpha}\right)^2}$$

für $0 \leqq \alpha \leqq \frac{\pi}{4}$ eine zehnstellige Genauigkeit verbürgt. Im Allgemeinen ist für kleines k

$$k_n \approx \frac{\sin^{2^{n-1}}\alpha}{2^{2^{n-2}}}.$$

Dieses Verfahren kann in sehr einfacher Weise beliebig weit fortgesetzt werden und liefert im Hauptgliede bei jeder neuen Transformation ungefähr eine Genauigkeit in verdoppelter Stellenzahl Die Reihen des § 1 konvergieren somit sehr stark für $0 \leqq k < a < 1$. Die Konvergenz hört jedoch auf für $k = 1$, und ist unbefriedigend für k in der Nähe von 1.

Im § 2 betrachten wir den Fall, dass k in der Nähe von 1 liegt. Unter Anwendung eines klassischen Hilfssatzes von GAUSS wird $F(a, b; c; z)$ in eine Potenzreihe nach $(1-z)$ transformiert, in der überdies noch ein logarithmisches Glied auftritt in dem hier interessierenden Fall, wo $c - a - b$ ganz $\geqq 0$ ist. (Hilfssatz 1).

Es ergibt sich dann die allgemeine Entwicklung

$$K(k) = \frac{1}{2^{q-1}c_q} \log\frac{4}{l_q} \cdot F\left(\tfrac{1}{2}, \tfrac{1}{2}; 1; l_q^2\right) - \frac{1}{2^{q-2}c_q\pi} \cdot \sum_{m=1}^{\infty} \frac{1}{(2m-1)2m} \sum_{n=m}^{\infty} \left\{\frac{\Gamma\left(\frac{1}{2}+n\right)}{n!}\right\}^2 l_q^{2n}$$

(Satz IV), mit einfach gebildeten l_q, und c_q, die nach der Methode des arithmetisch-geometrischen Mittels berechnet werden.

Wichtige Sonderfälle sind die stark konvergenten Gegenstücke von $(K\ III)$ und $(K\ IV)$, nämlich $(K^*\ III)$ und $(K^*\ IV)$ mit

$$q=3;\ c_q = \left(\frac{1+\sqrt{\sin\alpha}}{2}\right)^2;\ l_q = \left(\frac{1-\sqrt{\sin\alpha}}{1+\sqrt{\sin\alpha}}\right)^2;$$

$$q=4;\ c_q = \left(\frac{\cos\left(\frac{\pi}{4}-\frac{\alpha}{2}\right) + \sqrt[4]{\sin\alpha}}{2}\right)^2;\ l_q = \left(\frac{\cos\left(\frac{\pi}{4}-\frac{\alpha}{2}\right) - \sqrt[4]{\sin\alpha}}{\cos\left(\frac{\pi}{4}-\frac{\alpha}{2}\right) + \sqrt[4]{\sin\alpha}}\right)^2;$$

deren einfache Hauptglieder

$$K(k) \approx \frac{2}{(1+\sqrt{\sin\alpha})^2} \log 2\left(\frac{1+\sqrt{\sin\alpha}}{1-\sqrt{\sin\alpha}}\right),$$

und

$$K(k) \approx \frac{1}{\left(\cos\left(\frac{\pi}{4}-\frac{\alpha}{2}\right) + \sqrt[4]{\sin\alpha}\right)^2} \log 2\left(\frac{\cos\left(\frac{\pi}{4}-\frac{\alpha}{2}\right) + \sqrt[4]{\sin\alpha}}{\cos\left(\frac{\pi}{4}-\frac{\alpha}{2}\right) - \sqrt[4]{\sin\alpha}}\right)$$

dieselbe Genauigkeit verbürgen für $\frac{\pi}{4} \leqq \alpha < \frac{\pi}{2}$ wie die Hauptglieder von $(K\ III)$ und $(K\ IV)$ für $0 \leqq \alpha \leqq \frac{\pi}{4}$.

Im § 3 werden die Untersuchungen auf die Entwicklung der vollständigen elliptischen Integrale zweiter Art erweitert. Erst wird dazu im Hilfssatz 2 die (bekannte) Anwendung der LANDENschen Transformation auf die elliptischen Integrale zweiter Art vorgenommen. Endlich ergibt sich im Satz VI eine allgemeine Entwicklung folgender Art

$$E(k) = p_n F\left(-\tfrac{1}{2}, \tfrac{1}{2}; 1; k_n'^2\right) + q_n F\left(\tfrac{1}{2}, \tfrac{1}{2}; 1; k_n'^2\right), \quad n = 2,$$

wo p_n und q_n in einfacher Weise bestimmt werden.

Als sehr genaue Approximation geben wir das Hauptglied von E (IV')

$$E(k) = \frac{\pi}{2} \cdot \frac{\left(\cos\frac{\alpha}{2} + \sqrt[4]{\cos\frac{\alpha}{2}}\right)^4 - 4\sqrt{\cos\alpha}\,(1 + \sqrt{\cos\alpha} + \cos\alpha)}{\left(\cos\frac{\alpha}{2} + \sqrt[4]{\cos\frac{\alpha}{2}}\right)^2}$$

Die letzten Entwicklungen gelten für kleines k, also k nicht in der Nähe von l. Wenn k in der Nähe von 1 liegt, wird im Satz VII eine allgemeine Entwicklung der folgenden Form abgeleitet:

$$E(k) = c_n F\left(-\tfrac{1}{2}, \tfrac{1}{2}; 1; l_n'^2\right) + \frac{c_n}{2} l_n^2 \log\frac{4}{l_n} F\left(\tfrac{1}{2}, \tfrac{3}{2}; 2; l_n^2\right)$$

$$- \frac{2c_n}{\pi} \sum_{m=0}^{\infty} r_m \sum_{q=m}^{\infty} s_q\, l_n^{2q+2} + A_n K(k)$$

wo die Koeffizienten A_n, c_n, l_n, r_m und s_q in einfacher Weise bestimmt werden.

Das Hauptglied im Falle $n = 3$ wird

$$E(k) = \left(1 + \sqrt{\sin\alpha}\right)^2 + \frac{1}{2}\,\frac{(1 - \sin\alpha)(3 + \sin\alpha)}{(1 + \sqrt{\sin\alpha})^2} \log 2\left(\frac{1 + \sqrt{\sin\alpha}}{1 - \sqrt{\sin\alpha}}\right).$$

Im § 4 wird gezeigt, dass alle Entwicklungen für K und E der § § 1 und 2 (mit einer Ausnahme) bei gehöriger Definition der Argumente der in Betracht kommenden Grössen *für alle komplexen Werte von k in der von $k = +1$ nach $+\infty$ aufgeschlitzten rechten Halbebene $R(k) \geqq 0$ gelten.*

Schliesslich wird gezeigt, dass man bei geeigneter Wahl der Reihen K und E nach einigen Transformationen *immer für alle komplexen Werte von k mit $R(k) \geqq 0$ eine starke Konvergenz erzeugen kann.*

Die in dieser Arbeit enthaltenen Ergebnisse und Methoden sind auf ein weiteres Gebiet anwendbar. Insbesondere die von F. EMDE [1]) betrachteten vollständigen elliptischen Integrale

$$D(k) = \int_0^{\frac{\pi}{2}} \frac{\sin^2\varphi\, d\varphi}{\sqrt{1 - k^2 \sin^2\varphi}}$$

und

$$C(k) = \int_0^{\frac{\pi}{2}} \frac{\sin^2\varphi \cos^2\varphi\, d\varphi}{(1 - k^2 \sin^2\varphi)^{\frac{3}{2}}}$$

[1]) F. EMDE. Zur Zahlenrechnung bei vollständigen elliptischen Integralen. Archiv für Elektrotechnik XXX, 1936, S. 243.

können mit grosser Genauigkeit in ähnlicher Weise entwickelt werden. Ueber diese Ergebnisse hoffen wir an gegebener Stelle zu berichten.

Die Entwicklung des vollständigen elliptischen Integrals erster Art.

§ 1. *k liegt nicht in der Nähe von* 1.

Im folgenden wird vorläufig k reell vorausgesetzt, mit $0 \leqq k < 1$.

Wir setzen

$$k = \sin\alpha, \text{ mit } 0 \leqq \alpha < \frac{\pi}{2},$$

und definieren erst die doppelte Zahlenfolge (a_n, b_n) durch

$$\left.\begin{aligned} a_0 &= 1 + k = 1 + \sin\alpha; \quad b_0 = 1 - k = 1 - \sin\alpha; \\ a_n &= \frac{a_{n-1} + b_{n-1}}{2} \quad ; \; b_n = \sqrt{a_{n-1}\, b_{n-1}}; \quad (n \geqq 1) \end{aligned}\right\} \quad . \quad . \quad (1)$$

(arithmetisches und geometrisches Mittel).

Für $n \geqq 2$ ist

$$a_n = \frac{a_{n-2} + b_{n-2} + 2\sqrt{a_{n-2}\, b_{n-2}}}{4} = \left(\frac{\sqrt{a_{n-2}} + \sqrt{b_{n-2}}}{2}\right)^2. \quad . \quad (2)$$

Aus (1) und (2) folgt

$$\left.\begin{aligned} a_1 &= 1 \qquad\qquad\qquad\qquad ; b_1 = \sqrt{1-k^2} = \cos\alpha; \\ a_2 &= \frac{1+\cos\alpha}{2} = \cos^2\frac{\alpha}{2} \qquad ; b_2 = \sqrt{\cos\alpha}; \\ a_3 &= \left(\frac{1+\sqrt{\cos\alpha}}{2}\right)^2 \qquad ; b_3 = \cos\frac{\alpha}{2}\sqrt[4]{\cos\alpha}; \\ a_4 &= \left(\frac{\cos\frac{\alpha}{2} + \sqrt[4]{\cos\alpha}}{2}\right)^2 \qquad ; b_4 = \sqrt{\cos\frac{\alpha}{2}} \cdot \sqrt[8]{\cos\alpha} \cdot \left(\frac{1+\sqrt{\cos\alpha}}{2}\right); \\ a_5 &= \left(\frac{1+\sqrt{\cos\alpha} + 2\sqrt[8]{\cos\frac{\alpha}{2}} \cdot \sqrt[8]{\cos\alpha}}{4}\right)^2; \\ b_5 &= \sqrt[4]{\cos\frac{\alpha}{2}} \cdot \sqrt[16]{\cos\alpha} \cdot \sqrt{\frac{1+\sqrt{\cos\alpha}}{2}} \cdot \frac{\cos\frac{\alpha}{2} + \sqrt[4]{\cos\alpha}}{2}; \end{aligned}\right\} \quad (3)$$

u. s. w.

Weiter definieren wir

$$\left.\begin{aligned} k_n &= \frac{a_{n-1} - b_{n-1}}{a_{n-1} + b_{n-1}} \quad (n \geqq 1) \\ &= \left(\frac{\sqrt{a_{n-2}} - \sqrt{b_{n-2}}}{\sqrt{a_{n-2}} + \sqrt{b_{n-2}}}\right)^2 \quad (n \geqq 2) \end{aligned}\right\} \quad . \quad . \quad . \quad . \quad (4)$$

also, wegen (3)

$$\left.\begin{aligned} k_1 &= k = \sin\alpha \quad ; \\ k_2 &= \frac{1-\sqrt{1-k^2}}{1+\sqrt{1-k^2}} = \frac{1-\cos\alpha}{1+\cos\alpha} = tg^2\frac{\alpha}{2} \quad ; \\ k_3 &= \left(\frac{1-\sqrt[4]{1-k^2}}{1+\sqrt[4]{1-k^2}}\right)^2 = \left(\frac{1-\sqrt{\cos\alpha}}{1+\sqrt{\cos\alpha}}\right)^2 \quad ; \\ k_4 &= \left(\frac{\cos\frac{\alpha}{2}-\sqrt[4]{\cos\alpha}}{\cos\frac{\alpha}{2}+\sqrt[4]{\cos\alpha}}\right)^2 \quad ; \\ k_5 &= \left(\frac{1+\sqrt{\cos\alpha}-2\sqrt{\cos\frac{\alpha}{2}\cdot\sqrt[8]{\cos\alpha}}}{1+\sqrt{\cos\alpha}+2\sqrt{\cos\frac{\alpha}{2}\cdot\sqrt[8]{\cos\alpha}}}\right)^2 ; \\ &\text{u. s. w.} \end{aligned}\right\} \quad \ldots \quad (5)$$

Weiter ist zu bemerken, dass, wegen (4) und (1), für $n \geqq 1$

$$1+k_n = \frac{2\,a_{n-1}}{a_{n-1}+b_{n-1}} = \frac{a_{n-1}}{a_n}; \quad \ldots \quad (6)$$

$$1-k_n = \frac{2\,b_{n-1}}{a_{n-1}+b_{n-1}} = \frac{b_{n-1}}{a_n}; \quad \ldots \quad (7)$$

$$\sqrt{1-k_n^2} = \sqrt{\frac{a_{n-1}\,b_{n-1}}{a_n^2}} = \frac{b_n}{a_n}; \quad \ldots \quad (8)$$

$$\frac{1-\sqrt{1-k_n^2}}{1+\sqrt{1-k_n^2}} = \frac{a_n-b_n}{a_n+b_n} = k_{n+1}; \quad \ldots \quad (9)$$

$$\frac{1-k_n}{1+k_n} = \frac{b_{n-1}}{a_{n-1}} = \sqrt{1-k_{n-1}^2}; \quad \ldots \quad (10)$$

$$k_{n-1} = \frac{2\sqrt{k_n}}{1+k_n}; \quad \ldots \quad (11)$$

ist.

Satz I: Setzt man für ganzes $n \geqq 1$

$$\int_0^{\frac{\pi}{2}} \frac{d\varphi}{\sqrt{1-k_n^2\sin^2\varphi}} = K(k_n),$$

so ist

$$K(k_1) = \frac{K(k_2)}{a_2} = \ldots = \frac{K(k_n)}{a_n} = \frac{\pi}{2\,a_n} F(\tfrac{1}{2}, \tfrac{1}{2}; 1; k_n^2). \quad . \quad . \quad (12)$$

Beweis: Wegen (9) ist $0 \leq k_n < 1$ $(n \geq 1)$. Durch die LANDENsche Transformation

$$tg\,\varphi = \frac{sin\,2\omega}{p + cos\,2\omega}$$

geht

$$\int_0^{\alpha} \frac{d\varphi}{\sqrt{1-p^2\,sin^2\,\varphi}}$$

über in

$$\frac{2}{1+p} \int_0^{\beta} \frac{d\omega}{\sqrt{1 - \frac{4p}{(1+p)^2}\,sin^2\,\omega}}$$

mit

$$tg\,\alpha = \frac{sin\,2\beta}{p + cos\,2\beta}$$

(vgl. I, Proceedings XLIV, S. 607, Hilfssatz 1).

Wenn ω das Intervall $\left(0, \frac{\pi}{2}\right)$ durchläuft, so durchläuft φ das Intervall $(0, \pi)$ und findet man

$$\int_0^{\pi} \frac{d\varphi}{\sqrt{1-p^2\,sin^2\,\varphi}} = \frac{2}{1+p} \int_0^{\frac{\pi}{2}} \frac{d\omega}{1 - \frac{4p}{(1+p)^2}\,sin^2\,\omega},$$

also

$$2\,K(p) = \frac{2}{1+p} K\left(\frac{2\sqrt{p}}{1+p}\right). \quad . \quad . \quad . \quad . \quad . \quad . \quad . \quad (13)$$

Setzt man

$$\frac{2\sqrt{p}}{1+p} = k_{n-1},$$

somit

$$p = \frac{1 - \sqrt{1-k_{n-1}^2}}{1 + \sqrt{1-k_{n-1}^2}} = k_n \quad \text{(wegen (9))}$$

so geht (13) über in

$$K(k_n) = \frac{a_n}{a_{n-1}} K(k_{n-1}), \quad . \quad . \quad . \quad . \quad . \quad . \quad . \quad . \quad (14)$$

sodass

$$\frac{K(k_n)}{a_n} = \frac{K(k_{n-1})}{a_{n-1}} = \ldots = \frac{K(k_1)}{a_1}$$

ist. Endlich hat man

$$K(k_n) = \frac{\pi}{2} F(\tfrac{1}{2}, \tfrac{1}{2}; 1; k_n^2).$$

Bemerkung: (14) ist gleichwertig mit

$$F(\tfrac{1}{2}, \tfrac{1}{2}; 1; k_{n-1}^2) = (1 + k_n) \cdot F(\tfrac{1}{2}, \tfrac{1}{2}; 1; k_n^2) =$$
$$= \frac{2}{1 + \sqrt{1-k_{n-1}^2}} \cdot F\left(\tfrac{1}{2}, \tfrac{1}{2}; 1; \left(\frac{1 - \sqrt{1-k_{n-1}^2}}{1 + \sqrt{1-k_{n-1}^2}}\right)^2\right).$$

Dieses Ergebnis ist ein Sonderfall einer allgemeinen KUMMERschen Transformationsformel der hypergeometrischen Funktion [1])

$$F(\alpha, \beta; 2\beta; x) = \left(\frac{2}{1 + \sqrt{1-x}}\right)^{2\alpha} F\left(\alpha, \alpha - \beta + \tfrac{1}{2}; \beta + \tfrac{1}{2}; \left(\frac{1 - \sqrt{1-x}}{1 + \sqrt{1-x}}\right)^2\right).$$

Zu bemerken ist, dass die Reihe im rechten Gliede erheblich schneller konvergiert als die Reihe im linken Gliede, wegen

$$\left(\frac{1 - \sqrt{1-k_{n-1}^2}}{1 + \sqrt{1-k_{n-1}^2}}\right)^2 \approx \frac{k_{n-1}^4}{16}.$$

Aus (12), (5) und (3) ergeben sich für $n = 1, \ldots, 5$ die wichtigen Sonderfälle, die eine Folge immer stärker konvergenter Reihen für $K(k)$ bilden, nämlich

$$K(k) = \frac{\pi}{2} F(\tfrac{1}{2}, \tfrac{1}{2}; 1; k^2) = \frac{\pi}{2} F(\tfrac{1}{2}, \tfrac{1}{2}; 1; \sin^2 \alpha); \qquad (K.\,I)$$

$$K(k) = \frac{\pi}{1 + \sqrt{1-k^2}} F\left(\tfrac{1}{2}, \tfrac{1}{2}; 1; \left(\frac{1 - \sqrt{1-k^2}}{1 + \sqrt{1-k^2}}\right)^2\right) = \frac{\pi}{2\cos^2 \frac{\alpha}{2}} F\left(\tfrac{1}{2}, \tfrac{1}{2}; 1; tg^4 \frac{\alpha}{2}\right); \qquad (K.\,II)$$

$$K(k) = \frac{2\pi}{(1 + \sqrt[4]{1-k^2})^2} F\left(\tfrac{1}{2}, \tfrac{1}{2}; 1; \left(\frac{1 - \sqrt[4]{1-k^2}}{1 + \sqrt[4]{1-k^2}}\right)^2\right) = \frac{2\pi}{(1 + \sqrt{\cos \alpha})^2} F\left(\tfrac{1}{2}, \tfrac{1}{2}; 1; \left(\frac{1 - \sqrt{\cos \alpha}}{1 + \sqrt{\cos \alpha}}\right)^4\right); \qquad (K.\,III)$$

$$K(k) = \frac{2\pi}{\left(\cos \frac{\alpha}{2} + \sqrt[4]{\cos \alpha}\right)^2} F\left(\tfrac{1}{2}, \tfrac{1}{2}; 1; \left(\frac{\cos \frac{\alpha}{2} - \sqrt[4]{\cos \alpha}}{\cos \frac{\alpha}{2} + \sqrt[4]{\cos \alpha}}\right)^4\right); \qquad (K.\,IV)$$

[1]) CRELLE's Journal. Bd. **15**, 1836, S. 77, Formel (43), mit Druckfehler im rechten Gliede. $(2\alpha - 2\beta + 1$ statt $\beta + \frac{1}{2})$.

Uebrigens findet sich dieses Ergebnis schon wesentlich in GAUSS' Nachlass. Er ist vermutlich ± 1812 zu diesem Ergebnis gelangt, aber es wurde erst 1870 von SCHERING publiziert. (GAUSS, Werke III, S. 225, [101]).

$$K(k) = \frac{8\pi}{\left(1 + \sqrt{\cos\alpha} + 2\sqrt{\cos\frac{\alpha}{2}} \cdot \sqrt[8]{\cos\alpha}\right)^2} F\left(\tfrac{1}{2}, \tfrac{1}{2}; 1; \left(\frac{1 + \sqrt{\cos\alpha} - 2\sqrt{\cos\frac{\alpha}{2}} \cdot \sqrt[8]{\cos\alpha}}{1 + \sqrt{\cos\alpha} + 2\sqrt{\cos\frac{\alpha}{2}} \cdot \sqrt[8]{\cos\alpha}}\right)^4\right).$$

u. s. w. (*K. V*)

Wegen (9) ist

$$k_{n+1} = \frac{k_n^2}{(1 + \sqrt{1 - k_n^2})^2},$$

also

$$\frac{k_n^2}{4} \leqq k_{n+1} < k_n^2$$

und für kleine Werte von k ist

$$k_{n+1} \approx \frac{k_n^2}{4}$$

allgemein

$$k_n \approx \frac{\sin^{2^{n-1}}\alpha}{2^{2^n - 2}}.$$

Die Konvergenz der Reihen ist somit ausserordentlich stark, sodass man sich, zumal bei den Reihen *III*, *IV* und *V*, bei fast allen praktischen Rechnungen mit dem Gebrauche des ersten (Haupt-)Gliedes begnügen kann.

Diese Hauptglieder sind

$$K(k) \approx \frac{2\pi}{(1 + \sqrt[4]{1 - k^2})^2} = \frac{2\pi}{(1 + \sqrt{\cos\alpha})^2} \qquad (K.\ III')$$

$$K(k) \approx \frac{2\pi}{\left(\cos\frac{\alpha}{2} + \sqrt[4]{\cos\alpha}\right)^2} \qquad (K.\ IV')$$

$$K(k) \approx \frac{2\pi}{\left(1 + \sqrt{\cos\alpha} + 2\sqrt{\cos\frac{\alpha}{2}} \cdot \sqrt[8]{\cos\alpha}\right)^2} \qquad (K.\ V').$$

Die gemachten Fehler sind aus der folgenden Tabelle abzulesen.

α	$k_1 = \sin\alpha$	Fehler in		
		$K\,III'$	$K\,IV'$	$K\,V'$
$\leqq 45°$	$\leqq 0{,}70711$	$\leqq 2{,}6 \cdot 10^{-5}$	$\leqq 9{,}3 \cdot 10^{-11}$	$\leqq 1{,}1 \cdot 10^{-20}$
60°	0,86603	$4{,}7 \cdot 10^{-4}$	$2{,}6 \cdot 10^{-8}$	$7{,}5 \cdot 10^{-17}$
70°	0,93969	$3 \cdot 10^{-3}$	$8{,}7 \cdot 10^{-7}$	$7{,}6 \cdot 10^{-14}$
80°	0,98481	$2{,}3 \cdot 10^{-2}$	$4{,}2 \cdot 10^{-5}$	$1{,}4 \cdot 10^{-10}$
85°	0,99619	$8{,}5 \cdot 10^{-2}$	$5{,}1 \cdot 10^{-4}$	$1{,}7 \cdot 10^{-8}$
89°	0,99985	$5 \cdot 10^{-1}$	$1{,}6 \cdot 10^{-2}$	$1{,}1 \cdot 10^{-5}$

Obgleich die Reihen $K\,I - K\,V$ für $k = \sin\alpha = 1$ zu konvergieren aufhören, ist aus dieser Tabelle ersichtlich, dass die Reihen $K\,III - K\,V$ noch ausgezeichnet verwendbar sind, wenn der Unterschied zwischen k und 1 sehr gering ist.

Bemerkung: Die Formel (*K III'*) als Approximationsformel wird aus der Theorie der Thetafunktionen in SCHWARZ—WEIERSTRASS: Formeln und Lehrsätze zum Gebrauche der elliptischen Funktionen, S. 62, Formel (4) abgeleitet. Auch die vollständige hypergeometrische Entwicklung (*K III*) wird da, allerdings ohne Beweis, auf S. 68, Formel (10), angegeben.

Uebrigens ist (*K III*) ein Sonderfall der allgemeinen Transformationsformel von KUMMER (l.c. S. 129, Formel (13)):

$$F\left(\alpha, \frac{4\alpha+1}{6}; \frac{4\alpha+1}{3}; x\right) = \left(\frac{1+\sqrt[4]{1-x}}{2}\right)^{-4\alpha} F\left(\alpha, \frac{4\alpha+1}{6}; \frac{2\alpha+5}{6}; \left(\frac{1-\sqrt[4]{1-x}}{1+\sqrt[4]{1-x}}\right)^4\right).$$

Wendet man auf (12) die bekannte Transformationsformel

$$F(\alpha, \beta; \gamma; x) = (1-x)^{\alpha} F\left(\alpha, \gamma-\beta; \gamma; -\frac{x}{1-x}\right). \quad . \quad . \quad . \quad (15)$$

an, so ergibt sich, wegen (8)

Satz II: Für ganzes $n \geqq 1$ ist

$$K(k) = \frac{\pi}{2 b_n} F\left(\tfrac{1}{2}, \tfrac{1}{2}; 1; -\left(\frac{k_n a_n}{b_n}\right)^2\right). \quad . \quad . \quad . \quad . \quad . \quad (16)$$

Aus (16) und (5) ergeben sich nach einfacher Reduktion für $n = 1, \ldots, 5$ die wichtigen Sonderfälle mit ziemlich einfach gebildeten Hauptgliedern

$$K(k) = \frac{\pi}{2\cos\alpha} F\left(\tfrac{1}{2}, \tfrac{1}{2}; 1; -tg^2\alpha\right); \qquad (K.K.\,I)$$

$$K(k) = \frac{\pi}{2\sqrt{\cos\alpha}} \cdot F\left(\tfrac{1}{2}, \tfrac{1}{2}; 1; -\frac{\sin^4\frac{\alpha}{2}}{\cos\alpha}\right); \qquad (K.K.\,II)$$

$$K(k) = \frac{\pi}{2\cos\frac{\alpha}{2}\sqrt[4]{\cos\alpha}} \cdot F\left(\tfrac{1}{2}, \tfrac{1}{2}; 1; -\frac{\sin^8\frac{\alpha}{2}}{\cos^2\frac{\alpha}{2} \cdot \sqrt{\cos\alpha} \cdot (1+\sqrt{\cos\alpha})^4}\right); \qquad (K.K.\,III)$$

$$K(k) = \frac{\pi}{\sqrt{\cos\frac{\alpha}{2} \cdot \sqrt[8]{\cos\alpha} \cdot (1+\sqrt{\cos\alpha})}} \times$$

$$\times F\left(\tfrac{1}{2}, \tfrac{1}{2}; 1; -\frac{4\sin^{16}\frac{\alpha}{2}}{\cos\frac{\alpha}{2} \cdot \sqrt[4]{\cos\alpha} \cdot (1+\sqrt{\cos\alpha})^{10}\left(\cos\frac{\alpha}{2}+\sqrt[4]{\cos\alpha}\right)^4}\right); \qquad (K.K.\,IV)$$

$$K(k) = \frac{\pi}{\sqrt[4]{\cos\frac{\alpha}{2}} \cdot \sqrt[16]{\cos\alpha} \cdot \sqrt{\frac{1+\sqrt{\cos\alpha}}{2} \cdot \left(\cos\frac{\alpha}{2}+\sqrt[4]{\cos\alpha}\right)}} \cdot F\left(\tfrac{1}{2}, \tfrac{1}{2}; 1; \right.$$

$$\left. -\frac{2^7 \sin^{32}\frac{\alpha}{2}}{\sqrt{\cos\frac{\alpha}{2} \cdot \sqrt[8]{\cos\alpha} \cdot (1+\sqrt{\cos\alpha})^{17} \cdot \left(\cos\frac{\alpha}{2}+\sqrt[4]{\cos\alpha}\right)^{10}\left(1+\sqrt{\cos\alpha}+2\sqrt{\cos\frac{\alpha}{2} \cdot \sqrt[8]{\cos\alpha}}\right)^4}}\right). \qquad (K.K.\,V)$$

u. s. w.

Wegen $\frac{a_n^2}{b_n^2} = \frac{1}{1-k_n^2}$ ist die Stärke der Konvergenz der Reihen (K) und (KK) fast dieselbe. Die Konvergenzbereiche sind jedoch nicht gleich. Während die Reihen (K) für reelles k im Gebiet $0 \leqq \alpha < \frac{\pi}{2}$ konvergieren, konvergiert die Reihe (15), bzw. (16) im Gebiet $0 \leqq k_n^2 \leqq \frac{1}{2}$.

Wegen (11) bestätigt man ohne Schwierigkeit, dass

die Reihe	(KKI)	nur konvergiert für $\alpha \leqq 45°$
	$(KK\,II)$	$\alpha \leqq 80°.6'$
	$(KK\,III)$	$\alpha \leqq 89°.59'\,54''$
	$(KK\,IV)$	$\alpha \leqq 89°.59'\,59{,}99997''$

u. s. w.

W. v. IGNATOWSKI [1]) hat die folgende Approximationsformel aufgestellt

$$K(k) \approx \frac{\pi}{2\cos\frac{\alpha}{2}\,(\cos\alpha)^{\frac{1}{2}}}\left\{1 - \frac{\left(\sin\frac{\alpha}{2}\right)^8}{64\left(\cos\frac{\alpha}{2}\right)^4\cos\alpha}\right\} \quad . \quad . \quad . \quad (17),$$

die fast mit $(KK\,III)$ übereinstimmt. Diese Uebereinstimmung wird vollständig unter Anwendung der Transformationsformel [2])

$$(1+y)^{2\alpha}\,F(2\alpha, 2\alpha+1-\gamma; \gamma; y) = F\left(\alpha, \alpha+\tfrac{1}{2}; \gamma; \frac{4y}{(1+y)^2}\right)$$

auf $(K\,III)$. Man findet für $\alpha = \frac{1}{4}$, $\gamma = 1$

$$K(k) = \frac{2\pi\,(1+y)^{-\frac{1}{2}}}{(1+\sqrt{\cos\alpha})^2}\,F\left(\tfrac{1}{4}, \tfrac{3}{4}; 1; \frac{4y}{(1+y)^2}\right).$$

Wendet man nachher (15) an, so findet man für $y = \left(\frac{1-\sqrt{\cos\alpha}}{1+\sqrt{\cos\alpha}}\right)^2$

$$K(k) = \frac{2\pi\,(1+y)^{-\frac{1}{2}}}{(1+\sqrt{\cos\alpha})^2}\left(\frac{1-y}{1+y}\right)^{-\frac{1}{2}} F\left(\tfrac{1}{4}, \tfrac{1}{4}; 1; -\frac{4y}{(1+y)^2}\right) = \left.\begin{array}{l} \\ \\ = \dfrac{\pi}{2\cos\frac{\alpha}{2}\,.\,(\cos\alpha)^{\frac{1}{2}}}\,F\left(\tfrac{1}{4}, \tfrac{1}{4}; 1; -\dfrac{\sin^8\frac{\alpha}{2}}{4\cos\alpha\,.\left(\cos\frac{\alpha}{2}\right)^4}\right), \end{array}\right\} \quad (18)$$

also eine Formel, von der (17) die ersten beiden Glieder bildet.

Jedoch ist (18), und somit auch (17), nur der Sonderfall mit $\alpha = \frac{1}{2}$, $x = \sin^2\alpha$ der fast um ein Jahrhundert älteren Formel von KUMMER [3])

$$F\left(\alpha, \frac{4\alpha+1}{6}; \frac{4\alpha+1}{3}; x\right) = \left(\frac{\sqrt[4]{1-x}\,.\,(1+\sqrt{1-x})}{2}\right)^{-\alpha} \times$$

$$\times F\left(\frac{\alpha}{2}, \frac{2-\alpha}{6}; \frac{2\alpha+5}{6}; -\frac{(1-\sqrt{1-x})^4}{16\sqrt{1-x}\,.\,(1+\sqrt{1-x})^2}\right),$$

[1]) Acad. des sc. de l'U. R. S. S., III, 1 (Leningrad 1933). S. 88. (Zitat nach JAHNKE—EMDE, Funktionentafeln, 2e Aufl. S. 145).

[2]) GAUSS, Werke III, S. 225, [100].

[3]) l.c. S. 130, Formel 21.

(Fortsetzung folgt.)

Mathematics. — *Ueber die Entwicklung der unvollständigen elliptischen Integrale erster und zweiter Art in stark konvergenten Reihen.* I. Von S. C. VAN VEEN. (Communicated by Prof. J. G. VAN DER CORPUT).

(Communicated at the meeting of September 27, 1941.)

Die Reihenentwicklung der beiden *unvollständigen* elliptischen Integrale erster und zweiter Art

$$F(\sin\alpha, \beta) = \int_0^{\beta} \frac{d\varphi}{\sqrt{1-\sin^2\alpha \,.\, \sin^2\varphi}}$$

und

$$E(\sin\alpha, \beta) = \int_0^{\beta} \sqrt{1-\sin^2\alpha \,.\, \sin^2\varphi}\, d\varphi$$

für beliebige reelle Werte von α und β ist bisher, soviel mir bekannt ist, selten eingehend untersucht worden. Zwar gibt u.a. HOÜEL [1]) für alle vorkommenden Fälle ziemlich einfache Reihenentwicklungen, aber ihre Konvergenz ist nur dann befriedigend, wenn α und β entweder sehr wenig von 0 oder von $\frac{\pi}{2}$ verschieden sind.

Zweck der vorliegenden Untersuchungen ist, für alle vorkommenden Fälle Reihenentwicklungen für E und F abzuleiten, deren Konvergenz dermassen stark ist, dass mann sich in weitaus den meisten praktischen Rechnungen mit den Hauptgliedern begnügen kann.

Es ergibt sich nun, dass drei verschiedene Entwicklungen notwendig sind, je nachdem

1) α klein ist $\left(\text{nicht in der Nähe von } \frac{\pi}{2}\right)$,

2) α in der Nähe von $\frac{\pi}{2}$ liegt und β klein ist,

3) α und β beide in der Nähe von $\frac{\pi}{2}$ liegen

Im § 1 wird der erste Fall eingehend betrachtet. Unter wiederholter Anwendung der LANDENschen Transformation ergibt sich in (11) eine stark konvergente Entwicklung, deren erste Glieder sind:

$$F(\sin\alpha, \beta) = \frac{1}{(1+\sqrt{\cos\alpha})^2}\{\beta + \operatorname{arc\,tg}(\cos\alpha\, \operatorname{tg}\beta) + 2\operatorname{arc\,tg}(\sqrt{\cos\alpha}\,.\,\operatorname{tg}\beta)\}$$

$$+ \frac{1}{2(1+\sqrt{\cos\alpha})^2}\left(\frac{1-\sqrt{\cos\alpha}}{1+\sqrt{\cos\alpha}}\right)^4\left(\frac{\beta_3}{2} - \frac{\sin 2\beta_3}{4}\right) +$$

$$+ \frac{3}{8(1+\sqrt{\cos\alpha})^2}\left(\frac{1-\sqrt{\cos\alpha}}{1+\sqrt{\cos\alpha}}\right)^8\left(\frac{3\beta_3}{8} - \frac{\sin 2\beta_3}{4} + \frac{\sin 4\beta_3}{32}\right)$$

$$+ \frac{5}{16(1+\sqrt{\cos\alpha})^2}\left(\frac{1-\sqrt{\cos\alpha}}{1+\sqrt{\cos\alpha}}\right)^{12}\left(\frac{5\beta_3}{16} - \frac{15\sin 2\beta_3}{64} + \frac{3\sin 4\beta_3}{64} - \frac{\sin 6\beta_3}{192}\right) + \ldots$$

[1]) Recueil de formules et de tables numériques, 3me Ed. Paris 1885, S XLV u.f.

wo

$$\beta_3 = \beta + arc\,tg\,(\cos\alpha\,tg\,\beta) + 2\,arc\,tg\,(\sqrt{\cos\alpha}\,.\,tg\,\beta)$$

$0 \leqq \alpha < \frac{\pi}{2}$; β ist beliebig; jedoch kann ohne Beschränkung der Allgemeinheit $0 \leqq \beta \leqq \frac{\pi}{2}$ genommen werden. Dann sind für $arc\,tg\,(\cos\alpha\,tg\,\beta)$ und $arc\,tg\,(\sqrt{\cos\alpha}\,tg\,\beta)$ die Hauptwerte zu wählen.

Diese Reihe konvergiert nicht für $\alpha = \frac{\pi}{2}$. Jedoch ist sie noch sehr gut brauchbar für Werte von α, die ziemlich in der Nähe von $\frac{\pi}{2}$ liegen. Das Hauptglied (12)

$$F(\sin\alpha, \beta) \approx \frac{1}{(1+\sqrt{\cos\alpha})^2}\{\beta + arc\,tg\,(\cos\alpha\,.\,tg\,\beta) + 2\,arc\,tg\,(\sqrt{\cos\alpha}\,.\,tg\,\beta)\}$$

wird für die meisten praktischen Zwecke genügen.

In (23) wird das analoge, jedoch weniger einfache Ergebnis für $E(\sin\alpha, \beta)$ angegeben. Diese Reihe hat als Hauptglied (24)

$$E(\sin\alpha, \beta) \approx \frac{\sin 2\beta\,.\,\sin^2\alpha}{8\,\triangle} + \frac{tg\,\beta\,.\,\sin^2\frac{\alpha}{2}\,.\,\triangle}{1+\cos\alpha\,.\,tg^2\beta}$$

$$+ \frac{\cos^4\frac{\alpha}{2}}{(1+\sqrt{\cos\alpha})^2}\{\beta + arc\,tg\,(\cos\alpha\,tg\,\beta) + 2\,arc\,tg\,(\sqrt{\cos\alpha}\,.\,tg\,\beta)\}$$

mit

$$\triangle = \sqrt{1-\sin^2\alpha\,\sin^2\beta}.$$

Im § 2 wird der Fall, dass α in der Nähe von $\frac{\pi}{2}$ liegt und β klein ist, näher betrachtet. In (27) ergibt sich die in diesem Gebiet besonders stark konvergente Entwicklung

$$F(\sin\alpha, \beta) = \frac{1}{2\sqrt{\sin\alpha}}\,log\,w\sum_{n=0}^{\infty}(-1)^n\left(\frac{1\,.\,3\,.\,5\,\ldots\,(2n-1)}{2\,.\,4\,.\,6\,\ldots\,2n}\right)^2\left(\frac{x}{2}\right)^{2n}$$

$$+ \frac{1}{4\sqrt{\sin\alpha}}\sum_{n=1}^{\infty}\left(\frac{1\,.\,3\,.\,5\,\ldots\,(2n-1)}{2\,.\,4\,.\,6\,\ldots\,2n}\right)\left(\frac{xw}{4}\right)^{2n}\sum_{\substack{p=0\\ p\neq n}}^{2n}(-1)^p\binom{2n}{p}\frac{w^{-2p}}{n-p},$$

wo

$$x = \frac{1-\sin\alpha}{\sqrt{\sin\alpha}};\quad w = \frac{1+\sin\beta\sqrt{\sin\alpha}}{1-\sin\beta\sqrt{\sin\alpha}}.$$

Das Hauptglied ist

$$F(\sin\alpha, \beta) \approx \frac{1}{2\sqrt{\sin\alpha}}\,log\,\frac{1+\sin\beta\sqrt{\sin\alpha}}{1-\sin\beta\sqrt{\sin\alpha}}.$$

In (33) findet sich das analoge, weniger einfache Ergebnis für $E(\sin\alpha, \beta)$ mit dem Hauptglied

$$E(\sin\alpha, \beta) \approx \frac{1-\sin\alpha}{2\sqrt{\sin\alpha}} \log \frac{1+\sin\beta\sqrt{\sin\alpha}}{1-\sin\beta\sqrt{\sin\alpha}} + \sin\beta\sin\alpha.$$

Als *hinreichende* Bedingung für die Konvergenz der beiden Reihen (27) und (33) findet sich

$$0 \leqq \sin^2\beta < \frac{1}{\sin\alpha}\left(\frac{2-x}{2+x}\right).$$

Im § 3 wird endlich der letzte und schwierigste Fall, wobei α und β beide in der Nähe von $\frac{\pi}{2}$ liegen, eingehend betrachtet. In (46) findet sich die gesuchte Entwicklung für $F(\sin\alpha, \beta)$, nämlich

$$(F\sin\alpha, \beta) = K(\alpha) - \frac{1}{2\sqrt{\sin\alpha}} \log y \sum_{n=0}^{\infty}{}' (-1)^n \left(\frac{1.3.5....(2n-1)}{2.4.6...2n}\right)^2 \left(\frac{x}{2}\right)^{2n}$$

$$- \frac{1}{4\sqrt{\sin\alpha}} \sum_{n=1}^{\infty} \left(\frac{1.3.5....(2n-1)}{2.4.6....2n}\right) \left\{\frac{(\triangle+\cos\beta\sqrt{\sin\alpha})^2}{4\sqrt{\sin\alpha}(1+\sin\alpha\sin^2\beta)}\right\}^{2n} \sum_{\substack{p=0 \\ p\neq n}}^{2n}{}' (-1)^p \binom{2n}{p} y^{-2p}{}_{n-p},$$

wo

$$x = \frac{1-\sin\alpha}{\sqrt{\sin\alpha}}; \quad y = \frac{\triangle+\cos\beta\sqrt{\sin\alpha}}{\triangle-\cos\beta\sqrt{\sin\alpha}}.$$

$K(\alpha)$ ist das *vollständige* elliptische Integral erster Art, dessen Wert bestimmt, bzw. approximiert werden kann nach den Vorschriften meiner Arbeit „Stark konvergente Entwicklungen für die *vollständigen* elliptischen Integrale erster und zweiter Art" [1] **(weiter zitiert als; V. E. I.; I u.s.w.)**. Das Hauptglied dieser Entwicklung ist

$$F(\sin\alpha, \beta) \approx K(\alpha) - \frac{1}{2\sqrt{\sin\alpha}} \log \frac{\triangle+\cos\beta\sqrt{\sin\alpha}}{\triangle-\cos\beta\sqrt{\sin\alpha}}$$

In (55) wird die analoge Entwicklung für $E(\sin\alpha, \beta)$ mit dem Hauptglied

$$E(\sin\alpha, \beta) \approx E(\alpha) - \operatorname{cotg}\beta \cdot \triangle + \frac{\cos^2\alpha}{8\sin\alpha}(1-2\sqrt{\sin\alpha}) \log y + \frac{\triangle \cdot \cos\beta \cdot (1+\sin\alpha)}{2(1+\sin\alpha \cdot \sin^2\beta)}$$

gegeben, wo $E(\alpha)$ das *vollständige* elliptische Integral zweiter Art ist, dessen Wert in V. E. I. bestimmt wurde.

Hinreichende Bedingung für die Konvergenz der beiden Entwicklungen (46) und (55) ist

$$1 \geqq \sin^2\beta > \frac{1}{\sin\alpha}\left(\frac{x-2}{x+2}\right)$$

mit

$$x = \frac{1+\sin\alpha}{\sqrt{\sin\alpha}} \; (\geqq 2)$$

[1] Proc. Ned. Akad. v. Wetensch., Amsterdam, **44**, 964 (1941).

In der untenstehenden Figur sind die Konvergenzgebiete der Reihen angegeben,

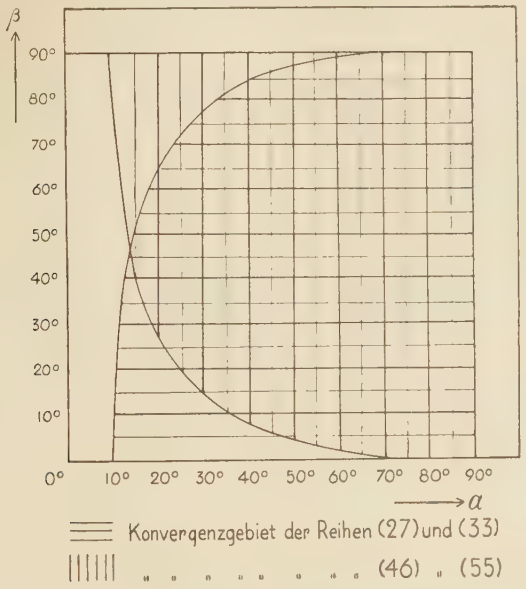

Fig. 1

Das horizontal schraffierte Gebiet stellt das Konvergenzgebiet der Reihen (27) und (33) da. (α in der Nähe von $\frac{\pi}{2}$; β nicht zu gross). Das vertikal schraffierte Gebiet stellt ebenso das Konvergenzgebiet der Reihen (45) und (55) da. Die Reihen (11) und (23) konvergieren im ganzen Quadrat $\left(0 \leqq \alpha < \frac{\pi}{2};\ 0 \leqq \beta \leqq \frac{\pi}{2}\right)$, die rechte Seite $\alpha = \frac{\pi}{2}$ ausgeschlossen.

Um die grösste Genauigkeit mit möglichst wenig Rechenarbeit zu erzielen, verfährt man am besten, wenn man die Reihen (11) und (23) aus § 1 bis etwa $\alpha = 70°$ benutzt. Die Reihen (27) und (33) aus § 2 verwendet man am besten für $70° \leqq \alpha \leqq 90°$; $0° \leqq \beta \leqq 70°$. Die Anwendung der Reihen (46) und (55) aus § 3 bleibt dann auf das Quadrat ($70° \leqq \alpha \leqq 90°$; $70° \leqq \alpha \leqq 90°$) beschränkt.

Schliesslich ist zu bemerken, dass im folgenden überall:

eine leere Summe $= 0$

und ein leeres Produkt $= 1$ bedeutet.

(*Fortsetzung folgt*).

Mathematics. — *Sur des séries et des intégrales définies contenantes les fonctions de* BESSEL. V. By J. G. RUTGERS. (Communicated by Prof. J. A. SCHOUTEN.)

(Communicated at the meeting of September 27, 1941.)

La substitution $\mu = \frac{1}{4}$ resp. $\mu = \frac{3}{4}$ dans (298) et (299) ou $\mu = \frac{1}{2}$ resp. $\mu = 1$ dans (300) et (301) donne après une légère réduction:

$$\left.\begin{aligned} \sum_{n=0}^{\infty} (-1)^n I_{n+\frac{1}{4}}(x) I_{n-\frac{1}{4}}(x) &= \frac{1}{\pi}\sqrt{\frac{2}{x}}\int_0^x I_0(x-\alpha)\cos(x-\alpha)\cos 2\alpha \frac{d\alpha}{\sqrt{\alpha}} = \\ &= I_{\frac{1}{2}}(x) I_{-\frac{1}{2}}(x) - \frac{1}{\sqrt{\pi}}\sqrt{\frac{2}{x}}\int_0^x I_0(x-\alpha)\sin(x-\alpha)\sin 2\alpha \frac{d\alpha}{\sqrt{\alpha}} = \\ &= \tfrac{1}{2} I_{\frac{1}{2}}(x) I_{-\frac{1}{2}}(x) + \frac{1}{\pi\sqrt{2x}}\int_0^x I_0(x-\alpha)\cos(x+\alpha)\frac{d\alpha}{\sqrt{\alpha}} \end{aligned}\right\} \quad (306)$$

(comme la demie somme des membres précédents),

$$\left.\begin{aligned} \sum_{n=0}^{\infty} (-1)^n I_{n+\frac{1}{4}}(x) I_{n+\frac{1}{4}}(x) &= \frac{1}{\pi}\sqrt{\frac{2}{x}}\int_0^x I_0(x-\alpha)\sin(x-\alpha)\cos 2\alpha \frac{d\alpha}{\sqrt{\alpha}} = \\ &= \frac{1}{\pi}\sqrt{\frac{2}{x}}\int_0^x I_0(x-\alpha)\cos(x-\alpha)\sin 2\alpha \frac{d\alpha}{\sqrt{\alpha}} = \\ &= \frac{1}{\pi\sqrt{2x}}\int_0^x I_0(x-\alpha)\sin(x+\alpha)\frac{d\alpha}{\sqrt{\alpha}} \end{aligned}\right\} \quad (307)$$

(comme la demie somme des membres précédents).

De l'égalité des membres intermédiaires de (306) et (307) suivent:

$$\int_0^x I_0(x-\alpha)\cos(3\alpha-x)\frac{d\alpha}{\sqrt{\alpha}} = \pi\sqrt{\frac{x}{2}}\, I_{\frac{1}{2}}(x) I_{-\frac{1}{2}}(x), \quad . \quad . \quad (308)$$

$$\int_0^x I_0(x-\alpha)\sin(3\alpha-x)\frac{d\alpha}{\sqrt{\alpha}} = 0. \quad . \quad . \quad . \quad . \quad . \quad (309)$$

La substitution $\mu = \frac{1}{2}$ dans (298) et (299) donne:

$$\sum_{n=0}^{\infty} (-1)^n I_{n+\frac{1}{2}}(x) I_n(x) = \sqrt{\frac{2}{\pi x}} \int_0^x I_0(2\alpha) I_0(x-\alpha) \cos(x-\alpha)\, d\alpha, \quad (310)$$

$$\sum_{n=0}^{\infty} (-1)^n I_{n+1}(x) I_{n+\frac{1}{2}}(x) = \sqrt{\frac{2}{\pi x}} \int_0^x I_0(2\alpha) I_0(x-\alpha) \sin(x-\alpha)\, d\alpha. \quad (311)$$

Ainsi la substitution $\mu = \frac{1}{4}$ resp. $\mu = \frac{3}{4}$ dans (302) et (303) ou $\mu = \frac{1}{2}$ resp. $\mu = 1$ dans (304) et (305) donne les formules particulières:

$$\left.\begin{aligned} &\sum_{n=0}^{\infty} (-1)^n I_{n+\frac{1}{4}}(x) \{\sin x\, I_{n-\frac{1}{4}}(x) - \cos x\, I_{n+\frac{3}{4}}(x)\} = \\ &\qquad = \frac{1}{\pi} \sqrt{\frac{2}{x}} \int_0^x I_0(x-\alpha) \cos 2\alpha \sin\alpha \frac{d\alpha}{\sqrt{\alpha}}, \end{aligned}\right\} \quad (312)$$

$$\left.\begin{aligned} &\sum_{n=0}^{\infty} (-1)^n I_{n+\frac{1}{4}}(x) \{\cos x\, I_{n-\frac{1}{4}}(x) + \sin x\, I_{n+\frac{3}{4}}(x)\} = \\ &\qquad = \frac{1}{\pi} \sqrt{\frac{2}{x}} \int_0^x I_0(x-\alpha) \cos 2\alpha \cos\alpha \frac{d\alpha}{\sqrt{\alpha}}, \end{aligned}\right\} \quad (313)$$

$$\left.\begin{aligned} &\sum_{n=0}^{\infty} (-1)^n I_{n+\frac{3}{4}}(x) \{\sin x\, I_{n+\frac{1}{4}}(x) - \cos x\, I_{n+\frac{5}{4}}(x)\} = \\ &\qquad = \frac{1}{\pi} \sqrt{\frac{2}{x}} \int_0^x I_0(x-\alpha) \sin 2\alpha \sin\alpha \frac{d\alpha}{\sqrt{\alpha}}, \end{aligned}\right\} \quad (314)$$

$$\left.\begin{aligned} &\sum_{n=0}^{\infty} (-1)^n I_{n+\frac{3}{4}}(x) \{\cos x\, I_{n+\frac{1}{4}}(x) + \sin x\, I_{n+\frac{5}{4}}(x)\} = \\ &\qquad = \frac{1}{\pi} \sqrt{\frac{2}{x}} \int_0^x I_0(x-\alpha) \sin 2\alpha \cos\alpha \frac{d\alpha}{\sqrt{\alpha}}, \end{aligned}\right\} \quad (315)$$

tandis que la substitution $\mu = \frac{3}{4}$ dans (304) et (305) donne:

$$\left.\begin{aligned} &\sum_{n=0}^{\infty} (-1)^n I_{n+\frac{1}{2}}(x) \{\sin x\, I_n(x) - \cos x\, I_{n+1}(x)\} = \\ &\qquad = \sqrt{\frac{2}{\pi x}} \int_0^x I_0(x-\alpha) I_0(2\alpha) \sin\alpha\, d\alpha, \end{aligned}\right\} \quad (316)$$

$$\left.\begin{aligned}\sum_{n=0}^{\infty}(-1)^n I_{n+\frac{1}{2}}(x)\{\cos x\, I_n(x)+\sin x\, I_{n+1}(x)\}&=\\ =\sqrt{\frac{2}{\pi x}}\int_0^x I_0(x-\alpha)\, I_0(2\alpha)\cos\alpha\, d\alpha.&\end{aligned}\right\}\quad\ldots\quad(317)$$

Par addition resp. soustraction de (312) et (315), ainsi de (313) et (314), on obtient:

$$\int_0^x I_0(x-\alpha)\sin 3\alpha\,\frac{d\alpha}{\sqrt{\alpha}}=\pi\sqrt{\frac{x}{2}}\sin x\, I_{-\frac{1}{2}}(x)\, I_{\frac{1}{2}}(x),\quad\ldots\quad(318)$$

$$\left.\begin{aligned}2\sum_{n=0}^{\infty}(-1)^n I_{n+\frac{1}{2}}(x)\{\cos x\, I_{n+\frac{1}{2}}(x)+\sin x\, I_{n+\frac{3}{2}}(x)\}-&\\ -\sin x\, I_{-\frac{1}{2}}(x)\, I_{\frac{1}{2}}(x)=\frac{1}{\pi}\sqrt{\frac{2}{x}}\int_0^x I_0(x-\alpha)\sin\alpha\,\frac{d\alpha}{\sqrt{\alpha}},&\end{aligned}\right\}\quad\ldots\quad(319)$$

$$\left.\begin{aligned}2\sum_{n=0}^{\infty}(-1)^n I_{n+\frac{1}{2}}(x)\{\sin x\, I_{n+\frac{1}{2}}(x)-\cos x\, I_{n+\frac{3}{2}}(x)\}+&\\ +\cos x\, I_{-\frac{1}{2}}(x)\, I_{\frac{1}{2}}(x)=\frac{1}{\pi}\sqrt{\frac{2}{x}}\int_0^x I_0(x-\alpha)\cos\alpha\,\frac{d\alpha}{\sqrt{\alpha}},&\end{aligned}\right\}\quad\ldots\quad(320)$$

$$\int_0^x I_0(x-\alpha)\cos 3\alpha\,\frac{d\alpha}{\sqrt{\alpha}}=\pi\sqrt{\frac{x}{2}}\cos x\, I_{-\frac{1}{2}}(x)\, I_{\frac{1}{2}}(x).\quad\ldots\quad(321)$$

Enfin la substitution $\mu=\frac{1}{2}$ resp. $\mu=1$ dans (304) et (305) donne les formules particulières:

$$\left.\begin{aligned}\sum_{n=0}^{\infty}(-1)^n I_{n+\frac{1}{2}}(x)\{\sin 2x\, I_{n-\frac{1}{2}}(x)-\cos 2x\, I_{n+\frac{1}{2}}(x)\}=&\\ =\frac{1}{\pi}\sqrt{\frac{2}{x}}\int_0^x I_0(\alpha)\sin 2\alpha\cos\alpha\,\frac{d\alpha}{\sqrt{x-\alpha}},&\end{aligned}\right\}\quad\ldots\quad(322)$$

$$\left.\begin{aligned}\sum_{n=0}^{\infty}(-1)^n I_{n+\frac{1}{2}}(x)\{\cos 2x\, I_{n-\frac{1}{2}}(x)+\sin 2x\, I_{n+\frac{1}{2}}(x)\}=&\\ =\frac{1}{\pi}\sqrt{\frac{2}{x}}\int_0^x I_0(\alpha)\cos 2\alpha\cos\alpha\,\frac{d\alpha}{\sqrt{x-\alpha}},&\end{aligned}\right\}\quad\ldots\quad(323)$$

$$\left.\begin{aligned}\sum_{n=0}^{\infty}(-1)^n I_{n+\frac{1}{2}}(x)\{\sin 2x\, I_{n+\frac{1}{4}}(x)-\cos 2x\, I_{n+\frac{3}{4}}(x)\}=\\ =\frac{1}{\pi}\sqrt{\frac{2}{x}}\int_0^x I_0(\alpha)\sin 2\alpha\sin\alpha\,\frac{d\alpha}{\sqrt{x-\alpha}},\end{aligned}\right\}\quad(324)$$

$$\left.\begin{aligned}\sum_{n=0}^{\infty}(-1)^n I_{n+\frac{1}{2}}(x)\{\cos 2x\, I_{n+\frac{1}{4}}(x)+\sin 2x\, I_{n+\frac{5}{4}}(x)\}=\\ =\frac{1}{\pi}\sqrt{\frac{2}{x}}\int_0^x I_0(\alpha)\cos 2\alpha\sin\alpha\,\frac{d\alpha}{\sqrt{x-\alpha}},\end{aligned}\right\}\quad(325)$$

tandis que l'addition resp. la soustraction des membres correspondants de (322) et (325), ainsi de (323) et (324) donne:

$$\int_0^x I_0(\alpha)\sin 3\alpha\,\frac{d\alpha}{\sqrt{x-\alpha}}=\pi\sqrt{\frac{x}{2}}\sin 2x\, I_{-\frac{1}{4}}(x)\, I_{\frac{1}{4}}(x),\quad(326)$$

$$\left.\begin{aligned}\sin 2x\, I_{-\frac{1}{4}}(x)\, I_{\frac{1}{4}}(x)-2\sum_{n=0}^{\infty}(-1)^n I_{n+\frac{1}{2}}(x)\{\cos 2x\, I_{n+\frac{1}{4}}(x)+\sin 2x\, I_{n+\frac{5}{4}}(x)\}=\\ =\frac{1}{\pi}\sqrt{\frac{2}{x}}\int_0^x I_0(\alpha)\sin\alpha\,\frac{d\alpha}{\sqrt{x-\alpha}},\end{aligned}\right\}\quad(327)$$

$$\left.\begin{aligned}\cos 2x\, I_{-\frac{1}{4}}(x)\, I_{\frac{1}{4}}(x)+2\sum_{n=0}^{\infty}(-1)^n I_{n+\frac{1}{2}}(x)\{\sin 2x\, I_{n+\frac{1}{4}}(x)-\cos 2x\, I_{n+\frac{3}{4}}(x)\}=\\ =\frac{1}{\pi}\sqrt{\frac{2}{x}}\int_0^x I_0(\alpha)\cos\alpha\,\frac{d\alpha}{\sqrt{x-\alpha}},\end{aligned}\right\}\quad(328)$$

$$\int_0^x I_0(\alpha)\cos 3\alpha\,\frac{d\alpha}{\sqrt{x-\alpha}}=\pi\sqrt{\frac{x}{2}}\cos 2x\, I_{-\frac{1}{4}}(x)\, I_{\frac{1}{4}}(x).\quad(329)$$

§ 13. En remplaçant dans (263) ϱ par $m+\frac{1}{2}$ resp. m (m entier positif ou nulle) et en multipliant les deux membres par $2(-1)^m$ resp. $\varepsilon_{2m}(-1)^m$ ou ε_{2m}, alors nous trouvons après la sommation sur m de 0 à ∞, à cause des séries connues $2\sum_{m=0}^{\infty}(-1)^m I_{2m+1}(x)=\sin x$, $\sum_{m=0}^{\infty}\varepsilon_{2m}(-1)^m I_{2m}(x)=$ $=\cos x$ et $\sum_{m=0}^{\infty}\varepsilon_{2m} I_{2m}(x)=1$, en appliquant le théorème de CAUCHY

$$\sum_{m=0}^{\infty}\sum_{n=0}^{\infty}\varphi(m,n)=\sum_{s=0}^{\infty}\sum_{p=0}^{s}\varphi(p,s-p),\quad(g)$$

où $\sum_{n=0}^{\infty} \varphi(m, n) = \psi(m)$ et $\sum_{m=0}^{\infty} \psi(m)$ sont des séries absolument convergentes:

$$\left.\begin{aligned} 2 \sum_{s=0}^{\infty} (-1)^s (s+1)\, I_{\nu+s+1}(x)\, I_{\nu+s+\frac{1}{2}}(x) = \\ = \frac{1}{\sqrt{x}} \int_0^x I_\nu(\alpha)\, I_{\nu-\frac{1}{2}}(\alpha)\, \sin 2(x-\alpha) \cdot \sqrt{\alpha}\, d\alpha, \quad R(\nu) > -\tfrac{1}{2} \end{aligned}\right\} \tag{330}$$

$$\left.\begin{aligned} \sum_{s=0}^{\infty} (-1)^s (2s+1)\, I_{\nu+s+\frac{1}{2}}(x)\, I_{\nu+s}(x) = \\ = \frac{1}{\sqrt{x}} \int_0^x I_\nu(\alpha)\, I_{\nu-\frac{1}{2}}(\alpha)\, \cos 2(x-\alpha) \cdot \sqrt{\alpha}\, d\alpha, \quad R(\nu) > -\tfrac{1}{2} \end{aligned}\right\} \tag{331}$$

$$\sum_{s=0}^{\infty} I_{\nu+s+\frac{1}{2}}(x)\, I_{\nu+s}(x) = \frac{1}{\sqrt{x}} \int_0^x I_\nu(\alpha)\, I_{\nu-\frac{1}{2}}(\alpha) \cdot \sqrt{\alpha}\, d\alpha, \quad R(\nu) > -\tfrac{1}{2}. \tag{332}$$

Si nous multiplions les deux membres de (331) par $\sin 2x$ resp. $\cos 2x$ et ceux de (330) par $\cos 2x$ resp. $\sin 2x$, alors nous obtenons après la soustraction resp. l'addition des membres correspondants:

$$\left.\begin{aligned} \sum_{s=0}^{\infty} (-1)^s I_{\nu+s+\frac{1}{2}}(x) \{(2s+1) \sin 2x\, I_{\nu+s}(x) - (2s+2) \cos 2x\, I_{\nu+s+1}(x)\} = \\ = \frac{1}{\sqrt{x}} \int_0^x I_\nu(\alpha)\, I_{\nu-\frac{1}{2}}(\alpha)\, \sin 2\alpha \cdot \sqrt{\alpha}\, d\alpha, \quad R(\nu) > -\tfrac{1}{2} \end{aligned}\right\} \tag{333}$$

$$\left.\begin{aligned} \sum_{s=0}^{\infty} (-1)^s I_{\nu+s+\frac{1}{2}}(x) \{(2s+1) \cos 2x\, I_{\nu+s}(x) + (2s+2) \sin 2x\, I_{\nu+s+1}(x)\} = \\ = \frac{1}{\sqrt{x}} \int_0^x I_\nu(\alpha)\, I_{\nu-\frac{1}{2}}(\alpha)\, \cos 2\alpha \cdot \sqrt{\alpha}\, d\alpha, \quad R(\nu) > -\tfrac{1}{2}. \end{aligned}\right\} \tag{334}$$

Par addition et soustraction des membres correspondants de (331) et (332) on trouve:

$$\left.\begin{aligned} \sum_{s=0}^{\infty} (2s+1) \{I_{\nu+2s+\frac{1}{2}}(x)\, I_{\nu+2s}(x) - I_{\nu+2s+\frac{3}{2}}(x)\, I_{\nu+2s+1}(x)\} = \\ = \frac{1}{\sqrt{x}} \int_0^x I_\nu(\alpha)\, I_{\nu-\frac{1}{2}}(\alpha)\, \cos^2(x-\alpha) \cdot \sqrt{\alpha}\, d\alpha, \quad R(\nu) > -\tfrac{1}{2} \end{aligned}\right\} \tag{335}$$

$$\left.\begin{aligned}\sum_{s=0}^{\infty}(2s+2)\{I_{\nu+2s+\frac{3}{2}}(x)\,I_{\nu+2s+1}(x)-I_{\nu+2s+\frac{1}{2}}(x)\,I_{\nu+2s+2}(x)\}=\\ =\frac{1}{\sqrt{x}}\int_0^x I_\nu(\alpha)\,I_{\nu-\frac{1}{2}}(\alpha)\sin^2(x-\alpha)\,.\sqrt{\alpha}\,d\alpha,\quad R(\nu)>-\tfrac{1}{2}.\end{aligned}\right\}\tag{336}$$

La substitution $\nu=0$, $\nu=\frac{1}{2}$ et $\nu=1$ dans (330) jusqu'à (336) nous donne les formules particulières:

$$2\sum_{s=0}^{\infty}(-1)^s(s+1)\,I_{s+1}(x)\,I_{s+\frac{1}{2}}(x)=\sqrt{\frac{2}{\pi x}}\int_0^x I_0(\alpha)\cos\alpha\sin 2(x-\alpha)\,d\alpha,\tag{337}$$

$$2\sum_{s=0}^{\infty}(-1)^s(s+1)\,I_{s+\frac{1}{2}}(x)\,I_{s+1}(x)=\sqrt{\frac{2}{\pi x}}\int_0^x I_0(\alpha)\sin\alpha\sin 2(x-\alpha)\,d\alpha,\tag{338}$$

$$2\sum_{s=0}^{\infty}(-1)^s(s+1)\,I_{s+2}(x)\,I_{s+\frac{3}{2}}(x)=\sqrt{\frac{2}{\pi x}}\int_0^x I_1(\alpha)\sin\alpha\sin 2(x-\alpha)\,d\alpha,\tag{339}$$

$$\sum_{s=0}^{\infty}(-1)^s(2s+1)\,I_{s+\frac{1}{2}}(x)\,I_s(x)=\sqrt{\frac{2}{\pi x}}\int_0^x I_0(\alpha)\cos\alpha\cos 2(x-\alpha)\,d\alpha,\tag{340}$$

$$\sum_{s=0}^{\infty}(-1)^s(2s+1)\,I_{s+1}(x)\,I_{s+\frac{1}{2}}(x)=\sqrt{\frac{2}{\pi x}}\int_0^x I_0(\alpha)\sin\alpha\cos 2(x-\alpha)\,d\alpha,\tag{341}$$

$$\sum_{s=0}^{\infty}(-1)^s(2s+1)\,I_{s+\frac{3}{2}}(x)\,I_{s+1}(x)=\sqrt{\frac{2}{\pi x}}\int_0^x I_1(\alpha)\sin\alpha\cos 2(x-\alpha)\,d\alpha,\tag{342}$$

$$\left.\begin{aligned}\sum_{s=0}^{\infty}I_{s+\frac{1}{2}}(x)\,I_s(x)=\sqrt{\frac{2}{\pi}}\int_0^x I_0(\alpha)\cos\alpha\,d\alpha=\\ =\sqrt{\frac{2}{\pi x}}\left\{\sin x\,I_0(x)+\int_0^x I_1(\alpha)\sin\alpha\,d\alpha\right\},\end{aligned}\right\}\quad\ldots\tag{343}$$

$$\sum_{s=0}^{\infty}I_{s+1}(x)\,I_{s+\frac{1}{2}}(x)=\sqrt{\frac{2}{\pi x}}\int_0^x I_0(\alpha)\sin\alpha\,d\alpha,\quad\ldots\tag{344}$$

$$\sum_{s=0}^{\infty}(-1)^s I_{s+\frac{1}{2}}(x)\{(2s+1)\sin 2x\, I_s(x)-(2s+2)\cos 2x\, I_{s+1}(x)\}= \left.\begin{aligned}&\\ &=\sqrt{\frac{2}{\pi x}}\int_0^x I_0(\alpha)\cos\alpha\sin 2\alpha\, d\alpha,\end{aligned}\right\} \tag{345}$$

$$\sum_{s=0}^{\infty}(-1)^s I_{s+1}(x)\{(2s+1)\sin 2x\, I_{s+\frac{1}{2}}(x)-(2s+2)\cos 2x\, I_{s+\frac{3}{2}}(x)\}= \left.\begin{aligned}&\\ &=\sqrt{\frac{2}{\pi x}}\int_0^x I_0(\alpha)\sin\alpha\sin 2\alpha\, d\alpha,\end{aligned}\right\} \tag{346}$$

$$\sum_{s=0}^{\infty}(-1)^s I_{s+\frac{1}{2}}(x)\{(2s+1)\sin 2x\, I_{s+1}(x)-(2s+2)\cos 2x\, I_{s+2}(x)\}= \left.\begin{aligned}&\\ &=\sqrt{\frac{2}{\pi x}}\int_0^x I_1(\alpha)\sin\alpha\sin 2\alpha\, d\alpha,\end{aligned}\right\} \tag{347}$$

$$\sum_{s=0}^{\infty}(-1)^s I_{s+\frac{1}{2}}(x)\{(2s+1)\cos 2x\, I_s(x)+(2s+2)\sin 2x\, I_{s+1}(x)\}= \left.\begin{aligned}&\\ &=\sqrt{\frac{2}{\pi x}}\int_0^x I_0(\alpha)\cos\alpha\cos 2\alpha\, d\alpha,\end{aligned}\right\} \tag{348}$$

$$\sum_{s=0}^{\infty}(-1)^s I_{s+1}(x)\{(2s+1)\cos 2x\, I_{s+\frac{1}{2}}(x)+(2s+2)\sin 2x\, I_{s+\frac{3}{2}}(x)\} \left.\begin{aligned}&\\ &=\sqrt{\frac{2}{\pi x}}\int_0^x I_0(\alpha)\sin\alpha\cos 2\alpha\, d\alpha,\end{aligned}\right\} \tag{349}$$

$$\sum_{s=0}^{\infty}(-1)^s I_{s+\frac{3}{2}}(x)\{(2s+1)\cos 2x\, I_{s+1}(x)+(2s+2)\sin 2x\, I_{s+2}(x)\}= \left.\begin{aligned}&\\ &=\sqrt{\frac{2}{\pi x}}\int_0^x I_1(\alpha)\sin\alpha\cos 2\alpha\, d\alpha,\end{aligned}\right\} \tag{350}$$

$$\sum_{s=0}^{\infty}(2s+1)\{I_{2s+\frac{1}{2}}(x)\, I_{2s}(x)-I_{2s+\frac{3}{2}}(x)\, I_{2s+1}(x)\}= \left.\begin{aligned}&\\ &=\sqrt{\frac{2}{\pi x}}\int_0^x I_0(\alpha)\cos\alpha\cos^2(x-\alpha)\, d\alpha,\end{aligned}\right\} \tag{351}$$

$$\sum_{s=0}^{\infty}(2s+1)\{I_{2s+1}(x)\,I_{2s+\frac{1}{2}}(x)-I_{2s+2}(x)\,I_{2s+\frac{3}{2}}(x)\}= \left.\begin{aligned}&\\ &=\sqrt{\frac{2}{\pi x}}\int_0^x I_0(\alpha)\sin\alpha\cos^2(x-\alpha)\,d\alpha,\end{aligned}\right\} \quad (352)$$

$$\sum_{s=0}^{\infty}(2s+1)\{I_{2s+\frac{1}{2}}(x)\,I_{2s+1}(x)-I_{2s+\frac{3}{2}}(x)\,I_{2s+2}(x)\}= \left.\begin{aligned}&\\ &=\sqrt{\frac{2}{\pi x}}\int_0^x I_1(\alpha)\sin\alpha\cos^2(x-\alpha)\,d\alpha,\end{aligned}\right\} \quad (353)$$

$$\sum_{s=0}^{\infty}(2s+2)\{I_{2s+\frac{3}{2}}(x)\,I_{2s+1}(x)-I_{2s+\frac{5}{2}}(x)\,I_{2s+2}(x)\}= \left.\begin{aligned}&\\ &=\sqrt{\frac{2}{\pi x}}\int_0^x I_0(\alpha)\cos\alpha\sin^2(x-\alpha)\,d\alpha.\end{aligned}\right\} \quad (354)$$

$$\sum_{s=0}^{\infty}(2s+2)\{I_{2s+2}(x)\,I_{2s+\frac{3}{2}}(x)-I_{2s+3}(x)\,I_{2s+\frac{5}{2}}(x)\}= \left.\begin{aligned}&\\ &=\sqrt{\frac{2}{\pi x}}\int_0^x I_0(\alpha)\sin\alpha\sin^2(x-\alpha)\,d\alpha,\end{aligned}\right\} \quad (355)$$

$$\sum_{s=0}^{\infty}(2s+2)\{I_{2s+\frac{1}{2}}(x)\,I_{2s+2}(x)-I_{2s+\frac{7}{2}}(x)\,I_{2s+3}(x)\}= \left.\begin{aligned}&\\ &=\sqrt{\frac{2}{\pi}}\int_0^x I_1(\alpha)\sin\alpha\sin^2(x-\alpha)\,d\alpha.\end{aligned}\right\} \quad (356)$$

Par addition resp. soustraction des membres correspondants de chacune des paires (337) et (341), (338) et (340), (351) et (354), (352) et (355), (353) et (356) on trouve:

$$\sum_{s=0}^{\infty}(-1)^s(4s+3)\,I_{s+1}(x)\,I_{s+\frac{1}{2}}(x)=\sqrt{\frac{2}{\pi x}}\int_0^x I_0(\alpha)\sin(2x-\alpha)\,d\alpha, \quad (357)$$

$$\sum_{s=0}^{\infty}(-1)^s\,I_{s+1}(x)\,I_{s+\frac{1}{2}}(x)=\sqrt{\frac{2}{\pi x}}\int_0^x I_0(\alpha)\sin(2x-3\alpha)\,d\alpha, \quad (358)$$

$$\sum_{s=0}^{\infty}(-1)^s\,I_{s+\frac{1}{2}}\,I_s(x)=\sqrt{\frac{2}{\pi x}}\int_0^x I_0(\alpha)\cos(2x-3\alpha)\,d\alpha, \quad (359)$$

$$\sum_{s=0}^{\infty} (-1)^s (4s+1)\, I_{s+\frac{1}{2}}(x)\, I_s(x) = \sqrt{\frac{2}{\pi x}} \int_0^x I_0(\alpha) \cos(2x-\alpha)\, d\alpha, \quad (360)$$

$$\sum_{s=0}^{\infty} \{I_{2s+\frac{1}{2}}(x)\, I_{2s}(x) + I_{2s+\frac{3}{2}}(x)\, I_{2s+1}(x)\} = \sqrt{\frac{2}{\pi x}} \int_0^x I_0(\alpha) \cos\alpha\, d\alpha, \quad (361)$$

$$\left.\begin{aligned} \sum_{s=0}^{\infty} \{(4s+1)\, I_{2s+\frac{1}{2}}(x)\, I_{2s}(x) - (4s+3)\, I_{2s+\frac{3}{2}}(x)\, I_{2s+1}(x)\} = \\ = \sqrt{\frac{2}{\pi x}} \int_0^x I_0(\alpha) \cos\alpha \cos 2(x-\alpha)\, d\alpha, \end{aligned}\right\} \quad (362)$$

$$\sum_{s=0}^{\infty} \{I_{2s+1}(x)\, I_{2s+\frac{1}{2}}(x) + I_{2s+2}(x)\, I_{2s+\frac{3}{2}}(x)\} = \sqrt{\frac{2}{\pi x}} \int_0^x I_0(\alpha) \sin\alpha\, d\alpha, \quad . \quad . \quad (363)$$

$$\left.\begin{aligned} \sum_{s=0}^{\infty} \{(4s+1)\, I_{2s+1}(x)\, I_{2s+\frac{1}{2}}(x) - (4s+3)\, I_{2s+2}(x)\, I_{2s+\frac{3}{2}}(x)\} = \\ = \sqrt{\frac{2}{\pi x}} \int_0^x I_0(\alpha) \sin\alpha \cos 2(x-\alpha)\, d\alpha, \end{aligned}\right\} \quad (364)$$

$$\sum_{s=0}^{\infty} \{I_{2s+\frac{3}{2}}(x)\, I_{2s+1}(x) + I_{2s+\frac{5}{2}}(x)\, I_{2s+2}(x)\} = \sqrt{\frac{2}{\pi x}} \int_0^x I_1(\alpha) \sin\alpha\, d\alpha, \quad . \quad (365)$$

$$\left.\begin{aligned} \sum_{s=0}^{\infty} \{(4s+1)\, I_{2s+\frac{3}{2}}(x)\, I_{2s+1}(x) - (4s+3)\, I_{2s+\frac{5}{2}}(x)\, I_{2s+2}(x)\} = \\ = \sqrt{\frac{2}{\pi x}} \int_0^x I_1(\alpha) \sin\alpha \cos 2(x-\alpha)\, d\alpha. \end{aligned}\right\} \quad (366)$$

Si nous multiplions les deux membres de (337) par $\sin x$ resp. $\cos x$ et ceux de (338) par $\cos x$ resp. $\sin x$, alors nous trouvons après la soustraction resp. l'addition des membres correspondants, et en faisant de même à l'égard de (340) et (341), ainsi de (343) et (344):

$$\left.\begin{aligned} 2 \sum_{s=0}^{\infty} (-1)^s (s+1)\, I_{s+1}(x) \{\sin x\, I_{s+\frac{1}{2}}(x) - \cos x\, I_{s+\frac{3}{2}}(x)\} = \\ = \sqrt{\frac{2}{\pi x}} \int_0^x I_0(x-\alpha) \sin\alpha \sin 2\alpha\, d\alpha, \end{aligned}\right\} \quad (367)$$

$$2\sum_{s=0}^{\infty}(-1)^s(s+1)\,I_{s+1}(x)\{\cos x\,I_{s+\frac{1}{2}}(x)+\sin x\,I_{s+\frac{3}{2}}(x)\}= \\ =\sqrt{\frac{2}{\pi x}}\int_0^x I_0(x-\alpha)\cos\alpha\sin 2\alpha\,d\alpha, \tag{368}$$

$$\sum_{s=0}^{\infty}(-1)^s(2s+1)\,I_{s+\frac{1}{2}}(x)\{\sin x\,I_s(x)-\cos x\,I_{s+1}(x)\}= \\ =\sqrt{\frac{2}{\pi x}}\int_0^x I_0(x-\alpha)\sin\alpha\cos 2\alpha\,d\alpha, \tag{369}$$

$$\sum_{s=0}^{\infty}(-1)^s(2s+1)\,I_{s+\frac{1}{2}}(x)\{\cos x\,I_s(x)+\sin x\,I_{s+1}(x)\}= \\ =\sqrt{\frac{2}{\pi x}}\int_0^x I_0(x-\alpha)\cos\alpha\cos 2\alpha\,d\alpha, \tag{370}$$

$$\sum_{s=0}^{\infty}I_{s+\frac{1}{2}}(x)\{\sin x\,I_s(x)-\cos x\,I_{s+1}(x)\}= \\ =\sqrt{\frac{2}{\pi x}}\int_0^x I_0(\alpha)\sin(x-\alpha)\,d\alpha=\sqrt{\frac{2x}{\pi}}\,I_1(x)\ \text{selon (189)}, \tag{371}$$

$$\sum_{s=0}^{\infty}I_{s+\frac{1}{2}}(x)\{\cos x\,I_s(x)+\sin x\,I_{s+1}(x)\}= \\ =\sqrt{\frac{2}{\pi x}}\int_0^x I_0(\alpha)\cos(x-\alpha)\,d\alpha=\sqrt{\frac{2x}{\pi}}\,I_0(x)\ \text{selon (187)}. \tag{372}$$

Si nous multiplions les deux membres de (359) par $\sin x$ resp. $\cos x$ et ceux de (358) par $\cos x$ resp. $\sin x$, alors nous trouvons après l'addition resp. la soustraction des membres correspondants:

$$\sum_{s=0}^{\infty}(-1)^s I_{s+\frac{1}{2}}(x)\{\sin x\,I_s(x)+\cos x\,I_{s+1}(x)\}=\sqrt{\frac{2}{\pi x}}\int_0^x I_0(x-\alpha)\sin 3\alpha\,d\alpha, \tag{373}$$

$$\sum_{s=0}^{\infty}(-1)^s I_{s+\frac{1}{2}}(x)\{\cos x\,I_s(x)-\sin x\,I_{s+1}(x)\}=\sqrt{\frac{2}{\pi x}}\int_0^x I_0(x-\alpha)\cos 3\alpha\,d\alpha. \tag{374}$$

Par la multiplication des deux membres de (359) par $\sin 2x$ resp.

$\cos 2x$ et ceux de (358) par $\cos 2x$ resp. $\sin 2x$, on trouve après la soustraction resp. l'addition des membres correspondants:

$$\left.\begin{aligned}\sum_{s=0}^{\infty}(-1)^s I_{s+\frac{1}{2}}(x)\{\sin 2x\, I_s(x) - \cos 2x\, I_{s+1}(x)\} = \\ = \sqrt{\frac{2}{\pi x}}\int_0^x I_0(\alpha)\sin 3\alpha\, d\alpha,\end{aligned}\right\} \quad . \quad . \quad (375)$$

$$\left.\begin{aligned}\sum_{s=0}^{\infty}(-1)^s I_{s+\frac{1}{2}}(x)\{\cos 2x\, I_s(x) + \sin 2x\, I_{s+1}(x)\} = \\ = \sqrt{\frac{2}{\pi x}}\int_0^x I_0(\alpha)\cos 3\alpha\, d\alpha.\end{aligned}\right\} \quad . \quad . \quad (376)$$

Botany. -- *The photoperiodic responses of Anthemis tinctoria in different ranges of wavelength.* By G. L. FUNKE. (Communicated by Prof. L. G. M. BAAS BECKING.)

(Communicated at the meeting of September 27, 1941.)

From 1936 till 1939 in Ghent, Belgium, I investigated the flowering photoperiodicity of a large number of plant species in different ranges of wave length. The plants received full day light from 7 a.m. till 3 p.m.; for the rest of the day they were covered, partly by dark cases, partly by white (limed), red and blue glass; check plants remained in the open air. "Dark" or "D" means plants which got full day light from 7 a.m. till 3 p.m.; "red" or "R", "blue" or „B" and „white" or „W" means plants which were exposed to full day light from 7 a.m. till 3 p.m. and resp. red, blue and white light from sunrise till 7 a.m. and from 3 p.m. till sunset. According to their reactions the species could be divided into 4 groups:

I. **W — R B — D**: "red" flowers at the same time as "white", "blue" at the same time as "dark".

II. **W — R — B D**: "red" and "blue" flower at the same time as "white", the colour of the light is of no importance.

III. **W R — B — D**: flowering of long day plants only in "white", neither "red" nor "blue" rays have any furthering influence; vice versa for short day plants.

IV. **W — B R — D**: the opposite of group I, "blue" flowers at the same time as "white", "red" at the same time as "dark".

Transitional cases occur between groups I, II and III; group IV seems to stand by itself.

During the summer of 1941 I continued these researches in the garden of the Botanical Institute at Leiden. The red and blue glasses which I had at my disposal were of a rather dark colour; they transmitted less than half of the solar energy than did those which I used in Ghent; especially on clouded days the light intensity in the different compartments was very low. RODENBURG (13 c) rightly points out the errors which may be caused under such conditions, but the species which I investigated under both types of glass appeared to be sufficiently sensitive to small quantities of light and they all gave results identical to those in former years.

Anthemis tinctoria is a "long-day plant" and belongs very distinctly to group I (see 4*d*, fig. 1). When investigating this species in 1939 I noticed some peculiarities which deserved closer attention and were therefore further investigated.

Although the number of plants used was restricted, 5 or 6 per division, their responses to the various treatments were so consistent with those of 1939 and also their further reactions so explicit, that I feel entitled to communicate the results as well-established facts.

Small specimens were potted during March and the experiments began on April 2nd. The development in the different divisions was as follows:

Specimens in "white" and "red"; control plants: the vegetative growth was normal; the stem reached a length up to about 70 cm, internodia up to 3½ cm; the anatomy of the stem (vascular bundles, lignification, sklerenchymatic tissue) was normal; diameter of the tracheae 28—34 micra; the first flowerbuds were visible on June 2nd; the growth of the flower stalks was normal, up to 20 cm; full blossoming on terminal and numerous lateral branches from the middle of June till the end of September; the ripening of the seeds took place from the end of August till the end of September; see fig. 1, no. 1.

Specimens in "blue": vegetative development normal, also the anatomy of the stem, as in "white", "red" and control; see fig. 1, no. 2; terminal flowerbuds appear towards the end of June, none on lateral branches; no or hardly any elongation of flower stalks (a

few cm at the utmost); most buds decay; the others did not open with the exception of two which took a great number of days to develop quite abnormal capitula with crippled marginal flowers (see 4*d*, fig. 2) (in a normal capitulum: diameter 45 mm, length of marginal flower 14 mm; in "blue" resp. 23 and 6 mm); they yielded only a few ripe seeds. The covering with the blue glass was discontinued on August 11th (the same holds true for the other divisions); this change, however, could not induce any more flowering. One specimen was put into full day length since July 11th; see fig. 1, no. 3; it formed a few more flowerbuds which, however, did not open with the exception of one and this gave an anomalous capitulum as described above.

Specimens in "dark": the longitudinal growth was extremely scanty, the utmost height reached about 10 cm; see fig. 1, no. 4; the foliage was dense owing to the shortness of the internodes; the lateral branches were rather numerous. The anatomy of the stem remains in the juvenile stage: separate vascular bundles, no lignification, no sklerenchymatic tissue; diameter of the tracheae 14—17 micra. This anatomical aspect is in striking contrast with that of control, "white", "red" and "blue" and illustrates the relativity of age; only towards the end of September a slight lignification sets in. Most leaves were shed towards the end of August and only terminal rosettes remain. Even microscopical examination showed no trace of flowerbuds. Since August 11th the plants were exposed to full day length, but this did not induce any further development. Also from July 11th some specimens received full day length; this extra month of long day induction caused an elongation of the stems to almost normal length; see fig. 1, no. 5; their anatomy gradually began to show the adult stage which was more or less reached towards the end of August; a few terminal flowerbuds were formed, but they remained very small, some of them hardly visible, and most of them were completely hidden by the topmost leaves.

Specimens in "control" and later in "dark"; a number of specimens stayed in full day length till May 2nd and were then transported to the dark compartment. Their longitudinal growth was more or less checked, but not nearly so markedly as that of the "dark" specimens. The plants reached a height of about 40 cm; see fig. 1, no. 6; the anatomy of the stems was normal. A small number of flowerbuds appeared on terminal and lateral branches in the beginning of June (3—4 per specimen against some dozens in control, "red" and "white"); the flower stalks elongated normally; the blossoming lasted till the end of August, while in control, "white" and "red" it continued till the end of September. The ripening of seeds was normal. Since July 11th part of them were put again in full day length; this did not change their aspect. The difference of treatment between these plants and those of "dark" which received also full day length since July 11th is that the latter ones got only 8 hours of daylight during April whereas the former ones were exposed during that month to the normal length of day.

During the last few years the fact has been established that we must distinguish two stages, and perhaps even more, in the reproductive phase. EGUCHI (3) says: "These facts show that there are two stages of different susceptibility to the photoperiod in the course of flowering, at first in the differentiation stage of bud and next in the succeeding stage of development respectively." And HAMNER (6*a*): "There is need for precise records showing the influence of photoperiod upon (1) the initiation of flower primordia as contrasted with (2) its influence upon the development of flowers, (3) its influence upon the development of fruits, and (4) its influence upon the development of seeds." And LOEHWING (9) advocates: "the possible desirability of subdividing the photophase of plant development into (*a*) an initial flowering phase as distinguished from a subsequent (*b*) gametogamic phase concerned with the formation of viable gametes." (See also BORTHWICK and PARKER (2 and 11), HARDER and VON WITSCH (8), MICHAJLOVA (10), PUVIS and GREGORY (12), ROODENBURG (13*b*).) Production of anomalous flowers, owing to insufficient photoinduction has also been stated in a number of cases, e.g. by GERHARD (5), HARDER (7), HARDER and VON WITSCH (8), LOEHWING (9: "It was soon

learned, however, that plants receiving minimal periods of photo-induction frequently produce flowers of anomalous shape and marked sterility.") The phenomena stated by BORGSTRÖM (1) in wild violets and by SCHAFFNER (15) in hemp are possibly related to the above mentioned ones.

Anthemis tinctoria presents a case where we should certainly distinguish at least 4 different reactions in: (1) the vegetative development, (2) the formation of flowerbuds, (3) the development of flowers and (4) the ripening of seeds.

(1) The vegetative development: only a long day allows sufficient formation of growth substance (compare ROODENBURG (13*a*) and ROODENBURG and TIDDENS (14), but the colour of the light is of no importance in this respect. This holds true for most species hitherto investigated, whether of the short day or of the long day character and in everyone of the groups I—IV (4). I cannot say whether that which has been observed about the anatomy is also a general feature. *Lycopus europaeus,* also belonging to group I, shows phenomena which, on the whole, are very parallel to those seen in *Anthemis*, but the very short stems in "dark" (11 cm) are anatomically equally well developed as the normal ones (40 à 50 cm) in control, "white", "red" and "blue"; other species have hitherto not been examined in this respect.

For the formation of flowerbuds, the development into flowering and the production of viable seeds a long day is needed. This species therefore belongs to the group LL as established by EGUCHI, but I think this is the first time we see that the different ranges of wave length have a different influence on these stages. The formation of flowerbuds is furthered by long "red"- and "blue days", but in a "red day" their number is normally great, while in "blue day" they are less numerous and many of them decay. The development of flowers is only brought forth by a long "red day"; 8 hours of full day light with additional blue light before and afterwards are not able to bring about the transition to this stage. At the utmost an exceptional anomalous capitulum develops, but this can hardly be considered as representing the reproductive stage because it yields only a very few viable seeds if at all. Control, "white" and "red" produce seeds in abundance; their percentage of germination is 94; their weight per 100 61 mgr. "Dark", preceeded by long day in April, yields less, but still some thousands; germination 85 %, weight per 100 only 33 mgr. One capitulum in "blue" gave no seeds at all, one other 24, germination 67 %, weight 5 mgr; one capitulum in "blue" and long day since July 11th gave 47 seeds, germination 65 %, weight 14 mgr. When we consider the scanty weight of the last mentioned seeds we wonder at their relatively high percentage of germination; it remains to be seen whether they will give healthy plants in the next year.

Anthemis tinctoria, moreover, shows a strongly decreasing sentitiveness to photoinduction as the season proceeds. The full length of the relatively short days of April, when flowerbuds are not visible by far, is sufficient to induce flowering in July, although they are followed by about 10 weeks of an eight hour day; full length of the much longer days since the middle of July, when flowerbuds have since long been formed, has, on the other hand, no influence on the development into flowers, although this goes on till the end of September in control, "white" and "red"; long days in midsummer have practically influence on the vegetative growth only.

A number of cleft grafts have been made in order to see whether the florigen can be transported under the different conditions of the experiment, and if so, how. Tops of "white" and "red" were grafted as scions on stocks of "blue" and "dark" and vice versa; they failed altogether, although most of them remained turgescent for nearly a week.

SUMMARY.

Anthemis tinctoria is a very sensitive long day plant; it shows photoperiodic responses in at least four different stages: (1) vegetative development; (2) formation of flowerbuds; (3) development of flowers; (4) ripening of seeds.

Eight hours ordinary daylight supplemented by red or blue light from sunrise till 7 a.m.

and from 3 p.m. till sunset is equally sufficient for (1) as natural day length; in short day it is extremely scanty.

(2), (3) and (4) are also brought forth normally by short day supplemented by red light. Supplemental blue light partly suppresses the formation of flower buds and nearly totally prevents the development of flowers and still more so the ripening of seeds.

Long day induction during April followed by short day treatment is sufficient for a nearly normal growth of the whole plant. Long day induction from the middle of July till the end of the summer restores the check of the vegetative development caused by a foregoing short day, but is not capable of inducing the reproductive phase, even though this foregoing short day was supplemented by blue light.

I want to express my heartfelt thanks to the Board of Trustees of the University of Leiden, to the Director of the Botanical Institute, to the scientific and technical staffs of the laboratory and gardens, to the Director, the scientific and technical staffs of the State Herbarium, who, with the utmost kindness, enabled me to continue my researchwork in my present circumstances.

Leiden, September 1941. *Botanical Institute.*

LITERATURE.

1. BORGSTRÖM, G., (1939), Nature, **144**, 514.
2. BORTHWICK, H. A. and PARKER, M. W., a. (1938), Bot. Gaz., **99**, 825; b. (1938), ibid. **100**, 245; c. (1938), ibid. **100**, 374.
3. EGUCHI, TS., (1937), Proc. Imp. Ac. Tokyo, **13**, 332.
4. FUNKE, G. L., a. (1936), Biol. Jaarb., **3**, 225; b. (1937), ibid. **4**, 345; c. (1938), ibid. **5**, 404; d. (1939), ibid. **6**, 351.
5. GERHARD, E., (1940), Journ. für Landw., **87**, 161.
6. HAMNER, K. C., a. (1938), Bot. Gaz., **99**, 615; b. (1940), ibid. **101**, 658.
7. HARDER, R., (1940), Ber. D. Bot. Ges., **58**, 70.
8. HARDER, R. und WITSCH, H. VON, a. (1940), Jahrb. wiss. Bot., **89**, 354; b. (1940), Planta, **31**, 192; c. (1940), ibid. **31**, 523.
9. LOEHWING, W. F., (1939), Science, No. **2346**, 552.
10. MICHAJLOVA, L. V., (1936), C. r. Acad. Sci. U.R.S.S., **2**, 102.
11. PARKER, M. W. and BORTHWICK, H. A., a. (1939), Bot. Gaz., **100**, 651; b. (1939), ibid. **101**, 145.
12. PURVIS, O. N. and GREGORY, F. G., (1937), Ann. Bot., N. S. **1**, 569.
13. ROODENBURG, J. W. M., a. (1937), Ber. D. Bot. Ges., **55**, 5; b. (1939), Weekbl. Ned. Mij. Tuinb. en Plantk., **13**, 2; c. (1940), Rec. trav. bot. néerl., **37**, 301.
14. ROODENBURG, J. W. M. and TIDDENS, B. A., (1938), Chron. Bot., **4**, 18.
15. SCHAFFNER, J. H., a. (1923), Ecology, **4**, 205; b. (1931), Amer. Journ. Bot., **18**, 424.

Fig. 1. The development of Anthemis tinctoria on September 4th 1941.
No. 1. Control, "white" and "red".
No. 2. "Blue".
No. 3. "Blue" and long day since July 11th.
No. 4. "Dark".
No. 5. "Dark" and long day since July 11th.
No. 6. Long day till May 2nd, then "dark".

Geology. — *Die permischen Alkaligesteine und die Ophiolithe des timoresischen Faltengebirges.* Von W. P. DE ROEVER. (Communicated by Prof. H. A. BROUWER.)

(Communicated at the meeting of September 27, 1941.)

In der vorliegenden Arbeit möchte ich die vorläufigen Ergebnisse meiner Untersuchungen an permischen Eruptivgesteinen von Timor mitteilen insbesondere mit Bezug auf die vor und während des eigentlichen Geosynklinalstadiums des timoresischen Faltengebirges auftretenden verschiedenen Eruptivstämme.

Die mir zur Untersuchung überlassenen Gesteine wurden während der von Prof. H. A. BROUWER geführten geologischen Expedition nach den Kleinen Sunda-Inseln 1937 gesammelt, und zwar der grösste Teil von F. A. H. W. DE MAREZ OYENS im Basleogebiet, und einige weitere bisher nicht eingehend beschriebene Gesteine von D. TAPPENBECK im Mollogebiet und A. L. SIMONS in Nordost Niederländisch Timor.

Nach der Publikation der wesentlichen Ergebnisse dieser Expedition, besonders der Untersuchungen von TAPPENBECK im Mollogebirge (Lit. 9), von VAN WEST im Miomaffogebiet (Lit. 12), und vom Verfasser im südwestlichen Moetisgebiet (Lit. 8), sind wir nun auf Grund meiner Untersuchungen der permischen Gesteine in der Lage, eine Mitteilung über das Auftreten von zwei charakteristischen Stammestypen von Eruptivgesteinen in den verschiedenen Formationen des timoresischen Faltengebirges zu machen, und eine Erklärung ihres Auftretens zu geben.

Wenn wir die Entwicklungsgeschichte der timoresischen Geosynklinale betrachten, so sehen wir dass im Perm, das die ältesten paläontologisch belegten Ablagerungen der Insel Timor umfasst, noch keine grösseren Meerestiefen vorhanden waren. Das eigentliche geosynklinale Stadium in der Entwicklung des Faltengebirges tritt erst im Mesozoikum ein, wo die geosynklinalen Ablagerungen an den Rändern der Geosynklinale von flyschartigen Sedimenten und von Riffkalken begleitet werden. Die Hauptorogenese des timoresischen Deckengebirges ist nach TAPPENBECK (Lit. 9) wahrscheinlich ins Oligozän zu stellen.

Vor der Expedition 1937 waren schon viele Eruptivgesteine von Timor bekannt, deren Beschreibung wir besonders WICHMANN (Lit. 13), RETGERS (Lit. 7), VERBEEK (Lit. 11), BROUWER (Lit. 1, 2, 3) und IMDAHL (Lit. 5) verdanken. Von den meisten dieser Gesteine war das geologische Alter nicht sicher bekannt.

Aus dem Perm von Timor waren ausser basischen Laven auch bereits Alkaligesteine beschrieben, deren Alter von BROUWER (Lit. 1, 2, 3) festgestellt wurde. Diese Gesteine gehören zu der Sonnebaitserie, deren Mesozoikum den Ablagerungen des zentralen Teils der Geosynklinale entspricht. Wie bereits erwähnt sind im Perm der Sonnebaitserie noch keine in grösseren Meerestiefen gebildeten Gesteine vorhanden: hier werden meistens Krinoidenkalke, begleitet von mehreren Typen von Eruptivgesteinen angetroffen. Diese Formation hat die meisten bekannten permischen Fossilfundorte von Timor, z.B. diejenigen von Somohole, Bitaoeni und Basleo geliefert. Nach meinen Untersuchungen gehören die wichtigsten primären Differentiationsglieder der permischen Effusivserie in den verschiedenen von der Expedition 1937 untersuchten Gebieten zu Olivinbasalten, Trachybasalten, Alkalitrachyten und Alkalirhyolithen. Diese Effusivreihe entspricht der von HOLMES (Lit. 4) aufgestellten trachybasaltischen (trachydoleritischen) Differentiationsreihe. Ausser auf einzelnen sich schroff aus den Ozeantiefen erhebenden Inseln (Ascension, Samoa, usw.) kommt diese Gesteinsserie vor allem in verschiedenen Typen von Bruchgebieten vor (Lit. 10). Neben den erwähnten primären Gesteinen sind im Perm der Sonnebaitserie Spilite und Poeneite (Lit. 8) gefunden worden. Die von mir unter-

suchten Proben des letztgenannten Gesteinstypus, nach dem Fluss Noil Poene [1]) benannt, zeigen Einsprenglinge von Kalifeldspat und in untergeordneter Menge von umgewandeltem Olivin inmitten einer Glasgrundmasse. Der Albit der Spilite und der Kalifeldspat der Poeneite sind durch metasomatische Prozesse aus basischem Plagioklas hervorgegangen. Das Vorkommen der charakteristischen Poeneite N. und S. des pliopleistozänen zentralen Beckens von Timor im Zusammenhang mit den gleichen Sedimenten und Eruptivgesteinen deutet darauf hin, dass die Decke der Sonnebaitserie nicht nur im nordwestlichen Teil von Timor vorhanden ist, sondern sich auch unter dem jungen Becken hindurch bis in das südöstliche Gebirge erstreckt.

Die postpermischen Eruptivgesteine von Timor werden hauptsächlich von den Ophiolithen gebildet. Von den in der früheren petrologischen Literatur erwähnten Gesteinen sind nur die Peridotite und Serpentine und die Gabbros eindeutig als Ophiolithe zu betrachten, während mehrere andere Gesteinstypen möglicherweise zu dieser Differentiationsreihe gehören, aber ihr nicht mit Sicherheit einzureihen sind. Die Gesteinsserie der Ophiolithe ist am besten bekannt von dem im Jahre 1937 vom Verfasser untersuchten südwestlichen Moetisgebiet (Lit. 8), wo der sogenannte Ophiolithspilitkomplex die folgenden Gesteinstypen umfasst: gabbroide Gesteine, Lherzolithe, Tremolitolivingesteine, Serpentine, Albitite und Alkalialbitite, albitisierte und analcitisierte Dolerite, Andesite und Keratophyre, Spilite, Basalte und Spilitaugitite. Die Gesteinsserie wird durch eine weitgehende Albitisierung und durch das Fehlen von Kalifeldspat charakterisiert. Das Alter des Ophiolithspilitkomplexes konnte nicht genügend bestimmt werden; es ist aber mit Sicherheit prämiozän. Diese Ophiolithe und spilitischen Gesteine gehören möglicherweise zu derselben Einheit als einige seltene Kalke und Hornsteine, deren Vorkommen aber nicht genau bekannt ist. Im Felde scheinen die Gesteine des Ophiolithspilitkomplexes ausserdem mit kristallinen Schiefern verknüpft vorzukommen, während die Eruptivgesteine der an andern Orten auf Timor mit den kristallinen Schiefern verbundenen Paleloserie eine weitgehende Ähnlichkeit mit Gesteinen des Ophiolithspilitkomplexes aus dem südwestlichen Moetisgebiet zeigen. Nach VAN WEST (Lit. 12) gehören die Eruptivgesteine des Schiefer-Palelo-Komplexes im Miomaffogebiet, wo sie am besten bekannt sind, zu Lherzolithen, Serpentinen, Quarzalbititen, Albitdiabasen, Keratophyren, Quarzkeratophyren und spilitischen Gesteinen. Die ältesten Sedimente der Paleloserie werden von Radiolariten gebildet (Lit. 12), während der jüngere Teil dieser Gesteinsserie alle Merkmale der Flyschfazies zeigt, ausserdem aber viel Eruptiva und Tuffe enthält, und meistens zum Oberjura und zur Kreide gehört. Stellenweise setzt sich nach TAPPENBECK (Lit. 9) und VAN WEST (Lit. 12) die Fazies der Paleloserie ins Eozän fort. Der Ophiolithspilitkomplex und die Eruptivgesteine des Schiefer-Palelo-Komplexes sind dem letzthin von KOSSMAT (Lit. 6) eingehend verfolgten ophiolithischen Magmagürtel der Kettengebirge des mediterranen Systems einzureihen. Für die Erstarrungsgesteine des Schiefer-Palelo-Komplexes scheinen besonders die Feststellungen von KOSSMAT zu gelten, dass diese Eruptivgesteine von sandig-tonigen, z.T. tuffitischen Flyschablagerungen begleitet werden und dass sie mindestens von untertertiärem, vorwiegend aber von mesozoischem Alter sind.

Ausser den obengenannten Gesteinen sind hier noch einige Eruptivtypen zu erwähnen, die möglicherweise zu andern, gleichaltrigen Differentiationsreihen gehören, die mit derjenigen des Perms der Sonnebaitserie zu vergleichen sind und die in der Keknenoserie und in dem Fatoekomplex auftreten. In der Keknenoserie, die Perm und Trias in Flyschfazies umfasst, sind bisher noch keine Eruptivgesteine gefunden worden, die mit Sicherheit dieser Serie einzureihen sind. Im Gebiet der permischen Aufschlüsse der Keknenoserie wurde jedoch eine Menge von metergrossen, losen Blöcken angetroffen, die alle zu mesokraten Alkalialbititen gehören (Lit. 8). Im Fatoekomplex, der permische und mesozoische Riffkalke enthält, sind nur in mehr oder weniger konglomeratischen Schichten kleine Gerölle von Sanidintrachyt (Lit. 8) oder von albithaltigen Eruptivgesteinen (Lit. 12) gefunden worden.

---

[1]) Für die Ortsnamen wird die niederländische Schreibweise gebraucht, wobei *oe* = *u*.

Die einzigen genügend bekannten Differentiationsreihen des prämiozänen Faltengebirges von Timor sind also diejenigen der Ophiolithe und Spilite und diejenige des Perms der Sonnebaitserie. Die ophiolithischen und spilitischen Gesteine sind für die geosynklinale Phase in der Entwicklung des Faltengebirges charakteristisch. Im Perm dagegen, das die ältesten nichtmetamorphen Gesteine von Timor enthält, waren noch keine grösseren Meerestiefen vorhanden, und hier tritt in der Sonnebaitserie, also im Zentrum der späteren Geosynklinale, eine trachybasaltische Differentiationsreihe auf, deren Entstehung wahrscheinlich mit Brucherscheinungen während des embryonalen Stadiums der Geosynklinalbildung zusammenhängt; das Auftreten der permischen Alkaligesteine stellt mithin eine Art vorgeosynklinale Eruptionsphase dar.

Amsterdam, Geologisches Institut.

ZITIERTE LITERATUR.

1. BROUWER, H. A., Neue Funde von Gesteinen der Alkalireihe auf Timor. Centralblatt f. Min. etc., 1913, 570—576 und 1914, 741—745.
2. ————, Gesteenten van Oost-Nederlandsch Timor. Jaarb. Mijnwezen Nederl. Oost-Indië, 1916, Verh. I, 67—260.
3. ————, On the age of alkaline rocks from the island of Timor. Proc. Kon. Akad. v. Wetensch., Amsterdam, **31**, 56—58 (1928).
4. HOLMES, A. und HARWOOD, H. F., The basaltic rocks of the Arctic region. Mineralogical Magazine, **18**, 180—223 (1919).
5. IMDAHL, H., Beiträge zur Petrographie von West-Timor. Centralblatt f. Min. etc., 1922, 65—76.
6. KOSSMAT, F., Der ophiolithische Magmagürtel in den Kettengebirgen des mediterranen Systems. Sitz.-Ber. preuss. Akad. Wiss., phys.-math. Kl., 1937, **24**, 308—325.
7. RETGERS, J. W., Gesteenten van Timor en onderhoorigheden. Jaarb. Mijnwezen Nederl. Oost-Indië, 1895, Wet. Ged., 139—148.
8. ROEVER, W. P. DE, Geological investigations in the southwestern Moetis region (Netherlands Timor). Geol. Exp. to the Lesser Sunda Islands under leadership of H. A. BROUWER. Amsterdam, **2** (1940). Auch publiziert als Diss. Amsterdam (1940).
9. TAPPENBECK, D., Geologie des Mollogebirges und einiger benachbarter Gebiete (Niederländisch Timor). Geol. Exp. to the Lesser Sunda Islands under leadership of H. A. BROUWER. Amsterdam, **1** (1940). Auch publiziert als Diss. Amsterdam (1939).
10. TYRRELL, G. W., The principles of petrology. London (1934).
11. VERBEEK, R. D. M., Rapport sur les Moluques. Reconnaissances géologiques dans la partie orientale d'Archipel des Indes Orientales Néerlandaises. Jaarb. Mijnwezen Nederl. Oost-Indië, 1908, Wet. Ged. (Sowohl in französischer als in niederländischer Sprache erschienen.)
12. WEST, F. P. VAN, Geological investigations in the Miomaffo region (Netherlands Timor). Diss. Amsterdam (1941). Wird auch erscheinen in: Geol. Exp. to the Lesser Sunda Islands under leadership of H. A. BROUWER. Amsterdam, **3**.
13. WICHMANN, A., Gesteine von Timor. Samml. geol. Reichsmus. Leiden, Serie 1, **2**, 1—172 (1882—1887).

Palæontology. — *Some eocene Foraminifera from the neighbourhood of Ričice near Imotski, E. Dalmatia, Yugoslavia.* By R. C. VAN BELLEN. (Communicated by Prof. L. RUTTEN.)

(Communicated at the meeting of September 27, 1941.)

The author collected during the summer of 1939 some samples of flysch marls near Ričice. The map indicates the exact position of the different localities. These marls contain numerous *Foraminifera*, smaller ones as well as larger ones. This paper only deals with the Smaller *Foraminifera*.

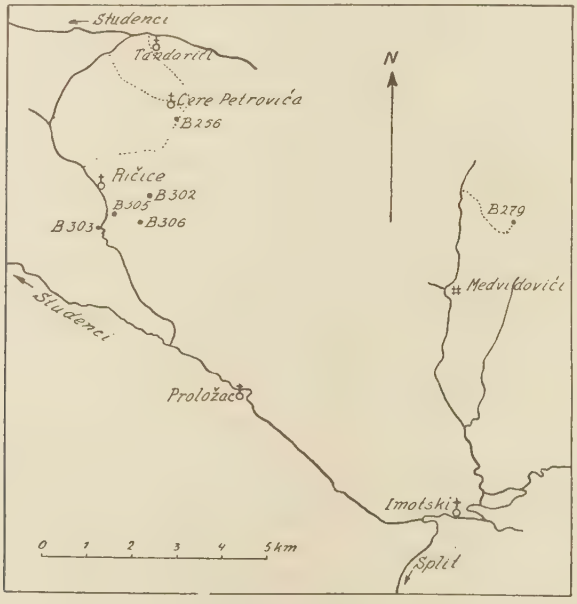

Many of the fossils were filled with pyrite, and this often obscured the details, especially of the apertures.

The tabular enumeration gives all the details with regard to the composition of the fauna, and of the stratigraphical range of its components [1]). Some remarks as to the nomenclature of the coiled

[1]) There are some errors in the tabular enumeration:

Cristellaria (R) *similis* TERQUEM with liter. 79 should be *Cristellaria* (R) *similis* D'ORB., non TERQUEM, liter. 65.

Lagena striata (D'ORB.) var. alata LIEBUS and var. *strumosa* RSS. should be *Lagena sulcata* W. a. J. etc. etc. (according to MATTHES, lit. 61).

Cibicides dorsmanni n.s. should be *Cibicides dorsmani* n.s.

Lagenidae are to be made. The genus *Cristellaria,* abandoned in the handbook by CUSHMAN, has been retained; while, where it was possible, *Lenticulina* and *Robulus* have been indicated as sub-genera by the figures *L* and *R*.

Of the 126 species and varieties 60 are known from the miocene, 60 from the oligocene, 65 from the eocene and 27 from the upper cretaceous. At first sight it seems — with regard to these figures — very difficult to state the age of the fauna. There are, however, various considerations which help us to limit the age with some precision:

1. The fact that not less than 7 species have not been found until now in deposits younger than cretaceous seems to be very suggestive. We must, however, take in mind that these species have been found only once or twice so that they do not have any real value as guide-fossils.

2. The fact that the genus *Marssonella* has been found until now only in cretaceous and eocene deposits and that *Hantkenina* is a strictly eocene genus suggest an eocene age of the fauna.

3. The fact that not less than 16 forms have been found up to now only in eocene deposits and that 10 of these, viz.: *Plectina dalmatina, P. eocaenica, Quinqueloculina carinata, Lagena sulcata* var. *alata, Plectofrondicularia trinitatensis, Bolivina nobilis, Uvigerina cocoaensis, U. lappa, Pleurostomella* cf. *acuta* and *Pl. incrassata* have been frequently encountered equally suggests an eocene age.

4. The occurrence of typical eocene larger *Foraminifera* (large *Camerinae* and *Discocyclinae*) proves the eocene age of the deposit.

5. On the other hand there are only 4 forms which have been found exclusively in oligocene deposits, and only 2 of these have been found more than once, viz. *Dorothia cylindrica* and *Cibicides dalmatina*.

The following species give rise to some remarks:

Vulvulina sp. I (fig. 1, × 22). Periphery acute, greatest part of the test biserial, in my specimens (10) there is at most one uniserial chamber. Outline dentate. Sutures depressed, especially those between the bi- and the uniserial part of the test. Aperture in the biserial portion a low transverse slit, in the adult an oblong slit. Length up to 1 mm., breadth up to 0.6 mm. This species differs from *V. pennatula* and *V. flabelliformis* in having depressed sutures.

Gaudryina eocaenica nov. sp. (fig. 2*a*, apertural face, × 35; 2*b*, × 20). Roughly agglutinated form. Length about 1.5 times breadth. Initial end with three chambers in a whorl. Sutures depressed, often hidden by the agglutination of the test. Chambers may be somewhat inflated or projecting, chiefly in the later, biserial part. Aperture an arch at the base of the last chamber. The triangular section at the initial end is invisible because of the roughness of the test. Sometimes the last chamber is somewhat terminal. Length up to 1 mm., breadth up to 0.7 mm.

Plectina sphaerica nov. sp. (fig. 3*a*, × 20; 3*b*, × 56; 3*c*, not oriented

section, × 56). Test almost spherical. Sometimes there is one suture visible. It is impossible to see the beginning or the end of the test, without using acid. The initial end has more than three chambers in the first whorl, probably four. Then follow one or two whorls with three chambers, and finally there are one or two biserial whorls. Aperture in the apertural face. Very roughly agglutinated. Diameter up to 0.5 mm. The spherical form is very typical.

Tritaxilina nov. sp. (fig. 4*a*, × 25; 4*b*, apical view, × 25). Initial end "five-serial". Each chamber corresponding with a depression. Sutures curved with the convexity upwards. Each chamber somewhat overhanging. Apertural end broken-off. Length of the fragment: 1.3 mm., breadth 0.6 mm. Only one specimen available.

Marginulina jonesi REUSS (fig. 5, × 50). Agrees fairly well with the description by REUSS. Broader at the base than at the top. About 12 costae running along the whole test, except along the last chamber. Section more compressed than section of *M. mülleri*. Length 0.5 mm., breadth 0.2 mm.

Marginulina mülleri REUSS (fig. 6, × 26). Agrees fairly well with the description by REUSS. About 14 costae running along the whole test, except along the last part. Thickness 0.55 mm., length 0.85 mm.

Marginulina sp. (fig. 7, × 30). Typical of this species is its very high apertural face as seen in the figure. Test ornamented in the coiled part with rows of knobs on the suture-lines. Later sutures only strongly limbate and raised. Length 0.8 mm., breadth 0.5 mm., height of the apertural face 0.5 mm., thickness 0.2 mm.

Cristellaria angustimargo (REUSS) (fig. 9, × 40). The only differences with the original description are the number of the chambers and the diameter. REUSS gives 7—8 chambers, and a diameter of 1.2 mm. Our specimens show only 6 chambers and a diameter of 0.4 mm.

Cristellaria secans REUSS (fig. 10, × 54). Although very badly preserved, it is possible to find the characteristics of this species of REUSS in our form. There are ten chambers in the last whorl. The sutures are strongly limbate and raised. They meet each other in an umbo, filled with clear shell-material. The periphery is sharply keeled. In accordance with the original description the aperture is invisible. Diameter 1 mm., thickness 0.4 mm.

Cristellaria similis D'ORB. (non TERQUEM) (fig. 8*a*, × 25; 8*b*, × 25). In the last whorl 6—7 chambers. Sutures curved, somewhat limbate and raised. Periphery with a broad thin carina. Thickness 0.4 mm., diameter 1 mm.

Cristellaria aff. *vortex* (F. a. M.). Agrees fairly well with *Crist.* aff. *vortex* (F. a. M.) described by NUTTALL in lit. 62.

Dentalina bohemiensis nov. sp. (fig. 11, × 20). The original description, given by REUSS of *D. annulata* in lit. 69, does agree with the figures on plate 8 (fig. 4) there, but does not agree with the figure on plate 13 (fig. 21). Our specimens agree closely with the last figure, but not so with

the first one. Particularly they do not show the typical raised sutures in the older part of the test. We propose the name of *D. bohemiensis* for the species in pl. 13, fig. 21.

Nodosaria sp. III (fig. 12, × 56). Only part of one specimen has been found. Apical end broken-off. Fragment consists of three chambers. All chambers inflated, last one more strongly so. Sutures depressed. All chambers striated with a number of oblique costae, the number of the costae on each chamber being different. Length of the fragment 0.5 mm.

Bulimina sp. (fig. 13, × 100). Test triangular with rounded edges. Initial end acute, apertural end rounded. Last three chambers making up almost $^2/_3$ of the length of the whole test. Sutures in the initial end not depressed, limbate, in the apertural end somewhat depressed, caused by the inflation of the last chambers, also limbate. Surface perfectly smooth. Aperture comma-shaped. Length 0.2 mm. This species differs from *B. affinis* D'ORB. in the shape of the test, from *B. ovata* in its triangular section, from *B. intermedia* REUSS in the less strong inflation of the last chambers.

? Bulimina sp. (fig. 14*a*, × 30; 14*b*, apertural view, × 30). Resembles the genus *Bulimina* in almost every respect. However, there are some differences: after a striated triserial part two chambers follow, non-striated and biserially arranged; finally follows the last chamber, non-striated and terminal, with a rounded aperture in the centre, in a somewhat sunken area. Only one specimen has been found in the sample B 303. We do not think, that it belongs to a new genus, but consider it to be a monstruosity of a *Bulimina*, perhaps of *B. buchiana* (lit. 65).

Uvigerina nov. sp. (fig. 15, × 65). Test about twice as long as broad. Chambers somewhat inflated, sutures obscured by the ornamentation. Wall ornamented in the middle and the upper part of the test with numerous small costae, crossing the sutures; in the lower part of the test there are small spines, irregularly scattered over the surface. Aperture with a very short neck. Length 0.6 mm., breadth 0.3 mm. We did not give this species a name, because only one specimen was available.

Gyroidina nov. sp. (fig. 16*a*, × 42; 16*b*, × 42; 16*c*, × 42). Ventral side convex, dorsal side flattened. Ventral side showing one whorl with 6 chambers. Ventral sutures limbate and raised. Dorsal sutures limbate, oblique, flush with the surface; spiral suture limbate, raised. Only somewhat more than two whorls visible on the dorsal side, rest hidden by a mass of secundary shell-substance. Aperture at the base of the last chamber, near the periphery. Diameter 0.5 mm., height 0.35 mm. We did not give this species a name, because only one specimen was available.

Valvulineria wittpuyti nov. sp. (fig. 17*a*—*c*, × 30). Test biconvex, ventrally more than dorsally. Only one whorl visible at the ventral side, with 7—8 chambers. Ventral sutures slightly curved and strongly limbate. The first five sutures on the ventral side are strongly raised near the depressed umbo, becoming flush with the surface towards the periphery.

Periphery at the beginning of the last whorl with a subacute keel; at the end bluntly rounded, without a keel. Dorsal side showing 2—2½ whorls. Dorsal sutures somewhat curved, limbate, partly raised. Aperture just above the periphery on the ventral side. The rests of the broken-off valvular lip are visible in the figure. Diameter up to 0.7 mm. Named in honour of my colleague J. F. C. DE WITTPUYT.

Eponides brückneri (REUSS) (fig. 18*a*—*b*, × 17). Corresponds very well with Reuss' description and figures.

Eponides ? karsteni (REUSS). The only difference with the original description (lit. 72) is the presence of a large knob of clear shellsubstance at the dorsal side. The species, named by FRANKE in lit. 50: *E. karsteni*, is certainly not the same as *E. karsteni* (REUSS).

Asterigerina rotula (KFM.) (fig. 19*a*—*c*, × 16). The only difference with the description by UHLIG is that the ramification of the ventral sutures lies nearer to the margin. Sometimes the dorsal whorls are slightly narrower than in UHLIG's figures.

Ceratobulimina perplexa (PLUMMER) (fig. 20*a*—*c* × 32½). The only difference with the original description is the limbation of the ventral sutures, which moreover show a very narrow depression in their predial part. Length up to 0,8 m.m.

Rogličia nov. gen. Shape of the test trochoid, like *Ceratobulimina*. All chambers visible from the dorsal side. Only those of the last formed whorl visible on the ventral side. Chambers distinct. Wall thick. Greatest part of the surface covered with short spines; only a region, surrounding the aperture smooth. The aperture, on the ventral side of the last formed chamber, circular, surrounded by a thickened ring, covered with a thin plate. This new genus differs from *Ceratobulimina* by the punctation of the test and the form of the aperture. Named in honour of Dr. J. ROGLIČ of Beograd.

Rogličia sphaerica nov. sp. (fig. 21*a*, ventral; 21*b*, peripheral; 21*c*, dorsal; 21*d*, not oriented section; 21*e*, section through aperture; all figures × 35). Test rounded, about spherical. Peripheral margin, especially near the last chamber, somewhat lobate. In the last whorl there are 5—6 chambers, rapidly increasing in size as added. Especially the last chamber forms a great part of the ventral side. Sutures ventrally flush with the surface, last one somewhat depressed. Dorsal side showing two whorls, dorsal sutures limbate, flush with the surface. Aperture at the ventral side of the base of the last chamber. Diameter 0,5—1 mm.

Globigerina ?tricamerata TOLM. (fig. 22*a*—*b*, × 38). Caused by the absence of the original literature it is impossible to determine this species with certainty. The figure, given by BRADY and renamed by THALMANN, resembles our species in having only three chambers, that give the lobate appearence to the test.

Globigerinella sp. I (fig. 23, × 60). This very small species shows only one whorl on the ventral side, with 5 chambers in it. The chamber-surfaces are coarsely punctated, with very small spines. Aperture on the ventral

side, with a lip over the umbilicus. Ventral sutures depressed, almost straight. Periphery rounded. Dorsal side showing two whorls. Dorsal sutures depressed, nearly straight. Chambers all inflated. Diameter 0.2 mm., thickness 0,1 mm.

Anomalina tenuissima (REUSS) (fig. 24*a*—*b*, × 32). Test almost equally biconvex. Ventrally only one whorl visible with 8 chambers. Ventral sutures strongly curved, sometimes depressed, sometimes flush with the surface. Ventral umbo filled with clear shellmaterial. Periphery with a small keel. Dorsal side showing two whorls; dorsal sutures strongly curved, limbate, flush with the surface or depressed. Greatest diameter 0,5 mm., thickness 0,1 mm.

Anomalina tenuissima (REUSS), var. *evoluta nov. var.* (fig. 25*a*—*b*, × 40). This variety differs from *A. tenuissima* (REUSS) in being more evolute and in having a ventral umbonal knob. Periphery lobate, sutures not always limbate and raised (by this characteristic the form differs from *Planulina wuellerstorfi* (SCHW.)). It differs from *Truncatulina costata* in having only 9 chambers in the last whorl, in being evolute ventrally and in having a ventral umbo-filling. Diameter 0,5 mm., thickness 0,12 mm.

Anomalina dalmatina nov. sp. (fig. 26*a*—*c*, × 35). Test equally biconvex. Ventral side only one whorl visible. Sunken umbilicus. Depressed sutures, curved near the periphery. Fourteen chambers in the last whorl. Periphery subacute without a definite keel. Dorsal side showing the chambers only in one whorl, but the limbate and raised spiral-suture can be followed for almost 2 whorls. Dorsal sutures, except the spiral suture, depressed. Aperture invisible. Its habit placed this species under the genus *Anomalina*. There is no *Anomalina* s.l. neither a *Rotalia* s.l., that shows this particular dorsal development. Diameter up to 0,8 mm., thickness up to 0,4 mm.

Anomalina sp. (fig. 27*a*—*b*, × 48). Ventral side convex, dorsal side almost flat. Ventral side showing only one whorl, with 8—9 chambers, last ones somewhat inflated. Ventral sutures flush with the surface, except the last ones, which are slightly depressed (caused by the inflation of the last chambers), all sutures limbate. Dorsal side showing $1\frac{1}{2}$ whorls. Sutures limbate, flush with the surface, except the last ones, which are depressed. This species differs from *Anomalina similis* HANTKEN (lit. 54), in being more involute dorsally and in being thicker. Diameter 0,6 mm., thickness 0,3 mm.

Cibicides cryptomphala (REUSS) (fig. 28*a*—*b*, × $27\frac{1}{2}$). Test biconvex, ventrally more than dorsally. Ventral side showing one whorl with 7—8 chambers. Ventral sutures depressed, the last ones more strongly than the first. Ventral umbo filled with a knob of clear shellmaterial. Last two or three chambers inflated. Periphery acute, not keeled. Dorsal side showing somewhat more than one whorl. Dorsal sutures depressed, the first ones somewhat limbate, curved. Spiralsuture limbate. Dorsal side with a knob

of clear shellmaterial. Last part of the periphery lobulated. Diameter 0,8 mm, thickness 0,35 mm.

Cibicides granosus (HANTKEN) (fig. 29*a*—*b*, × 35). Corresponds very well with HANTKEN's description and figures. The species has been figured here again because only one set of figures is available in the literature.

Cibicides dalmatina nov. nom. (fig. 30, × 30). Our specimen can be determined as *Truncatulina dutemplei* d'ORB. as described by REUSS in lit. 77. This description and the original one by d'ORBIGNY in lit. 65 as well as the figures do not agree inter se. The following differences are to be noticed:

REUSS:	d'ORBIGNY:
12 chambers in the last whorl.	8 chambers in the last whorl.
dorsal side showing only one whorl, rest hidden by secundary shellmaterial.	dorsal side showing two whorls, rest hidden by secundary shellmaterial.
curvature of the ventral and dorsal sutures very strong.	curvature of the sutures not so strong.

Because d'ORBIGNY used the name *"dutemplei"* first, it is necessary to give a new name to the *Truncatulina dutemplei* of REUSS. The following description can be given: Test planoconvex. Ventral side strongly convex, showing only the last whorl. Ventral sutures depressed, curved. Periphery sharp, not keeled. Dorsal side flat, showing somewhat more than one whorl, rest hidden by a somewhat raised boss of clear shellmaterial. Twelve chambers in the last whorl. Aperture over the periphery. Diameter 0,6 mm., thickness 0,35 mm. According to the position of the aperture this species belongs to the genus *Cibicides*.

Cibicides keijzeri nov. sp. (fig. 31*a*—*b*, × 20; 31*c*, × 35). Test variable, sometimes almost equally biconvex, sometimes planoconvex (dorsal side flat, ventral side convex). Ventral side with an umbo, filled with clear shellmaterial. Only one whorl visible on the ventral side. Sutures ventrally limbate, curved, mostly flush with the surface. The ventral umbo surpasses the convex outline of the ventral side. Periphery somewhat rounded, with a subacute keel of clear shell-material. Dorsal side with three visible whorls. In the last one 10—11 chambers. Dorsal sutures limbate, curved, mostly flushed with the surface. Spiral suture limbate and raised. First two whorls somewhat hidden by secundary shell-substance. Ventrally finely porous, dorsally more coarsely so. Diameter 1 mm., thickness 0,5 mm. Named in honour of my colleague F. KEIJZER.

Cibicides trinitatensis NUTTALL (fig. 32, × 30). Our species agree very well with the american ones.

Cibicides dorsmani nov. sp. (fig. 33*a*—*c*, × 40). Ventral side convex, dorsal side more strongly so. Ventral side showing only the last whorl, with 7 chambers. Ventral sutures depressed, sometimes with a limbate ridge

in the depression. Last chamber inflated. Umbonal area depressed. Periphery subacute. Dorsal side showing two whorls. The last whorl covers a part of the preceeding one. Aperture invisible. The general appearance of the test places it under the genus *Cibicides*. Diameter up to 0,6 mm., thickness up to 0,3 mm. This species is named in honour of my colleague L. DORSMAN.

LITERATURE.

1. W. R. BARKER, Bull. Am. Ass. Petr. Geol., **20**, 433—451 (1936).
2. J. BEISSEL, Abh. kön. pr. geol. Anst. N.F., Hft. **3**, 1—76; plt. I—XVI (1891).
3. P. J. BERMUDEZ, Mem. Soc. Cub. Hist. Nat., **11**, 91—96 (1938).
4. K. BEUTLER, N.J., 140—162, plt. XVIII (1909).
5. J. G. BORNEMANN, Z. D. G. G., **7**, 307—351, plt. XII—XIX (1855).
6. H. B. BRADY, Report on the scientific results of the exploring voyage of H. M. S. "Challenger", 1873—1874; Zoology, **9**, 1—814, plt. I—CXV (1884).
7. H. N. CORYELL and J. B. EMBICH, J. Pal., **11**, 289—305, plt. XLI—XLIII (1937).
8. J. A. CUSHMAN, U. S. Nat. Mus. Bull., **71**, prt. II (Textulariidae), 1—108, 156 textfig. (1911).
9. ——— U. S. Nat. Mus. Bull., **71**, prt. III (Lagenidae), 1—118, plt. I—XLVII (1913).
10. ——— U. S. Nat. Mus. Bull., **71**, prt. V (Rotalidae), 1—87, plt. I—XXXI (1915).
11. ——— U. S. Nat. Mus. Bull., **71**, prt. VI (Miliolidae), 1—103, plt. 1—XXXIX (1917).
12. ——— U. S. Geol. Surv. Bull., **676**, 1—100, plt. I—XXX (1918).
13. ——— U. S. Nat. Mus. Bull., **100**, vol. 4, 1—608, plt. I—C (1921).
14. ——— U. S. Nat. Mus. Bull., **104**, prt. III (Textulariidae), 1—149, plt. I—XXVI (1922).
15. ——— U. S. Geol. Surv. Prof. Pap., **129**E, 79—122, plt. XIV—XXVIII (1922).
——— U. S. Geol. Surv. Prof. Pap., **129**F, 123—152, plt. XXIX—XXXV (1928).
16. ——— U. S. Nat. Mus. Bull., **104**, prt. IV (Lagenidae), 1—228, plt. I—XLII (1923).
17. ——— U. S. Nat. Mus. Bull., **104**, prt. V (Globigerinidae), 1—56, plt. I—VIII (1924).
18. ——— Cont. Cush. Lab. For. Res., **1**, 65—71, plt. X (1925).
19. ——— Bull. Scripps Inst. Oc. Techn. Ser., **1**, 119—188, plt. I—VI (1927).
20. ——— Contr. Cush. Lab. For. Res., **3**, 156, plt. XXVIII (1927).
21. ——— Contr. Cush. Lab. For. Res., **3**, 180—185, plt. XXXI—XXXII (1927).
22. ——— J. Pal., **8**, 147—172, plt. XXIII—XXVIII (1927).
23. ——— U. S. Nat. Mus., Bull., **104**, prt. VI (Miliolidae .....), 1—129, plt. I—XXII (1929).
24. ——— Contr. Cush. Lab. For. Res., **5**, 67—72, plt. XI (1929).
25. ——— Contr. Cush. Lab. For. Res., **5**, 77—101, plt. XII—XIV (1929).
26. ——— Contr. Cush. Lab. For. Res., **5**, 102—105, plt. XV (1929).
27. ——— U. S. Nat. Mus. Bull., **104**, prt. VIII (Rotalidae.....), 1—179, plt. I—XXVI (1931).
28. ——— Contr. Cush. Lab. For. Res., **7**, 33—46, plt. V—VI (1931).
29. ——— Contr. Cush. Lab. For. Res., **8**, 75—85, plt. X (1932).
30. ——— U. S. Geol. Surv. Prof. Pap., **181**, 1—88, plt. I—XXVII (1935).
31. ——— Contr. Cush. Lab. For. Res., **13**, 54—61, plt. VII—VIII (1937).
32. ——— Contr. Cush. Lab. For. Res., **13**, 74—86, plt. XI—XII (1937).
33. ——— Contr. Cush. Lab. For. Res., Spec. Publ., **7**, 1—157, plt. I—XX (1937).

34. J. A. CUSHMAN, Contr. Cush. Lab. For. Res., Spec. Publ., **8**, 1—120, plt. I—XXIV (1937).
35. ——— Contr. Cush. Lab. For. Res., Spec. Publ., **9**, 1—228, plt. I—XXIV (1937).
36. ——— Contr. Cush. Lab. For. Res., **15**, 49—76, plt. IX—XII (1939). plt. V—VI (1936).
37. J. A. CUSHMAN and P. J. BERMUDEZ, Contr. Cush. Lab. For. Res., **12**, 27—38.
38. J. A. CUSHMAN and P. G. EDWARDS, Contr. Cush. Lab. For. Res., **15**, 33—40, plt. VIII (1939).
39. J. A. CUSHMAN and R. W. HARRIS, Contr. Cush. Lab. For. Res., **3**, 171—179, plt. XXIX—XXX (1927).
40. ——— Contr. Cush. Lab. For. Res., **3**, 128—135, plt. XXV (1927).
41. J. A. CUSHMAN and H. D. HOBSON, Contr. Cush. Lab. For. Res., **11**, 53—64, plt. VIII—IX (1935).
42. J. A. CUSHMAN and P. W. JARVIS, Contr. Cush. Lab. For. Res., **4**, 85—103, plt. XII—XIV (1928).
43. ——— Contr. Cush. Lab. For. Res., **5**, 6—17, plt. II—III (1929).
44. ——— Proc. U. S. Nat. Mus., **80**, art. 14, 1—60, plt. I—XVI (1931).
45. J. A. CUSHMAN and B. LAIMING, J. Pal., **5**, 79—120, plt. IX—XIV, 5 textfig. (1931).
46. J. A. CUSHMAN and F. L. PARKER, Contr. Cush. Lab. For. Res., **14**, 53—62, plt. IX—X (1938).
47. ——— Contr. Cush. Lab. For. Res., **14**, 90—94, plt. XV—XVI (1938).
48. J. A. CUSHMAN, R. E. and K. C. STEWART, Trans. S. Diego. Soc. Nat. Hist., **6**, 41—94, plt. I—VIII (1930).
49. C. FORNASINI, Mem. d. R. Acad. d. Sc. dell'Ist. di Bologna, (VI), **1**, 59—70, plt. I—IV (1904).
50. A. FRANKE, Abh. geol. pal. Inst. Univ. Greifswald, **6**, 4—96, plt. I—VIII (1925).
51. J. J. GALLOWAY and M. MORREY, Bull. Am. Pal., **55**, 1—56, plt. I—VI (1929.
52. C. W. GÜMBEL, Abh. Bayer. Ak. Wiss. II Cl., **10**, 581—730, plt. I—IV (1870).
53. R. HAÜSLER, N. J., **1**, 178—189, plt. IV—V (1887).
54. M. VON HANTKEN, Mitt. Jahrb. k. Ungar. geol. Anst., **4**, 1—93, plt. I—XVI (1875).
55. R. JONES and K. PARKER, Q. J. G. S., London, **28**, 103—131 (1872).
56. F. KARRER, Sitzber. Ak. Wiss. Wien, Math. Naturw. Cl., **58**, 111—193, plt. I—V (1868).
57. F. KEIJZER, Proc. Kon. Ned. Akad. v. Wetensch., Amsterdam, **41**, 987—991 (1938).
58. A. LIEBUS, Jahrb. k. k. geol. R. A., 351—366, fig. 1—8 (1906).
59. ——— Sitzber. Ak. Wiss., Wien, Math.-Naturw. Cl., **120**, 865—956, plt. I—III (1911).
60. ——— Palaeontographica, **70**, 41—114, textfig. (1928).
61. H. W. MATTHES, Palaeontographica, **90** A, 49—104, plt. III—VIII (1939).
62. W. L. F. NUTTALL, Q. J. G. S., London, **84**, 57—115, plt. III—VIII (1928).
63. ——— J. Pal., **6**, 3—35, plt. I—IX (1932).
64. A. D'ORBIGNY, Foraminifères; in: DE LA SAGRA: Hist. phys. de l'île de Cuba (1859).
65. ——— Foraminifères fossiles du bassin tertaire de Vienne, 1—132, XX plt. (1846).
66. D. PALMER and P. J. BERMUDEZ, Mem. Soc. Cub. Hist. Nat., **10**, 227—316, plt. XIII—XX (1936).
67. P. J. PIJPERS, Geogr. Geol. Meded. Phys. Geol. Reeks, **8**, 1—103, textfig., Utrecht (1933).
68. B. VAN RAADSHOVEN, Nat. Hist. Maandblad Limburg, **29**, 11—12 (1940).
69. A. E. REUSS, Die Versteinerungen der Böhmischen Kreideformation I, 25—40, plt. I—XII (1845).
70. ——— Denkschr. Ak. Wiss. Wien, **1**, 365—390, plt. XLVI—LI (1850).
71. ——— Z. D. G. G., **3**, 49—92, plt. III—VII (1851).
72. ——— Z. D. G. G., **7**, 261—292, plt. VIII—XI (1855).

1
2a
2b
3a
3b
3c
4a
4b
5
6
7
8a
8b
9
10
11
12
13
14a
14b
15
16a
16b
16c
17a
17b
17c
18a
18b
19a
19b
19c
20a
20b
20c
21a
21b
21c
21d
21e
22a
22b
23
24a
24b
25a
25b
26a
26b
26c
27a
27b
28a
28b
29a
29b
30
31a
31b
31c
32
33a
33b
33c

Eocene Foraminifera from the neighbourhood of Ričice near Imotski (E.Dalmatia).	Text a/o fig.	N.Dalm. Lieb. 1911	Alb. Lieb. 1928	M.Dal. Keyz. 1938	B256	B279	B302	B303	B305	B306	Upper Cret.	L.Eo-cene.	M.Eo-cene.	U.Eo-cene.	Oli-go-cene	Mioc. and Rec.	Literature:
Textularia corrugata Costa	-	-	-	-	-	-	-	x	-	-							6,77,80.
Vulvulina sp.I	x	-	-	-	-	-	-	x	-	-							29
sp.II	-	-	-	-	-	-	-	x	-	-							
Tritaxia tricarinata (Rss.)	-	-	-	-	-	-	-	-	x	-							50,59,69,74.
Gaudryina eocaenica nov.sp	x	-	-	-	x	-	-	-	-	-							
Clavulinoides haeringensis Cushm	-	-	-	-	-	-	-	x	-	-							33.
szaboi (Htk.)	-	x	-	-	-	-	-	x	-	-							33,54,59.
Marssonella indentata (Cushm.& Jarvis)	-	-	-	x	-	x	-	x	-	x							34,42,57,82.
Dorothia cylindrica (Nuttall)	-	-	-	-	-	-	-	x	-	-							34,63.
eocaenica Cushm	-	-	-	-	-	-	-	x	-	-							34.
sp.I	-	-	-	-	-	-	-	x	-	-							
sp.II	-	-	-	-	-	-	-	x	-	-							
sp.III	-	-	-	-	-	-	-	x	-	-							
Plectina dalmatina (Schub.)	-	x	-	x	-	-	-	x	-	-							34,57,59.
eocaenica Cushm	-	-	-	x	-	-	-	x	-	-							34,57.
sphaerica nov.sp	x	-	-	-	x	-	x	x	-	x							
Tritaxilina nov.sp	x	-	-	-	-	-	-	-	x	-							
Quinqueloculina carinata d'Orb	-	-	-	-	-	-	-	x	-	-							49,79.
pygmaea Rss	-	-	-	-	-	-	-	x	-	-							6,70,80.
vulgaris d'Orb	-	-	-	-	-	-	x	-	-	-							11,23.
sp.(?form.juv.Q.plana d'Orb.)								x									49,79.
Cristellaria(R) angustimargo (Rss)	x	-	-	-	-	-	-	x	-	-							5,71.
(R) arcuatostriata (Htk)	-	x	x	-	-	-	-	x	-	-							54,66.
(L) cultrata (Mtf)	-	x	x	x	-	-	-	x	-	-							65.
(R) gutticostata (Gümb.)	-	-	-	-	-	-	-	x	-	-							20,30,52,54,63,66.
(R) inornata (d'Orb.)	-	-	x	-	-	-	x	x	-	-							5,54,60,63,65,66,67.
(R) megalopolitana (Rss.)	-	-	-	-	-	-	-	x	-	-							72.
(L) rotulata (Lam.)	x	x	x	x	-	-	-	x	-	-							6,15.
(L) secans Rss	x	x	-	-	-	-	-	x	-	-							74.
(R) similis Terquem	x	-	-	-	-	-	-	x	-	-							79.
(R) vortex (F.a.M.)	-	x	-	x	x	x	-	-	-	-							6,57.
(R) aff.vortex (F.a.M.)	x	-	-	-	-	-	-	x	-	-							62.
Marginulina jonesi Rss	x	-	-	-	-	-	-	x	-	-							44,75.
mülleri Rss	x	-	-	-	-	-	-	x	-	-							75.
subaculeata (Cushm.)	-	-	-	-	-	-	-	x	-	-							6,16,80.
var.glabrata (Cushm.)	-	-	-	-	-	-	-	x	-	-							16,25,62.
sp.I	x	-	-	-	-	-	-	x	-	-							
Dentalina bohemiensis nov.sp	x	-	-	-	-	-	-	x	-	-							69.
consobrina d'Orb	-	x	x	-	-	-	-	x	-	-							6,54,65,71,80.
cf.megapolitana Rss	-	-	-	-	-	-	-	x	-	-							72.
Nodosaria ewaldi Rss	-	x	x	x	x	-	-	x	-	-							57,71.
hirsuta d'Orb	-	x	x	-	-	-	-	x	-	-							6,65,71,80.
radicula (Linn.)	-	x	-	x	-	-	-	x	-	-							6,57.
raphanus (Linn.)	-	-	-	-	-	-	-	x	-	-							6.
sp.I	-	-	-	-	-	-	-	x	-	-							
sp.II	-	-	-	-	-	-	-	x	-	-							
sp.III	x	-	-	-	-	-	-	x	-	-							
Saracenaria acutauriculauris (F.a.M.)	-	-	x	-	-	-	-	x	-	-							6,25,82.
?Frondicularia sp	-	-	-	-	-	-	-	x	-	-							
Lagena marginata (W.a.B.)	-	x	-	x	-	-	-	x	-	-							6,57,76.
?orbignyana (Seg.)	-	x	x	x	-	-	-	x	-	-							6,52,57,61.
striata(d'Orb.) var.alata Liebus	-	x	-	x	-	-	-	x	-	-							57,59,61.
var.strumosa Rss	-	-	-	-	-	-	-	x	-	-							6,9,13,16,36,80.
sulcata (W.a.J.) var.apiculata Cushm.	-	-	-	-	-	-	-	x	-	-							9,24,61.
Plectofrondicularia trinitatensis C.a.J	-	-	-	-	-	-	-	x	-	-							30,43.
Bulimina affinis d'Orb	-	-	-	x	-	-	-	x	x	-							6,8,13,14,57.
costata d'Orb	-	-	-	-	-	-	-	x	-	-							46.
inflata Seg	-	x	x	x	-	-	-	x	-	-							46,57,67.
sp	x	-	-	-	-	-	-	-	x	-							
?Bulimina sp	x	-	-	-	-	-	-	x	-	-							
Bolivina antiqua d'Orb	-	-	-	-	-	-	-	x	-	-							4,35,65.
nobilis Htk	-	x	-	-	-	-	-	x	-	-							35,54,58.
Uvigerina cocoaensis Cusman	-	-	-	-	-	-	-	x	-	-							18,30,32.
lappa Cushm.a.Edw	-	-	-	-	-	-	-	x	-	-							31,54.
cf.urnula Orb.var.semiornata d'Orb.	-	-	-	-	-	x	-	-	-	-							38,65.
nov.sp	x	-	-	-	-	-	-	x	-	-							
Pleurostomella cf.acuta Htk	-	x	-	x	-	-	-	x	-	-							39,54,57.
alternans Schw	-	-	x	x	-	-	-	x	-	-							39,57,60.
incrassata Htk	-	x	-	x	-	-	-	x	-	-							20,39,57.
Ellipsolagena apiculata (Rss.)	-	x	x	-	-	-	-	x	-	-							6,53,54,76.
Discorbis araucana (d'Orb.)	-	-	-	-	-	-	-	x	-	-							6,15,55,63,80.
eximia (Htk.)	-	-	-	-	-	-	-	x	-	-							6,55,57,80.
Valvulineria araucana (d'Orb.)	-	-	-	-	-	-	-	x	-	-							19,48,64.
witt-puyti nov.sp	x	-	-	-	-	-	-	x	-	-							
Gyroidina orbicularis d'Orb	-	-	-	x	-	-	-	x	-	-							6,10,57,80.
soldanii d'Orb	-	x	x	x	-	-	-	x	-	-							41,56.
nov.sp	x	-	-	-	-	-	-	-	-	x							
Eponides bruckneri (Rss.)	x	-	-	-	x	-	x	x	-	x							72.
concentricus (P.a.J.)	-	x	-	-	x	x	x	x	-	-							6,10,80,81.
?karsteni (Rss.)	x	-	-	-	-	-	-	x	-	-							6,10,50,72,80.
nanus Rss	-	-	-	-	-	-	-	x	-	-							45,51,66,70.
praecinctus (Karrer)	-	x	x	-	-	-	-	x	-	-							6,10,56,80.
repandus (F.a.M.)	-	-	-	-	-	-	-	x	-	-							6,10,12,27,80.
tschoppi van Bellen	-	-	-	-	-	-	-	x	-	-							83.
umbonatus (Rss.)	-	x	x	x	-	-	-	x	-	x							6,10,30,51,80.
Epistomina elegans (d'Orb.)	-	-	-	-	x	x	-	x	x	-							6,21,65,80.
Asterigerina rotula (Kfm.)	x	x	-	-	-	x	x	-	-	-							50,81.
Ceratobulimina perplexa (Plummer)	x	-	-	-	x	x	x	x	-	x							40.
Rogličia sphaerica nov.gen.,nov.sp	x	-	-	-	-	-	-	x	-	-							
Pulvinulinella pacifica Cushm	-	-	-	-	-	-	-	x	-	-							19,48.
Cassidulina havanensis Cushm.a.Boys	-	-	-	-	-	-	-	x	-	-							37.
sp.I	-	-	-	-	-	-	-	x	-	-							
Sphaeroidina bulloides d'Orb	-	x	x	-	-	x	-	-	-	-							6.
Globigerina bilobata d'Orb	-	-	-	-	-	-	-	-	x	-							65.
bulloides d'Orb	-	x	x	x	x	-	-	x	x	-							6.
conglomerata Schw	-	-	-	-	-	-	-	x	-	-							57,78.
cretacea d'Orb	-	-	-	-	-	-	-	-	x	-							2,6,28.
inflata d'Orb	-	x	-	x	-	-	-	x	-	-							6,17.
?tricamerata Tolm	x	-	-	-	-	-	-	x	-	-							6,80.
triloba Rss	-	-	-	-	-	x	-	x	x	-							6,70,80.
Globigerinoides conglobatus (Brady)	-	-	x	x	-	-	-	x	-	-							6,57,70,80.
Globigerinella sp	x	-	-	-	-	-	-	-	x	-							
Hantkenina liebusi Shokhina	-	-	-	-	-	-	-	x	-	-							59.
Globorotalia crassa (d'Orb.)	-	x	-	-	-	-	-	x	-	x							10.
tumida (Brady)	-	-	-	-	-	x	-	-	x	x							6,80.
Anomalina ammonoides (Rss)	-	x	x	x	-	x	-	x	-	-							6.
badenensis d'Orb	-	-	-	-	-	x	-	-	-	-							65.
dalmatina nov.sp	x	-	-	-	-	-	x	x	-	-							
lucida (Rss.)	-	-	-	-	-	-	-	x	-	x							77.
tenuissima (Rss.)	-	-	-	-	-	-	-	x	-	-							73.
var.evoluta nov.var	x	-	-	-	-	-	-	x	-	-							
sp.I	x	-	-	-	-	-	-	-	-	x							
Planulina ariminensis d'Orb	-	x	-	-	-	-	-	x	-	-							6,26,80.
ornata(d'Orb.)	-	-	-	-	-	-	-	x	-	-							48,64.
wullerstorfi (Schw.)	-	x	x	x	-	-	-	x	-	-							6,26,57,80.
Cibicides cryptomphalus (Rss.)	x	-	-	-	-	-	-	x	-	-							70.
dalmatina nov.nom	x	-	-	-	-	-	-	x	-	-							54,77.
dorsmanni nov.sp	x	-	-	-	-	-	-	x	-	-							
granosus (Htk.)	x	-	-	-	-	-	-	x	-	-							54.
keijzeri nov.sp	x	-	-	-	-	-	-	x	-	-							57.
lobatulus (W.a.J.)	-	x	x	-	-	-	-	x	-	-							6,15,65,80.
pseudoungerianus (Cushm.)	-	-	-	x	-	-	-	x	-	-							6,7,15,80.
refulgens Mtf	-	x	x	x	-	-	-	x	-	-							6,57,66,80.
trinitatensis Nuttall	x	-	-	-	-	-	-	x	-	-							62,63,83.
ungerianus (d'Orb.)	-	x	x	-	x	-	x	x	-	-							54,65.
Gypsina globulus (Rss.)	-	-	-	-	x	x	x	-	x	x							6,81.

73. A. E. Reuss, Sitzber. Ak. Wiss. Wien, Math. Naturw. Cl., **18**, 197—296, plt. I—X (1855).
74. ———— Sitzber. Ak. Wiss. Wien, Math. Naturw. Cl., **40**, 147—238, plt. I—XIII (1860).
75. ———— Sitzber. Ak. Wiss. Wien, Math. Naturw. Cl., **46**, 1, 5—100, plt. I—XIII (1863).
76. ———— Sitzber. Ak. Wiss. Wien, Math. Naturw. Cl., **46**, 1, 308—342, plt. I—VII (1863).
77. ———— Die Foraminiferen ..... des Septarienthones, 1—98, plt. I—XI (1866).
78. C. Schwager, Fossile Foraminiferen von Kar Nikobar. Reise der ... Novara. Geol. Theil, **2**, 18—268, plt. IV—VII (1866).
79. O. Terquem, Mém. Soc. Géol. France, **2**, 3, 1—193, plt. I—XX (1882).
80. H. E. Thalmann, Ecl. Geol. Helv., **25**, 293—312, **26**, 251—255 (1932 and 1933).
81. V. Uhlig, Jahrb. k. k. geol. R. A., 142—241, plt. II—V (1886).
82. M. P. White, J. Pal., **2**, 177—215, plt. XXVII—XXIX; 280—316, plt. XXXVIII—XLII (1928).
83. R. C. van Bellen, A. Rutgers, J. van Soest, J. F. C. de Wittpuyt, Oligocene Foraminifera from Cuba, Proc. Ned. Ak. Wet., in litt.

Palæontology. — *Eine neue eozäne Foraminiferengattung aus Dalmatien.* Von F. KEIJZER. (Communicated by Prof. L. RUTTEN.)

(Communicated at the meeting of September 27, 1941.)

Die beschriebene Form entstammt den mitteleozänen Flyschmergeln vom Längstal zwischen Omiška Dinara und Stupina, oberhalb Omiš an der adriatischen Küste [1]). In einer Foraminiferenliste war die vorliegende Form benannt als *Heterohelicidae* genus indet. [2]). Bei einer eingehenden Betrachtung stellte sich aber heraus, dass das Gehäuse sehr fein agglutiniert ist, und dass die Form den Textulariden zugestellt werden muss.

Septigerina nov. gen.

Gehäuse keilförmig, agglutiniert, jüngerer Teil spiralig, später biserial angeordnet. Die biserialen Kammern sind von einer Zwischenwand geteilt. Von den beiden so entstandenen Teilkämmerchen trägt das innere den halbkreisförmigen Mund, der auf die vorhergehende Kammerwand stützt. Das äussere Kämmerchen hat nur Kommunikation mit dem inneren, jedoch keinen direkten Weg zur Aussenwelt.

Septigerina dalmatica nov. sp.
Textularia an *Spiroplecta* sp. nov. indet. LIEBUS, 1911.
(Sitzber. Ak. Wiss. Wien, Math. Nat. Kl., Bd. 120 I, 1911, S. 932, Taf. II, Fig. 6*a*, *b*.)

Gehäuse stark abgeplattet keilförmig, sehr fein agglutiniert, mit reichlichem Zement. Auf die kugelige Embryonalkammer folgen 3 spiralig angeordnete Kammern. Der folgende biseriale Teil enthält wenigstens 18 alternierende Kammern. Weil keine vollständige Exemplaren gefunden worden sind, konnte die genaue Anzahl nicht bestimmt werden. Die gebogenen Suturen sind in mehreren Exemplaren verdickt, in einigen werden sie jedoch nur von einer feinen Linie angedeutet. Im Dünnschliff stellte sich heraus, dass die biserialen Kammern von einer Art Scheidewand geteilt werden in ein kleines äusseres, in der Randwulst gelegenes Kämmerchen, und einen grösseren an der inneren Seite gelegenen Teil, der deutlich aufgeblasen hervortritt. Dass die Scheidewand nicht nur vorgetäuscht wird von einem nicht genau medianen Schnitt, der einen stark eingebuchteten Teil der

---

[1]) G. H. VOORWIJK, Geologie und Palaeontologie der Umgebung von Omiš (Dalmatien). Dissertation, Utrecht 1938.

[2]) F. KEIJZER, Proc. Kon. Ned. Akad. v. Wetensch., Amsterdam, Vol. XLI, 9, S. 987—991 (1938).

Seitenwand getroffen hat, bewies ein Querschnitt (Fig. 3). Die Form der Scheidewand konnte nicht genau bestimmt werden. Die Figuren 4*a*, *b*, *c*, geben verschiedene Möglichkeiten. Die Figuren 1 und 2 (× 50) sind nach verschiedenen gebrochenen Exemplaren rekonstruiert. Der Bauplan weist mit Sicherkeit auf die Textulariden hin.

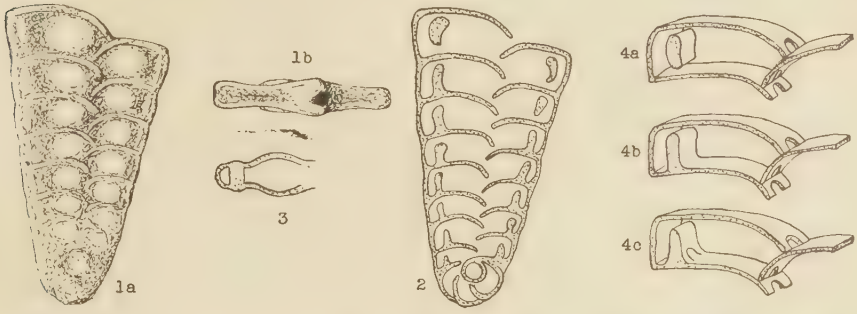

Die Genotypen befinden sich in der Dünnschliffsammlung des Geologischen Institutes der Reichsuniversität zu Utrecht (Nummer 18743, 20976—20979).

Histology. — *On the structure of the connective tissue of the anterior lobe of the hypophysis cerebri and the nature of the intraprotoplasmic networks described by Tello in and around the cells of the anterior lobe.* By F. P. BOL. (From the Histological and Embryological Laboratory of the University of Utrecht.) (Communicated by Prof. J. BOEKE.)

(Communicated at the meeting of September 27, 1941.)

As is well-known, the hypophysis cerebri is a very composite structure, composed of glial, epithelial and connective tissues and nerve fibres. Embryologically the hypophysis arises from two separate anlagen. The pars buccalis arises from an evagination of the buccal mucosa, first described by RATHKE (1838) and known as RATHKE's pouch. It is generally assumed that this pouch is of ectodermal origin, but according to LUPS (1929) and ATWELL (1926) the anterior wall of the hypophysial anlage from which the anterior lobe originates, is clearly ectoderm, but it is impossible to tell whether the posterior wall, which gives rise to the pars intermedia, is formed from ectoderm or entoderm.

At all events the anterior lobe of the hypophysis is of ectodermal origin, and so are the paired lateral lobes which unite in the embryo in the midline and grow laterally to become the pars tuberalis.

The anterior lobe, which constitutes on an average about 75 % of the total of the gland by weight (RASMUSSEN, 1928, BUCY, 1932), is composed of polygonal epithelial cells of two types, chromophobe and chromophile cells. The latter are filled with eosinophilic and basophilic granules. The epithelial cells of the anterior lobe lie in groups and columns which are supported in a delicate reticular connective tissue mixed with thicker membranous formations and septa of collagenous connective tissue. Between these groups of epithelial cells are dilated sinusoids and other bloodvessels. According to BUCY the connective tissue forms a loose network throughout the pars anterior; the fenestrations of this net are smallest in the posterosuperior part of the anterior lobe near its junction with the pars intermedia. This connective tissue is composed of collagenous fibers with numerous reticulin fibers attached to them; at times the reticulin fibers cross from one band of collagen to another. According to BUCY this causes fibrosis of individual alveoli of epithelial cells and the number of epithelial cells in such a fibrosed alveolus is greatly reduced or they may be completely absent (BUCY, 1932, p. 733).

The innervation modus of the anterior lobe is difficult to study. According to DANDY (1913) the sympathetic nerves enter the lobe together with the bloodvessels from the circle of WILLIS, accompany the larger vessels and finally separate to wind among the epithelial cells. TELLO (1912) found it extremely difficult to impregnate the nerve fibers and could only find them in some of the specimens studied. GREVING (1926) and CROLL (1928) experienced the same difficulty. BUCY (1932) was unable to demonstrate "to his own satisfaction" any nerve fibers within the anterior lobe, using CAJAL's silver pyridine technique. Only PINES (1925) describes a very fine intercellular nervous network between the epithelial cells with pericellular loops and knoblike endings lying close to the surface of the cells. In the pictures accompanying the description of PINES the resemblance of the structures described by him as nervous to the reticulin networks of BUCY and others is very striking.

In 1903 GEMELLI described inside the protoplasm of the epithelial cells a reticulated structure, a network extending throughout the protoplasm, in the epithelial cells of the whole lobe but particularly in the cells of the anterior lobe near the infundibulum. It was not comparable with the GOLGI-apparatus. In 1909 CELESTINO DA COSTA described intraprotoplasmic filaments inside the epithelial cells which he compared with the

ergastoplasma of PRENANT. In 1912 TELLO described (by means of the ACHúCARRO's tannic silver method) large and very clearly impregnated reticulate structures inside the protoplasm of the epithelial cells, surrounding the nucleus and sometimes drawn out into a fibrous ligament, remaining independant of the connective tissue networks. In fact, TELLO got the most perfect pictures of these networks in preparations, in which the connective tissue was but faintly impregnated. With the GOLGI-apparatus these networks had nothing to do. The ergastoplasmic filaments described by DA COSTA he thought to be a part of the network described by him. DA COSTA himself (1923) was not able to come to a decisive opinion ("je ne peux pas me prononcer d'une façon définitive sur les rapports qu'il y a entre ce que TELLO a vu chez l'homme et ce que j'ai rencontré chez le COBAYE").

BUCY working with the ACHúCARRO method used by TELLO could not find any trace of these reticulate structures (1932), ROMEIS does not even mention them in his very elaborate study of the histology of the hypophysis in MÖLLENDORFF's Handbook (1940).

Thus we see, that the histology of the lobus anterior of the hypophysis is by no means clear. It being however of high importance to get a solid histological base for the complicated (and inconstant) physiological functions of this part of the gland, we tried to get at the bottom of this controversy by studying the structure of the lobus anterior with the aid of the same methods used by TELLO, viz. the ACHúCARRO method and the silver method of BIELSCHOWSKY. We studied the hypophysis of the cow, which we got as fresh as possible from the abattoir. A number of specimens was investigated, and after following as well as possible the instructions given by TELLO as to the methods used bij him, every possible variation of the methods used was tried.

The preparations made with the aid of the ACHúCARRO tannine silver method showed in the first place thick membranous and fibrous formations and septa of collagenous connective tissue surrounding the groups and islands of epithelial cells on all sides, as described by BUCY. These collagenous formations were everywhere mixed with more delicate reticulated reticuline fibres, which are thickest in the neighbourhood of the blood vessels, surrounding these vessels. The reticuline fibers are of different size, very thick fibers being mixed with extremely delicate reticular fibers. The impregnation is often rather granular (fig. 1).

From these networks surrounding the groups of epithelial cells very delicate fibers arise at different places, which traverse the group of cells, running between them towards the opposite side, where they are lost again in the network mentioned above. These fibers, which are as a rule very delicate, sometimes not only run from one side of the group of epithelial cells to the other, but form a network around one or more of these cells (fig. 1 and 2). These very fine and loose networks are irregular, and are lying close to the surface of the cells they surround. As the nucleus of these cells often has an excentric position and is lying close to the surface of the cell, these fibers sometimes give the impression of running through the protoplasma of the cell they surround and of surrounding the nucleus intraprotoplasmatically. In many cases it was extremely difficult to decide for or against the intraprotoplasmic course of these delicate reticular fibers (for example in fig. 3 and 4). Especially when we study thin sections as in preparations treated after the method of BIELSCHOWSKY it is often impossible to decide this question as the connection with the dense network around the group of epithelial cells is severed. Then these networks appear as loose reticular fibers surrounding the cell and the nucleus and they suggest a close resemblance to the networks described by TELLO. Distinct pictures of the reticular structures TELLO described inside the epithelial cells we have never seen, neither in preparations made with the use of the method of ACHúCARRO nor in BIELSCHOWSKY-preparations.

So we are tempted to ask whether the pictures given by TELLO in 1912 are not of delicate reticuline networks surrounding the epithelial cells and being connected with the reticuline network of the connective tissue surrounding the groups of epithelial cells. In

many parenchymatous organs (like the liver for example) the dense interlacing network of reticuline fibers ("Gitterfasern") surrounding the sinusoids lies very close to the epithelial cells they surround. Here in the lobus anterior of the hypophysis this network is much looser but it presents the same pecularities.

The same question may be asked in the case of the so-called networks of sympathetic nerve fibers described by PINES. Here too the resemblance of the pictures given by PINES to those we got in our preparations of the reticuline structures is often rather striking. But as in our BIELSCHOWSKY-preparations no nerve fibers were impregnated, we are not able to express a distinct opinion in this matter. But for the description by PINES the investigation of the nervous supply of the anterior lobe of the hypophysis has produced but very poor results indeed.

Our investigations of the hypophysis being nearly finished, there was published a paper by Mrs. STAUDACHER–DALLE ASTE (March 1941), in which the reticulin structure of the follicules of epithelial cells of the thyroid gland was described. The authoress gives pictures of the reticular structures surrounding the epithelial follicules resembling the networks we found in the hypophysis. Moreover those drawings remind us of the pictures of the sympathetic fibers in the lobus anterior given by PINES and mentioned above. Thus our conclusion expressed above that the networks described by TELLO in the cells of the lobus anterior of the hypophysis and perhaps at least part of the structures described by PINES are in reality of reticular connective tissue nature, seems to be strengthened by the observations of Mrs. STAUDACHER in the thyroid gland.

LITERATURE CITED.

ATWELL, W. J., Amer. J. of Anat., Vol. **37** (1926).
BUCY, P. C., in Penfield, Cytology of Nerv. Syst. II (1932).
CELESTINO DA COSTA, A., C. R. Assoc. Anat., Lyon, Mars 1923.
CROLL, M. M., J. of Physiol., Vol. **66** (1928).
DANDY, W. E., Amer. J. Anat., Vol. **15** (1913).
GEMELLI, A., Boll. Soc. Med. Chir. di Pavia (1903).
GREVING, R., Zeitschr. ges. Neurol. u. Psych., **89** (1926).
PINES, J. L., Journ. f. Psych. u. Neurol., Bd. **32** (1925).
STAUDACHER, DALLE ASTE, E. V., Anat. Anz., Bd. **91** (1941).
TELLO, F., Trabaj. del Lab. de biol. de Madrid, Tomo X (1912).

F. P. BOL: ON THE STRUCTURE OF THE CONNECTIVE TISSUE OF THE ANTERIOR LOBE OF THE HYPOPHYSE CEREBRI AND THE NATURE OF THE INTRAPROTOPLASMIC NETWORKS DESCRIBED BY TELLO IN AND AROUND THE CELLS OF THE ANTERIOR LOBE.

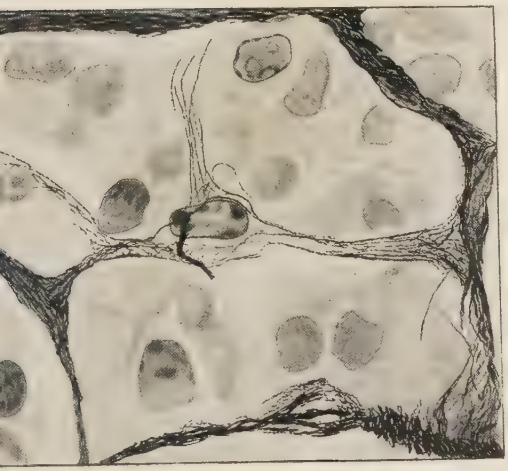

Fig. 1.

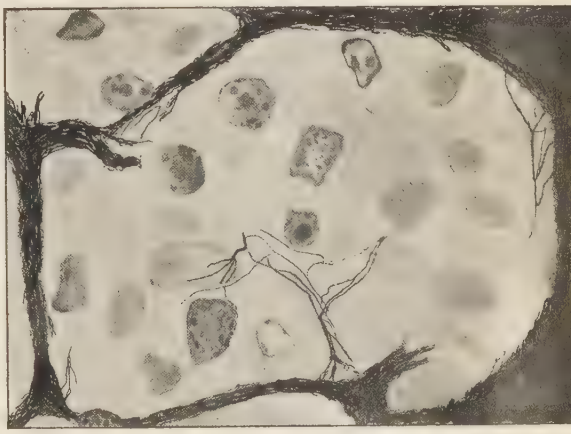

Fig. 2.

Fig. 3.

Fig. 4.

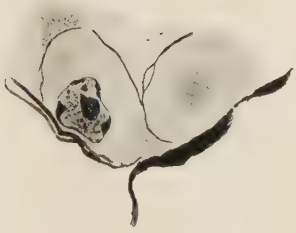

Fig. 5.

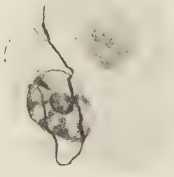

Fig. 6.

Fig. 1 and 2, sections through the midst of a follicule of epithelial cells of the lobus ant. of the hypophysis of a cow with reticular fibers traversing the follicule, method of ACHúCARRO. Fig. 3, 4, 5 and 6. Details of the reticular structures surrounding the epithelial cells, thin sections. BIELSCHOWSKY-method. Highly magnified.

Anatomy. — *Microgyria and retarded migration.* By R. BRUMMELKAMP. (Communicated by Prof. C. U. ARIËNS KAPPERS.)

(Communicated at the meeting of September 27, 1941.)

Microgyria is a congenital defect, hence its mode of genesis should be looked for during the foetal growth. It takes its name from the well-known *manifest* form in which the gyrations of the affected areas are narrow and small, their number being great and their shape and course deviating greatly from the normal. In number and shape of the gyrations true or primary microgyria is distinct from secondary or acquired microgyria (also called ulegyria) in which the gyrations are also narrow and small, but agree in number and course with the normal gyration relief. In this article we shall exclusively discuss primary or true microgyria.

By the side of the manifest form we also find a *non-apparent* form of microgyria (fig. 1). Here the gyrations visible on the exterior surface — although deviating from the normal — are not narrower, but sometimes even broader than normal. This form may be macroscopically recognized by a finally noduled surface (status verrucosus deformis, RANKE). In this form we repeatedly observe a type of gyration which has some resemblance to that of Ungulates resp. Carnivores (BIELSCHOWSKY). This non-apparent form we count among true microgyria, because the microscopic aspect of the cellcontaining cortex layers (or cellular cortex i.e. the part of the cortex below the lamina zonalis) fundamentally agrees with that of the manifest form (BIELSCHOWSKY).

In the manifest form as well as in the non-apparent form the thickness of that part of the cellular cortex which strongly participates in fissuration is less than normal. In accordance with the rule that a thin layer is more pliable than a thick one, the number of fissures of the cortex will increase when its thickness decreases and vice versa [1]). When the fissuration of the cellular cortex layer is followed by the exterior surface, the exterior aspect of the cerebrum has many small, narrow gyrations, and we have the manifest form of microgyria. When the surface layer does not follow, or only partly follows the manifold fissuration of the underlying cellular layers, we have the non-apparent form of microgyria (non-apparent microgyria), (fig. 2). Places coïnciding with inward fissuration of the cellular layers may look like a shallow pit or groove, places coïnciding with outward fissuration may occur as a slight elevation, a combination of the two processes results in a finely noduled aspect of the surface. — In ulegyria (secondary microgyria) cell groups have fallen out.

To the above we add the following. It may happen that *the cellular cortex divides into two parts* separated by a pauci-cellular zone (fig. 3a). In this zone their may be many tangential nervous (BIELSCHOWSKY) resp. glial fibres. The exterior cellular layer is then fissured most strongly, the interior one to a less extent. Altogether we can then distinguish four layers: an exterior pauci-cellular layer of tangential fibres (lam. zonalis); followed by a cellular layer with numerous fissures, again a pauci-cellular zone of tangential fibres followed against by a cellular layer, which is straighter than the upper cellular layer and in the part facing the marrow is incompletely occupied and not clearly demarcated. VAN NIEUWENHUISE and also BIELSCHOWSKY have devoted an extensive

---

[1]) This rule holds also true for the normal cortex, e.g. the motor cortex being thick and less fissured, the visual cortex thin and much fissured; also in Ungulates the cortex is thin and has many fissures whereas in Carnivores the cortex is thick and has few fissures.

study to this form of microgyria. Besides a division of the cellular part of the cortex into two layers, there also occurs a *division into three layers* (fig. 3b).

We further mention the *heterotopies,* larger or smaller islands (resp. peninsulas, when they are partly attached to the cortex) of gray substance amidst white substance. Sometimes the heterotopies are very extensive and fissurated like the cortex. At other times they occur as globules (fig. 4a), or as groups of cells only visible through the microscope. As smallest occuring heterotopies we may consider the cortex cells scattered individually in the white substance, where they do not occur normally; these cells may be abnormally enlarged (SCHOB), (fig. 4b). The localization of these heterotopies may reach as far as the ventricles.

In the molecular layer (lamina zonalis) we often find cells of CAJAL; the nerve cells under them are often small and of an embryonic character (little protoplasm, no separation between tigroid substance and cytoplasm, more than one nucleolus). It is a remarkable fact that in *every case of microgyria a large amount of neuroblasts remain in the embryonic stage.*

As we said VAN NIEUWENHUISE starts from those forms of microgyria in which the cellular cortex has divided into two superimposed cellular systems. Normally the demarcations of these systems are not so evident as in microgyria. The exterior system is supposed to coïncide with the first four layers of BRODMANN, the interior system with the fifth and sixth layer of BRODMANN. The layer of tangential fibres between the two systems is normally found between the fourth and fifth layers of BRODMANN (stripe of BAILLARGER) as in VAN NIEUWENHUISE [2]). According to VAN NIEUWENHUISE the exterior system is relatively hypertrophic, on account of which fissures are formed. The primary disturbance would be owing to a lesion of the thalamus opticus. VAN NIEUWENHUISE assumes that the exterior system (the four upper layers of BRODMANN) which according to the investigations of NISSL is independent of the thalamus, continues its growth independently, whereas the interior system, dependent on the thalamus is restricted in its growth. SCHAFFER rightly objects that duplication of the cortex is by no means found in all the parts of unmistakable microgyria, and therefore cannot serve as a general base of genesis. Moreover the condition of the stemganglia is often remarkably good (BIEMOND) and the changes in the thalamus opticus may be also explained from atrophy in this organ, secondary to the changes in the cortex. Sometimes, as was said above, division of the cellular cortex into more than two layers is found, which can hardly be explained by VAN NIEUWENHUISE's theory. Moreover, the growth of the exterior system also may be reduced in size and number of cells (see fig. 5).

Mechanical influences through pressure on the surface of the growing cerebrum were supposed o.a. by VIRCHOW, SCHÄFFER (premature cranial synostosis) and by BRESLER (pressure of the exudate in meningitis or pressure through hydrocephalus). BIEMOND also thinks that exterior pressure may act as *causa efficiens.* This author published a case of non-apparent microgyria (under the name of micro-engyria) in a microcephalic child whose cranial sutures were prematurely obliterated; the shape of the cranium was abnormal. He thinks that — at least in his case — lack

---

[2]) On account of a study on pachygyria BIELSCHOWSKY believes that this layer of tangential fibres is homologous to the fibrae arcuatae and therefore, the upper system of cellular layers homologous to the whole cortex, while the underlying cellular system should be an abnormal formation in the sense of a plane-like heterotopy. BIELSCHOWSKY gives no figures which are conclusive in this respect. ROSE points to his lamina dissecans in this respect. As BECK could show this lamina does not exist in the former stages of cortical growth. Following LORENTE DE NÒ the lamina dissecans depends on the development of a protoplasmic plexus in layer IV.

of space and deformation of the cranium are primary, deformation of the cortex he assumes to be secondary, the cortex growing inward in the direction of the white substance, on account of want of space, hence the name of micro-engyria. This theory he supported by experiments on kittens, in which the growth of the cranium was prevented by means of steel caps. From this point of view, however, the heterotopies and the division of the cellular cortex into separated layers are unconceivable; on the other hand BIEMOND's experiments may help us to understand the way in which the mechanical component realizes itself in the process of fissuration.

By the side of mechanical factors autochtonic development factors claim our attention. RANKE's investigations took this direction (abnormal persistence as to form and duration of the status verrucosus simplex described by this author); also SCHAFFER (error in peri- and tectogenesis owing to the elimination of certain cell layers, a. o. of the third layer of BRODMANN, resulting in division into two parts of the original cellular layer); BIELSCHOWSKY (abnormal location and insufficient growing power of perivascular growth centres — to which power BIELSCHOWSKY also ascribes normal fissuration — by the side of compensatory new centres; combined with insufficient cell differentiation and migration, the latter causing heterotopies). Against RANKE and SCHAFFER we remark that neither by their theories the heterotopies are explained. Against BIELSCHOWSKY that his theory on fissuration (perivascular growth centres) is not in accordance with the histological facts of the fissuring cortex.

HIS showed that the wall of the brain vesicles originally consists of 2 layers: a densely cellular layer, located on the ventricle side (matrix) and a layer containing no cells on the exterior side (lamina zonalis or "Randschleier"). After a short time a tissue of loose texture is inserted between lamina zonalis and matrix. The cortex now forms, owing to the cells detaching themselves from the matrix and migrating through the intersuscepted layer, until they reach the lamina zonalis, where they assemble and are again subjected to growth. So the formation of the cortex is determined by three processes, distinct as to space and time: the formation of the matrix, the migration and the growth of the migrated cells after they have reached the lamina zonalis.

As stated in a former communication [3]) *these ontogenetic migrations may best be considered as movements in a field of power.*

This field of power is dependent on the existence of stimuli-conducting fibres (stimulogenous centres) in the cortex [4]). In the palaeo- and archicortex these fibres are of olfactory origin and run in the zonal layer. On this system of ancient, scarcely distributed fibres in the neocortex a system of ascending thalamic fibres is superposed, to which is added a fibre system issuing from the cortex cells themselves, giving rise to long callosal

---

[3]) Equal distribution of the neo-cortical nucleus mass and equal growth intensity of the neo-cortex. (The significance of neurobiotaxis for this problem.) Proc. Ned. Akad. v. Wetensch., **44**, no. 5, 1941.

[4]) KUHLENBECK (Anat. Anz. Bd. 67, 1929) has pointed to a difference in migration intensity in amphibians, reptiles and mammals. In the palaeocortex of amphibians we find on the surface only marrowless olfactory fibres which send forth only few stimuli, so that here migration does not occur. In the archicortex of amphibians the number of fibres on the exterior surface is much greater and they are myelinated, here migration is stronger. In reptiles the fibres have developed all over the cortex and accordingly we see a more general migration. In mammals the fibre development is strongest, accordingly in mammals the migration is completest. Evidently the power of the field and with it the intensity of the migration increases with the degree of development of the fibres. As the power of this field is of neurobiotactic origin (ARIËNS KAPPERS) we may speak of a neurobiotactic field of power.

axons and short intracortical axons. So in the neocortex the field of power originates from at least three sources: Firstly from the scarcely ancient fibre system giving rise to but a weak field of power which causes only few migration and a primitive arangement of cortex cells in a lamina granularis, which has mainly receptive functions and a deeper layer of pyramids having a corticofugal and commisural function. Secondly from the system of ascending thalamic fibres. Thirdly from the fibres issuing from the cortex cells themselves (long callosal and short intracortical fibres). The second and third fibre system highly strengthen the primitive field of power giving rise to a much greater outgrowth of matrix cells in a superficial direction and thus to the formation of supragranular cell-layers, which at the meantime acquire a larger size (ARIËNS KAPPERS) [5]).

As in microgyria many neuroblasts remain on an embryonic stage of development [6]) the number of stimuli-conducting axons will be highly reduced and therefore the force of the field will be weakened. What will happen when the power of the field has weakened is, that the migration becomes less than normal, and therefore the cortex-anlage is disturbed. We will try to explain the pictures in microgyria from this point of view.

When the field has only slightly weakened the cortex-anlage will only be little disturbed. When, however, the field has considerably weakened, so that its power is not sufficient to overcome the resistance of the intersuscepted layer, there is no migration at all, but the cells remain located near the ventricle. A scale of gradation is possible between the two extremes.

In the case of moderate weakening of the field, where migration still takes place, the rapidity with which the migration occurs will decrease and it will not be possible for all the matrix cells to reach the exterior surface within the appointed time. This will cause a catastrophe to the retarded cells. While they are still on the way the intersuscepted layer (which will ultimately become the white substance) becomes denser, owing to ingrowth and myelinization of nerve fibres; the resistance is increased with the result that the retarded cells are as it were imbedded on the spot. We find them in groups, or individually in the white substance, where normally they should hardly, if at all be found. They may still increase by division, but migration in the direction of the lamina zonalis is impossible. These cells, scattered or grouped together in the white substance, are the heterotopies of fig. 4a and 4b.

Sometimes we see pictures in which the cellular cortex is divided into two parts, but in which the superior cellular layer is very thick as compared with the inferior layer (fig. 3c). In that case there is no trace of microgyria exteriorly: the breadth of the fissure is normal, its surface is smooth, and microscopic examination only reveals a light, narrow zone in the lower part of the cortex poor in cells, followed by a narrow zone rich in

---

[5]) The cell arrangement is in accordance with the general rule that in the central nervous system the receptive cells are of granular size and the effective cells of large, pyramidal size. So in cortex areas, where many sensory fibres enter the number of granular cells is much increased and inversely, in areas from which long effectory fibres arise, we find many pyramidal cells. As the prime function of the upper layers consists in the reception of a multitude of separate impulses it is conceivable that the cells of the upper layers form as many separated entities as possible and therefore are small and numerous. It may be that under the influence of the sensory fibres the neuroblasts preserve their granular size, they had in the embryonic stage of growth. On the other hand the large size of the pyramidal cells depends on the long axon which arises from them, and on the integrating function of these cells. Between the granular and pyramidal layers a layer of plexiform fibres develops.

[6]) This weakening in differentiation potency possibly depends on a deficiency in vital foodstuffs. In this respect the investigations of GAILLARD are of importance. He showed that in explantates of neuroblasts an addition of *aneurin* (vitamine B_1) is necessary for the growth of axons and for the differentiation into the adult form of the neuroblasts.

cells. These pictures may be found near areas of true microgyria and may be explained from a slight weakening of the neurobiotactic field of power in the final stage of migration owing to which the last cells cannot quite reach the cortex anlage. A preparation taken from a foetal mouse (fig. 3d) shows the course of such a thin layer of migrating cells, checked by the investigation.

In the case described by VAN NIEUWENHUISE an other type of division of the cellular cortex into two parts exists. Between the exterior and interior parts of the cellular cortex there is in that case a plexus of tangential fibres. Normally this plexus is penetrated by cells and therefore not clearly marked in Nissl' preparations. In consequence of the diminished field of power the matrix cells are attracted with less force and they migrate more slowly than normal, sothat this fibre plexus has ample time to form and to develop some degree of resistance against the cells which follow later. Their way is barred, as it were and the barrier prevents further penetration, bringing about a separation between the upper and lower layers, clearly visible in cell preparations of microgyria (fig. 3a). — The cells of the 6th (last) layer of BRODMANN are in the most unfavourable position. Their course will be increasingly impeded by the progressing condensation of the white substance. Even if they are not imbedded in the white substance as heterotopies they cannot quite catch up with the cells of the cortex anlage to which the demarcation between cortex and marrow is incompletely and not very sharp.

Sometimes the cellular cortex is divided into more than two parts as is the case in fig. 3b, taken from the occipital cortex. Possibly this type of division depends on the development of the two layers of tangential fibres, normally existing in layer IVb and V—VI.

Meanwhile the migration of the inner layers is retarded, the upper layers, which have already reached the lamina zonalis continue to grow, the result being surface extension of the upper layers.

In a former publication [7]) I have shown that the number of superimposed cells, constituting the cortex, is exclusively determined by the degree of migration and that the process of growth in the cortex itself only causes extension of the cortex in a tangential plane. But the growth in the tangential plane is checked o.a. by the lack of space within the cranial capsule and this limitation is compensated for by a deformation of the cortex surface in the sense of fissuration [8]).

Owing to slight thickness of the layers, the manifest microgyrous cortex offers but little resistance to deformation, the pressure which arises in the cellular part of the cortex during the growth compels the layers soon to form numerous narrow, short fissures: narrow on account of the slight thickness of the cortex, short because the longitudinal axis of the narrow fissure is easily flexed. As the internal structure of the affected part is greatly different from the normal structure, the fissuration type will also be greatly different resulting in a gyration relief which can hardly be compared with the normal relief. Many narrow atypical gyrations thus form the picture of manifest microgyria.

In the non-apparent form of microgyria the fissuration of the cellular layers is not followed by an equally strong fissuration of the exterior surface, but there is a discrepancy between the two. It is striking that the strongly fissuring layer although well formed is *thin* in this form of microgyria. When owing to growth, the cell layer extends in the tangential place, and forms fissures, then apparently the connection it has with the lamina zonalis (probably owing to lack of differentiation of its cells) is not sufficient to involve it in the fissuration process. Thus the lamina zonalis remains unfissured, at the same time its stretching direction is less than normal and therefore it remains thicker than in the fissured areas. To what extent the spaces between the fissures will be filled by subsequent neuroblasts depends on the degree of disturbance of the migration of the deeper layers.

---

[7]) Loc. cit. note 3.

[8]) On this object an article will appear in the next number of the Acta neerl. morph. 1941/1942, called: Sur la fissuration de l'écorce.

When the subsequent neuroblasts have little or no opportunity to depose themselves between the fissure-lamellae of the exterior cell layer, there is nothing to prevent the formation of the most irregular fissuration figures. On section we then find pictures which strongly resemble sections of papillomatous growth (fig. 6) with this difference that the growth of papillomatous epithelium is directed towards the free surface (extroversion) whereas the fissure forming cell layer of the cortex in non-apparent microgyria is directed inwards (introversion). Probably the counter pressure of the enveloping cranial capsule on the growing cortex (as in the experiments of BIEMOND), which is of course absent in papillomatous growth causes the introverse direction taken by the cortex layer; it is evident that the resistance of the cranial capsule is greater than the resistance found in the underlying layer of loose texture. So the idea of micro-engyria introduced in literature by BIEMOND, is seen to apply to some extent to this form of non-apparent microgyria.

LITERATURE.

ARIËNS KAPPERS, Vergleichende Anatomie des Nervensystems, Haarlem 1920—1921.

BECK, Morphogenie der Hirnrinde, Monographie, Ges. d. Neur. u. Pathol., 69, 1940.

BIELSCHOWSKY, J. Psych. u. Neurol., 22, 1915; 30, 1923.

BIEMOND, Annales d'Anatomie pathologique, T. 15, N°, 8, 1938; Ned. Tijdschr. v. Geneeskunde, 1940.

BRUMMELKAMP, Proc. Ned. Akad. v. Wetensch., Amsterdam, **44**, 5, 1941.

GAILLARD, Ned. Tijdschr. v. Geneesk. 1941.

HIS, Ueber die Entwicklung des menschlichen Gehirns während der ersten Monate, Leipzig, 1904.

KUHLENBECK, Anat. Anz., 67, 1929.

LORENTE DE NÒ, J. Psych. u. Neurol., 45, 1934.

VAN NIEUWENHUISE, Neurol. Bl., 1913.

RANKE, Beitr. pathol. Anatomie, 47, 1910.

ROSE, J. Psych. u. Neurol., 30, 1923.

SCHAFFER, Z. f. Neurol., 38, 1917.

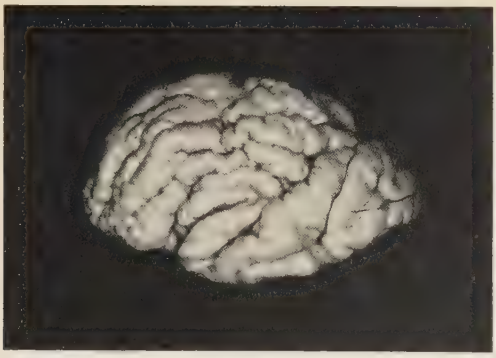

Fig. 1. Non-apparent microgyria.

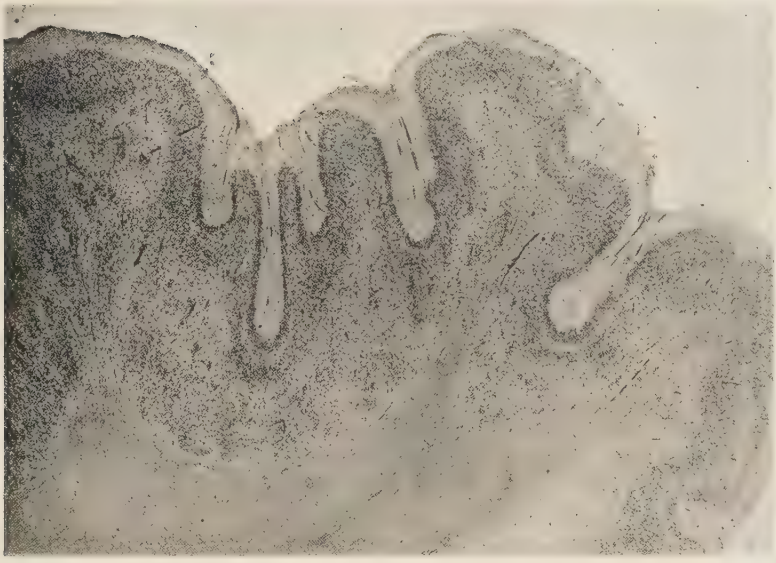

Fig. 2. Microscopic picture of non-apparent microgyria: division into two layers, the outer layer has many fissures, the inner layer only few.

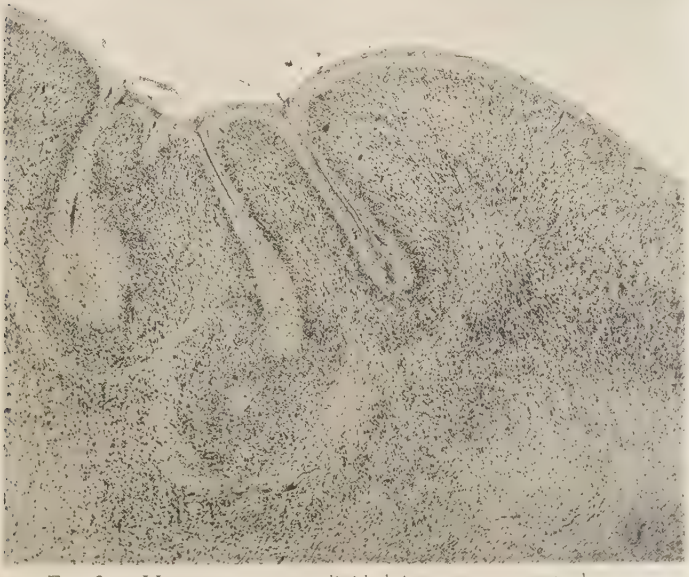

Fig. 3a. Microgyric cortex divided into two separate layers.

Fig. 3b. Microgyric cortex divided into three separate layers.

Fig. 3c. Retardation of the migration in the surroundings of microgyric cortex.

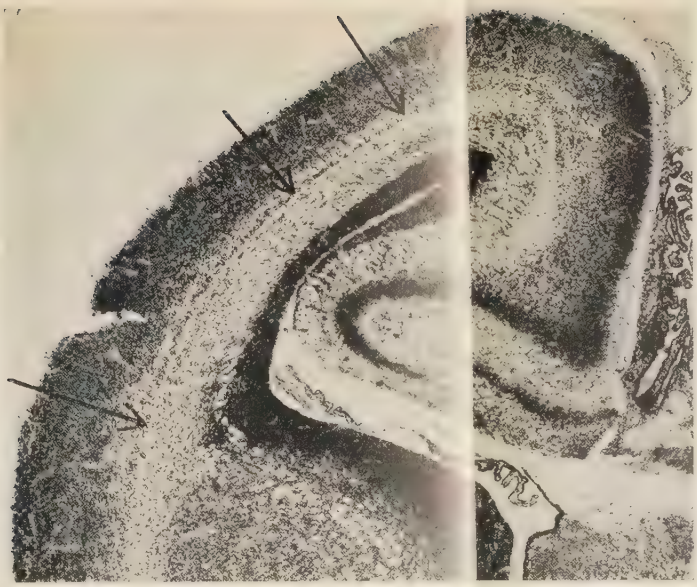

Fig. 3d. Foetal cortex of the mouse, checked in its process of migration: see the resemblance with the picture of fig. 3c.

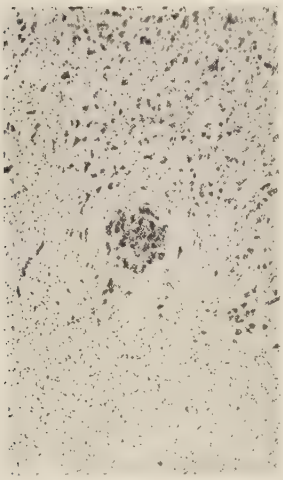

Fig. 4a. Nodule-like form of heterotopy just beneath the cortex.

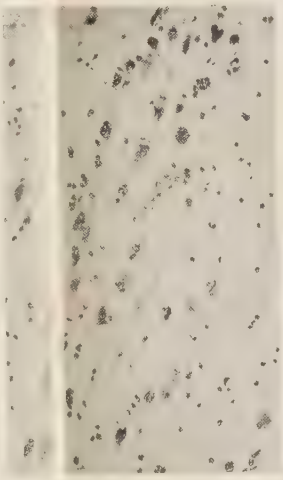

Fig. 4b. Heterotopies of single cells in the white substance.

Fig. 5. Microgyric cortex divided into two layers separated by a light zone.

Fig. 6. Papilliformous growth of the cortex, taken from SCHOB.

Comparative Physiology. — *Der Einfluss von Kohlensäure auf die Atmungsbewegungen von Crustaceen.* II. Von J. SEGAAR. (Aus der Zoologischen Station zu Neapel und dem Institut für vergleichende Physiologie der Universität zu Utrecht.) (Communicated by Prof. H. J. JORDAN.) [1])

(Communicated at the meeting of September 27, 1941.)

HOMARUS VULGARIS.

Abb. 6. Wenn wir einem Homarus bei diesem Versuch normales Seewasser geben, zählen wir einen Frequenz von ungefähr 60/Min. Wenn wir nun den Hahn des Apparates so drehen, dass das normale durch kohlensäurehaltiges Seewasser von 35.84 ccm/l ersetzt wird, dann treten auch bei Homarus die drei Phasen *a*, *b* und *c*, die wir bei Palinurus kennen lernten, auf. Für Phase *a* gilt dasselbe, was wir bei Palinurus bemerkten. Es tritt eine deutliche Frequenzsteigerung auf. Gleichzeitig zeigt sich häufig aber eine allgemeine Unruhe des Tieres, welches offenbar „etwas bemerkt hat". Zuweilen versucht es sich zu entfernen. Bei den Versuch muss daher streng darauf geachtet werden, dass das Versuchsobjekt, ausgenommen die Bewegung der Skaphognatiten, vollkommen ruhig ist.

Die zweite Phase (*b*) zeichnet sich bei Homarus nicht lediglich durch eine Frequenzverminderung, sondern sogar durch einen vollkommenen Atmungsstillstand aus. Dieser Teil der Kurve stimmt hierdurch überein mit der Hemmungsphase bei Astacus, wie GUITTART diese fand (GUITTART Abb. 2, Seite 8).

Die Hemmungsphase *b* ist bei Homarus sehr hardneckig. Nicht selten treten erst dann Atembewegungen auf, wenn wir dem Tiere normales Wasser geben, aber selbst dann tritt keine deutliche Verschnellungsphase *c* auf. Wir bringen dies in Zusammenhang mit der Tatsache, dass nach BOSWORTH und Mitarbeiter (1936) ein Teil der Kohlensäure durch den Panzer neutralisiert wird. Dadurch wird offenbar der Durchtritt der Kohlensäure in das Blut stark gehemmt. Dahingegen sehen wir in *sehr wenig* Fällen (und dann noch mit grossen Schwankungen der Resultate) die Frequenzerhöhung von Phase *c* (Siehe Abb. 6). In den Schwankungen drückt sich daher meiner Meinung nach die konkurrierende Wirkung von endoceptiv verursachter Beschleunigung und exteroceptiv verursachter Verzögerung aus.

Die Wahrnehmung von Kohlensäure bei Homarus.

Diese Wahrnehmung verläuft bei Homarus anders als bei Eriocheir (nach VAN HEERDT), und teilweise auch anders als bei Palinurus. Weder

[1]) Die erste Abteilung dieser Mitteilung ist im vorigen Heft erschienen.

die Antennulae noch die Taster der Mundteile haben Sinnesorganfunktion gegenüber Kohlensäure. Abb. 6 ist vollkommen identisch mit der Kurve eines Tieres, bei dem die Antennulae und die Taster entfernt worden waren. Dahingegen stimmt Homarus insofern mit Astacus überein, dass die Hemmungsphase durch einen homolateralen Reflex entsteht, dessen Rezeptoren sich auf den Kiemen befinden. Nur die Kiemen sind Träger dieser Sinnesorgane. Hierdurch ist es auch der Mühe wert, die Antennulae

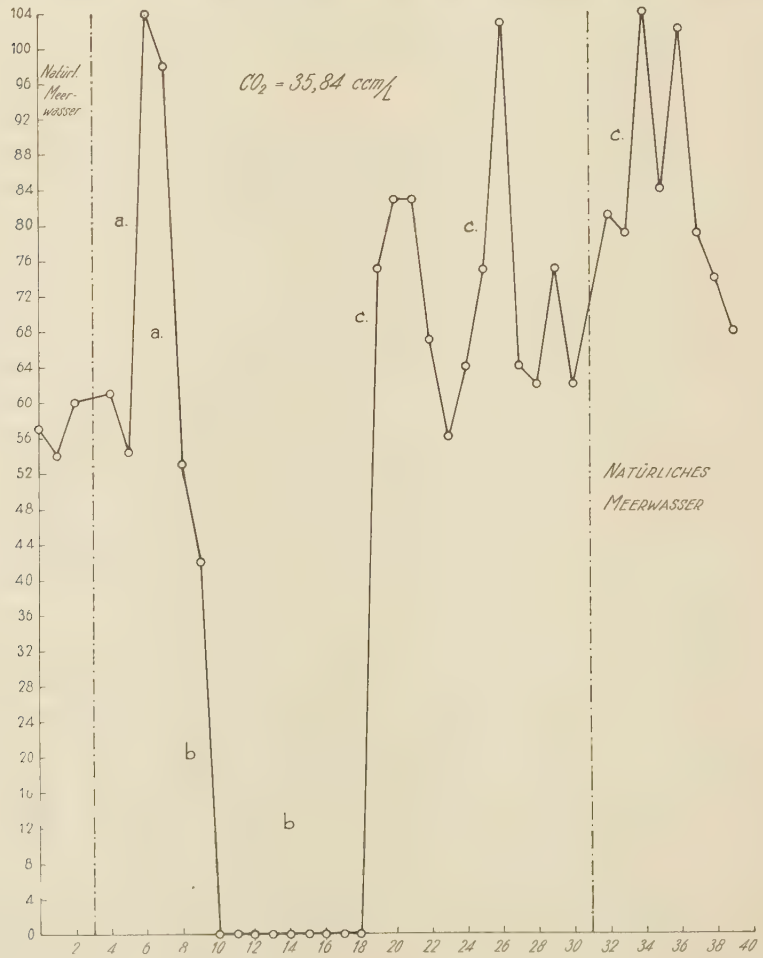

Abb. 6. Homarus.
Dreiphasige Atmungsreaktion nach Zufuhr von Wasser mit einer CO_2-Konzentration von mehr als 3 % (35,84 ccm/l). *a* = Frequenzzunahme; *b* = Apnoë; *c* = periodische Frequenzzunahme. Abszisse: Versuchszeit in Minuten, Ordinate: Minutenfrequenz der Skaphognatiten.

von Astacus und Homarus einerseits mit denen von Eriocheir und Palinurus anatomisch zu vergleichen. Während Palinurus auf zweierlei Weise

(Antennulae und Kiemen) vor schlechtem Atemwasser gewarnt wird, besitzt für diese Warnung Homarus (und Astacus?) nur ein einziges Organ, nämlich die Kiemen. Ob bei Eriocheir die Kiemen einen Sinnesfunktion haben, ist noch nicht untersucht worden.

ERIPHIA SPINIFRONS.

Abb. 7. Eine Kohlensäurekonzentration von 11.20 ccm/l hat deutliche Erniedrigung der Atmungsfrequenz zur Folge. Dies stimmt überein mit Phase *b* bei Palinurus, diese Phase dauert bei Eriphia aber länger. Die Form der Kurve ist daher anders als bei Palinurus und stimmt in dieser Hinsicht mehr mit derjenigen von Homarus überein. Nur ist die Frequenzerniedrigung nicht so stark dass ein totaler Atmungsstillstand eintritt. Bei Eriphia habe ich keine Phase *a* finden können. Wenn am Schluss wieder normales Seewasser zugefügt wird, dann wird die exteroceptiv verursachte Hemmung aufgehoben und Dyspnoë macht sich geltend.

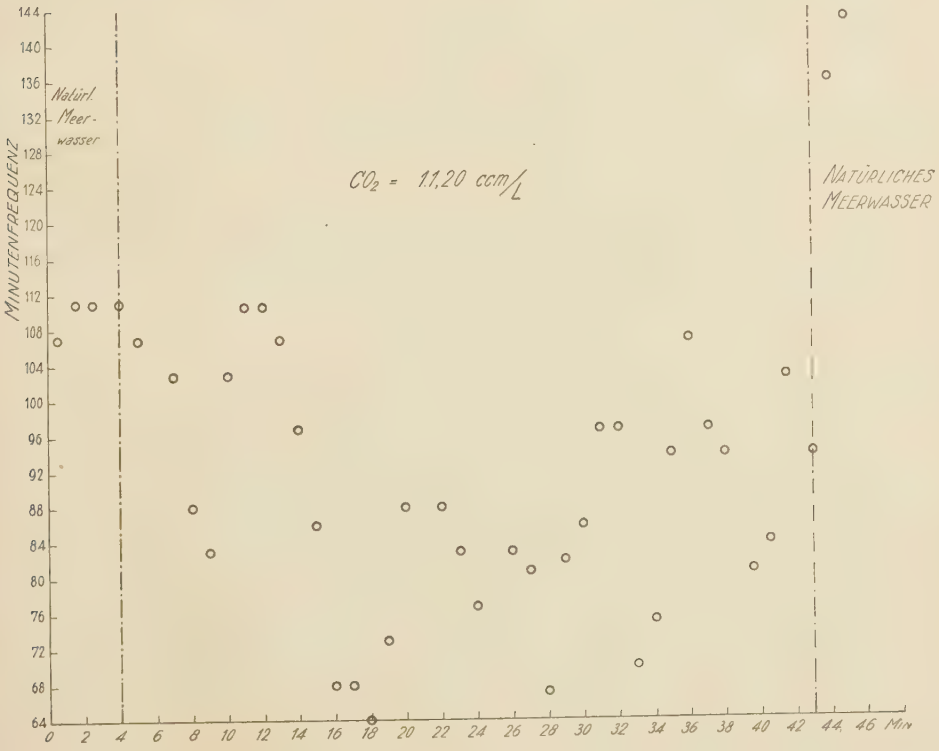

Abb. 7. Eriphia.

Änderung der Atemfrequenz nach Zufuhr von Wasser verschiedenen CO_2-Gehaltes. Abszisse: Versuchszeit in Min., Ordinate: Minutenfrequenz der Skaphognatiten. Die Frequenz nimmt in Wasser mit einer CO_2-Konzentration von ungefähr 1 % (11,20 ccm/1) ab (Phase *b*), um in natürlichem Wasser wieder steil emporzusteigen (Phase *c*). Phase *a* fehlt.

Abb. 8. Eine höhere Kohlensäurekonzentration, nämlich 36.96 ccm/l verursacht erstens eine sehr deutliche Frequenzverminderung und einen totalen Atmungsstillstand. Nach einigen Unterbrechungen dieser Hemmung kommt zweitens starke Dyspnoë.

Abb. 8. Eriphia.
Zweiphasige Atmungsreaktion nach Zufuhr von CO_2 reichem Wasser. Phase *a* fehlt. Phase *b* = Frequenzabnahme bis zum Atmungsstillstand. Phase *c* = Frequenzzunahme. Abszisse: Versuchszeit in Min., Ordinate: Minutenfrequenz der Skaphognatiten.

Bei noch höheren Kohlensäurekonzentrationen, z.B. 58.24 ccm/l (hierfür haben wir keine Abb. gegeben), tritt die Hemmungsphase nicht auf. Sie wird unmittelbar durch Dyspnoë verdrängt.

DROMIA VULGARIS.

Abb. 9. Bei einer Kohlensäurekonzentration von 26.88 ccm/l wird die Atmungsfrequenz deutlich erniedrigt. Diese Kurve erniedrigter Frequenz kann mit derjenigen verglichen werden, die wir bei Eriphia fanden. Als Unterschied zwischen beiden fällt auf, dass in manchen Fällen bei Dromia

diese Frequenzerniedrigung einer kurz dauernden Frequenzerhöhung voranging (auf der Figur ist diese Frequenzerhöhung nicht wiedergegeben).

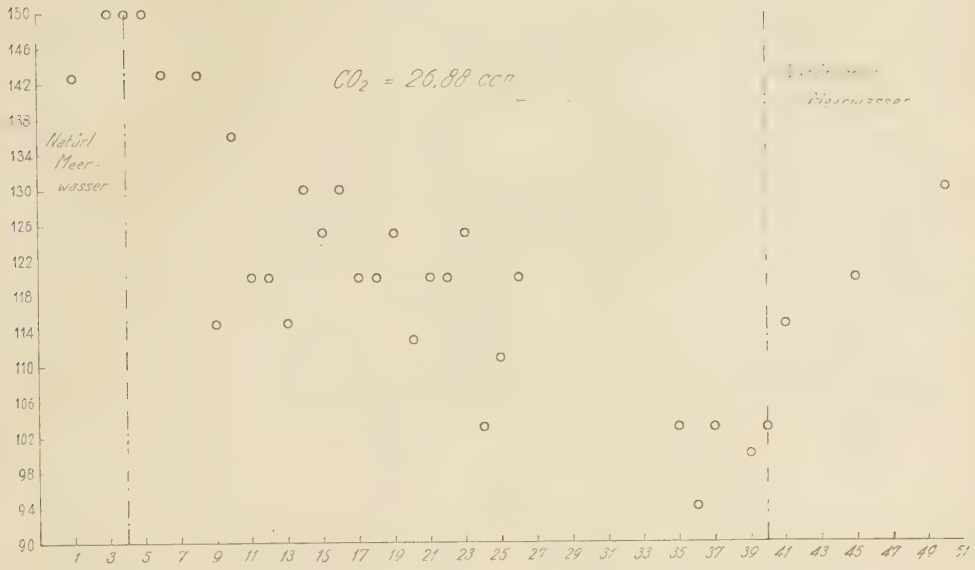

Abb. 9. Dromia.
Änderung der Atemfrequenz nach Zufuhr von Wasser verschiedenen CO_2-Gehaltes. Abszisse: Versuchszeit in Min., Ordinate: Minutenfrequenz der Skaphognatiten. Phase *a* könnte anwesend sein, tritt hier aber nicht auf. Die Frequenz nimmt in Wasser mit eine CO_2-Konzentration von 26.88 ccm/1 ab (Phase *b*).

Abb. 10. Eine Kohlensäurekonzentration von 45.92 ccm/l verursacht drei auf einander folgende Phasen. *a*) kurz dauernde Frequenzsteigerung. *b*) Frequenzerniedrigung, die sich jedoch darauf beschränkt, dass nach der genannten Frequenzerhöhung *a* wieder normaler Rhythmus auftritt. *c*) die Kohlensäure wirkt nun im Blut und verursacht Dyspnoë. Dromia stimmt also mit Eriphia darin überein, dass beide langdauernde Hemmungsphasen bei niederer Kohlensäurekonzentration haben (Abb. 7 und 9). Dromia stimmt mit Palinurus und Homarus überein, durch das Auftreten einer kurz dauernde Verschnellungsphase *a* (Abb. 6 und 10).

Zusammenfassung.

1. Palinurus vulgaris, Homarus vulgaris, Eriphia spinifrons und Dromia vulgaris haben das Vermögen sich durch Regulierung der Atmungsfrequenz an Veränderungen der Kohlensäurekonzentration im Atemwasser anzupassen. In dieser Beziehung unterscheiden sich Crustaceen, die im tiefen Wasser leben, nicht von den Arten, die in der Brandung oder im untiefen Wasser leben.

2. Bei zunehmender Kohlensäurekonzentration kann man 4 Phasen dieser Reaktion von einander unterscheiden:

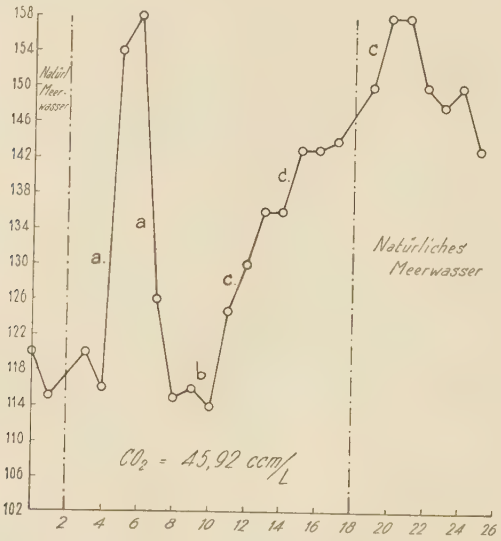

Abb. 10. Dromia.
Dreiphasige Atmungsreaktion nach Zufuhr von Wasser mit einer CO_2-Konzentration von 45,92 ccm/1. Abszisse: Versuchszeit in Min., Ordinate: Minutenfrequenz der Skaphognatiten.

a) exteroceptiv verursachte Frequenzzunahme (diese wurde bei Eriphia nicht gefunden),
b) exteroceptiv verursachte Frequenzverminderung oder totale Hemmung der Atmungsbewegungen,
c) endoceptiv verursachte Frequenzsteigerung,
d) Narkose.

3. Die Schwellenwerte, die nötig sind um die verschiedenen Reaktionsformen hervorzurufen, sind bei den verschiedenen Arten, aber auch bei verschiedenen Individuen gleicher Art, verschieden. Hierzu kommt, dass bei Homarus (wie auch bei Astacus) ein Teil der dem Wasser zugesetzten Kohlensäure durch den Panzer neutralisiert wird. Daher sind die Kohlensäurewerte, die angegeben werden, lediglich Annäherungswerte der Kohlensäurekonzentration, die bei dem betreffenden Versuche zur Anwendung kam. Bei Palinurus treten die vier Phasen auf, bei den folgenden Kohlensäurekonzentrationen:

Phase	*a*)	ungefähr bei	1 %	Kohlensäure
„	b)	„ „	2 %	„
„	*c*)	„ „	5 %	„
„	*d*)	„ „	10 %	„

4. Die Sinnesorgane, die durch die Kohlensäure gereizt werden, befinden sich bei Homarus auf den Kiemen.

5. Die eigentliche Sinnesorgane kommen bei Palinurus auf den Antennulae und den Kiemen vor. Die Sinnesorgane für geringe Konzentrationen befinden sich hier auf den Antennulae, die vorhanden sein müssen, wenn Phase *a* und *b* hervorgerufen werden soll. Höhere Konzentrationen erregen die Sinnesorgane auf dem Kiemen. Hierbei treten zwei Möglichkeiten auf:

1) Die höhere Konzentration tritt langsam auf. In diesem Fall konkurriert die Hemmung, die durch die im Aussenmedium vorhandene Kohlensäure ausgelöst wird, mit der endoceptiven Dyspnoë, ausgelöst durch den Kohlensäuregehalt des Blutes.
2) Die höhere Konzentration tritt schnell auf. Ebensoschnell ergibt sich nun Hemmung.

6. Die Erregbarkeit der Kiemen durch Kohlensäure ist spezifisch. Der Schwellenwert der Kohlensäure liegt bei einem viel höheren pH als für andere Säuren. Ob die Reizung der Antennulae von Palinurus, wie VAN HEERDT dies bei Eriocheir angegeben hat, unspezifisch ist, habe ich nicht nachuntersucht.

Am Schluss dieser Mitteilung ist es mir eine angenehme Pflicht der Niederländischen Regierung für die Zuweisung eines Stipendiums und des Niederländischen Arbeitsplatzes, Herrn Prof. Dr. R. DOHRN und Dr. G. KRAMER, sowie dem gesammten Personal der Zoologischen Station zu Neapel für die Weise, wie sie alle dazu beigetragen haben, meinen Aufenthalt in Neapel nützlich und angenehm zu gestalten, meinen herzlichsten Dank auszudrücken. Herrn Prof. JORDAN und seinen Mitarbeitern im Laboratorium voor vergelijkende Physiologie zu Utrecht danke ich für ihre grosse Anteilnahme an meiner Arbeit und für ihre Hilfe.

LITERATUR.

BALSS, H.: Tierwelt der Nord- und Ostsee VI von G. Grimpe und E. Wagler.
FOX, H. M. and M. L. JOHNSON: J. of exper. Biol. **11**, 1 (1934).
DAMBOVICEANU, Mlle ARISTIE: Arch. Roum. de path. exp. et de microbiol. Extrait 2 (1932).
JOHNSON, M. L.: J. of exper. Biol. **13**, 4 (1936).
VAN HEERDT, P. F. und B. J. KRIJGSMAN: Z. vergl. Physiol. **27**, 29 (1939).
JORDAN, H. J. and J. GUITTART: Proc. Ned. Akad. v. Wetensch., Amsterdam, **41**, 1 (1938).
KRUMBACH: Handbuch der Zoöl. von Kükenthal, 931 (1927).
PETERS, F.: Z. vergl. Physiol. **25**, 591 (1938).
SEGAAR, J.: Z. vergl. Psysiol. **21**, 492 (1934).
VERWEY, J.: Treubia **12**, 169 (1930).

Medicine. — *Biophysique. Spectres d'absorption de l'extrait et des protéines du poumon normal et du poumon intoxiqué par le phosgène dans l'ultra-violet.* (Troisième mémoire.) Par ONG SIAN GWAN. (Communicated by Prof. W. H. KEESOM.)

(Communicated at the meeting of September 27, 1941.)

1. Nous avons montré qu'on pouvait vacciner des cobayes et des souris contre une dose sûrement mortelle de phosgène en les soumettant préalablement à des doses inframortelles de phosgène [1]). Pour expliquer ce résultat obtenu, nous avons pensé que le phosgène agirait sur les protéines du poumon. Il en résulterait une combinaison chimique nouvelle; cette protéine modifiée agirait comme antigène et il vaccinerait l'animal contre l'action mortelle du phosgène.

Dans le deuxième mémoire nous avons mis en évidence la présence de cette protéine nouvelle dans le poumon intoxiqué par le phosgène [2]). En effet, il existe une différence nette entre la solubilité, l'indice de réfraction et le pouvoir rotatoire des protéines du poumon normal et du poumon intoxiqué par le phosgène. Ces résultats montrent qu'il s'agirait d'une modification chimique de la structure moléculaire des protéines du poumon après l'action du phosgène. Nous avons poursuivi l'étude de ces protéines nouvelles à l'aide de la spectrophotométrie dans l'ultra-violet, afin de savoir comment cette modification de la structure moléculaire se traduiront dans le spectre d'absorption.

2. *Technique expérimentale.* Dans ce travail on a employé un spectrographe à optique de quartz construit par HILGER. La cuve en quartz utliisée avait une épaisseur fixe de 5 mm. La source de lumière était une lampe à arc de mercure (3 ampères, 110 volts), qui donnait une lumière rigoureusement constante. Les plaques photographiques utilisées étaient les suivantes: Radio GEVAERT, Graphic process extra GEVAERT 25 H. et D. et Autofilter ILFORD 400 H. et D. Dans certains cas les plaques ont été sensibilisées à l'aide d'une couche de vaseline. Pendant le développement les plaques furent brossées pour éviter la contamination des parties non exposées par les parties exposées.

Dans toutes ces expériences on a utilisé le poumon de porc. Le même poumon fut divise en deux parties, la première était destinée à l'intoxication phosgénique et la deuxième servait de témoin. La préparation de l'extrait de poumon et l'isolément des protéines pures à partir de cet extrait ont été décrits dans le deuxième mémoire [2]).

3. *Spectres d'absorption de l'extrait de poumon normal et de poumon intoxiqué par le phosgène.* Déjà à l'aide d'un simple spectroscope à vision directe on peut distinguer l'extrait de poumon normal de celui de poumon intoxiqué. En effet, on constatait dans le premier les deux bandes d'absorption caractéristiques de l'oxyhémoglobine ($\lambda_1 = 5890$—5770 et $\lambda_2 = 5500$—5360 Å), tandis qu'elles manquaient dans le second. La disparition de ces bandes d'absorption d'oxyhémoglobine a été constaté pendant la guerre de 1915—1918 dans le sang des hommes gazés.

La spectrophotographie nous montre, toutes conditions égales, que l'extrait de poumon normal présente une absorption plus prononcée que celui de poumon intoxiqué (fig. 1). La différence d'absorption se manifeste dans le visible et surtout dans l'ultra-violet.

4. Dans d'autres cas, quand l'extrait de poumon intoxiqué était plus opalescent que celui de poumon normal on observait le contraire: le poumon intoxiqué montrait dans l'ultra-violet une absorption plus marquée que le poumon normal. L'absorption était également augmentée vers les grandes longueurs d'onde (fig. 2). Dans ce cas on constatait que l'extrait de poumon intoxiqué donnait une lumière diffuseé à angle droit (phénomène de TYNDALL) plus intense que l'extrait de poumon normal. La couleur observée était bleu clair.

[1]) ONG SIAN GWAN, Proc. Ned. Akad. v. Wetensch., Amsterdam, **44**, 205 (1941).
[2]) ONG SIAN GWAN, Ibid., **44**, 871 (1941).

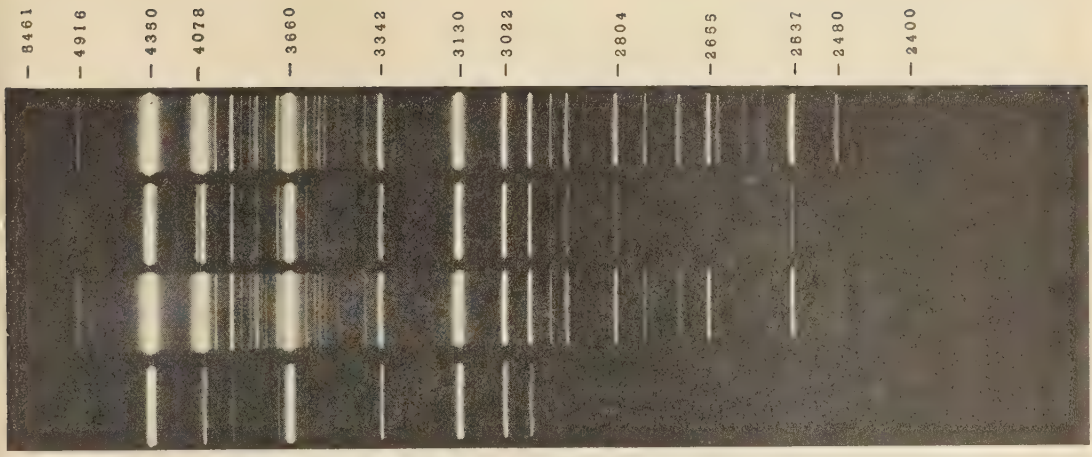

Fig. 1. Extrait de poumon 51.

1. Poumon intoxiqué par le phosgène $c =$ 88 mg de protéines p. 100 cc Temps de pose $t = 15$ sec.
2. Poumon normal $c =$ 88 mg de protéines p. 100 cc $t = 15$ sec.
3. Poumon intoxiqué $c = 157$ mg/100 cc $t = 20$ sec.
4. Poumon normal $c = 176$ mg/100 cc $t = 20$ sec.

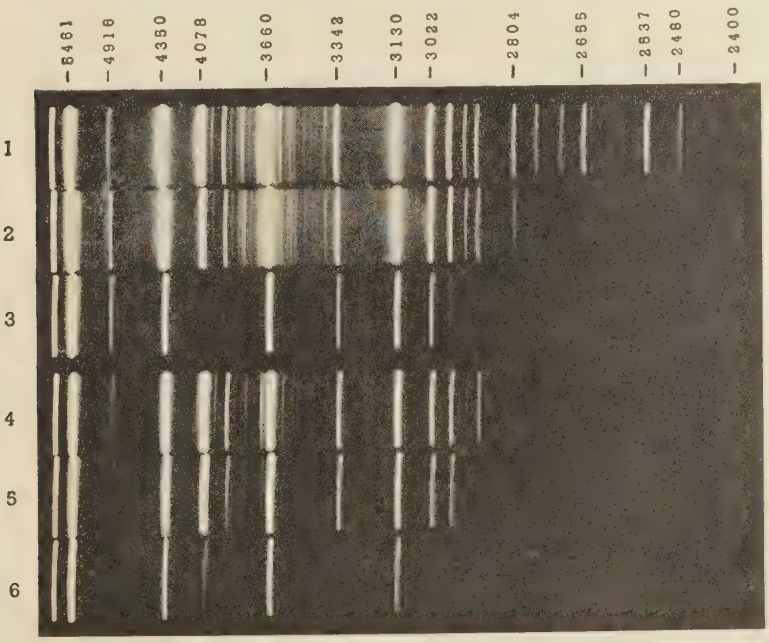

Fig. 2. Extrait de poumon 124.

1. Poumon normal $c = 132$ mg/100 cc $t = 45$ sec.
2. Poumon normal $c = 265$ mg/100 cc $t = 90$ sec.
3. Poumon normal $c = 794$ mg/100 cc $t = 270$ sec.
4. Poumon intoxiqué $c = 132$ mg/100 cc $t = 45$ sec.
5. Poumon intoxiqué $c = 265$ mg/100 cc $t = 90$ sec.
6. Poumon intoxiqué $c = 794$ mg/100 cc $t = 270$ sec.

D'après la loi bien connue de Lord RAYLEIGH [3]) l'intensité de la lumière diffusée est égale à

$$I = K \frac{I_0 N v^2}{\lambda^4 x^2} \left(\frac{n_1^2 - n_0^2}{n_1^2 + 2 n_0^2} \right)^2 \sin^2 \theta \quad . \quad . \quad . \quad . \quad . \quad (1)$$

où I, l'intensité de la lumière diffusée à une distance x du particule, I_0, l'intensité de la lumière incidente, N, le nombre de particules par unité de volume, v^2, le carré moyen du volume des particules, λ, la longueur d'onde, n_1, l'indice de réfraction des particules, n_0, l'indice de réfraction du solvant et θ l'angle de la direction de la lumière incidente avec la lumière diffuseé. Cette loi suppose que les dimensions des particules sont petites par rapport à la longueur d'onde.

Si la concentration $c = Nvd$ (d = densité) est constante, on voit que l'intensité de la lumière diffusée augmente en même temps avec le volume des particules. C'est ce que nous avons constaté dans le cas considéré.

Considérons la loi de LAMBERT–BEER

$$I = I_0 e^{-kcd}. \quad . \quad . \quad . \quad . \quad . \quad . \quad . \quad . \quad . \quad . \quad (2)$$

où I_0 représente l'intensité de la lumière initiale et I, l'intensité de la lumière après avoir traversé l'épaisseur d.

RAYLEIGH a montré que le coefficient d'absorption (densité optique) k est défini par la relation

$$k = K \frac{N v^2}{\lambda^4} \left(\frac{n_1^2 - n_0^2}{n_1^2 + 2 n_0^2} \right)^2 \quad . \quad . \quad . \quad . \quad . \quad . \quad . \quad (3)$$

où K désigne une constante.

Pour des solutions d'une même concentration $c = Nvd$, la relation devient

$$k = K_1 \frac{v}{\lambda^4} \left(\frac{n_1^2 - n_0^2}{n_1^2 + 2 n_0^2} \right)^2. \quad . \quad . \quad . \quad . \quad . \quad . \quad . \quad (4)$$

Si pour des solutions d'une même concentration les particules grossissent par accollement entre elles, de sorte que le volume v' d'une nouvelle particule est égal à la somme des volumes des particules composantes, l'indice de réfraction de la particule ne change pas. Le coefficient k est dans les deux cas proportionnel au volume des particules.

Si k' désigne le coefficient d'absorption après l'augmentation du volume des particules, on voit que pour toutes les radiations le rapport $\frac{k'}{k}$ est contante et il est proportionnel à $\frac{v'}{v}$. Mais la différence absolue $| k' - k |$ est proportionnelle à $\frac{v' - v}{\lambda^4}$ de sorte qu'elle est beaucoup plus grande dans le violet que dans le rouge. Ainsi s'explique l'augmentation de l'absorption vers le visible quand le volume des particules augmente. Le coefficient $1/\lambda^4$ est 16 fois plus grand pour $\lambda = 0\ \mu$, 20 que pour $\lambda = 0\ \mu$, 40.

5. L'expérience suivante montre l'exactitude de ce raisonnement. On sait qu'en sérologie on peut obtenir des émulsions de lipoïdes d'une opacité différente suivant le mode de préparation. Ainsi en projetant 0,5 cc d'un extrait alcoolique de coeur de veau (antigène syphilitique préparé d'après BORDET–RUELENS) dans un vase cylindrique contenant 20 cc d'eau salée à 0,9 p. 100, on obtient une émulsion limpide. Si l'on ajoute d'abord 0,5 cc d'extrait dans le vase et on verse ensuite d'un seul coup 20 cc d'eau salée à 0,9 p. 100, on obtient une émulsion à peine opalescente. Si dans la dernière opération on ajoute l'eau salée par petites fractions, on obtient une émulsion opaque. En modifiant le temps de dilution on peut avoir des émulsions de lipoides d'une opacité différente.

[3]) Lord RAYLEIGH (J. W. STRUTT), Phil. Mag. **41**, p. 107, 274, 447 (1871); **47**, p. 375 (1899).

La figure 3 montre les spectres d'absorption des émulsions de lipoïdes ainsi préparées. On constate, que des émulsions contenant la même quantité de lipoïdes, mais d'une opacité différente ne donnent pas des spectres d'absorption identiques. A mesure que le volume des particules augmente, l'absorption est augmentée vers le visible pour le même temps de pose. Cet effet peut être également obtenu, si pour une même émulsion on diminue le temps de pose. On peut le constater en comparant par exemple les spectres 1, 4 et 7 dans la figure 3.

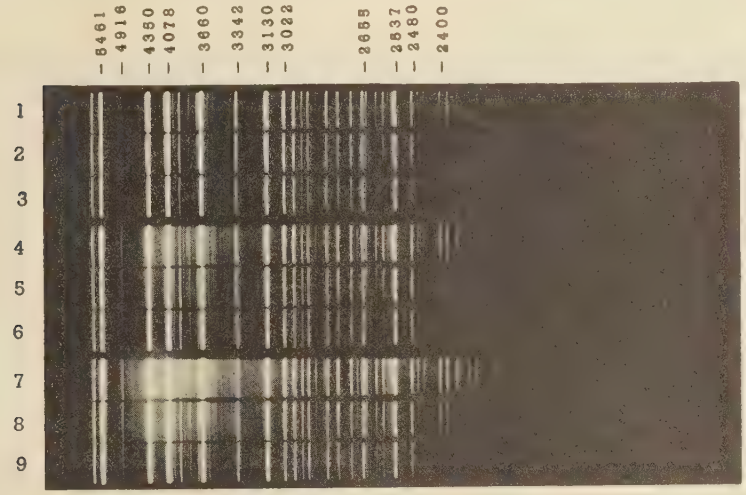

Fig. 3. Emulsion de lipoïdes dans l'eau salée à 0,9 p. 100.
1, 2, 3 c = 16,5 mg de lipoïdes p. 100 cc t = 20 sec.
L'opacité et par conséquent la dimension des particules augmente dans l'ordre indiqué.
4, 5, 6 mêmes émulsions t = 40 sec.
7, 8, 9 mêmes émulsions t = 80 sec.

Il est probable qu'on peut obtenir le même phénomène avec des solutions de protéines, dont les particules ont des dimensions différentes.

6. *Spectres d'absorption des protéines pures isolées à partir des poumons normal et intoxiqué.* Aves les protéines pures les résultats sont très nets. Le spectre d'absorption des protéines de poumon normal montre toujours une absorption plus prononcée et elle augmente vers le visible. Ce résultat a été obtenu sur plusieurs poumons. La figure 4 montre un exemple type d'un même poumon, dont une partie fut intoxiqué et l'autre partie servait de témoin. En comparant les spectres 3 et 4 avec les spectres 7 et 8 on constate une différence nette dans l'ultra-violet au dessous de 3000 Å, mais on peut également remarquer une différence d'absorption entre les raies 4078 et 3660 Å.

7. Nous présentons ici également les courbes de spectres d'absorption obtenues par enregistrement photométrique. L'appareil employé était un microphotomètre enregistreur MOLL construit par KIPP & ZONEN à Delft.

Les figures 5 et 6 montrent respectivement les courbes des spectres d'absorption de l'extrait de poumons normal et intoxiqué. (Spectres No. 4 et 3 de la figure 1.)

En comparant les deux figures on constate que la différence d'absorption est déjà très nette dans le visible. En effet l'extrait du poumon normal (fig. 5) contenant environ la même quantité de protéines montre un pouvoir absorbant plus important que celui du poumon intoxiqué (fig. 6). Cette différence d'absorption est encore plus accentuée dans l'ultra-violet. Tandis que le poumon normal montre des maxima d'absorption au dessus de 80 unités arbitraires, le poumon intoxiqué par contre ne présente que des maxima au dessous de 60 unités. Ceci est vrai pour les raies au dessus de 3000 Å. A partir de

3000 Å et au dessous de celui-ci on constate dans la courbe du poumon normal, la disparition de la plupart des raies spectrales.

Les figures 7 et 8 représentent respectivement les courbes des spectres d'absorption des protéines pures isolées à partir des poumons normal et intoxiqué (spectres No. 4 et 8 de la figure 4). On peut ici également remarquer la différence d'absorption entre les raies

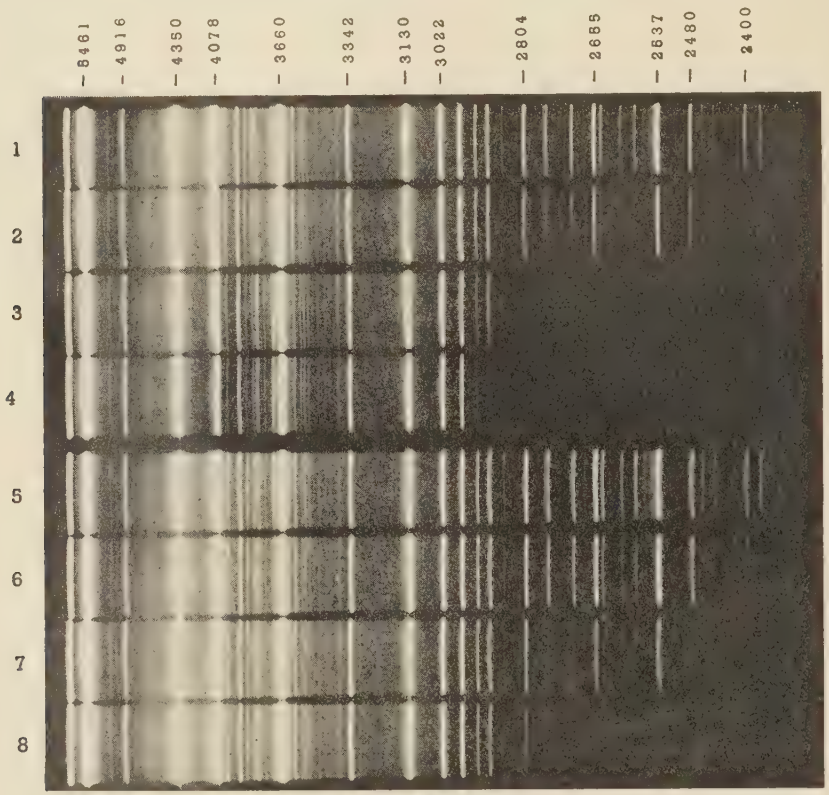

Fig. 4. Protéines pures isolées à partir du poumon 125.

1. Poumon normal $c = 106$ mg/100 cc $t = 100$ sec.
2. Poumon normal $c = 211$ mg/100 cc $t = 150$ sec.
3. Poumon normal $c = 422$ mg/100 cc $t = 200$ sec.
4. Poumon normal $c = 422$ mg/100 cc $t = 250$ sec. Epaisseur de la cuvette = 8 mm.
5. Poumon intoxiqué $c = 106$ mg/100 cc $t = 100$ sec.
6. Poumon intoxiqué $c = 211$ mg/100 cc $t = 150$ sec.
7. Poumon intoxiqué $c = 422$ mg/100 cc $t = 200$ sec.
8. Poumon intoxiqué $c = 422$ mg/100 cc $t = 250$ sec. Epaisseur de la cuvette = 8 mm

4078 et 3660 Å, mais elle est surtout très nette au dessous de 3000 Å, où on constate la disparition de plusieurs raies spectrales dans la courbe du poumon normal.

Ces résultats montrent une différence quantitative dans les spectres d'absorption des poumons normal et intoxiqué. On peut en conclure qu'il s'agirait d'une modification chimique superficielle de la structure moléculaire des protéines après l'action du phosgène. Cette conclusion confirme les résultats du travail précédent où l'on a constaté une diffé-

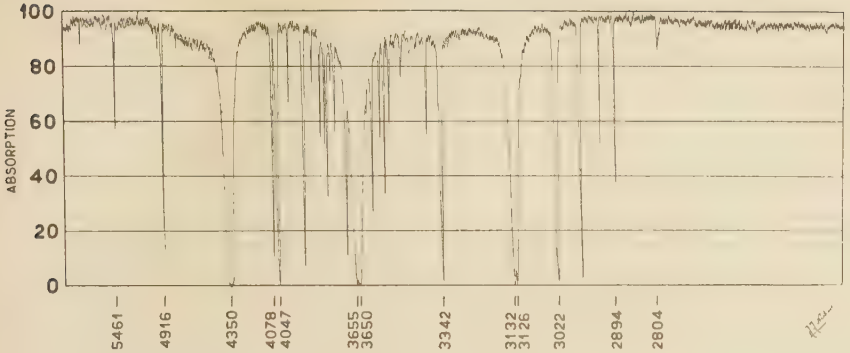

Fig. 5. Courbe d'absorption de l'extrait de poumon normal 51.
Courbe du spectre d'absorption No. 4 de la figure 1. $c = 176$ mg/100 cc. Les courbes dans les figures 5, 6, 7 et 8 ont été retouchées aux endroits où les traits ne sont pas assez nets. Mais rien n'est changé en ce qui concerne la valeur d'absorption de la lumière.

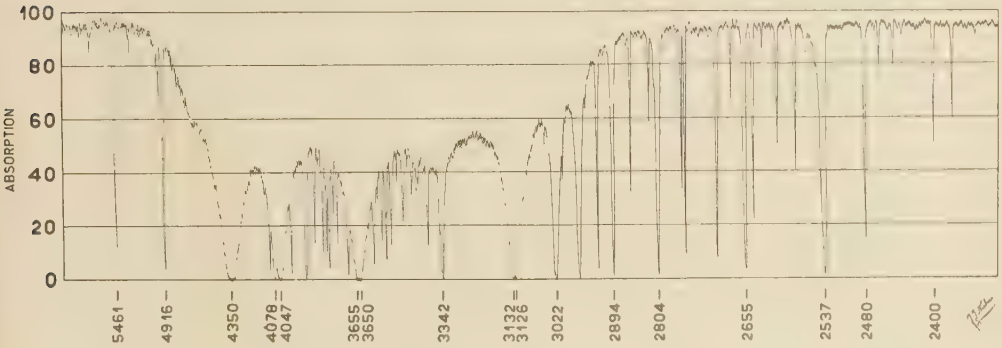

Fig. 6. Courbe d'absorption de l'extrait de poumon intoxiqué 51.
Courbe du spectre d'absorption No. 3 de la figure 1. $c = 157$ mg/100 cc.

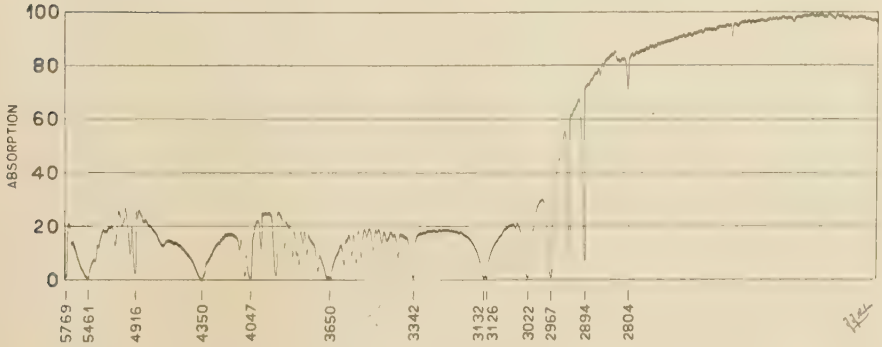

Fig. 7. Courbe d'absorption des protéines pures isolées à partir du poumon normal 125.
Courbe du spectre d'absorption No. 4 de la figure 4. $c = 422$ mg/100 cc.

rence de solubilité, d'indice de réfraction et de pouvoir rotatoire entre les protéines de poumons normal et intoxiqué.

Ce travail a été poursuivi à l'annexe du laboratoire KAMERLINGH ONNES à Leyde. Je remercie M. le Professeur W. H. KEESOM pour les suggestions qu'il a bien voulu me

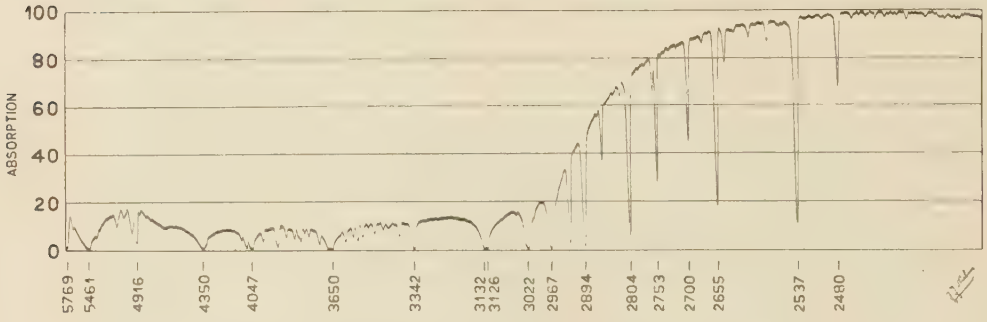

Fig. 8. Courbe d'absorption des protéines pures isolées à partir du poumon intoxiqué 125. Courbe du spectre d'absorption No. 8 de la figure 4. $c = 422$ mg/100 cc.

faire et à M. le Professeur W. J. DE HAAS, qui m'a permis de poursuivre ces recherches. Je remercie M. C. A. CROMMELIN et M. le Professeur H. B. G. CASIMIR de l'intérêt qu'ils ont bien voulu porter à ce travail. Je dois également remercier le conseil de l'organisation „Toegepast-natuurwetenschappelijk Onderzoek", qui m'a facilité de poursuivre mes recherches.

RÉSUMÉ.

1. Les spectres d'absorption de l'extrait de poumons normal et intoxiqué par le phosgène montrent une différence nette dans le visible et surtout dans l'ultra-violet. L'extrait de poumon normal donne une absorption plus prononcée que celui de poumon intoxiqué.
2. On constate le contraire, quand l'extrait de poumon intoxiqué, contenant la même quantité de protéines, est plus opalescent c'est-à-dire que les particules sont plus grosses que celles du poumon normal. Ceci pourrait être expliqué par la loi de Lord RAYLEIGH.
3. Il est dèmontré expérimentalement et conforme à la loi de RAYLEIGH, que des émulsions de lipoïdes d'une même concentration, donnent une absorption plus prononcée et augmentant vers le visible à mesure que le volume des particules augmente.
4. En comparant les spectres d'absorption des protéines pures isolées à partir de poumons normal et intoxiqué, on constate que le poumon normal donne une absorption plus prononcée entre les raies 4078 et 3660 Å. Au dessous de 3000 Å la différence est encore plus grande.
5. Les courbes d'absorption, obtenues par enregistrement photométrique montrent également une différence d'absorption entre l'extrait ou les protéines des poumons normal et intoxiqué.
6. La différence d'absorption étant quantitative, elle indiquerait une modification chimique superficielle de la structure moléculaire des protéines de poumon après l'intoxication par le phosgène.

Medicine. — *Investigations about stimulation and paralysis of the labyrinth by methylamine.* By P. G. GERLINGS. (Communicated by Prof. A. DE KLEYN.)

(Communicated at the meeting of September 27, 1941.)

At the onset of inflammatory affections of the labyrinth some symptoms can be noted which must be interpreted as labyrinth stimulus phenomena. WITTMAACK [1]) tried to elicit these symptoms experimentally and found in methylamine a substance which, when brought into the middle ear and resorbed through the round window, first caused for some time a distinct nystagmus to the injected side, after which this nystagmus disappeared and was followed by a typical nystagmus to the other side, if the concentration of the methylamine-solution was strong enough. WITTMAACK remarked that he had been looking for such a substance for several years; we must point to the fact, however, that in literature some publications can be found about experimental labyrinth stimulus phenomena by chemical substances.

1. BREUER's [2]) *interpretation of the experiments of* KÖNIG [3]).

C. J. KÖNIG made a series of experiments bringing cocaine into the canals after opening of the bony semicircular canals, while the membranous canals were intact; by this the extremities of the sensory organs in the ampuls were made insensible. It appeared that after cocainisation of two corresponding semicircular canals the same disturbances developed as seen after cutting of the canals: head-movements ("Pendeln") in the plane of the semicircular canals: "Kreis- und Reitbahngang" etc. KÖNIG held that cocaine not had a stimulating but a paralyzing influence. Therefore he thought the symptoms seen by him were caused by a loss of function of the ampuls. BREUER also found that there is hardly any difference between a pigeon with cocainisized horizontal canals and one whose canals are cut. So the experiments of KÖNIG seemed to supply a new confirmation of the idea that the FLOURENS' symptoms are due to a loss of function of the labyrinth. KÖNIG, however, did not investigate whether the extremities of the nerves were really paralyzed. BREUER therefore repeated these experiments and came to the following conclusion:

"Es erfolgt zuerst *Erregung* der Ampulle durch die Wasserentziehung; dann tritt allmählich die Anästhesie ein. Die erste Kopfbewegung wird von der Ampulle der operierten Seite aus hervorgerufen, die zweite, durch die Anästhesie dieser Ampulle bedingt, von der intakten Ampulle der anderen Seite."

2. *The experiments of* VAN ROSSEM [4]) *with ether.*

It appeared that injection of ether in the middle ear of caviae caused the same movements of eyes, trunk and head as injection of cocaine, except that immediately after the injection eye-movements to the opposite direction developed for some minutes. VAN ROSSEM stresses the fact that his experiments are insufficient for conclusive evidence.

3. *Experiments with hypertonic salt solution* (DE KLEYN [5])).

If, after opening of the bulla, a hypertonic salt solution (1,5 per cent NaCl) is injected

---

[1]) WITTMAACK, Acta Otolaryng., **25**, 109 (1937).

[2]) BREUER, Studien über den Vestibular-Apparat, Wien 1903, page 39.

[3]) KÖNIG, C. J., Contribution à l'étude expérimentale des canaux sémicirculaires, Thèse, Paris 1897.

[4]) VAN ROSSEM, Gewaarwordingen en reflexen, opgewekt vanuit de half-cirkelvormige kanalen. Thesis, 1907.

[5]) DE KLEYN, A., Arch. f. d. ges. Physiol., **145**, 549 (1912).

into the vestibulum through the foramen rotundum, the head is immediately strongly turned to the side which has not been operated upon. If now some 0,1 cc. 20 per cent cocaine are injected into the vestibulum, contrary movements develop to the operated side, caused by paralysis of the labyrinth.

4. *Cocaine experiments of* MAGNUS *and* DE KLEYN [6]) *in caviae.*

Sometimes it can be noticed that the paralysis caused by cocaine is preceded by a stimulation lasting only for some minutes. In these cases an eye-deviation or "Grunddrehung" to the other side develops.

So the above-mentioned investigations of BREUER, VAN ROSSEM, MAGNUS and DE KLEYN prove that labyrinth stimulus phenomena by chemical substances were already known before the experiments with methylamine.

Methylamine is a volatile substance, smelling like ammonia, which is on the market in a 33 per cent solution. The dilutions vary from 1 : 9 to 1 : 14 in aqua dest. A needle was inserted into the tympanum and by means of a Pravaz syringe attached to it, methylamine was injected into the middle ear and the auditory canal. After about 15—20 minutes a typical nystagmus to the treated side develops, lasting for about half an hour, sometimes longer, sometimes shorter. This nystagmus disappears after which, if the concentration is strong enough, a nystagmus to the opposite side occurs. The following day a turning of the head is sometimes found. When weaker concentrations are used the nystagmus does not change, so that "der Nystagmus zur behandelten Seite die einzige, relativ schnell vorübergehende Reaktion vonseiten des Vestibularapparates bleibt".

The histological symptoms (i.e. the tonus syndrome of WITTMAACK) consisted of a paradoxhypotonic reaction of the cupulae, the otolithic membranes of the maculae and of the organ of *Corti*.

MAGNUS and DE KLEYN not only found that in caviae after injection of cocaine in the middle ear a paralysis of the labyrinth can be preceded by a stimulation, but also that the separate labyrinthine reflexes do not disappear simultaneously but always in a definite succession.

After unilateral loss of function of the labyrinth in rabbits and caviae the following symptoms are noted:

1. Inclining of the head to the side of the failing labyrinth;
2. "Grunddrehung"; turning of the head to the side of the failing labyrinth.
3. Turning of the trunk;
4. Loss of tonus of the extremities at the same side (in dorsal position).
5. Compensatory eye-positions: both eyes are looking to the side of the failing labyrinth. At the normal side the eye is directed vertically upward and somewhat dorsal, the other eye vertically downward and somewhat forward.
6. Horizontal nystagmus, quick component to the side of the normal labyrinth.
7. Labyrinthine righting reflexes a-symmetric loss of function of the right labyrinth; in right lateral position: head in lateral or dorsal position; in left lateral position: head in normal position.

The disappearing of the labyrinthine reflexes after injection of cocaine in the middle ear in caviae was explained as follows:

a. Paralysis of the sacculus causes, while the other labyrinth was intact, an *unilateral abolishment of the "a-symmetric" labyrinthine righting reflexes* and *vertical deviation of the eye* without nystagmus. The "symmetric" righting reflexes remained intact and therefore it was thought that they were probably dependent on the utriculi.

b. Paralysis of the utriculus, while the other labyrinth was intact, caused a "Grunddrehung" turning to the injected side.

c. As soon as the paralysis of the semicircular canals developed, *a turning of the head*

---

[6]) MAGNUS–DE KLEYN, A contribution concerning the function of the vestibular apparatus. Proc. Kon. Akad. v. Wetensch., Amsterdam, **27**, 201 (1923).

and *a spontaneous nystagmus of head and eyes* were seen; at the same time the turning reactions (turning to the right and to the left) became a-symmetric.

MAGNUS and DE KLEYN gave it as their opinion that the cocaine first reached the macula sacculi by the round window, then the macula utriculi, after which the ampullae were anaesthesized. Later investigations of VERSTEEGH [7]) made it improbable that the maculae sacculi had a static function, so that WERNER [8]) gave the following explanation: The cocaine propagates from the cysterna perilymphatica, reaches the nerve-roots of the rampa lateralis in the connective tissue around the macula utriculi and causes a loss of those labyrinthine functions which MAGNUS and DE KLEYN thought were due to the macula sacculi. After that the nerve roots of the rampa anterior of the utriculus were reached, eliciting a loss of those reflexes of which it was thought previously that they were caused by the whole utriculus (see experiments of QUIX and EGMOND [9]) with iron- and cocaine salts).

It now appears that after injection of methylamine in the middle ear of rabbits a similar "Gesetzmäszigkeit" exists, both in stimulation and paralysis of the labyrinth.

Here follows the protocol of a typical experiment.

Red-brown rabbit; on examination normal labyrinthine reflexes. No spontaneous nystagmus, no head nystagmus. The turning nystagmus can be well elicited to both sides. Marked lift reaction, "Sprungbereitschaft" somewhat less. The tilting reactions around the longitudinal and bitemporal axis are present, just as the compensatory (vertical) eye-positions and the labyrinthine righting reflexes on the head in the right and left lateral position, head upright and head downward.

9.38 a.m. Some cc. of methylamine $^1/_{10}$ are injected into the *left* tympanic cavity (through tympanic membrane); the left auditory canal is filled.

9.40 a.m. Examination of the different reflexes shows no disturbances.

9.44 a.m. The labyrinthine righting reflex on the head is absent in the right, present in the left lateral position. Head downward: head is turned *to the right* (Grunddrehung $\rightarrow R$). The compensatory eye-positions are absent in the right, markedly present in the left lateral position. If the rabbit sits quietly the trunk inclines a little to the right.

9.48 a.m. The "Grunddrehung" to the right diminishes, after that the "Grunddrehung" is absent when the head is directed downward. Some moments later the labyrinthine righting reflex on the head is present in the right lateral position, but absent in the left lateral position.

9.50 a.m. Now a distinct "Grunddrehung" $\rightarrow L$ is present; labyrinthine righting reflexes are present in the right, absent in the left lateral position. No spontaneous nystagmus, no head nystagmus. The compensatory eye-positions showed a completely inverse picture: present in the right lateral position, absent in the left lateral position of the head.

9.52 a.m. *Distinct but unfrequent nystagmus* $\rightarrow L$, *the slow phase can be seen distinctly. No head nystagmus. "Grunddrehung"* $\rightarrow L$. *The lift reaction is present, tilting reactions can be elicited only with difficulty. The labyrinth righting reflexes are unchanged.*

10. a.m. The spontaneous nystagmus to the left decreases and disappears completely, after which a slowly developing nystagmus $\rightarrow R$ occurs. No head nystagmus, the tilting reactions are doubtful. The labyrinthine righting reflexes remain unchanged.

10.5 a.m. Marked spontaneous nystagmus $\rightarrow R$ (right eye 26 movements in 10"). Distinct head nystagmus.

---

7) VERSTEEGH, C., Acta Otolaryng., **11**, 393 (1927).

8) WERNER, C. F., Das Labyrinth, 1940.

9) QUIX, F. H. and V. EGMOND, A. A. J., Zeitschr. Hals usw. Heilk., **32**, 26 (1932).

So the rabbit shows the typical syndrome of a loss of function of the left labyrinth.

From the test it appears that four phases can be distinguished:

I. Stimulation of the left labyrinth as far as tonic labyrinthine reflexes are concerned.
II. Paralysis of the left labyrinth as far as tonic labyrinthine reflexes are concerned.
III. *At the same time stimulation of the labyrinth as far as the semicircular canals and paralysis as far as the tonic reflexes are concerned.*
IV. Paralysis of the whole labyrinth.

According to DE BURLET [10]) the membranous labyrinth can be divided into a pars superior (semicircular canals with utriculus) and a pars inferior (sacculus and cochlea) seperated by a tectorial membrane. According to the above-mentioned investigations of VERSTEEGH and to the hypothesis of WERNER, the labyrinthine reflexes are elicited in the pars superior. It is, however, very questionable whether a further anatomical localisation of these reflexes is possible.

Both the cocaine experiments of MAGNUS and DE KLEYN and the investigations of DE KLEYN and VERSTEEGH [11]) (destroying of the nervus utricularis with a galvanocauter after extirpation of the sacculus) emphasize an essential difference between the tonic labyrinthine reflexes and the labyrinthine moving reflexes.

This difference was disputed by HUIZINGA [12]) in consequence of his experiments which demonstrated that in pigeons not only dynamic reflexes but also a tonic influence upon the neck muscles proceeds from the cristae.

As is mentioned by HUIZINGA, MAGNUS and DE KLEYN already accepted the property of the sensory epithelium of the cristae to produce reflexes incessantly.

Physiologically a marked difference exists, however, between the tonic labyrinthine reflexes of the utriculus and the non-tonic reflexes of the semicircular canals. Besides, the methylamine experiments gave new evidence for the above-mentioned conception of MAGNUS and DE KLEYN.

Pathological processes in the vestibular apparatus cause disturbances of the equilibrium which are either permanent or compensated centrally. It can make a great difference whether this pathological process occupies the peripheral labyrinth, the nervus vestibularis, the vestibular region or the supranuclear tracts. It is the merit of BARRÉ that he has emphasized this fact; the first syndrome is described as "Syndrome vestibulaire harmonieux", the second as "Syndrome vestibulaire dysharmonieux". The first investigations of BARRÉ [13]) were made in some cases of cerebellar disturbances; later some cases were published of other affections of the fossa cranii posterior. ARSLAN [14]) gives the following summary about the syndrome of the "dysharmonie vestibulaire": "Le syndrome dû à une lésion périphérique est "harmonieux", puisque les réflexes qui le composent ont tous le même signe; le syndrome dû à une lésion centrale est au contraire dysharmonieux puisque les réflexes qui la composent ou manquent en partie, ou ont des signes différents."

From our investigations (injection of methylamine in the middle ear of rabbits), however, the above-mentioned classification of BARRÉ proves to be an incomplete one, as the observed symptoms pointed to a vestibular disharmony, whereas a peripheral affection was present.

The clinical importance of the experimental investigations follows from the case mentioned below.

---

[10]) DE BURLET, Anat. Anzeiger, **53**, 302 (1920).
[11]) DE KLEYN and VERSTEEGH, Acta Otolaryng., **22**, 327 (1935).
[12]) HUIZINGA, Acta Otolaryng., **24**, 83 (1938); **27**, 662 (1939).
[13]) BARRÉ, Revue d'O.N.O., 1938, page 419.
[14]) ARSLAN, Revue d'O.N.O., 1938, décembre.

Girl, 8 years of age. Patient became ill on Dec. 27th 1939 with a left-sided ear-ache and high temperature (103°). On Dec. 28th paracentesis was performed, which was immediately followed by an abundant purulent secretion. On Dec. 29th patient was dizzy, everything turned around her; she showed a tendency to fall to the right. She also complained of pain in the neck, lay in bed with her knees pulled up, and *turned her head to the right.*

Examination on Dec. 30th. Patient is seriously ill, lying in bed with her head turned to the right. Slight rigidity of the neck, the head is only moved carefully. The abdominal reflexes are present, the knee jerks and *Achilles*-tendon reflexes are vivid. Perhaps a slight left-sided paresis of the facialis. Abundant purulent excretion from the left ear, pain on pressure on the left processus mastoideus, slight swelling of the glands in the left neck.

The right tympanum is normal. The acuity of hearing for the whispering voice was 6 metres at the right side; at the left side ad concham. Lateralisation of the test of WEBER to the left, RINNE positive at the right, negative at the left; duration of hearing (tuningfork of STRUYCKEN, C 5) at the right 20″, at the left 12″ (normal: 35″). No spontaneous nystagmus.

Caloric reaction: 10 cc. cold water at the right: nystagmus → L.
15 cc. cold water at the left: no nystagmus.

Lumbar puncture: pressure of liquor 120 mm, clear, PANDY positive, NONNE negative, cells $^3/_3$. No bacteriological examination.

Examination on Dec. 31st: Patient is very ill, but compos mentis, no mental disturbances. Temperature 101.3°. Pulse 90. The patient is lying in bed with her head in right lateral position. This position is partly forced: when the patient is placed in the sitting position the head is resting completely if turned to the right. There is also a turning to the right in the horizontal plane. If the physician turns the head of the patient to the left, it is immediately turned back to the middle position and then to the right. The same takes place if primarily the middle position is taken. Patient states that turning of the head to the left causes no pain. It is, however, impossible to decide whether the slight glandular swelling at the left has any influence upon the forced position of the head.

There is a *marked spontaneous nystagmus to the left,* when looking to the left; looking straight forward and looking to the right causes no nystagmus. This nystagmus does not change in the different positions of the head, only when the head is in the left lateral position, a rotatory component exists. The peripheral labyrinth can now be stimulated, at least with ice-water. In dorsal position a distinct horizontal nystagmus to the right developed, which changed into a nystagmus II to the left when the abdominal position was taken. Lateralisation of the test of WEBER to the left. Duration of hearing of tuningfork-STRUYCKEN C 5 at right 20″, at left 12″ (normal 35″). A spontaneous past-pointing is present: at the left, pointing outward; at the right sometimes normal, sometimes inward.

The co-ordination tests show no cerebellar disturbances. Perhaps slight paresis of the left nervus facialis.

Mastoid operation at the left: extensive pneumatisation, also in the petrosal angle and in the processus zygomaticus. The cells were filled with pus and granulations; a larger cavity existed towards the point, the trabeculae around the cavity were also softened. The cells alongside the sinus transversus proceeded to the bulbus jugularis. They also contained pus and granulations.

Culture of pus: haemolytic streptococci. Administration of dagénan twice a day.

Course: January 1st, 1940. Patient has vomited once, is lying in the supine position, head turned to the right. In dorsal position, head somewhat bent forward: slight horizontal nystagmus to the left when looking to the left. No nystagmus when looking straight forward and to the right. Three times a day 3 cc. dagénan.

Jan. 2nd, 1940. Temperature normal. Rigidity of the neck has somewhat improved.

Slight nystagmus to the left when looking to the left. Patient vomited some times this morning, has diarrhea and cyanosis, probably caused by the dagénan. Therefore the administration of dagénan was not continued.

Jan. 3rd, 1940. Temperature normal. No forced position of the head, no spontaneous nystagmus, no spontaneous past-pointing (in three planes).

Undisturbed wound course.

Discussion. This patient with an acute left-sided otitis showed a distinct spontaneous nystagmus to the left. The left peripheral labyrinth could be stimulated. The fact that a nystagmus $\rightarrow R$ could only be elicited with ice-water must be explained by the strong spontaneous nystagmus $\rightarrow L$, which had to be conquered. The development of a nystagmus II to the other side, when the patient was placed in the abdominal position, proves the irritability of the left labyrinth. The whole syndrome was strongly suggestive of an over-stimulation of the left labyrinth; an objection against this diagnosis was brought forth by the fact that there was spontaneous past-pointing to the left.

No symptoms of intracranial affection, the lumbar fluid was normal, no cerebellar symptoms. A striking feature was the position of the head: turning to the right in the horizontal plane. All symptoms disappeared after the operation of the mastoid.

For the explanation of the symptoms observed the forced position of the head is of great importance. Forced positions of the head and eyes are often found in neurological literature (f.i. STENVERS [15])) but they also occur in complications of inflammatory affections of the ear. BECK and LOSSEN [16]) described the oblique position of the head as pathognomic for an otogenic abscess of the brain; MUCK [17]) explained it by the fact that a different venous filling of the brain vessels should be present in the separate positions of the head. WAGNER [18]) in an article "Zwangstellung des Kopfes bei Ohrenerkrankungen" recorded a case of otitis with nystagmus and meningitis in which the forced position of the head was attributed to an intracranial process. Exact auditory and vestibular examinations, however, failed.

In our patient the forced position might be caused by the inflammatory process in the mastoid, especially from the perisinual cells, which proceed to the bulbus venae jugularis. The torticollis can then be explained by the necessity to relax the glands under the M. sternocleidomastoideus. As a rule in such cases the head is inclined to the affected side and turned to the healthy side, whereas in our case the head was turned to the healthy side in the horizontal plane.

BRUNNER [19]) in consequence of two of his cases, comes to a more probable conclusion. He writes: "Der Torticollis musz vielmehr als eine direkte Labyrinthwirkung angesehen, demnach dem labyrinthären Schwindel gleich geordnet werden." The forced position in our case must then be due to a vestibular torticollis, a so-called "Grunddrehung" a stimulation-symptom of the labyrinth, just as the spontaneous nystagmus to the left. The only symptom which does not belong to the clinical picture of the labyrinthine stimulation is the spontaneous past-pointing to the left with the left arm, except when this should be interpreted as "dysharmonie vestibulaire" (BARRÉ [20])) of *peripheral* origin.

---

[15]) STENVERS, Arch. of Neurology and Psych., **13**, 711 (1925).

[16]) BECK–LOSSEN, Cit. BRUNNER, Monatsch. f. Ohrenheilk., **55**, 331 (1921).

[17]) MUCK, Cit. BRUNNER, Monatschr. f. Ohrenheilk., **55**, 331 (1921).

[18]) WAGENER, Dtsch. Otol. Gesellsch., 1911, page 196.

[19]) BRUNNER, Monatschr. f. Ohrenheilk., **55**, 331 (1921).

[20]) BARRÉ, Revue d'Otol., **16**, 419 (1938).

Medicine. — *Some considerations concerning our knowledge of the action of the auditory organ.* Part I. By J. BIJTEL. (Communicated by Prof. A. DE KLEYN.)

(Communicated at the meeting of September 27, 1941.)

In spite of many contributions, in ever increasing number, towards our knowledge of the action of the auditory organ, one cannot yet speak of a definite or satisfactory conception. No manner of viewing the matter has been able to maintain itself as conclusive, not a single experiment has furnished an arresting proof of any theory. The present state of affairs has made us ask ourselves whether our investigations are well founded, whether the leading thoughts are indeed the right ones. One cannot escape from the impression that there will have to be a vision of biological processes different from that which now predominates. We have certainly not yet come to a formulation, in a definite form, of other notions about the matter. For the present we shall have to limit ourselves to considering the elements of our present knowledge critically and collecting data from this for determining new lines of action. If one concentrates on the main points of the predominating views, one can say that the analytical function is considered essential and that the thoughts about this move between two antipoles, namely central and peripheral analysis. For the solution of this antithesis the knowledge of the process of conduction in the auditory nerve is of great importance. For, if the process of conduction of excitation in the auditory nerve should prove a phenomenon of vibration, more or less identical with the mechanical process of vibration that comes from outside, this would point more or less to central analysis. If, on the other hand, the process of conduction in the auditory nerve appears to be, according to the old general law of specific nervous energies, a process not specific as regards the outer stimulus, equal for all nerve-fibres, one should assume peripheral analysis. If this is the case, the peripheral organ will contain a number of receivers, each for a separate quality of excitation, in this case a certain pitch. When the receiver is excited specifically, one or more nerve-fibres belonging to this receiver will bring about a corresponding perception in the central nervous system, by a process of conduction of their own.

The right means to orientate oneself about the conduction of excitation in the auditory nerve is the registration of the action current of the nerve. Now it is only with great difficulty that one can apply this means rightly with regard to the auditory nerve. Derivation with two unpolarisable electrodes of a part of the auditory nerve that is lying free has really not yet succeeded. Anatomical situations are the principal cause of this. Derivation in other ways, when, moreover, use is made of powerful amplifiers cannot furnish conclusive proof. The effects of the alternating current, derived in this way, have always potentials that must be considered microphone-effects of the cochlea. DAVIS [1]) distinguishes two parts in the effect of the alternating current, namely the cochlea-effect and the action-potential of the auditory nerve.

The cochlea- effect occurs within 0.1 millisecond after the sound-stimulus, it follows the form of the mechanical excitation closely, the phase of the cochlea-effect turns with the phase of the stimulus. This effect must be considered a microphone-effect. Some tenths of a millisecond later an electric effect occurs, which has more a characteristic of its own and which DAVIS looks upon as an action-potential of the auditory nerve. DAVIS succeeded in obtaining this action-potential more isolated from the auditory nerve itself. Up to a frequency of 3000—4000 cycles a second this gives an alternating current

1) DERBYSHIRE, A. J. and DAVIS, H., Amer. Journal of Physiology, **113**, 476 (1935). DAVIS, H., The Journ. of the Acoustical Society of America, **6**, 205 (1934—35). BÉKÉSY, G. VON, Ztschr. f. techn. Physik, **17**, 522 (1936).

of the same frequency as the sound-stimulus, but independent of it as regards the phase. Above this frequency the alternations of the currents of action are no longer synchronous with the soundvibrations. At about 900 cycles a second, the maximum that is possible in connection with the refractory period of a nerve-fibre, if one assumes that every cycle of the sound corresponds to a nerve-impulse, the strength of the action-potential drops by half, at 1800 cycles a second by a third.

It is sometimes assumed that in a group of nerve-fibres which takes part in the conduction, alternating conduction occurs, each nerve-fibre in itself only transmitting half the number of cycles. This would be attended with an extension of the number of nerve-fibres which takes part in the conduction. If we imagine that up to 900 cycles a second two fibres transmit the impulses at the same time, then at above 900 cycles a second one fibre will conduct the odd impulses, the other the even ones. One can also put it thus: up to 900 cycles a second one fibre transmits the impulses and above this a second fibre is switched in. That in reality the proportions are a little more intricate does not change the thus described principle. One can remark against this that one cannot understand how one fibre begins to conduct at the first and another only at the second impulse. Nor is it clear why with common derivation from all conducting fibres the action-potential weakens through alternating conduction. Meanwhile these experimental results have been explained as indications of the transmitting, in form, of the vibrational process through the auditory nerve to the centre which would be a plea in favour of central analysis. We can say besides that the cochlea is an organ which can never admit sharp analysis in a physical sense. Sharp resonances are certainly impossible in this very muted system. An important contribution, which undoubtedly opens new possibilities, comes from VON BÉKÉSY [1]). VON BÉKÉSY, using enlarged models, concluded that there are whirling currents in the liquid, for different frequencies in different places. On account of this the cochlea would become an a-periodical analyser. Apart from the question whether this phenomenon will occur in the same way in the cochlea, in spite of the precautions taken by VON BÉKÉSY in constructing the enlarged model, it certainly does not explain a sharp analytical power. VON BÉKÉSY himself also thinks that peripheral analysis is certainly not possible to the extent that was formerly assumed and best formulated in the resonance-theory according to HELMHOLTZ.

Attempts were made to gain other data from the study of the overtones. The peripheral auditory organ is not at all a linear system, i.e. it does not pass on a vibrational phenomenon untransformed. So overtones are formed in the peripheral organ. VON BÉKÉSY [2]) established that the intensity of overtones may even amount to 30% of the intensity of the fundamental tone. The greater part of them can be found again in the electric effect of the cochlea and so must mainly arise in the peripheral organ. It is sometimes assumed, however, that some of them also arise in the auditory nerve.

Now if we limit ourselves to the part which arises in the peripheral organ, these overtones can again be divided into 2 groups, namely 1°, the overtones coming from the middle ear and 2°, those coming from the cochlea. One can infer from experiments made by VON BÉKÉSY [3]) that the overtones which arise from conduction through the middle ear have only a small intensity. The effect which the tympanic membrane ought to have on the arising of the overtones, on account of its form, is again made worthless by effective impedance-situations, at least the greater part.

VON BÉKÉSY [4]) showed further that these overtones of the cochlea arise after the sound has been split up in its components, which are then each included in a separate system, which points to peripheral analysis.

---

[1]) BÉKÉSY, G. VON, Physik. Ztschr., **29**, 793 (1928); Acta Otolaryngologica, **27**, 388 (1939).

[2]) BÉKÉSY, G. VON, Annalen der Physik, **20**, 809 (1934).

[3]) BÉKÉSY, G. VON, Acta Otolaryngologica, **27**, 281 (1939).

[4]) BÉKÉSY, G. VON, Annalen der Physik, **20**, 809 (1934).

The experiment is then conducted in this way:

As a primary tone a pure tone of 500 vibrations a second is made to act on the ear. There arises, among other things, a first overtone of 1000 cycles a second. One can perceive this, because when a secondary tone of 1004 cycles a second is provided, 4 beats a second occur. Now with the primary and the secondary tone a tertiary tone is provided, of a relatively low frequency, namely 100 cycles a second. Phenomena of modulation do not occur then. This would be the case if the three tones together passed one and the same physical system.

We ask ourselves, however, how it is possible that beats arise when the components of a compound sound are already separated in such a way that modulation is excluded. It also seems to us that the occurring of 4 beats a second in perceiving the tones of 500 and 1004 cycles a second does not yet prove the formation of a tone of 1000 cycles a second. It is possible that from these two tones a different tone of 504 cycles a second arises, which then together with the tone of 500 cycles a second gives the 4 beats.

Attempts have been made to approach the problem, already mentioned before, of the character of the process of conduction in the auditory nerve with the help of the tone-beats. If namely a process of a vibrational character runs through the auditory nerve, identical with the sound-vibrations that are provided, beats will have to be perceived, even if one makes two tones with a small difference in frequency act each on one ear of the same person on whom the experiment is made. That the two stimuli unite centrally can be derived from the binaural summation of two tones of the same frequency each with an intensity, beneath the threshold-value, up to an audible tone.

As regards this question the only investigations found by us in literature were those of STEWARD and LANE [1]). LANE concludes that so-called subjective beats can occur, distinguished from so-called objective beats, which occur when the sounds brought to both ears mingle outside the auditory nerve. Our own experiments [2]) did not confirm this, however. When the possibility of the two sounds mingling outside the auditory nerve was really excluded, none of the persons on whom our experiments were made could perceive beats. This would point to a process of conduction specific of all nerve-fibres, at least a process that lacks the vibrational character. We noticed already that this is sometimes considered as pointing to peripheral analysis.

The sensitivity of the auditory organ, so much varying for different pitches and which has occupied so many investigators, can also be included among these considerations. As far as we could ascertain, the investigators have chiefly limited themselves to measuring the sensitivity without speculating too much on it. We remark the following:

The curve which illustrates the sensitivity of the ear to different pitches can be considered as a resonance-curve. We think that in the organ of perception — tympanic membrane, tympanic bones and cochlea — we may see a pressure-receiver. Now in contrast with the auditory organ in its entirety a pressure-receiver is little dependent on the frequency. One might derive from this fact that the difference in sensitivity for different pitches cannot be dependent on the organ of perception alone, but must be resident in the central nervous system. On the other hand, however, the electric cochlea-effect is in its strength dependent on the frequency with a maximum at 1000 cycles a second, from which it would follow again that the difference in sensitivity is for different frequencies a quality of the cochlea. It should be remembered that for the electric cochlea-effect other rules obtain than for the auditory power.

Our insight, meanwhile, into the intensity-perception of sound has as yet developed very little.

The principle of central analysis was, as far as we could ascertain, first formulated in 1886 by RUTHERFORD in his telephone-theory (derived from WILKINSON and GRAY [3])).

---

[1]) LANE, C. E., Physical Reviews, **26**, 401 (1925).

[2]) BIJTEL, J., Ned. Akad. v. Wetensch., Amsterdam, **44**, 198 (1941).

[3]) WILKINSON, G. and GRAY, A. A., The mechanism of the cochlea, London, 1924.

Here it is assumed that the membrana basilaris follows the sound-vibrations in its entirety and that the integral image is passed on to the auditory centre to be dealt with further. In their critical view of the different theories concerning the auditory function WILKINSON and GRAY say one cannot assume that an analysis of compound mechanical vibrations can take place in the brain. For this would mean a time-measurement, namely of the duration of a vibrational period by the brain. They take as their basis the relativity-theory, that time can only be measured by movement. Now the brain, WILKINSON and GRAY say, does not contain a clock, a chronometer, one can really only consider the pendulum as such. It is especially in the membrana basilaris with its resonators that one can see, according to WILKINSON and GRAY, an excellent chronometer.

Here we certainly have the crux of the whole matter, namely in how far the action of an organ must be seen as a purely physical process and the apparatus of the organ as an instrument. We think that the psychical atmosphere has been considered too little.

In the psychical atmosphere the ideas of pitch are not at all exclusively connected with an instrument with a pendulum. A composer can work with ideas of pitch in endless variations and that not only as regards mutual relations, but often also with the right absolute values (absolute hearing of tones). We learnt on good authority that MAX REGER worked out music contrapuntally without the help of any instrument. Nor, when sound-images are called back to memory, i.e. are seen introspectively by the ego, do we dispose of a physical chronometer in this psychical process.

The way in which living organs react on stimuli cannot be compared with the qualities of a physical measuring-apparatus. We do not mean to say by this that the living organism should not be subject to physical laws. However, too little attention has been paid to that which is typical of the living organ. As an example we take the sensation of pressure. It is a well-known fact that a constant pressure is perceived for some time. Then there is adaptation. When the pressure-stimulus is removed, an after-image arises, as it were; for some time the pressure is still perceived. One can also apply the argument to the otolith-apparatus, where a constant pressure does not lead, it is true, to a direct perception, but maintains a state of tension in the nervous system, which presupposes a constant activity in the organism. Physically speaking we do not know of such a state. A constant pressure cannot provide energy nor can activity come from it. It is clear that in living nature there are other possibilities.

As we have still a very incomplete knowledge of the essential facts in the action of living organs, in spite of all our investigations, it is impossible to get a more profound insight into the importance of such data. However, they will have to divert our attention from a one-sided physical way of considering the matter.

We add to this a curious example of how organ-stimuli are dealt with centrally, in an unexpected way. We know that according to the physical view of perceiving forms on the retina we can only perceive a dark line in a luminous field if this line has a certain breadth, namely is seen under an angle of 60 seconds. With suitable illumination, however, we can see very thin threads in a luminous field, so that the adjoining angle amounts to no more than 2 seconds. EINTHOVEN [1]) showed that perceptions of intensity in this case lead to a certain perception of form. An analogue to the auditory organ is not known to us. We point to the fact, however, that in general the central treatment of organ-stimuli is by no means always bound with physical systematicalness. In this connection the difference between the hearing of tones and the hearing of speech is curious. We find every imaginable variation. The hearing of speech is sometimes weakened when there is a predominant defect in the low tones, in other patients again when there are predominant defects in the high tones. We also found that the hearing of speech had grown much weaker, while the hearing of tones had only grown a little weaker. Several patients whose hearing of tones has weakened in divergent ways, can have equal hearings of speech.

---

[1]) EINTHOVEN, W., Kon. Akad. v. Wetensch., Amsterdam, **29**, 388 (1920); Pflügers Arch. f. d. ges. Physiologie, **191**, 60 (1921).

One patient had a good hearing of speech, while the hearing of tones had weakened. We know that the hearing of speech is strongly influenced by psychical factors. The diversity which we noted in our routine-investigation with whispered speech and tuning-forks, certainly cannot be entirely attributed to diversity in power of concentration, psychic predisposition etc. A minute peripheral analysis with following reconstruction of the sound-image in more central parts would certainly give a more constant relation between hearing of speech and hearing of tones. We have too few data to assume that there are separate organs for hearing of speech and hearing of tones. Meanwhile we point to the fact that the idea of a differentiation in the peripheral organ has sometimes come to the fore. Formerly it was sometimes assumed that the perception of murmurs and the perception of pure tones were separate peripherally, in sacculus and cochlea respectively. One might also imagine that distinct nerve-elements in the cochlea form the basis of such a differentiation. Anyhow in this case the accent would fall on the nervous system. Meanwhile, as we lack exact data, such considerations are for the present mere speculation.

A plea, more meant for use in the discussion about the way in which peripheral analysis must be imagined, is derived from the perception of trills. One can perceive very well two quickly alternating pitches, the one after the other. If we accept the resonance-theory as true, this fact presupposes a great muting-value. For muted resonators need a short period of time to stop resonation and to come into action, little muted resonators need longer periods of time to stop resonation and to come into action. A strongly muted system, however, loses again in analytical power. If one attributes a great analytical power to the ear, localised in the cochlea, then one meets with a contradiction: little muting to explain the analytical power, strong muting to explain the short period of time needed to stop resonation and to come into action. JUNG [1]) has tried to solve this contradiction. In doing so he has applied a method that is used more often: he constructed an electric analogue to study the mechanical phenomena.

JUNG has succeeded in constructing an electric system, in which this contradiction has been removed. He also thinks that the structure of the cochlea-organ need not necessarily bring with it the above-mentioned contradiction for mechanical vibrations. It remains to be asked here in how far the analogy can be applied. A very complicated reasoning is necessary to fix the analogy.

VON BÉKÉSY [2]) has measured the just perceptible period during which a sound is interrupted. If one compares pure tones with murmurs, one finds that these periods are fairly equal. If we were dealing with a system of selective resonators this equality could not exist. For murmurs consist of many tones, each of a short duration, which cannot make a rather sharply tuned resonator vibrate with them at full strength. The periods of time needed to stop resonation must also be short, shorter than is the case with pure tones. These considerations especially bear on the way in which the peripheral organ works. However, they strongly speak against sharp resonances in the end-organ in any form and as any other way of analysing is necessarily less sharp than that through resonance, they again make us view the matter in a way that goes in the direction of central analysis.

In another way one also comes to the conclusion that central analysis, at least partly, must be assumed and that is on account of the phenomena attending the perception of tones of a short duration. For frequencies beneath 500 cycles a tone of short duration of together 8—10 cycles sounds like a click, in which, it is true, one can recognise a certain pitch, but where the threshold of distinction has been considerably increased. Such short series of cycles can be divided again into e.g. 3 groups of 3 cycles, which, separated by intervals of time, are brought to the ear. From the time-values it is concluded that nervous processes play a part here, which determine the perception of a click or tone.

We want to make a few more remarks about the perceptions of intensity. Taking the "all-or-none law" as our starting-point, we must assume that for every pitch a great

---

1) JUNG, H., Akustische Ztschr., **5**, 268 (1940).

2) BÉKÉSY, G. VON, Physik. Ztschr., **29**, 793 (1928).

number of nerve-fibres is present to distinguish the different degrees of intensity. If one assumes peripheral analysis with separate paths of conduction for different pitches, there would have to be no less than 340.000 different nerve-elements to perceive all frequencies at all degrees of intensity, but this is not the case. We know from the work of ADRIAN that a greater perception of intensity can also be transmitted by a greater number of impulses in one nerve-fibre. If, however, it is true that the number of impulses in the auditory nerve is determined by the pitch, at least to a certain extent, we are again faced with inexplicable facts.

LORENTE DE NO assumes that the inner and the outer hair-cells have different functions, in this way that one group serves to determine frequency and the other to determine intensity. MINK even assumes that the intensity is determined through stimuli from the middle ear. But we have no positive indications for this.

We now want to conclude the enumeration of those data which are important to determine the character of the auditory process, especially the process of conduction of excitation. We think that we have provided sufficient data to come to the conclusion that not a single physical consideration gives us a definite answer to the question as to how an auditory impression really originates. The peripheral recording-apparatus, which naturally supports the physical way of considering the matter, cannot at all be called a suitable tone-analyser. It is true that a few data point to a greater accuracy than the structure would make us suspect at first sight. We pointed this out already, by saying namely that on account of certain impedance-situations the non-linear conduction through the tympanic membrane is for the greater part prevented, so that the part that the middle ear plays in the originating of overtones becomes very small. This demonstrates very clearly how intricate are the instruments of living nature and how much their construction deviates from our technical apparatuses, which again makes a comparison between the living organ and the technical instrument extremely difficult. The supposition that also in other respects such complicated situations occur in the acoustic organ is justified, especially when we note the fact that the central nervous system has a correcting influence on phenomena transformed in such a rough receiver as the cochlea. Years ago already BÁRÁNY expressed himself in this way. Also in BUDDE [1]) we found an indication in this direction. We have not yet come to a fixed notion, meanwhile, of the activities in the nervous system. We can only say that undoubtedly processes work in it that to a great extent follow biological principles of their own, though they are always attended with physical and chemical phenomena.

---

[1]) BUDDE, E., Mathematische Theorie der Gehörsempfindung, Berlin 1920. (Handbuch der biologischen Arbeitsmethoden V, 7. 1.).